EXAMINING THE USE OF THE PARTITION COEFFICIENT IN QUANTIFYING SORPTION OF HEAVY METALS IN PERMO-TRIASSIC SANDSTONE AQUIFERS

By

TIMOTHY ALEXANDER BATTY

A thesis submitted to
The University of Birmingham
for the degree of DOCTOR OF PHILOSOPHY

Department of Earth Sciences
School of Geography, Earth & Environmental Sciences
College of Life and Environmental Sciences
The University of Birmingham

July 2015

UNIVERSITY OF
BIRMINGHAM

University of Birmingham Research Archive

e-theses repository

This unpublished thesis/dissertation is copyright of the author and/or third parties. The intellectual property rights of the author or third parties in respect of this work are as defined by The Copyright Designs and Patents Act 1988 or as modified by any successor legislation.

Any use made of information contained in this thesis/dissertation must be in accordance with that legislation and must be properly acknowledged. Further distribution or reproduction in any format is prohibited without the permission of the copyright holder.

ABSTRACT

Hydrogeologists using the partition coefficient, or K_d approach, to quantify attachment (sorption and / or ion exchange) of heavy metal(s) in aquifers have expressed reservations about its oversimplification of the geochemistry involved, potentially undermining predictions of contaminant fate and therefore jeopardising effective remediation efforts. The aims of this project were to determine the validity of the K_d approach for the Permo-Triassic sandstone – a common aquifer type worldwide – and to propose a better way of quantifying attachment for metal ions.

In Stage 1 (of four), computer simulations of batch experiments explored the sensitivity of the processes governing Cd attachment on synthetic hydrous ferric oxide, hypothesised to be an analogue of the haematite coating on the surface of the sandstone, to factors such as pH, metal concentration, and overall water chemistry. These showed that pH is highly influential, with very little attachment at low pH, and almost 100 % attachment at high pH, demonstrating that K_d values vary from effectively zero to infinity over a pH interval of about 2 pH units. They also suggested that Ca and Mg were important *competing* ions. In Stage 2, laboratory batch experiments using Zn were undertaken using a sample of carbonate-free Permo-Triassic sandstone. These showed that ion exchange was very important; however, the strong pH dependence suggested that sorption was also involved. The sorbing phase was not identified, and could be a mixture of Fe oxide, Mn oxide and clay mineral edges. Full equilibration took up to 170 hours. In Stage 3, the geochemical code PHREEQC was used to interpret the results of

the laboratory experiments using simulations incorporating both surface complexation theory and ion exchange. These demonstrated, by approximately matching attachment isotherm plots of Zn, that the model was a robust representation of the sandstone. In Stage 4, this model was adapted to simulate transport of Zn through a representative aquifer in a range of conditions to determine the potential importance of sorption in metal transport. The results confirmed the variability in the system with regard to pH influences, the fluctuating dominance of ion exchange and sorption, the presence of competing ions, and the resultant outcomes for Zn transport. It is expected that these results are similar for metals with chemistry similar to that of Zn.

The project has contributed to the field of contaminant hydrogeology by comprehensively substantiating the existing reservations regarding the use of the K_d approach, demonstrating the high degree of complexity in the Permo-Triassic sandstone system. The project has also shown how geochemical models incorporating surface complexation theory can be employed to make much more realistic predictions, potentially improving the outcome of predictions of contaminant fate for aquifer management and remediation efforts.

ACKNOWLEDGEMENTS

I am sincerely thankful to my principal supervisor, Professor John Tellam, for his guidance, insight, technical expertise and general support. This project would not have been possible without his input. I was also helped along the way in various ways by Dr Steve Buss, Dr Joanna Renshaw and Dr Michael Rivett, my secondary supervisors.

Aruna Mistry, Gretchel Coldicott, Jane Harris, and Steve Baker were key support staff in various phases of the project, and I am thankful for their invaluable help.

I gratefully acknowledge the financial and technical support provided by the CASE project partner, ESI Ltd.

I am deeply indebted to Dr David Mair, Stephen Hartland, Alistair Dow, Chris and Julie Grove, Andrew and Jill Veitch, Charles Eaves, David Lassey, Andrew Leo, Kate Waplington, Sezer Sarfraz, Kate Walker, Andy Clarke, and the staff and congregation of The Church at Carrs Lane, Birmingham, for supporting me in various ways. My fellow PhD students and post-docs have been a source of inspiration and moral support, along with a number of friends who wish to remain nameless!

Finally, my parents, Robert and Sandra Batty, and my brother, Peter Batty, have offered steadfast support throughout this work, for which I am truly thankful.

CONTENTS

LIST OF FIGURES

LIST OF TABLES

1 - BACKGROUND, AIMS, APPROACH & THESIS STRUCTURE

1.1 Overview

This chapter gives an introduction to the project, presenting the context for the research and also the main questions arising. An overview of the approach taken to answer those questions is then given, followed by an outline of the thesis structure.

1.2 Background to the Project

1.2.1 The Importance of Groundwater

Groundwater forms a key part of the global hydrological cycle (Brassington, 1998) and is generally considered to be an inexpensive, reliable and high-quality source of water for human consumption (Downing, 1998). Globally, it provides 25% to 40% of the world's drinking water, with around 2,058 million people obtaining their water from boreholes and other wells in 2010, an increase of 4.5% over the dependence in 1990 (NGWA, 2016). Its availability and use is dependent upon the distribution of suitable aquifers and the local climate; arid countries, such as Bahrain, Oman and the United Arab Emirates, and island nations such as Malta and Barbados are entirely dependent on groundwater resources to supply domestic, agricultural and industrial needs (Margat & van der Gun, 2013), with India, China and the United States drawing considerable demand, particularly for agricultural irrigation. It is expected that groundwater will play a progressively

more crucial role in ensuring water and food security as predicted changes in climate (Ruddiman, 2002) increasing the variability in precipitation, soil moisture and surface water (Taylor, et al., 2013). It is therefore important to protect and responsibly steward this valuable natural resource.

1.2.2 Contamination of Groundwater

Whilst groundwater is commonly safe for human consumption with minimal treatment, it is vulnerable to contamination – normally by human activities at the land surface. Urban development, industrial development, and agricultural activity, can each give rise to localised (*point source*) or widespread (*diffuse*) pollution (Environment Agency, 2013). Contemporary sources of contamination include: domestic septic tanks; storm water drains; agriculture; mining; industries such as food and drink manufacturing, textiles, chemicals production, petrochemicals, power generation, and various engineering works; household wastes; and landfill. These activities give rise to a multitude of potential contaminants, such as bacterial contamination, suspended solids, ammonia, nitrate, phosphate, sulphate, chloride, suspended solids, and various other chemicals and metals (Hiscock, 2005).

Groundwater is recharged by the percolation of surface water through the upper layers of soil to the water table (Fetter, 2000). Therefore, if contaminants are released into the soil or surface water – due to accidental spillage, incorrect or malignant disposal, or other means – they may find their way into the groundwater system (Figure 1-1).

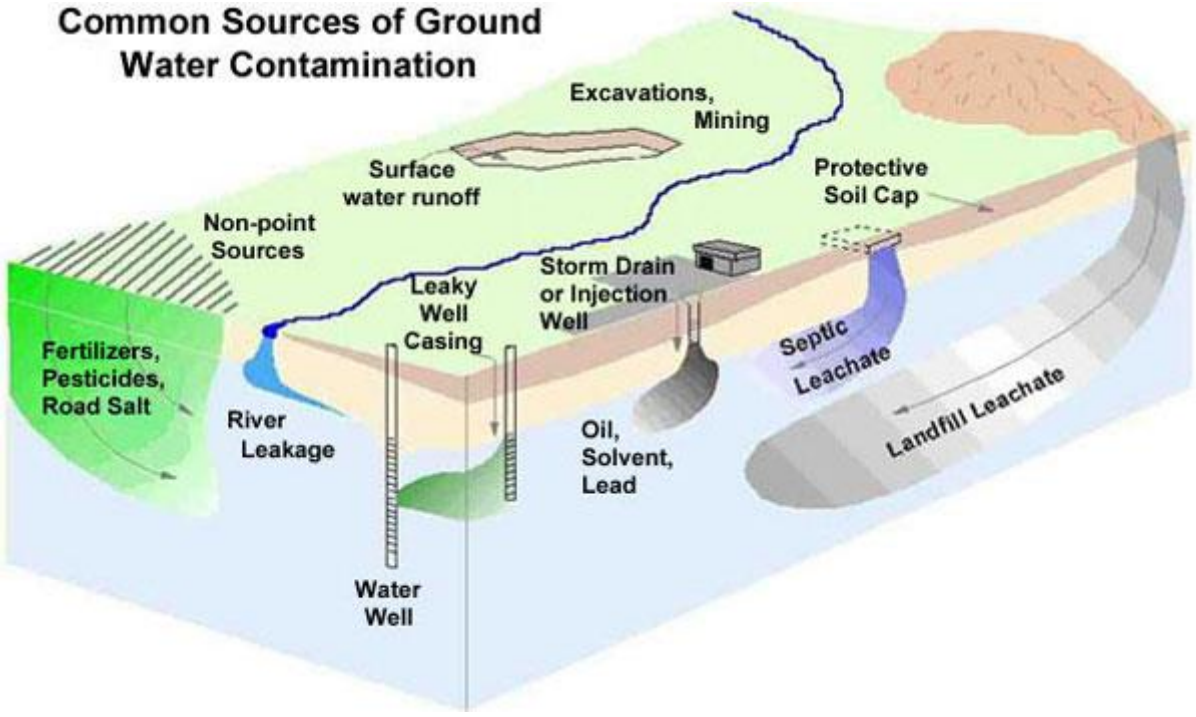

Figure 1-1: Common sources of groundwater contamination[1]

Contaminants may then migrate through the groundwater system, potentially reaching a location where they may cause harm to the environment and biota, and jeopardise formerly potable abstraction wells and boreholes (Rose, 2004).

1.2.3 Incidence of Contamination

Evidence is mounting that the incidence of soil contamination worldwide is growing – mostly in areas of industrial activity. Across Europe, there are an estimated 2.5 million potentially contaminated sites, of which around 14% (340,000 sites) are expected to require remediating measures (EEA, 2014). Production sectors were

[1] (Source: www.idahogeology.org/services/hydrogeology/PortneufGroundWaterGuardian/my_drinking_water/water_quality_reports/reports_images/contam.jpg)

largely responsible, accounting for around 60% of contamination incidents, with service sectors contributing around 32% and mining responsible for the rest, in certain countries. In England and Wales, 781 sites had been determined as contaminated land, of which over 90% had residential buildings (Environment Agency, 2009(b)). The United States Environmental Protection Agency reported tracking more than 530,000 sites and approximately 23 million acres affected by contamination across the United States of America (USEPA, 2013) from a wide range of sources. In 2014, China's Ministry of Environmental Protection and the Ministry of Land published the results of a soil pollution study (BBC, 2014) which suggested that, in a study area of approximately 6.3 million km^2 – two-thirds of China's land area – nearly a fifth (mostly arable land) exhibited excessive concentrations of potentially harmful substances (EPM, 2014). The sources are attributed to mining, other industry, and agricultural activities.

These statistics give an idea of the scale of the problem in some of the more developed countries, and where the government is taking action to improve the situation. In other (especially developing) countries, however, there is little or no understanding of the issue of soil and water contamination (Fowler, 2007) despite evidence that groundwater contamination may be widespread (Kao, 2004). This may be because issues such as poverty and poor health present more pressing concerns for the resident population than environmental harm (USITC, 2004). In an effort to address these uncertainties, the Blacksmith Institute began compiling a global inventory of contaminated sites (Blacksmith Institute, 2012).

1.2.4 Heavy Metals

Heavy metals feature prominently in the lists of common contaminants found in site investigations:

- In Europe, the preponderance of heavy metals was calculated as 34.8%, mineral oil as 23.8%, with hydrocarbons, cyanides, phenols and others making up the rest (EEA, 2014);
- In England and Wales, metals, metalloids and organic compounds constituted the majority of the pollutants in these sites (Environment Agency, 2009(b));
- Contaminated land in China was found to have excessive levels of cadmium, mercury, arsenic, copper, lead, chromium, zinc and nickel, along with miscellaneous other contaminants (EPM, 2014; Cheng, 2003);
- In the United States and Canada, dioxins, furans, lead, mercury, asbestos, arsenic, PCBs, benzene, cadmium PAHs and benzene by-products were common (UNEP, 2002);
- In developing countries, mercury, arsenic, chromium, lead, cadmium, cyanide, PCBs, pesticides, coal, volatile organic compounds, PAHs and several other contaminants were often found (Erickson, 2011).

Used in many facets of industry (Lenntech B.V., 2016), the presence of heavy metals in soils and groundwater raises concerns because they pose a considerable risk to the environment and to human health (W.H.O., 2011; Liu, et al., 2005; Zhuang, et al., 2009). An outline review of the uses of some of these heavy metals - of cadmium, lead and mercury – is given in Table 1-1.

Table 1-1: Sources and uses of common heavy metals

Metal	Source / Manufacture	Typical Use(s)
Cadmium (Cd)	Mostly as a by-product of Zn ore refining (Evans, 2005). Key producers: China (8,090 tons), Rep. of Korea (4,250 tons), Japan (1,970 tons) (USGS, 2016(a)).	Ni-Cd rechargeable batteries; sacrificial corrosion-resistant coatings for iron and steel; pigments; stabilisers for PVC; in alloys and electronic compounds; in photovoltaic cells (Lenntech B.V., 2016; OSHA(a), 2013).
Lead (Pb)	Mined as naturally-occurring metal (Evans, 2005). Key producers: China (2,300,000 tons), Australia (633,000 tons), USA (385,000 tons) (USGS, 2016(b)).	Natural sources; batteries; petrol additives (banned in EU); alloys; pigments; cable sheathing; munitions; radiation shielding; fishing weights (Lenntech B.V., 2016; OSHA(b), 2014).
Mercury (Hg)	Mined as a naturally-occurring metal; also a by-product of gold-silver mining. Key producers: China (1,600 tons), Mexico (500 tons), Kyrgyzstan (70 tons) (USGS, 2016(c)).	Instruments such as thermometers, manometers, barometers; electrical components (switches, batteries, high-intensity discharge lamps); amalgams in dentistry; heat transfer technology, pigments, catalysts, lubricating oils (Lenntech B.V., 2016; OSHA(c), 2012).

1.2.5 Remediation of Heavy Metal Contamination

In land where substances are present in potentially harmful concentrations (Environment Agency, 2009(a); Environment Agency, 2005(a)), and where there is a pathway for migration and a target location at risk of contamination, a clean-up strategy for the affected land and groundwater may be implemented (Downing, 1998; Environment Agency, 2014). Once analysis is complete, steps may then be taken to enact the remediation strategy (Environment Agency, 2010). Measures may include: containment of the contamination using physical barriers such as impermeable membranes; removal of contaminated soil; pumping to remove contaminated groundwater ("pump-and-treat"); and other approaches (Reddy, 2008; Downing, 1998).

In contaminated groundwater investigations, hydrogeologists need to be able to understand and predict the movement of contaminants through the system (Environment Agency, 2005(b)). One of the primary assessments that must be undertaken is the interaction of the contaminant and the aquifer: as contaminants migrate through an aquifer, a portion of them remain dissolved in solution, and the other portion becomes attached ("sorbed") to the aquifer material (Fetter, 2000; Stumm, 1992). This governs how the contaminant will be 'retarded' in the system, influencing its concentration at a given point. The task, then, is to quantify the degree of sorption and desorption occurring as the contaminant plume moves through the groundwater system (de Marsily, 1986). This project is essentially concerned with the way in which we quantify sorption, of heavy metals in particular.

1.2.6 The Partition Coefficient (K_d)

Historically, these interactions have been simplified by assuming that the concentration of the metal sorbed to the aquifer material (i.e. permeable rock) is proportional to the concentration of the metal in solution, the ratio being called the "K_d", or partition coefficient (Appelo & Postma, 2007). This concept originates from work on the interaction between water and gases by Henry (1803) and developed by Nernst (1891), who was perhaps the first to use the term "distribution coefficient", now in common environmental parlance. Their observations suggested that chemical solutes will partition predictably between liquid, gaseous and solid phases. The concept evolved to include thermodynamic factors by Gibbs (1876; 1878) and Lewis (1901). Early applications of this work were in anaesthesia and toxicology, which prompted research by Meyer (1899) and Overton (1901) to grapple with the mechanisms underlying anaesthesia; the concept also underpins the theory of chromatography (Zechmeister & Cholnoky, 1941). Researchers later attempted to quantify partition coefficients between other pairs of phases, such as air-water, soil-water and biota-water (Mackay, et al., 2016). Amongst these studies were experiments undertaken to ascertain the effect of pH (Kipton, et al., 1992; Lee, et al., 1996; Pankow, et al., 1997; Zhang, et al., 2015) and temperature (Mackay, et al., 2006; Li, et al., 2007); these influences will be discussed later. The theoretical foundations of the partition coefficient are outlined in Chapter 2.

Regardless of the nature of the phases being investigated, calculating the partition coefficient essentially requires determination of the concentration of the substance

in question in each phase. Generally using laboratory batch experiments, the two phases in question are brought into equilibrium under steady-state conditions and the concentrations either directly measured, or inferred from mass-balance calculations (Lee, et al., 1996; Mackay, et al., 2006; Boethling & Mackay, 2000; Lyman & Reehl, 1982). Such is the current dependence on partition coefficient calculations that many aspects of their determination have been standardised by recommended procedures, for example BSI (1990; 2004; 2008) and elsewhere.

Partition coefficients have been used extensively in many environmental investigations. These include, but are not limited to, assessment of landfill performance, e.g. (EA, 2000; EA, 2003(a); EA, 2003(b)); studies of soils and clays and their behaviour with regard to different metals, e.g. Carriere et al. (1995), Appel & Ma (2002), Altin et al. (1999), Balistrieri & Murray (1982), Bibak (1994), Bruemmer et al. (1988), Forbes et al. (1976), Hooda & Alloway (1998), Puls et al. (1991), and others.

This approach has persisted because of its simplicity and ease of application in practice, and is incorporated into many reaction transport models used to describe sorption, such as ConSim (Golder, 2009) and Landsim (Golder, 2006) – both used extensively in hydrogeological investigations to predict the migration of contaminants. However, several authors (Brusseau, 1994; Carriere, et al., 1995; Evanko & Dzombak, 1999; Kohler, et al., 1996; Reed, et al., 1995; Tuin & Tels, 1990; McMahon, 2001; Bethke & Brady, 2000(b)) have raised concerns regarding the use of the partition coefficient.

1.2.7 Criticism of the Partition Coefficient (K_d) Approach

Many complex geochemical reactions govern sorption behaviour – these are outlined in Chapter 2. The K_d approach can work well for contaminants that sorb weakly to soil and aquifer solids, are present in low concentrations, and where pH and other chemical conditions vary little (Essington, 2004). However, these conditions may not apply to heavy metals, which sorb strongly and react to form various species and complexes (Baun & Christensen, 2004; Santos, et al., 2002; Tamunobereton-ari, et al., 2011). Also, pH and other conditions within a pollutant plume can fluctuate widely between pH 4.5 and 9 (Umar, et al., 2010; Christensen, et al., 2001; Abbas, et al., 2009; Bohdziewicz & Kwarciak, 2008; Tatsi & Zouboulis, 2002). When the K_d approach is used under these conditions, predictions of the movement of contaminants may well be in great error. For example, Bethke & Brady (2000(b)) found that during laboratory experiments on Cd-contaminated water in soil, a “tail” of Cd-contamination was present in the water during the flushing phase, which contradicted the predictions made by a K_d-based transport model, which had suggested a prompt recovery without tailing. More importantly, the concentrations in the flushing phase were higher than that allowed by drinking water regulations. Similarly, this would not have been predicted by the K_d-based transport model. This was suspected as being due to inadequate representation of the interactions between Cd and the soil surfaces. Other authors (Brusseau, 1994; Carriere, et al., 1995; Reed, et al., 1995; Selim, et al., 1992; Tuin & Tels, 1990) have suggested that factors such as bypassing of flow around portions of sediment; variations in kinetic rates between the sorption and desorption phases; and interactions with organic matter may also contribute to variability.

In a real investigation, the choice of remediation strategy may be incorrectly recommended by such disparities (Bethke & Brady, 2000(a)), consequently undermining the clean-up efforts and potentially putting public health at risk. There is therefore a strong case to develop a more realistic model of sorption.

1.2.8 The growing impetus to develop alternatives to the partition coefficient

Building on continued research into the factors associated with metal sorption in soils and rock surfaces, for example Ainsworth et al. (1994), Brown et al. (1998), Comans & Middleburg (1987), Glynn & Brown (1996), Jung & Thornton (1997), Kohler et al. (1996), Kuo et al. (2006), Liu et al. (2005), Markiewicz-Patkowska et al. (2005), Payne et al (1994), Stollenwerk (1995), Twardowska & Kyziol (2003), Wen et al. (1998), Zachara & Smith (1994) and others, efforts have progressed in building more sophisticated computer models, capitalising on the increased processing power available in recent years. Earlier transport codes (Cederberg, et al., 1985; Jennings, et al., 1982; Kent, et al., 1995) incorporated Langmuir and Freundlich representations of sorption; these in turn gave rise to codes such as HYDROGEOCHEM (Yeh & Tripathi, 1990), CHESS (van der Lee, 1997), and PHREEQC (Parkhurst & Appelo, 2015), which includes a surface complexation model based on hydrous ferric oxide (Dzombak & Morel, 1990); it is used in this project and described later. The confluence of more sophisticated models of metal-surface interactions and enhanced computer processing capability has boosted research in this area in a wide range of environmental applications

(Halim, et al., 2005; Hu & Dai, 2013; Randall, et al., 1999; Runkel, et al., 1999; Stollenwerk, 1994; Wang, et al., 1997).

1.3 Aim of the Project

This project seeks to determine the validity of the K_d approach for a continental red bed sandstone aquifer, the Permo-Triassic ("P-T") sandstone, an important aquifer in the United Kingdom (Allen, et al., 1997) and representing a common aquifer type worldwide. If it seems not to be valid, then a secondary aim is to suggest another way of quantifying sorption. It is hoped that the answers to these questions will thus lay the foundation for more accurate and realistic environmental assessments for this rock type.

This CASE (Collaborative Awards in Science and Engineering) project was a collaboration between the University of Birmingham and the environmental consultancy, Environmental Simulations International, Ltd (ESI Ltd). The project was jointly funded by the Natural Environment Research Council (NERC) and ESI Ltd.

1.4 Approach

1.4.1 Introduction

The main questions to answer for this project are:

- Is such a simple approach as K_d likely to give valid predictions, given the complexity of the sorption process?
- Is the K_d approach valid for describing metal uptake on P-T sandstone?

- If it is not valid, then is there a better way?

1.4.2 Project Outline

The project uses a combination of laboratory batch and geochemical modelling and is divided into four main stages: Stage 1, An assessment of sorption in sandstones using a surface complexation model; Stage 2, Laboratory testing of sandstone samples; Stage 3, The development of a revised model representation; and Stage 4, A revised theoretical assessment of sorption in sandstones.

Stage 1: An assessment of sorption in sandstones using a surface complexation model

A series of comparisons were undertaken of K_d-based predictions of metal mobility with predictions based on an existing surface complexation model. The computer code chosen was PHREEQC (Parkhurst & Appelo, 2015) (see Chapter 2).

Stage 2: Laboratory testing of sandstone samples

The standard surface complexation models have been developed using synthetic hydrous ferric oxide (HFO). In order to determine whether the surface complexation model adequately represents sorption on sandstone surfaces, this phase involved obtaining detailed information on the chemical behaviour of a rock system. Samples of sandstone from the UK Permo-Triassic sequence were used in a set of batch experiments to examine the sorption behaviour of a metal at a variety of concentrations and chemical conditions. The data obtained from these

experiments were then used to produce isotherms. The results of this work then drove the next stage of the project:

- If the isotherms were linear, then the priority in Stage 3 would be to quantify the contribution of the processes involved in order to:
    a. understand how the linear relationship is produced
    b. provide a means of predicting K_d values using process-based parameter values, not empirically, under the same conditions as the K_d values were derived.
- If the isotherms were not linear, then in Stage 3 it was important to:
    a. quantify the contribution of the processes involved, and
    b. to devise a method for predicting the isotherms, again using a process-based approach.

Experimentation on the sandstone was not straightforward because of the presence of several mineral phases. As a result, Stage 2 required the development of a new experimental approach to try and isolate sorption behaviour.

Stage 3: The development of a revised model representation

The chemical properties of the sandstone gathered from the laboratory experimentation were interpreted using PHREEQC with the aim of quantifying the processes involved, as outlined in Section 1.3.3.

Stage 4: A revised theoretical assessment of sorption in sandstones

In the final phase, the model developed in Stage 3 was incorporated in a solute transport model and used to examine the implications of the findings for predicting metal mobility in the field.

1.4.3 Choice of a Representative Metal

In order to research the answers to these questions, the project required a representative sandstone and metal. The sandstone sample chosen is described in Section 4.3.5.1.

The most commonly-found heavy metals in cases of land contamination include mercury, cadmium, zinc, copper, lead and chromium. These metals can pose significant health risks when they exceed certain concentrations in drinking water, such that guidelines regarding the maximum tolerable levels are published and regularly updated by the World Health Organisation (W.H.O., 2011). In weighing the requirements of this project against the potential risks to health during the laboratory phase of the project, zinc was chosen as it posed less of a risk. Zinc is an important groundwater pollutant in its own right, but in addition it has similarities in its chemistry to several other important metal pollutants, including cadmium, lead and copper. It is not a good analogue for a range of other metals (nor metalloids), including chromium.

1.5 Thesis Outline

This thesis has seven chapters.

This chapter has introduced the research project, providing some background to the field and explaining why the project was initiated, along with an overview of the approach.

A detailed explanation of sorption processes is given in Chapter 2, along with an overview of a theoretical model of surface complexation on hydrous ferric oxide (HFO), proposed by Dzombak and Morel (Dzombak & Morel, 1990). This is incorporated into the geochemical modelling software, PHREEQC, whose capabilities are utilized in initial scoping investigations.

Chapter 3 discusses the initial laboratory stage of the project: standard batch experiments providing data to produce sorption isotherms for Zn for the sandstone. The main aim of this work was to determine the likely form of the isotherms and whether, as expected from the surface complexation model, they were pH-dependent.

Chapter 4 is the main part of the laboratory stage, involving the development of the methods for isolating sorption reactions, and the use of these methods to explore Zn sorption behaviour on the sandstone, including how factors such as pH, time, and ionic strength affect the system. The results of the experiments are

interpreted where appropriate with the help of PHREEQC, and a set of pH-dependent isotherms produced.

The isotherms obtained from the laboratory work are used in Chapter 5 to develop a numerical model representation of the sorption of the sandstone.

In Chapter 6, the computer model is incorporated into a field-scale contaminant transport model which is then used to predict Zn movement in various scenarios.

Chapter 7 presents a summary of the project, the overall conclusions and implications for contaminant hydrogeological assessment of metal mobility, and suggestions for future work.

2 - A BRIEF INTRODUCTION TO SORPTION PROCESSES AND MODELS

2.1 Overview

This chapter provides an introductory guide to the theory used and developed later in the thesis. Part 1 presents the theoretical underpinnings of ion exchange and sorption processes, concluding with a summarised form of surface complexation theory. In Part 2, a brief account of the geochemical modelling software, PHREEQC - which numerically represents surface complexation theory - is given.

2.2 Part 1: Surface Complexation Theory

2.2.1 Introduction

As a dissolved contaminant migrates through an aquifer, a proportion of ions will become attached to the surfaces of the aquifer - this is called *partitioning*. *Sorption* is the umbrella term for three types of interaction of a dissolved chemical species (sorbate) with a surface (sorbent). Ions may also desorb from the surface into the aqueous phase (Environment Agency, 2013). The three types of interaction are (Appelo & Postma, 2007):

- *Adsorption* - which occurs where an ion binds to the surface of a sorbent;
- *Absorption* - which occurs where an ion is taken up within the sorbent; and

- *Ion exchange* - which occurs where an ion is electrostatically attached to a surface that may be external to the solid phase or internal (e.g. between the sheets of clay minerals).

This is summarised in Figure 2-1.

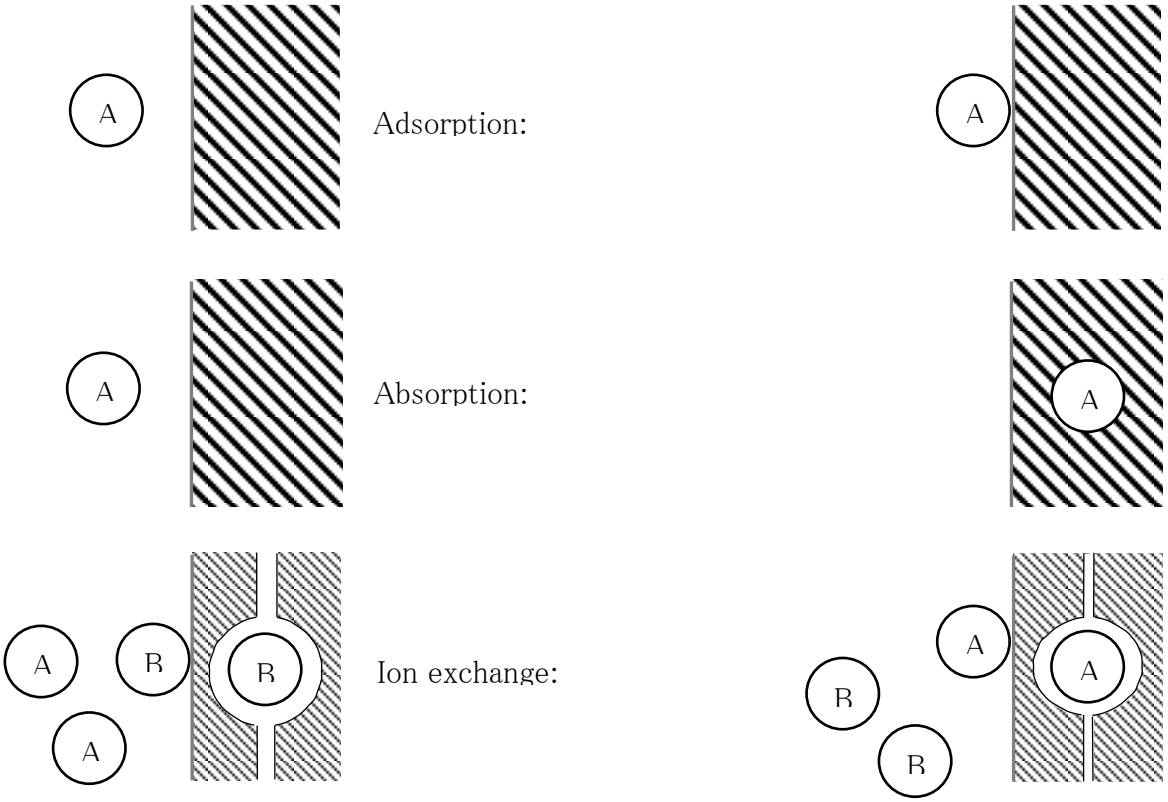

Figure 2-1: Summary of sorption processes (Appelo & Postma, 2007).

2.2.2 Definitions

For the purposes of this project:

- *Attachment* refers to the attachment of an ion to a surface by an unidentified process;

- *Sorption* refers to both adsorption and absorption (but usually adsorption), a process that involves bonding and an electrostatic component;
- *Ion exchange* refers to electrostatic attachment without bonding;
- *Sorber* or *sorbent* is a solid material that binds dissolved chemicals by means of sorption mechanisms;
- An *exchanger* is a solid material that interacts with dissolved chemicals by means of ion exchange mechanisms.
- *Sorbate* refers to a binding ion.

Here follows a brief overview of the current theory regarding the respective attachment mechanisms of ion exchange and sorption, to the level of detail required to understand this project. More detailed accounts may be accessed available via the citations provided.

2.2.3 Ion Exchange Process

Ion exchange involves the substitution of an existing ion within an exchanger for an incoming ion (or ions) that is electrostatically attracted to the exchanger. It generally occurs on clay mineral surfaces, involving small cationic species such as $\mathrm{Ca}^{2+}, \mathrm{Na}^{+}, \mathrm{NH}_4^{+}, \mathrm{Sr}^{2+}, \mathrm{Mg}^{2+}$ and K^{+}.

The cause of the electrostatic attraction is the existence of a permanent charge on the clay surfaces. This charge imbalance is an inherent feature of the mineral lattice, and is therefore primarily contingent upon the type of clay, owing little consequence to the environmental conditions in which the clay resides (Hellferich,

1995; Troeh & Thompson, 2005; Essington, 2004). However, there is a potential for exchange or sorption to occur on clay sheet edges, and this may be a pH-dependent mechanism: it is usually assumed to be a minor component of the total cation exchange capacity of a clay.

A potential difference results from the disparity between the negatively-charged clay surface and the surrounding bulk solution. This gives rise to a *solid-solution interface* – a transitional zone that is neither mineral nor bulk solution. It is in this region that the flux of ions between the bulk solution and the exchanger occurs.

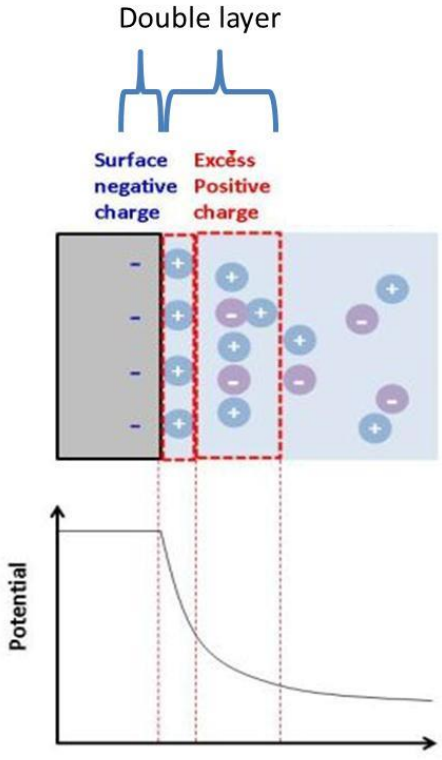

Figure 2-2: The electric double layer in proximity to a clay surface (modified after Hara (2013))

The action of electrostatic forces attracts cations ('counter ions') and repels anions ('co-ions') from the bulk solution toward / away from the clay surface. This trend is countered by an opposing diffusion force, moving some cations away from the surface. This eventually results in the formation of a diffuse layer (the Gouy layer) of cations (Figure 2-2) in the vicinity of the surface which together with the surface's negative charge form the double layer (the Gouy-Chapman double layer model). A fuller description recognises the presence of an entirely positive layer of cations bound to the surface, the Stern layer, thus forming a triple layer model (Essington, 2004). The diffuse layer becomes an increasingly-balanced mixture of cations and anions with distance from the surface, with the potential also decreasing away from the surface of the mineral.

2.2.4 Ion Binding

Upon reaching the surface, exchangeable cations are held to it by 'outer-sphere complexation' (Hellferich, 1995; Hubbard, 2002; Kirk, 2004; Essington, 2004). This means that there is at least one water molecule between the exchanger surface and the attached species. It is a non-specific, weak bond, attained by electrostatic attraction. (This is in contrast to the comparatively strong, inner-sphere complexes formed by adsorption, described later.) Coulomb's law describes the retention of these cations (Equation 2-1):

$$F = \frac{q_+ q_-}{\varepsilon r^2}$$

Equation 2-1

where F is the force of attraction between opposing charges;

- q_+ and q_- are charges;

- r is the separation distance; and
- ε is a dielectric constant of water.

Thus, for a given exchangeable ion, its effective size and valence will determine how strongly and where on the surface it will exchange. This means that, for increasing valence:

- the force of attraction on the ion toward the surface increases; and therefore
- the selectivity of the surface for the ion increases.

A further implication of Coulomb's law is that, for a given valence, the hydrated radius of the ion influences exchangeability: F increases as the hydrated radius (r) of an exchangeable cation decreases. Therefore, in exchange reactions involving two ions of the same valence, ions with a smaller hydrated radius will be preferentially exchanged (Pauley, 1953). Generally, ion exchange reactions involve small cationic species, such as Ca^{2+}, Na^{+}, NH_4^{+}, Sr^{2+}, and Al^{3+}.

2.2.5 Cation Exchange Capacity

There is limit to the number of cations that a mineral can accommodate (Hellferich, 1995; Essington, 2004). This is called the 'Cation Exchange Capacity' (CEC). More strictly, it is defined as the moles of adsorbed cation charge that can be displaced by an index ion per unit mass of solid, and can be expressed in units of meq / 100 g. Like surface charge, it is an inherent feature of the mineral surface and often assumed unlikely to alter significantly.

2.2.6 Quantification of Ion Exchange: Models

Ion exchange models take account of all ions involved in the reaction: the incoming exchangeable cations, and the ions relinquishing their positions on the exchanger. (In contrast to this, comparative models for sorption focus on only one chemical, explained later.) The general binary reaction for cation exchange (Equation 2-2) attempts to describe how ions I_i and I_j are distributed between the exchanger and the solution (Bond, 1995).

$$z_j I_i^{z_i+}(aq) + z_i I_j^{z_j+}(exch) = z_i I_j^{z_j+}(aq) + z_j I_i^{z_i+}(exch)$$

Equation 2-2

where:

- I_i and I_j are exchangeable cations on the exchanger and in solution, respectively;
- z_i and z_j are the valences of cations I_i and I_j; and
- (exch) and (aq) are the exchanger and solution phases, respectively.

Generally, there is not an equal distribution of counter-ions between the solid and dissolved phases at equilibrium; instead, certain ions are preferentially exchanged. This attribute is called ‘selectivity’, and is defined in terms of the selectivity coefficient (Equation 2-3) (Bond, 1995):

$$K_{ij} = \frac{\alpha_i^{z_j} A_j^{z_i}}{\alpha_j^{z_i} A_i^{z_j}}$$

Equation 2-3

where:

- K_{ij} is the thermodynamic equilibrium constant;
- α_i and α_j are the activity of cations I_i and I_j in the exchanger phase; and
- A_i and A_j are the activity of cations I_i and I_j in the solution phase.

Given that most exchangers are non-ideal, the variation in this constant reflects the differing selectivity of the surface for different chemicals under different conditions (e.g. attached ion population composition).

When considering solution phases, the activity of the chemicals must be related to the molar concentration of the solution. This is achieved using the activity coefficient λ, which may be calculated by the Davies or extended Debye-Hückel equation (Appelo & Postma, 2007).

Synthesis of the components of the ion exchange process into a summary cation exchange reaction may be achieved by way of the Gaines-Thomas Convention (Essington, 2004). This model assumes that the solid phase activities are equal to equivalent fractions, defined as (Equation 2-4):

$$\{\beta_i\} = \frac{\mathrm{meqI}}{\sum_{I,\,J,\,K,\ldots} \mathrm{meqI}} = \frac{\mathrm{meqI}}{\mathrm{CEC}}$$

Equation 2-4

where:

- I, J, K… are exchangeable cations with charges z_i, z_j, z_k…;
- meq I indicates the milliequivalents of cation I.

As described above, and allows for calculation of (the Gaines-Thomas) selectivity coefficient, K_{ij}, as given by equation (Equation 2-5).

$$K_{ij} = \frac{\{\beta_I\}^{z_j}\left(A_j\right)^{z_i}}{\{\beta_J\}^{z_i}(A_i)^{z_j}}$$

Equation 2-5

where:

- A_i and A_j represent the activities of I_i and I_j in the solution;
- $\{\beta_i\}$ and $\{\beta_j\}$ are the equivalent fractions of cation I_i and I_j on the exchanger X, and z_i and z_j are the valences of cation I_i and I_j.

Other models include the Vanselow convention (Vanselow, 1932), the Gapon convention (Gapon, 1933) and the Rothmund-Kornfeld convention (Rothmund & Kornfeld, 1919), but this project has assumed the Gaines-Thomas convention in the modelling, described later.

2.2.7 Surface Complexation

Like ion exchange, sorption also involves a solid phase and a liquid phase containing a species to be sorbed. Taking the example of hydrous ferric oxide (HFO), cations form surface complexes by way of bonds with surface oxygen atoms (Dzombak & Morel, 1990). This can be summarised (Equation 2-6), very briefly, as:

$$\equiv \mathrm{XO^-} + \mathrm{H^+} = \equiv \mathrm{XOH^0}$$

$$\equiv \mathrm{XOH^o} + \mathrm{H^+} = \equiv \mathrm{XOH_2^+}$$

$$\equiv \mathrm{XOH^o} + \mathrm{M^{2+}} = \equiv \mathrm{XOM^+} + \mathrm{H^+}$$

Equation 2-6

where:

- ≡ indicates a bond to the solid lattice;
- X is a metal species (in the case of HFO, FeIII); and
- M is a cation.

Note that there are also other possible interactions between cations and anions and the surface complexes as suggested by Dzombak and Morel (1990). The hydroxyl groups, able to bond and dissociate protons, are thus highly sensitive to the pH of the surrounding environment.

Dzombak and Morel (1990) developed a consistent generalised double layer complexation model theory for HFO based on Equation *2-6* and including sorbed ion effects on surface potentials. In their model, the equilibrium constants are calculated using equations of the form (Equation 2-7):

$$\mathrm{K}= \frac{(\equiv XOM^{+})(H^{+})}{(\equiv \mathrm{XOH^{o}})(\mathrm{M^{2+}})} \exp\left[-\frac{F\psi}{RT}\right]$$

Equation 2-7

where the final term takes account of the energy required to move an ion away from the surface against electrostatic attraction, and where

- F is the Faraday constant (C/mol)
- ψ is the surface potential (V)
- R is the gas constant (J/mol/K)
- T is the temperature (K).

They tested their model against published experimental data for a wide range of cations and anions. They found that it was necessary to involve two site types to represent cation sorption, possibly because sorption density is not proportional to dissolved concentration. The two site types were named “high affinity” (or type 1, or strong) and “low affinity” (or type 2, or weak). These are differentiated using a superscript “s” and “w” notation (Dzombak & Morel, 1990).

The process of adsorption continues until an equilibrium is established between the solid and liquid phases. It is a reversible process.

2.2.8 Semi-Empirical Sorption Isotherm Models

2.2.8.1 Introduction

An “isotherm” is the relationship between dissolved and sorbed concentrations in a particular water/solid system. There are several isotherm models that are

commonly used as they fit a variety of experimentally-determined isotherms. Some of these (e.g. the Langmuir isotherm) can be derived using simple assumptions as to the nature of the partitioning (e.g. sorption being dependent on sorbed concentration). These models have found favour in applications as they are in general simply applied, but in the context of predicting metal movement in groundwaters have also been criticised for giving misleading results (Bethke & Brady, 2000(b)). Though all the models described in this section (linear, Langmuir, and Freundlich) have been applied to predict contaminant movement in groundwaters, the linear model has been most commonly applied.

2.2.8.2 Linear Isotherm Model (the "K_d" model)

The linear isotherm is defined by Equation 2-8:

$$C^* = K_d C$$

Equation 2-8

where:

- K_d is the partition coefficient (l/kg);
- C^* is the mass of solute sorbed per dry unit weight of solid (mg/kg); and
- C is the concentration of solute in solution in equilibrium with the mass of solute sorbed onto the solid (mg/l).

The following caveats apply to the linear isotherm model:

- It assumes infinite sorption capacity. This is unrealistic (Erskine, 2000; Mostbauer, 2003), as solids have a limited number of sites that can sorb cations.

- Due to the issue above, the linear model is best suited to situations where there is a low solute concentration that can be assumed to be far below the maximum sorption capacity of the solid.
- At solute concentrations anticipated to be much higher, then a non-linear sorption model (see below) should be used.
- Values for the model are derived under controlled conditions (usually in a laboratory). This means that the data available for K_d values are strictly only applicable for the same conditions under which the values were obtained. It ignores speciation, pH, competing ions, etc.

2.2.8.3 Langmuir Isotherm Model

The Langmuir model is described by Equation 2-9:

$$C^* = \beta \frac{\alpha C}{1 + \alpha C}$$

Equation 2-9

where:

- α is the partition coefficient (l/mg);
- β is the maximum amount of solid that can be sorbed by the solid (mg/kg);
- C^* is the mass of solute sorbed per dry unit weight of solid (mg/kg); and
- C is the concentration of solute in equilibrium with the mass of solute sorbed onto the solid (mg/l).

The Langmuir isotherm model offers an improvement over the linear type in that it assumes that the sorption capacity of the rock is finite, due to a limited number of sorption sites. At equilibrium between the sorbed and dissolved phases of the

solute, it is assumed that a fraction C* / β of the site is occupied, and a fraction 1-C* / β is not occupied. However, it still ignores other factors such as pH, speciation, competing ions, and other factors.

2.2.8.4 Freundlich Isotherm Model

The Freundlich isotherm model is described by Equation 2-10:

$$C^{*}=K_{f}C^{N}$$

Equation 2-10

where:

- K_f and N are empirical constants;
- C^* is the mass of solute sorbed per dry unit weight of solid (mg/kg); and
- C is the concentration of solute in solution in equilibrium with the mass of solute sorbed onto the solid (mg/l).

The Freundlich model affords *some* scope for variable exchanger properties, by way of K_f and N. However, like the linear model, which is a special case of the Freundlich isotherm, it does not provide a limit for sorption capacity.

The limitations of these four models have already been noted. When they are used in predicting the fate of metals in groundwater contamination incidents, they are likely to give misleading results (Bethke & Brady, 2000(b)). It is possible, however, to use a much better representation of the processes taking place by appealing to geochemical modelling software.

2.3 Part 2: Geochemical Modelling Software

2.3.1 Choice of Modelling Software

Out of the geochemical computer codes available (e.g. MICROQL, MINTEQA2, PHREEQC), PHREEQC was chosen because of its robust treatment of surface complexation, its ability to simulate solute transport and the fact that it is the most commonly used geochemical modelling code in groundwater research and application.

2.3.2 Introduction to PHREEQC

PHREEQC is a general-purpose geochemical computer program (Parkhurst & Appelo, 1999). It has the ability to perform a wide range of low-temperature aqueous geochemistry calculations. Of particular interest here is its incorporation of Dzombak and Morel's (1990) surface complexation theory, which has been summarised into sets of simultaneous equations that PHREEQC then solves. It is beyond the scope of this chapter to give a detailed account of the numerical representation, but full details are available in the User's Guide (Parkhurst & Appelo, 1999). Essentially, for a given simulation, PHREEQC solves the mass action and mass balance equations accounting for surface reactions, using iterative processes until convergence is obtained. The representation in PHREEQC is not an identical formulation to that used by Dzombak and Morel (1990), but the differences are mainly of importance in the case where multi-dentate attachment occurs, a type of attachment not considered by Dzombak and Morel (1990). Likewise, the calculated concentrations of ions in the diffuse layer

are approximate because of the way that PHREEQC deals with charge imbalance between solution and surface (Parkhurst and Appelo, 1999).

2.3.3 Modelling Process

The user creates an input file for each simulation. Using data blocks, various parameters may be specified; examples of such input files may be found in the User's Guide (Parkhurst & Appelo, 1999) and in Chapters 3 and 5 of this thesis. Data for individual chemicals and other aspects may be found in the extensive databases provided, or they may be specified by the user.

In the case of the sorption processes simulated in this project, once the surface and exchange properties have been specified and the simulation initiated, PHREEQC "speciates" the HFO surface and determines the "surface species" iteratively by either modifying the surface concentrations in the presence of a fixed aqueous composition, or by adjusting both the surface and aqueous compositions.

PHREEQC can provide a range of output data, such as the final solution composition, the surface composition, the composition of weak and strong sites, the pH, and other aspects. The output is "raw" and must be processed using appropriate software (e.g. Excel) in order to produce useful data.

2.4 Summary

This chapter has provided a brief overview of the relevant theory regarding surface complexation, followed by a brief account of the geochemical modelling software employed in this project. Further details will be provided as these two aspects are used in the study.

3 - INITIAL INVESTIGATIONS OF SORPTION THEORY REGARDING METAL MOBILITY IN GROUNDWATER

3.1 Overview

After an introduction to this stage of the project, there is a series of comparisons of computer simulations using PHREEQC that begin to explore the differences of using the surface complexation approach rather than the K_d method. The implications of these differences will then be discussed.

3.2 Introduction

This chapter is primarily concerned with using the surface complexation theory as presented by Dzombak and Morel (Dzombak & Morel, 1990). As described in Chapter 2, the geochemical computer code, PHREEQC, embodies this theory, and it is therefore able to simulate surface reactions. Here, a number of initial investigations were undertaken using PHREEQC to begin to understand the effects that materials represented by hydrous ferric oxide (HFO) might have on metal mobility in groundwaters.

In light of the theory presented in Chapter 2, the purpose of the investigations here is to try to answer the following question:

- If a given medium possessed the ('perfect') characteristics assumed by the Dzombak and Morel theory, what effect would this have on sorbing pollutants?

A concise suite of simulations was designed by which to explore some of the implications of the Dzombak and Morel theory. The outcomes of these were designed to inform two possible paths of action thereafter:

I. If the model made similar predictions to K_d, or were otherwise very simple and predictable, then the investigation could conclude at that point.

II. If the model indicated there was some complexity in the system not accounted by K_d and not readily predictable, then this would prompt a more thorough investigation. It would also demand scrutiny of the implications of the K_d approach.

As highlighted in Chapter 2, major deficiencies in the K_d approach relate to its disregard of, amongst many other factors:

- any ions apart from the one it attempts to quantify;
- the pH;
- the nature of the surface.

In contrast to this, PHREEQC permits full account of all of these factors (as far as its databases allow), and so allowing a wider consideration of the effects of the "whole" chemistry of the system.

3.3 Approach and Methods

3.3.1 Introduction

In order to begin to ascertain the main variables affecting sorption of heavy metals to HFO, according to Dzombak and Morel (1990), a sequence of models were designed that increase in complexity until they begin to represent the complexity of the real system, examining, in turn, factors expected to influence sorption: pH, ionic strength, other competing ions, and HFO properties.

Initially, cadmium was chosen as a representative heavy metal, since there is a lot of existing data on cadmium with which to compare. (It should be noted that safety considerations prompted the use of Zn, as opposed to Cd, in the laboratory experiments and in subsequent stages. This is explained in Chapter 4.)

The main suite of models used the batch simulation capability of PHREEQC. In these, one could liken the simulation to a laboratory experiment consisting of an enclosed vessel with a mass of HFO mixed with a solution, and allowed to reach equilibrium. (The laboratory method it replicates is described in detail in Chapter 4.) This is helpful, because it allows direct comparison with the laboratory experiments undertaken later in the project. Some tentative transport models were also undertaken.

A sample of the code used for these experiments is given in Appendix 9.1, and some points to note are now described.

3.3.2 Numerical Experiment Design

Table 3-1 shows the generic data block for the solution composition. This was repeated six times, with the Cd concentration increasing through the range of: 0, 0.05, 0.1, 0.15, 0.2, 0.25 mg/l.

Table 3-1: Solution composition specification

```
SOLUTION 1
        Temp        25
        pH          3
        pe          4
        redox       pe
        units       ppm
        density             1
        Cd          0.0
        -water      0.1 # kg
```

Table 3-2 shows the generic data block for the specification of the surface properties for the sorption sites. It is divided into properties for the weak and strong sites, and takes results from Dzombak and Morel (1990). These remained the same through the whole simulation. The initial surfaces have been assumed to be protonated.

Table 3-2: Surface specification data block [in contact with 0.1 kg water (continued from Table 3.1)]

```
SURFACE 1
        Hfo_sOH  0.000055          600     1
#‘strong’ sites, protonated        moles of site          specific surface area (m2/g)    mass of
HFO (g)
        Hfo_wOH  0.0022
#’weak’ sites    moles of site {surface area and mass already defined in previous line}
```

Table 3-3 shows the arbitrary filename and also the quantities chosen to write to the output file. In this case, it was decided to look at the molalities of Cd^{2+} ion, and the Cd^{+} ions complexed with the weak and strong sites, respectively.

Table 3-3: Output data selection

```
SELECTED_OUTPUT
        -file [filename].sel
        -molalities     Cd+2    Hfo_wOCd+       Hfo_sOCd+
```

The output data were then used to plot isotherms and to investigate pH relationships, together with the composition of the weak and strong sites.

3.3.3 Batch Simulations

3.3.3.1 System 1: H_2O – Cd – HFO; fixed pH

The first sets of simulations were intended to show the sorption behaviour of Cd on HFO, using only pure water. Of particular interest were investigations into the effects of pH and initial Cd solution concentration. PHREEQC runs the simulations as though they were taking place in a laboratory, so that one could imagine a set of beakers with 1g of HFO and 100ml of Cd solution, at concentrations of 0, 0.1, 0.15, 0.2, and 0.25 mg/l. This range was chosen since it encompasses the likely (and permitted) range of concentrations found in aquifers. For each set of six concentrations, the pH was fixed at 1, 3, 5, 7, 9, 11, and 13. Although in reality outside extreme pollution cases, only pH 4-9 is the likely range to be measured, it was decided to cover a larger range in order to investigate more fully the sorption behaviour. In this first model, the pH was fixed throughout the sorption process by addition of HCl or NaOH, depending on the value required. This fix was applied because, as described in later models, pH tends to vary during the sorption behaviour, equilibrating in parallel with sorption, and the aim of this model was to look at the effects of initial dissolved concentration of cadmium. In real life, this fix would represent buffering of pH by other ions, such as carbonates. The results of the numerical experiment are shown in Figure 3-1 to Figure 3-4.

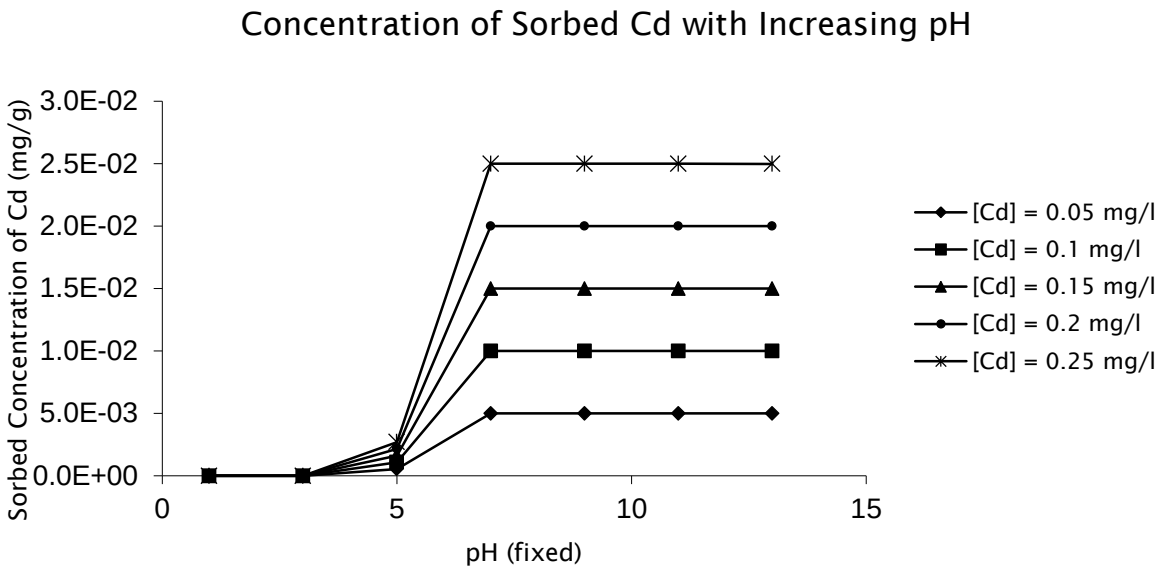

Figure 3-1: Predicted relationship between Cd sorption on HFO and pH. (Pure water, pH fixed.)

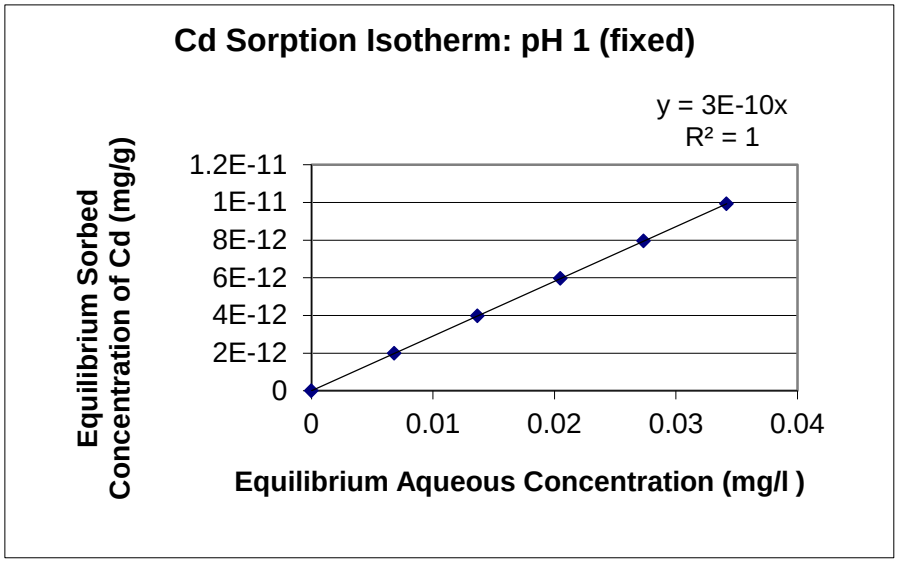

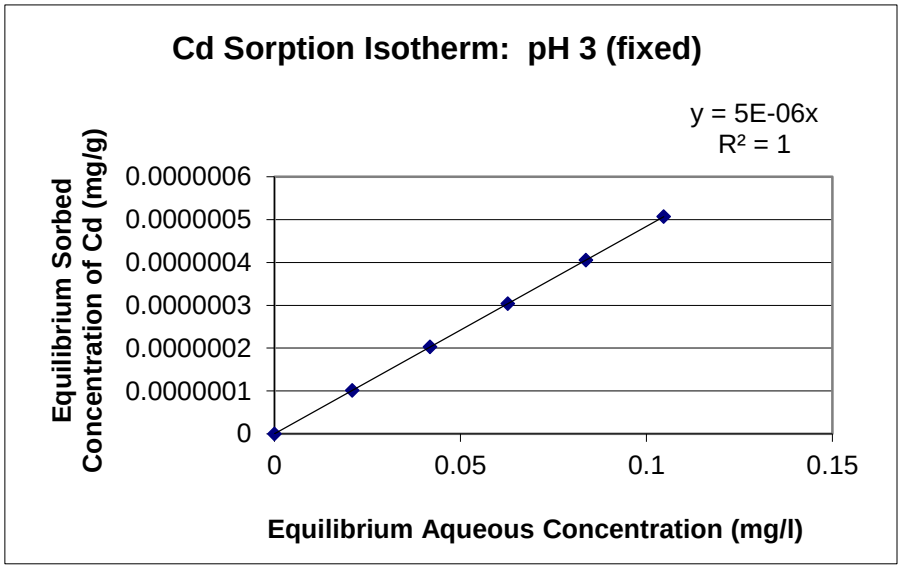

Figure 3-2: Cd sorption isotherms, pH 1 and pH 3. Note that the sorbed concentrations are effectively zero until the pH rises above about 5

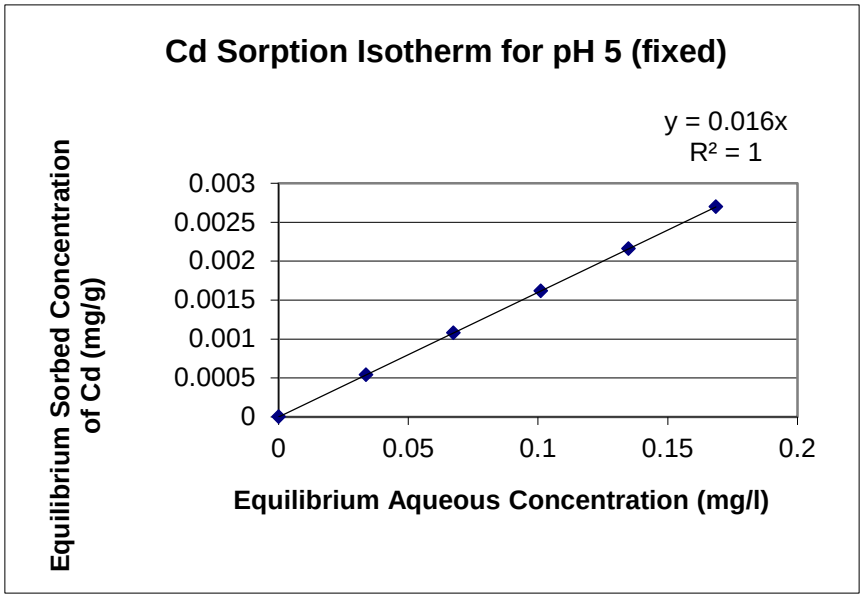

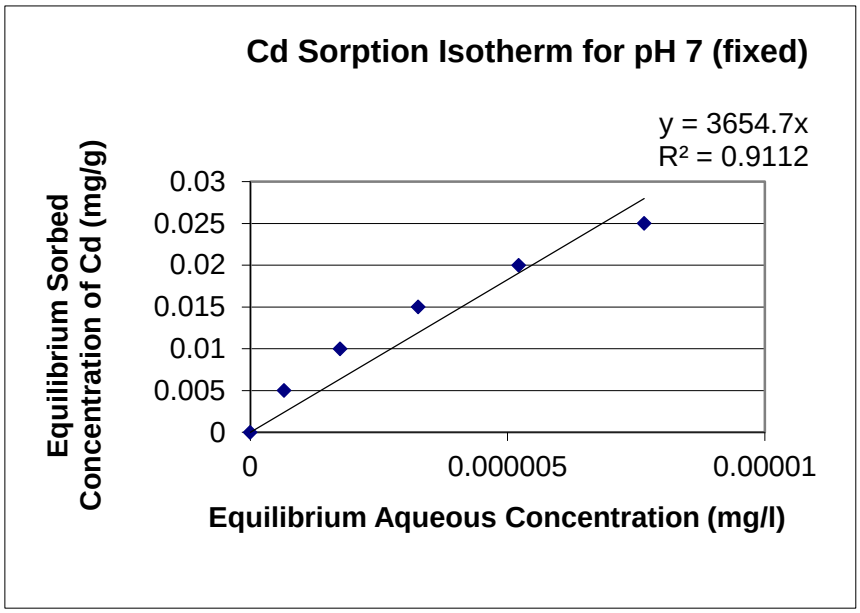

Figure 3-3: Cd sorption isotherms, pH 5 and pH 7. Note that the aqueous concentrations for pH = 7 and higher are effectively zero, and are just included here for completeness

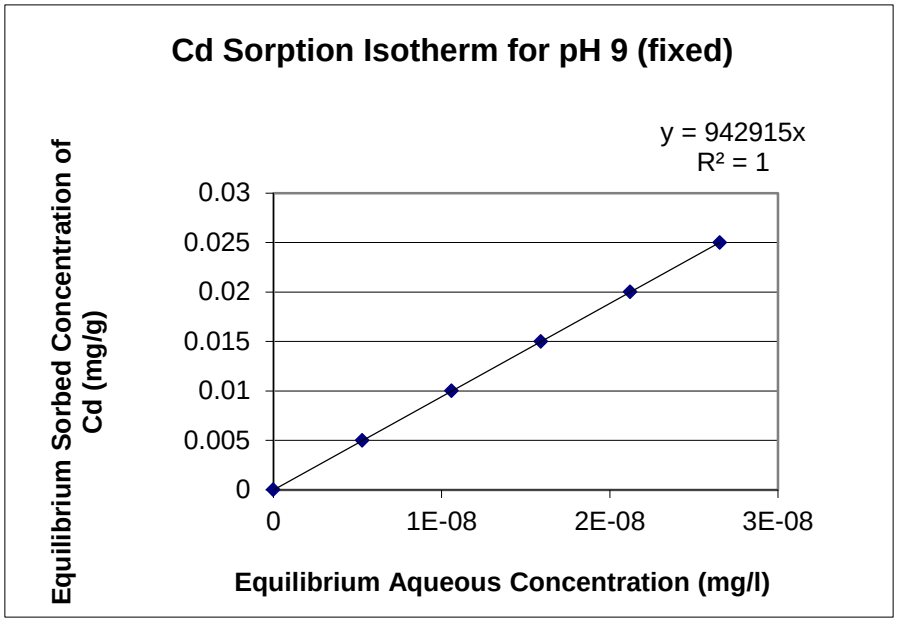

Figure 3-4: Cd sorption isotherms, pH 9

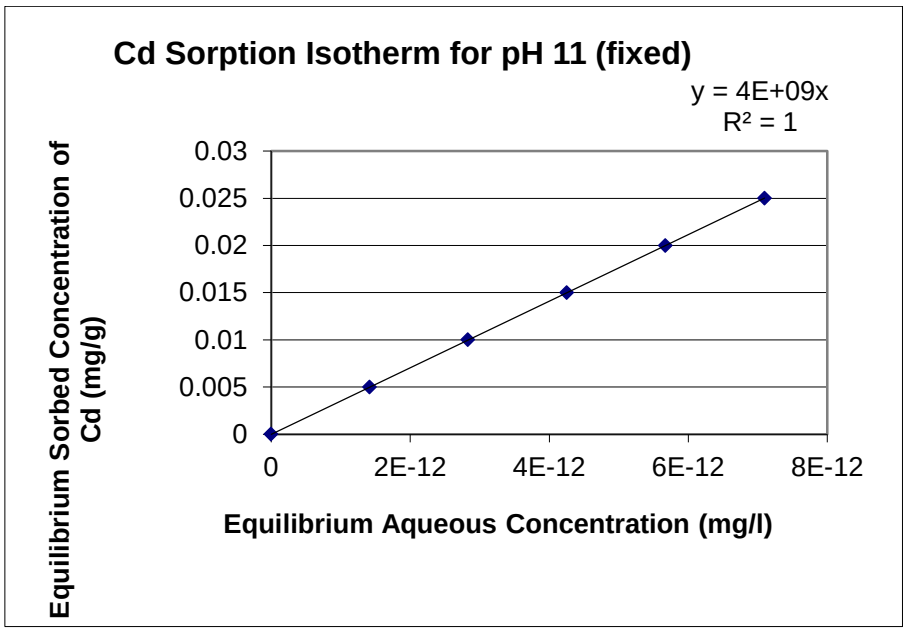

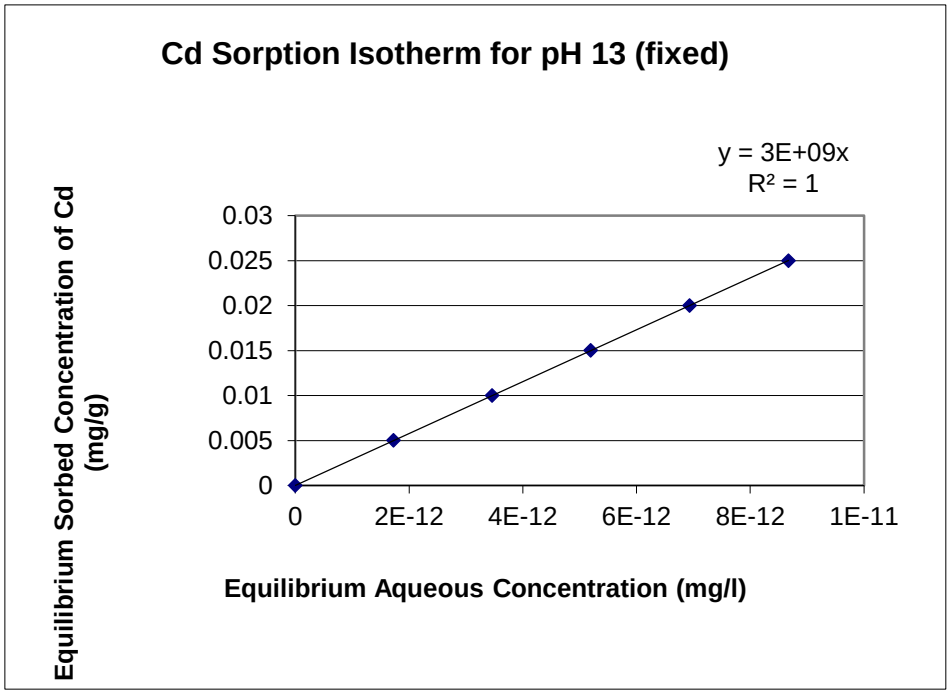

Figure 3-5: Cd sorption isotherms, pH 11 and pH 13

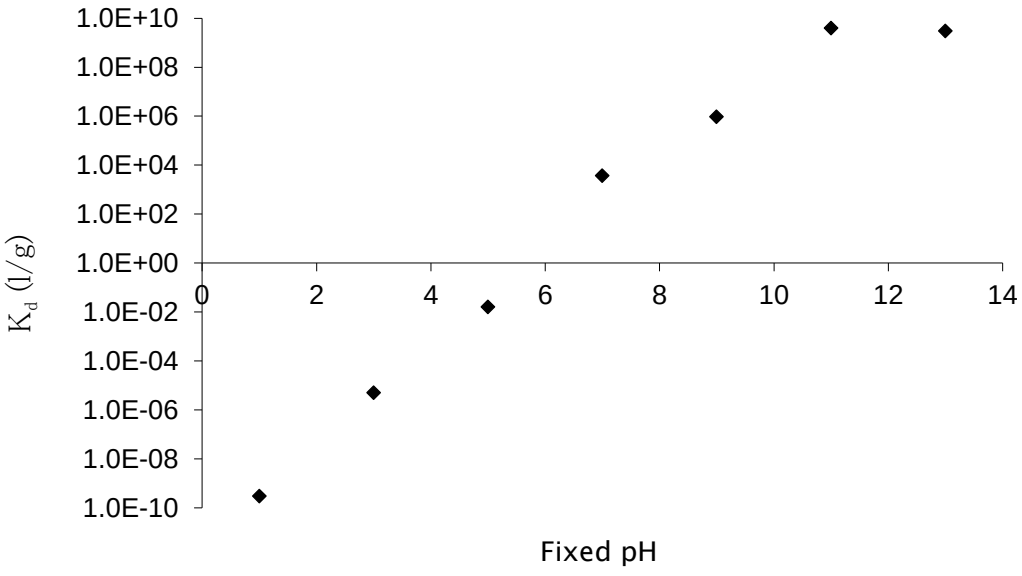

Figure 3-6: Predicted 'K_d' / pH relationship (log 'K_d') for sorption of Cd onto HFO in pure water, where pH was externally fixed. Since the sorbed concentration / dissolved concentration relationship is not exactly linear, it cannot strictly be called K_d, hence 'K_d' until an alternative notation is decided upon.

Figure 3-1 clearly shows that pH is a strong control on sorption, and agrees with pH-related behaviour for cadmium observed by Dzombak and Morel (1990). According to surface complexation theory, cations sorb onto HFO by bonding with surface oxygen atoms, with a concurrent release of protons. This reaction is represented by Equation 3-1:

$$\equiv \mathrm{XOH}^{\circ} + \mathrm{M}^{2+} = \equiv \mathrm{XOM}^{+} + \mathrm{H}^{+}$$

Equation 3-1

where M^{2+} represents a divalent cation – in this case, cadmium. However, at low pH, H^{+} 'sorption' out-competes M^{2+} sorption and the dominant reaction is (Equation 3-2):

$$\equiv \mathrm{XOH}^{\circ} + \mathrm{H}^{+} = \equiv \mathrm{XOH}_{2}^{+}$$

Equation 3-2

The influence of pH on cation sorption can be explained by considering that the reactive surface sites are hydroxyl groups, which can coordinate and dissociate protons.

Another way of considering this is using the point of zero charge (PZC) concept: at low pHs, the HFO surface is positively charged ($\equiv \mathrm{XOH}_{2}^{+}$) and hence cation sorption (e.g. Cd^{2+}) does not occur. At pHs greater than the PZC, the dominant

surface species can be considered to be $\equiv XO^-$ and hence Cd^{2+} sorption is very likely.

Figures 3-2 to 3-5 show that the K_d concept is broadly valid in this system in that, although their slopes vary with pH, isotherms are linear. In the mid-range pHs, there is some evidence of non-linearity, but only at concentrations that are effectively zero.

On the basis of the results from Figures 3-2, 3-3 and 3-4 show the variation of K_d with pH; as expected from Figure 3-1, K_d ranges from extremely small, where there is no effective sorption, to extremely large, where sorption is effectively 100 %. The change occurs over an interval in log (K_d) is linear in pH (the odd result for a pH of 13 may be a numerical issue, but has not been explored).

According to surface complexation theory, it is necessary to use two site types to model cation sorption. This effect is illustrated in Figure 3-7. In the case shown, the concentrations on the weak sites are far less than on the strong sites.

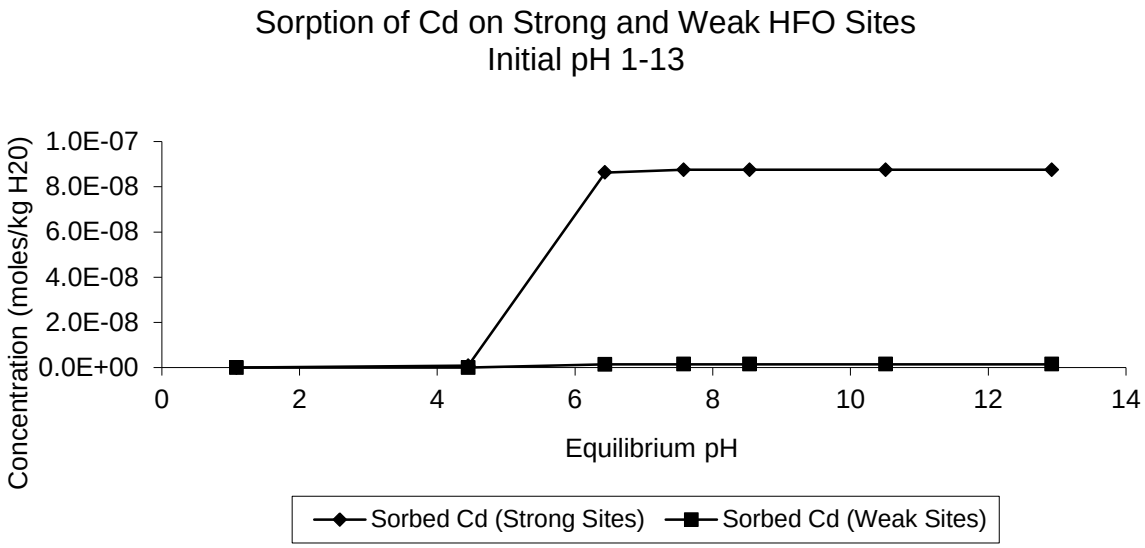

Figure 3-7: Pattern of Cd sorption onto weak and strong sites on HFO, related to increasing equilibrium pH. (Pure water; [Cd]i = 0.1 mg/l)

Figure 3-8 shows how the two site types vary in their in sorption behaviour as the pH changes in the H_2O-Cd-HFO system. Comparison of Figure 3-7 and Figure 3-8 indicates that Cd is mostly present on the strong sites, and H+ dominates on the weak sites.

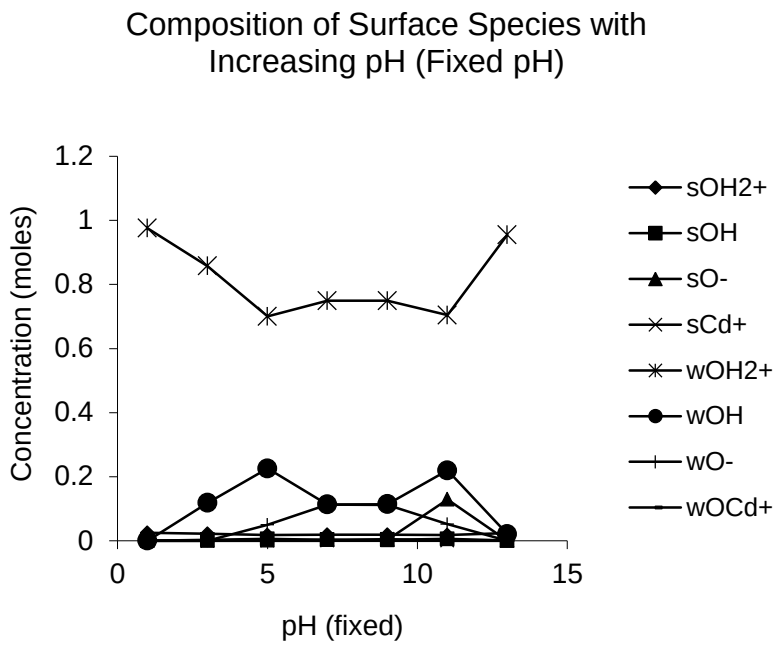

Figure 3-8: The variation of species on the HFO surfaces with pH in the system H_2O-Cd-HFO, with initial [Cd] of 0.1 mg/l.

3.3.3.2 System 2: Groundwater – Cd – HFO; fixed pH

System 1 is simplistic in that it only considers Cd sorption in pure water. System 2 was therefore devised to investigate sorption behaviour in a groundwater composition taken from real data. This adds complexity due to increased ionic strength, and competition between cations for sites on the HFO surfaces. The simulations here were run exactly the same as for System 1, except for the composition of the water.

The groundwater composition is given in Table 3-4, which is based on the composition observed in boreholes at Haydock Park (Tellam, 2013). The Cd concentrations were as for the numerical experiments in System 1.

Table 3-4: Groundwater composition in System 2 experiments

Species	Concentration (mg/l)
Cl	54.4
SO_4	151.3
NO_3	33.4
Ca	97.3
Mg	33.1
Na	32.3
K	4.9
Fe	0.03
Zn	0.11
Mn	0.02
Cu	0.1
Pb	0.2
Ba	0.1
Si	5.7

Figures 3-9 to 3-14 show the results of the numerical experiments, and correspond to Figures 3-1 to 3-4 for System 1. No carbonate species were included in order to reduce the complexity of the pH buffering at high pH, though carbonate (calcite and otavite ($CdCO_3$) for example) could have been suppressed in the model.

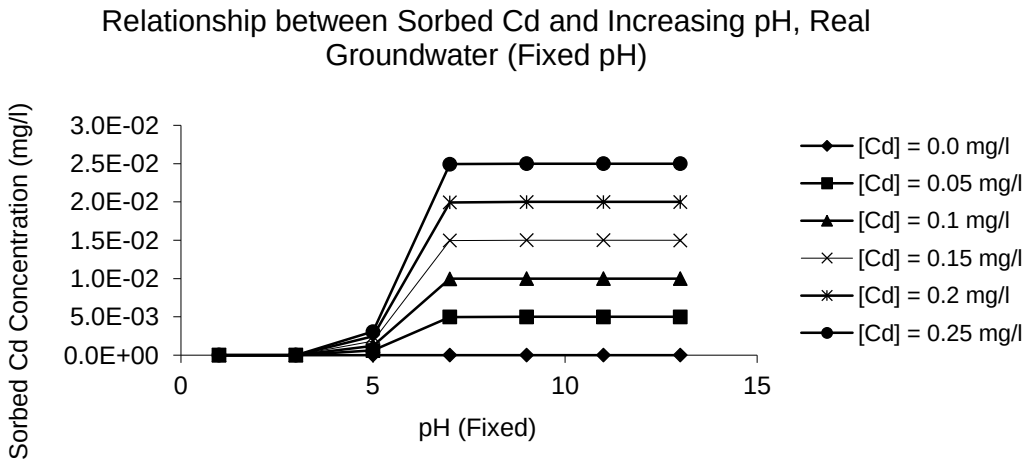

Figure 3-9: Relationship between Sorbed Cd and Increasing pH, Real Groundwater (Fixed PH)

Figure 3-9 gives exactly the same result as Figure 3-1, again showing that pH exerts a strong influence on K_d, for the reasons given for Figure 3-1, and that the presence of the other constituents of the groundwater have no significant effect.

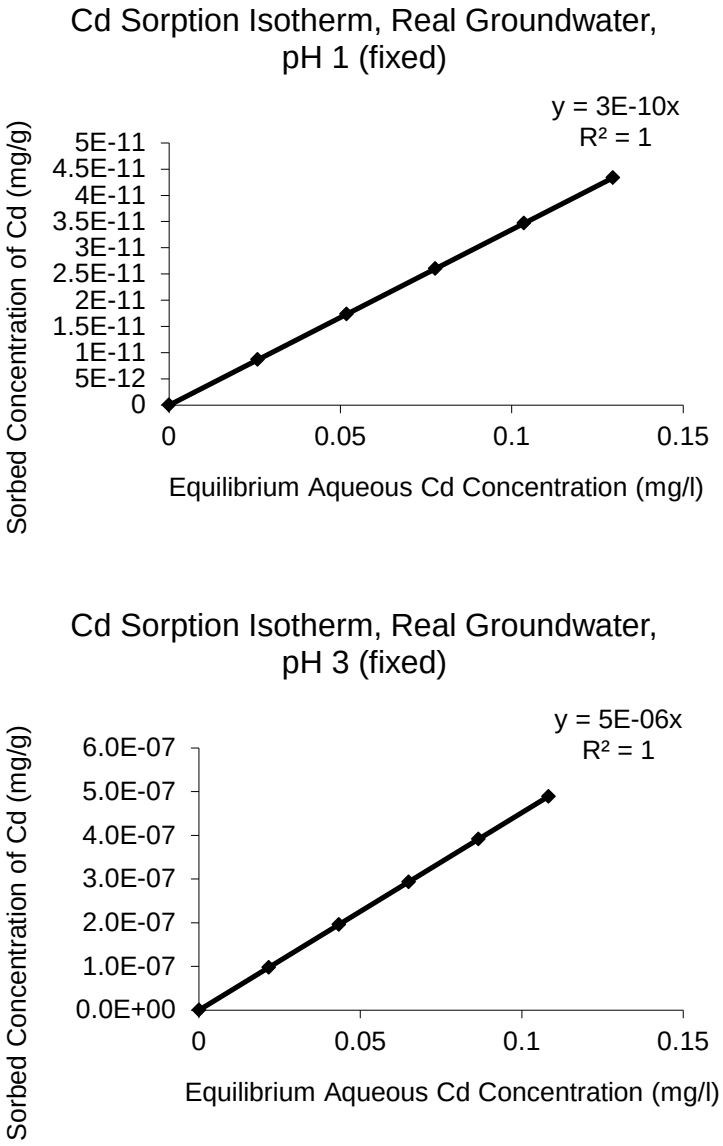

Figure 3-10: Cd Sorption Isotherms, Real Groundwater, pH 1 and pH 3 (Fixed pH). Note that the sorbed concentrations are effectively zero until the pH reaches about 5

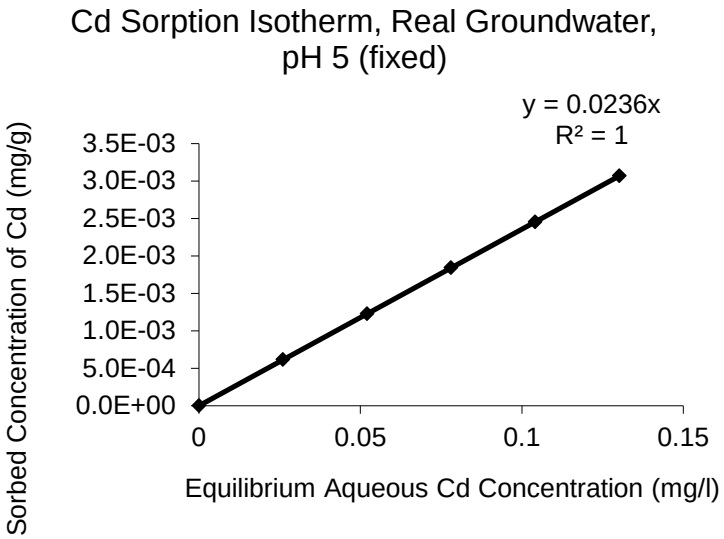

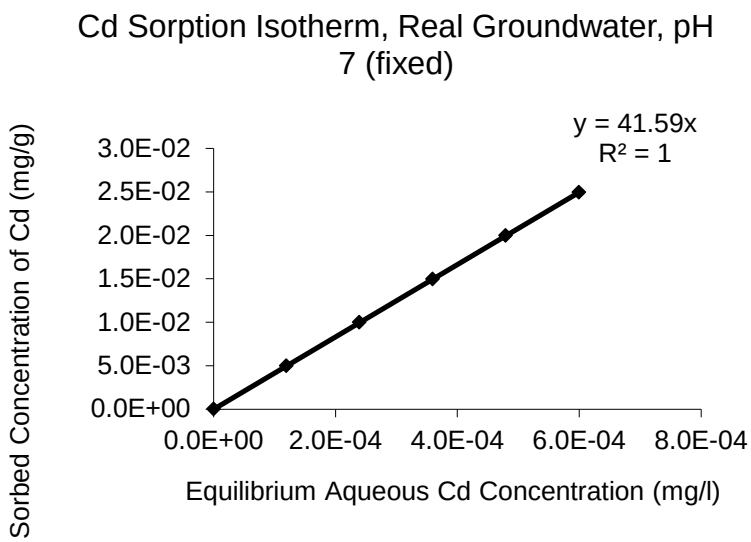

Figure 3-11: Cd Sorption Isotherms, Real Groundwater, pH 5 and pH 7 (Fixed pH). Note that the dissolved concentrations are effectively zero about a pH of about 7

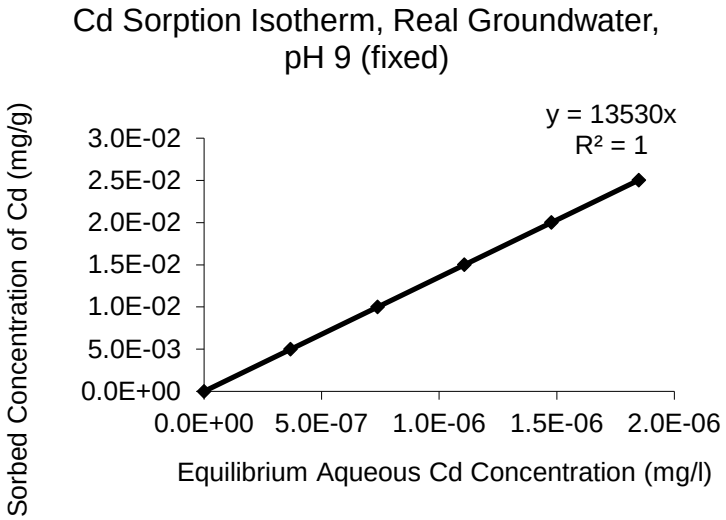

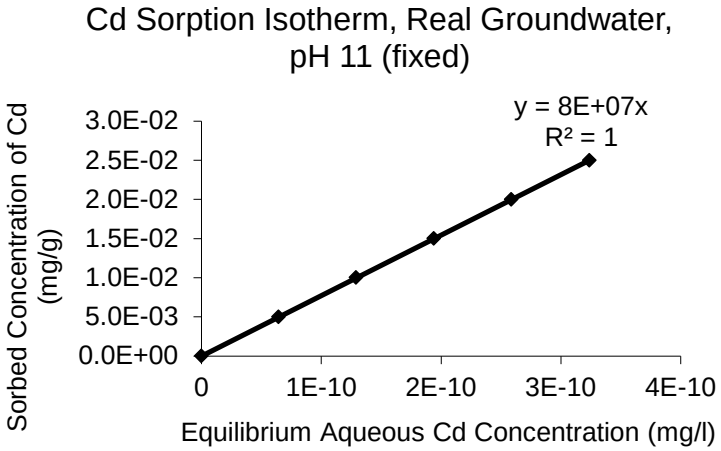

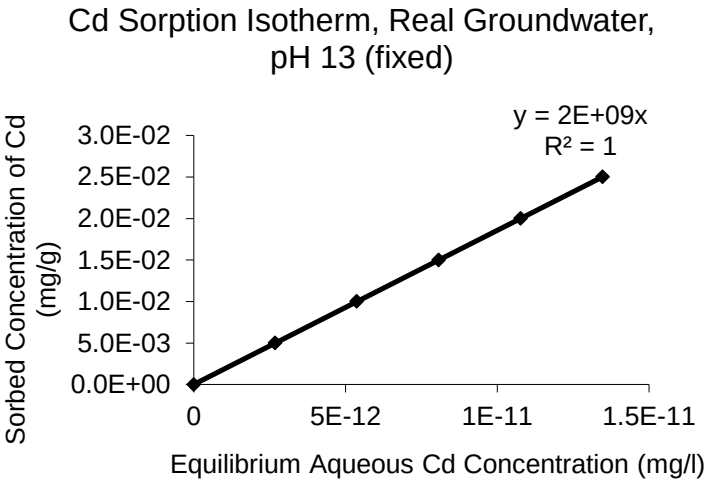

Figure 3-12: (Above) Cd Sorption Isotherms, Real Groundwater, pH 9 (Fixed pH).

Figure 3-13: (Right) Cd Sorption Isotherm, Real Groundwater,

pH 11 and 13 (Fixed pH)

When the results used for Figure 3-9 are broken down into individual isotherms (Figures 3-10 to 3-13), they each show that a linear relationship holds when the pH is held constant during the sorption reactions. However, the K_ds are different for similar pH when considering pure water with groundwater. For groundwater at pH 7, for instance, the K_d is 42 l/g, but for groundwater it is 3655 l/g. This is presumably due to a higher ionic strength or possibly competition for sites between other ions in the groundwater, but requires further investigation.

Figure 3-14 shows K_d variation with pH, the pattern being as expected from the results of Figures 3-10 to 3-12.

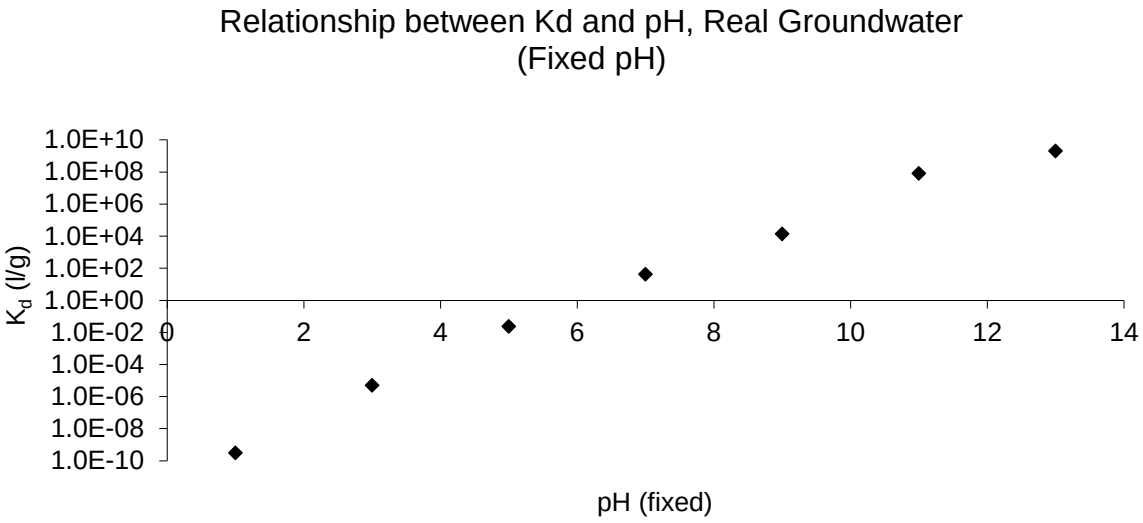

Figure 3-14: Relationship between K_d and pH, Real Groundwater (Fixed pH)

It would appear that the equilibration of a Cd-spiked groundwater with an originally protonated HFO surface results in very similar Cd sorption as for the case in pure water.

3.3.3.3 System 3: H_2O – Cd – HFO; varying pH

In the experiments so far described, pH was fixed in order to obtain as precise a relationship between sorption and pH as possible. However, in a real system, there will be an interaction between a new solution and the surface, and this will result in a change in pH. This change in pH and its effects on sorption are explored in this section. System 3 is exactly the same as System 1, except that the pH was allowed to vary as the sorption reaction took place. The initial surfaces again were protonated, and may hence represent an extreme case.

Figure 3-15 shows the relationship between sorption and final (equilibrium) pH. As expected, the pattern is as in previous experiments.

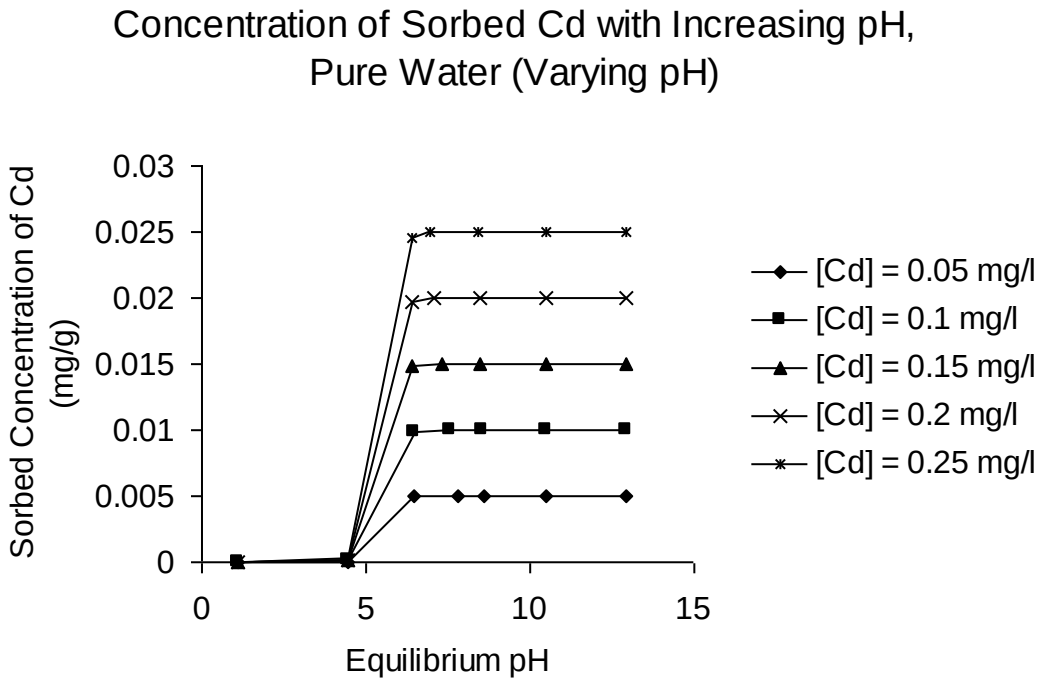

Figure 3-15: Concentration of Sorbed Cd with Increasing pH, Pure Water (Varying pH)

Figures 3-16 to 3-22 show the isotherms for each of the initial pH values. For initial pHs of between 3 and 11, the sorption isotherms are not linear – therefore at first glance 'K_d' does not hold. However, the equilibrium pH varies with initial Cd aqueous concentration, and these isotherms are not at constant pH.

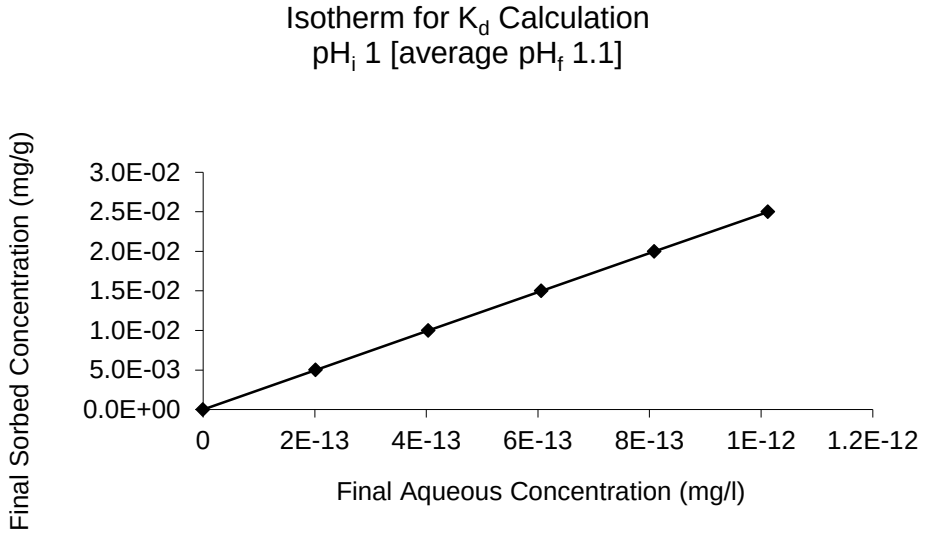

Figure 3-16: note that the sorbed concentrations are effectively zero for pHs below about 4

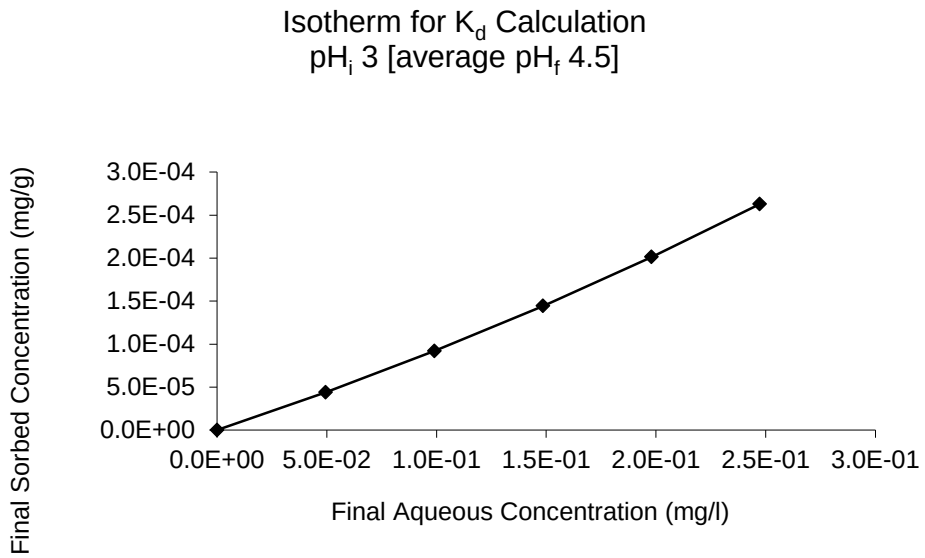

Figure 3-17: Isotherm for K_d Calculation pH 3 [average pH 4.5]

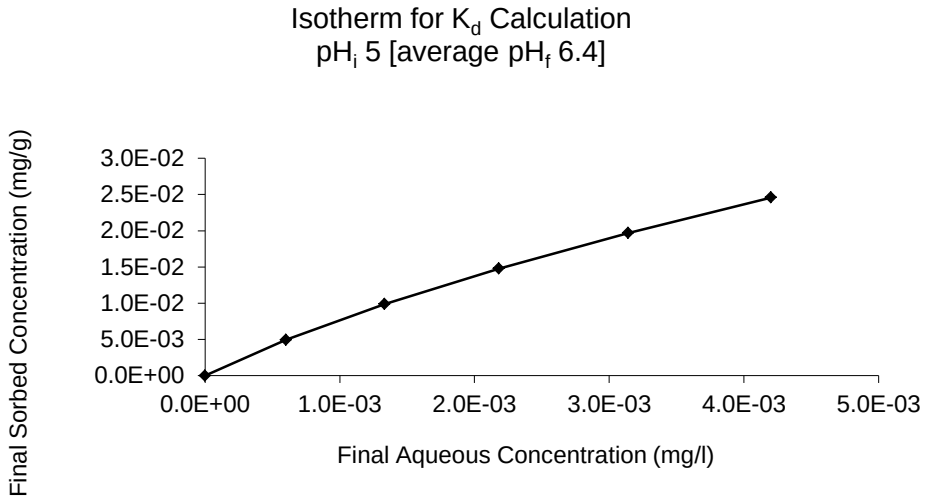

Figure 3-18: Isotherm for K_d Calculation pH5 [average pH 6.4]

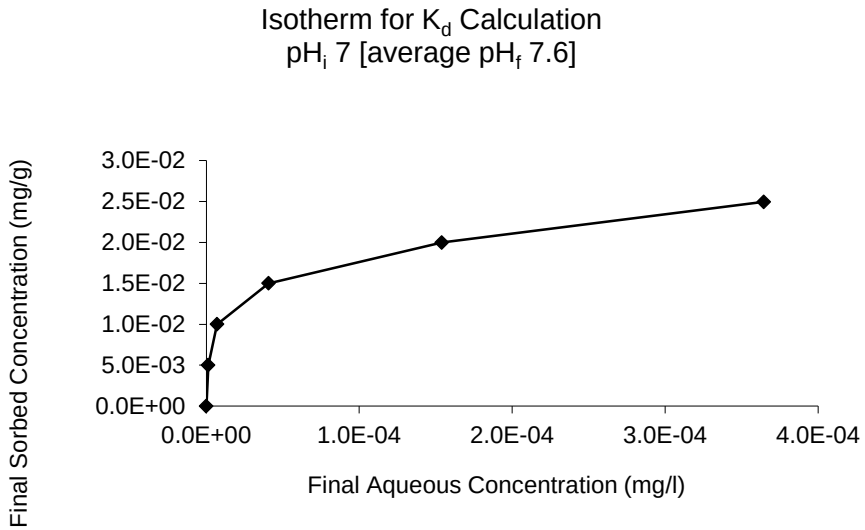

Figure 3-19: Isotherm for K_d Calculation pH 7 [average pH 7.6]

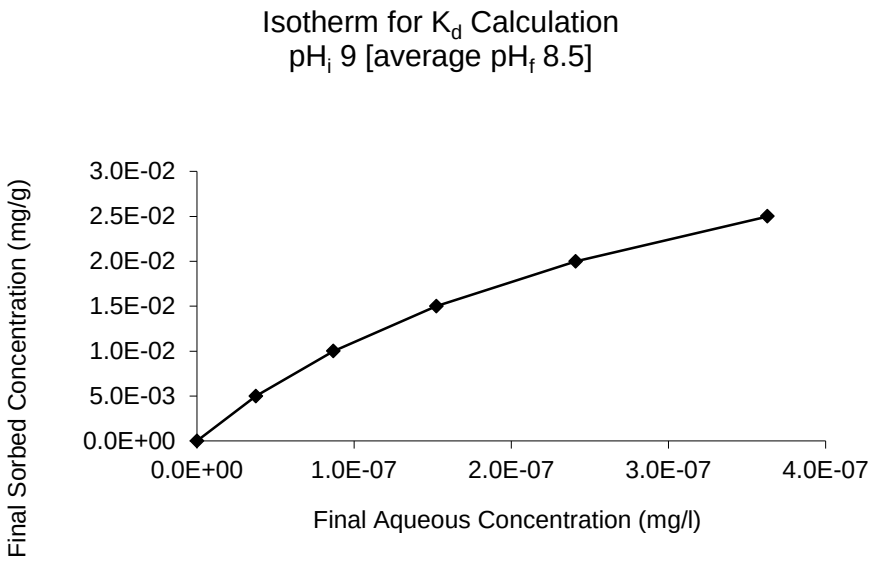

Figure 3-20: note that the aqueous concentrations are effectively zero for systems where pH is greater than about 8.

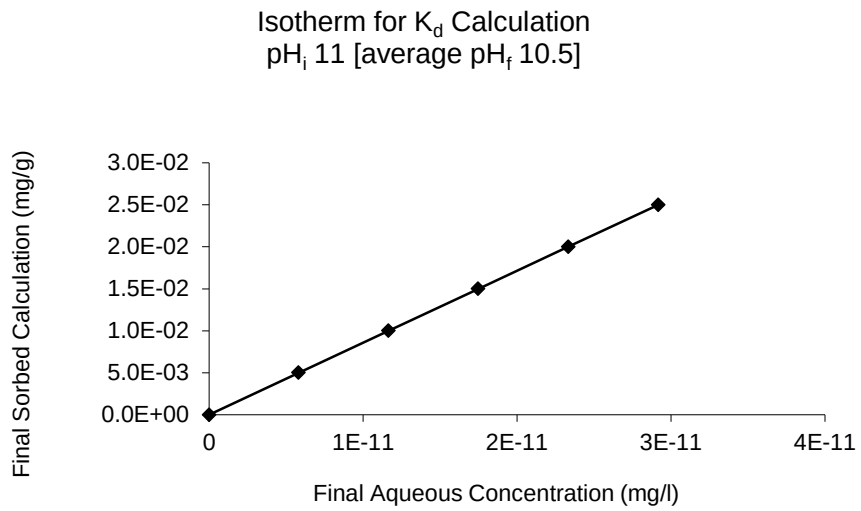

Figure 3-21: Isotherm for K_d Calculation pH 11 [average pH 10.5]

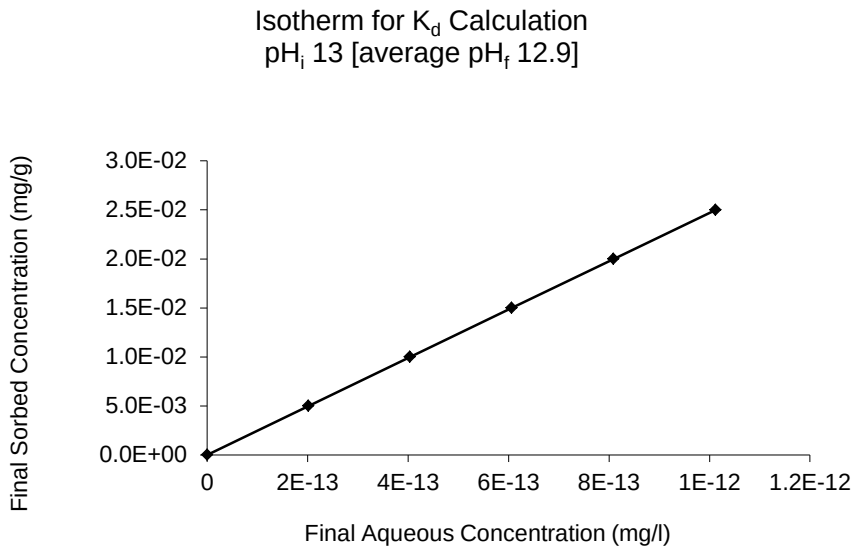

Figure 3-22: Isotherm for K_d Calculation pH 13 [average pH 12.9]

Figure 3-23 shows how the pH changes during the experiments in the [Cd] = 0.1 ppm case, with the zero Cd concentration case for comparison (Figure 3-24): at low initial pH the final pHs are higher than the initial pH, and at high initial pH the final pHs are lower than the initial pHs. This is qualitatively as expected: at low initial pH, reaction (Equation 3-3) will occur, thus increasing the pH.

$$\equiv \mathrm{XOH}^{\circ} + \mathrm{H}^{+} = \equiv \mathrm{XOH}_2^{+}$$

Equation 3-3

At higher pHs, the reaction will go in the opposite direction, thus decreasing the pH. Figure 3.14 shows how pH changes during the experiments with initial pHs of 3 and 7. It is clear that Cd makes a difference to the final pH, presumably through reaction (Equation 3-4).

$$\equiv XOH^{\circ} + M^{2+} = \equiv XOM^{+} + H^{+}$$

Equation 3-4

The pH change with Cd concentration is not always negligible (pH 7 case, for example), and thus the presence of Cd is enough to change the K_d appreciably.

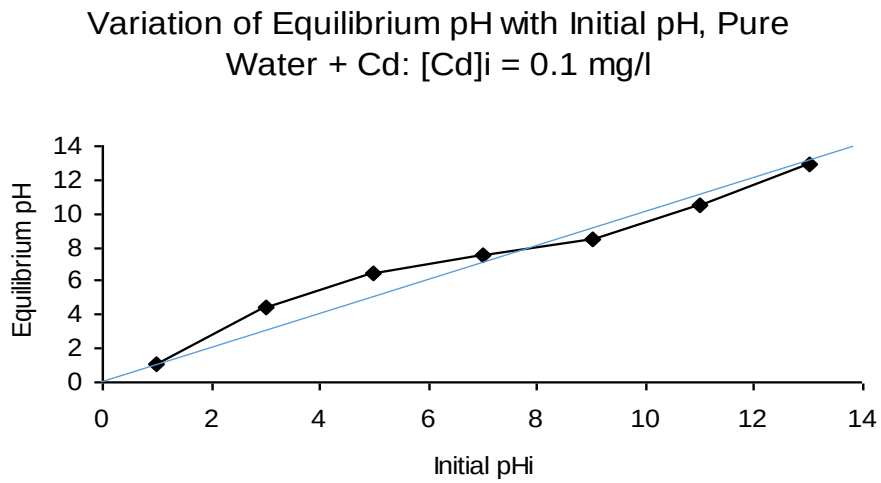

Figure 3-23: Relationship between initial pH and equilibrium pH as Cd sorbs to HFO in pure water. [Cd]i = 0.1 mg/l

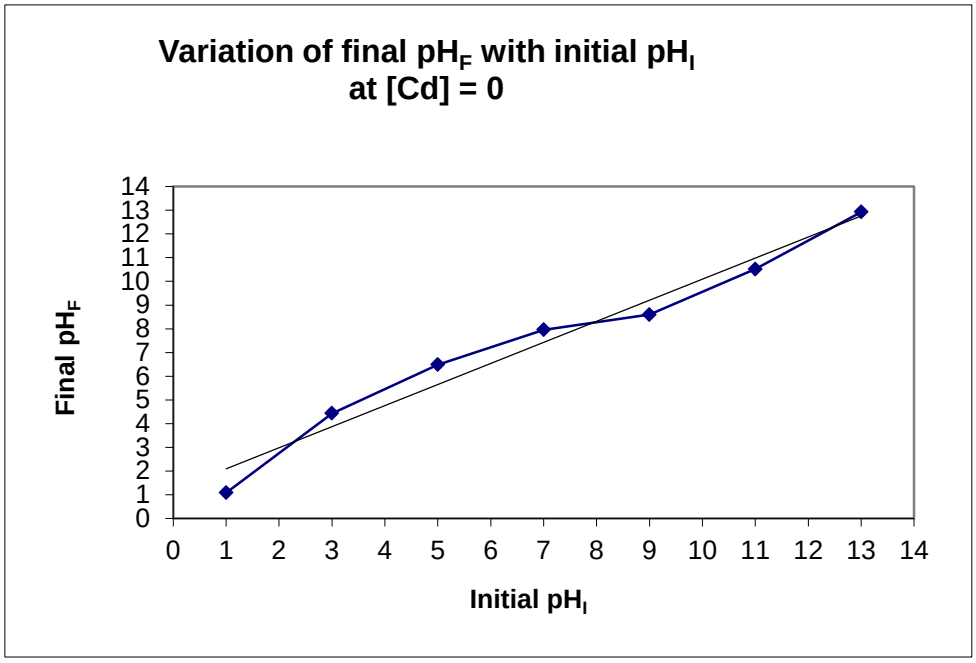

Figure 3-24: Relationship between initial pH and equilibrium pH as Cd sorbs to HFO in pure water. [Cd]i = 0 mg/l

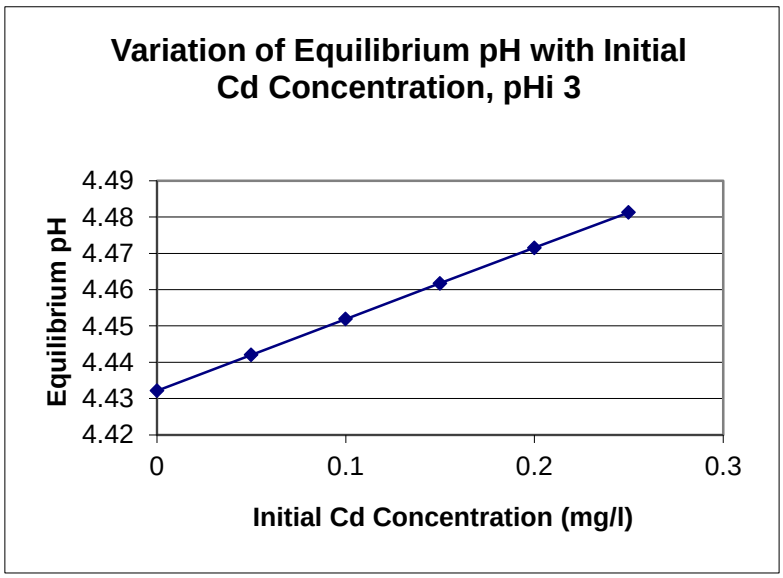

Figure 3-25: Variation of equilibrium pH with initial Cd concentration, pHi 3

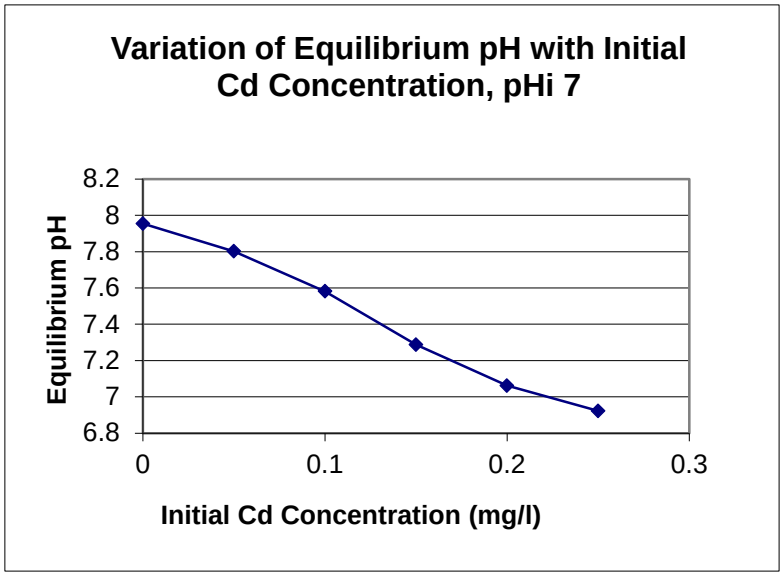

Figure 3-26: Variation of equilibrium pH with initial Cd concentration, pHi 7

3.3.3.4 System 4: Groundwater – Cd – HFO; varying pH

System 4 is exactly the same as System 2, except that the pH was not externally fixed, but allowed to vary as sorption took place (as System 3). Comparison with System 3 results allow a qualitative assessment of the effects of other ions to be gauged.

An immediate difference is noticed with these runs in that, although the runs with initial pH values of 1 and 13 remain approximately at these pHs throughout the equilibration with the HFO surface, all the other cases are buffered to a pH between 7 and 8 (Figures 3-27 and 3-28). Thus the isotherms appear more similar to each other than in the previous cases investigated (Figures 3-28 and 3-29).

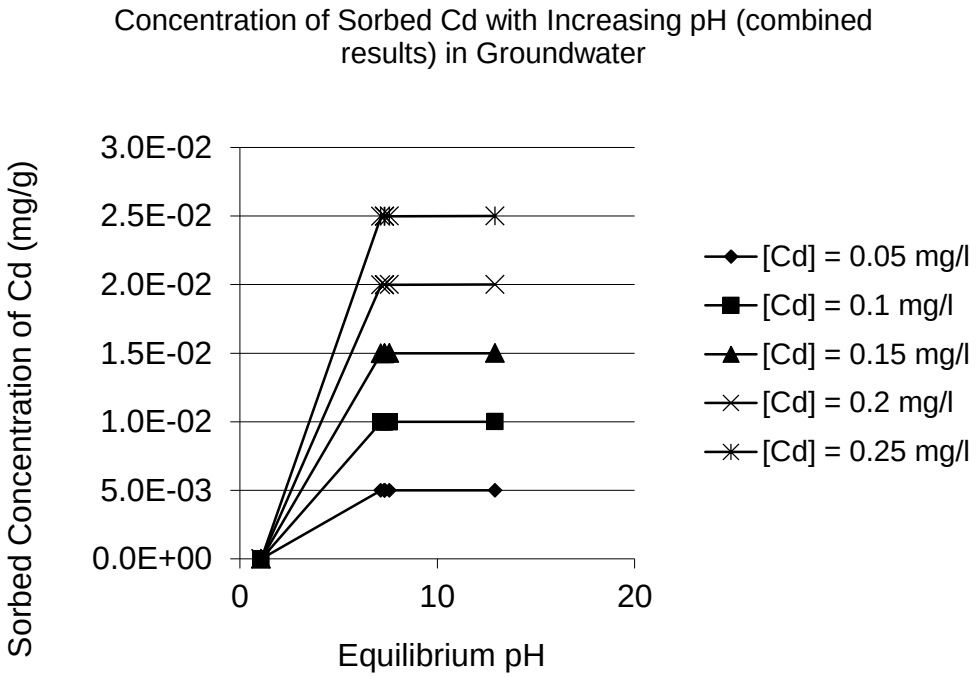

Figure 3-27: Predicted relationship between Cd sorption on HFO and pH: combined results for all concentrations (Groundwater, pH allowed to vary.)

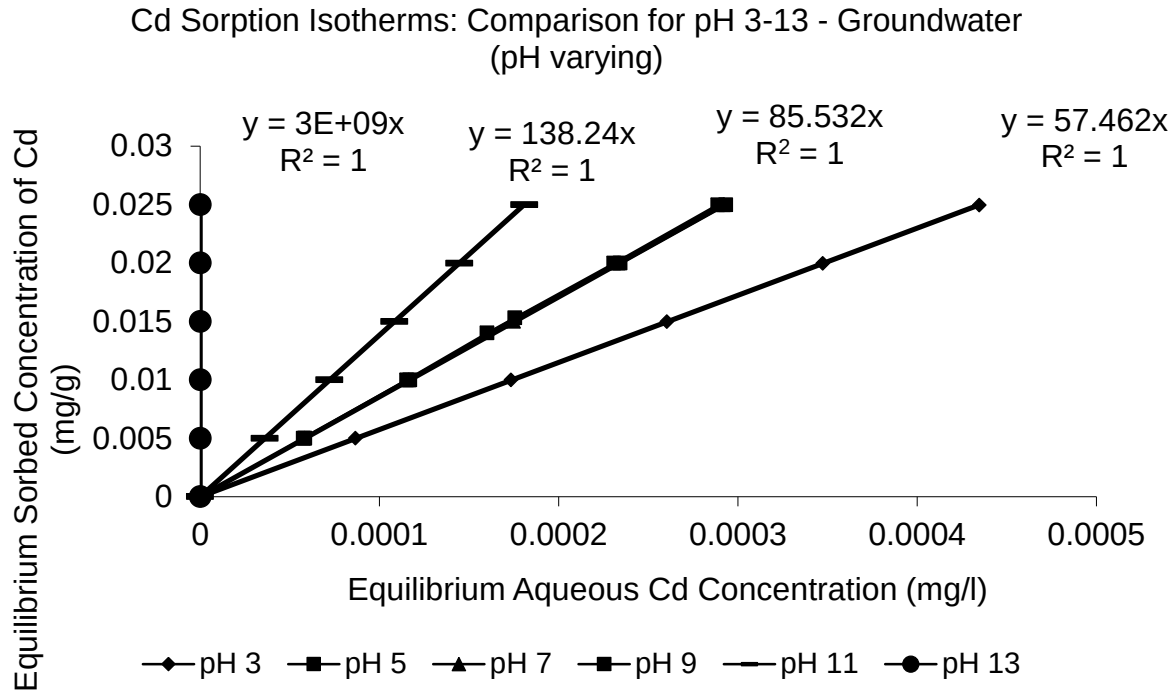

Figure 3-28: Cd Sorption Isotherms: Comparison for pH 3-13 Real Groundwater (pH varying)

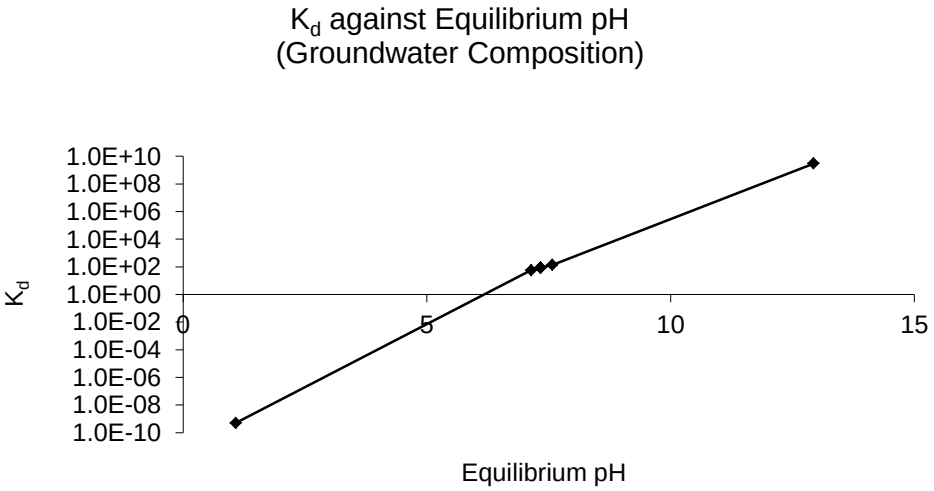

Figure 3-29: Predicted K_d / pH relationship for sorption of Cd onto HFO in groundwater. pH allowed to vary.

Figure 3-27 shows that for initial pHs greater than 3, sorption approaches 100%, but for initial pHs less than 3, sorption is approximately 0%.

Linear sorption isotherms occur across the narrow equilibrium pH range, as shown in Figure 3-29. This indicates that the pH is being fixed by buffering reactions arising due to this groundwater composition. Examination of the speciation model results shows how important Ca is. For the pH 9 case, Ca-surface complex reaction (Equation 3-4) are at least 5 times greater in concentration than protonated surfaces for the strong sites, and for the weak sites, the Mg and Ca complexes significantly lower the proportion of protonated sites. In both cases, H+ is released into solution, thus lowering the pH. In the pure water runs, this reaction does not occur, except to a minor extent with the low concentrations of Cd, and pHs therefore are not lowered as much.

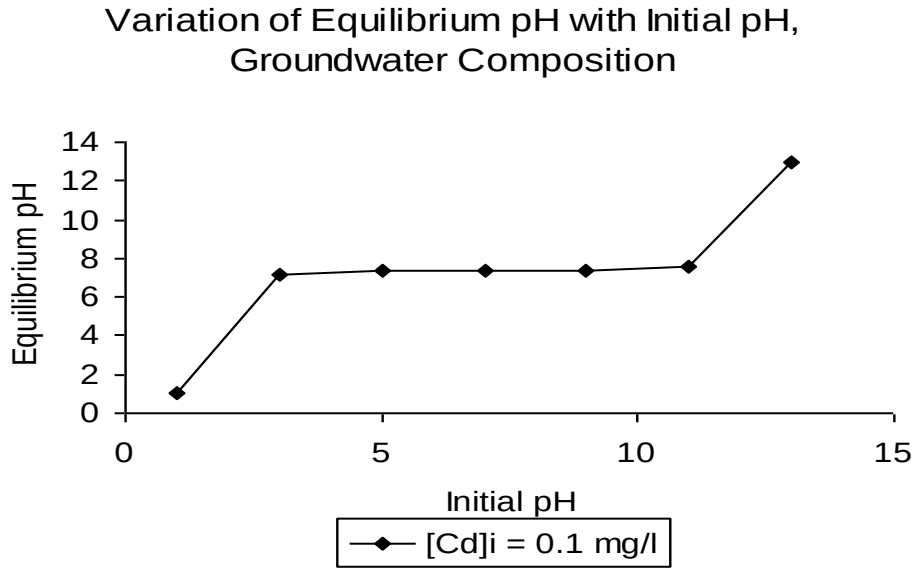

Figure 3-30: Relationship between initial pH and equilibrium pH as Cd sorbs to HFO in real groundwater. [Cd]i = 0.1 mg/l

3.3.3.5 System 5: H_2O – Cd – HFO in equilibrium with calcite

System 5 was devised to investigate the effects of high carbonate levels in groundwater, as might be expected in some parts of the Permo-Triassic Sandstone, due to carbonate cement. PHREEQC maintained equilibrium with calcite at all times. The pH was not otherwise fixed.

Figures 3-31 to 3-37 show the isotherms obtained for initial pHs from 3 to 13. Though the combination of initial pH and initial HFO surface composition is a little artificial, it does show that initial conditions produce a range of apparent K_d values, even if the system is strongly buffered by the presence of calcite.

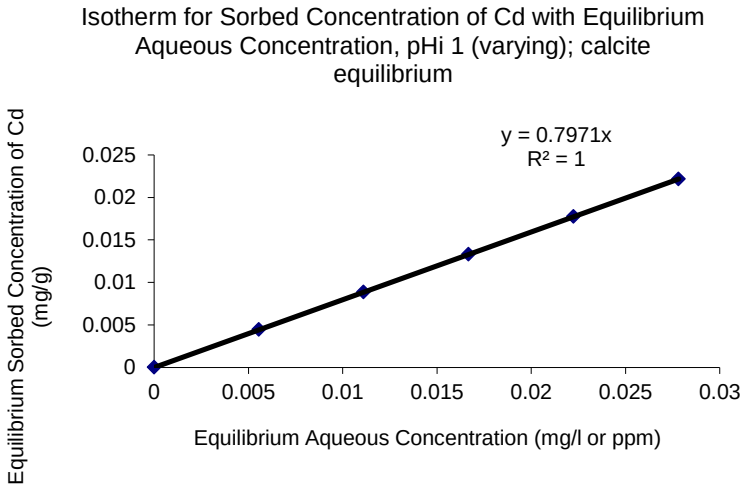

Figure 3-31: Cd sorption isotherm, pHi = 1 (varying); calcite equilibrium.

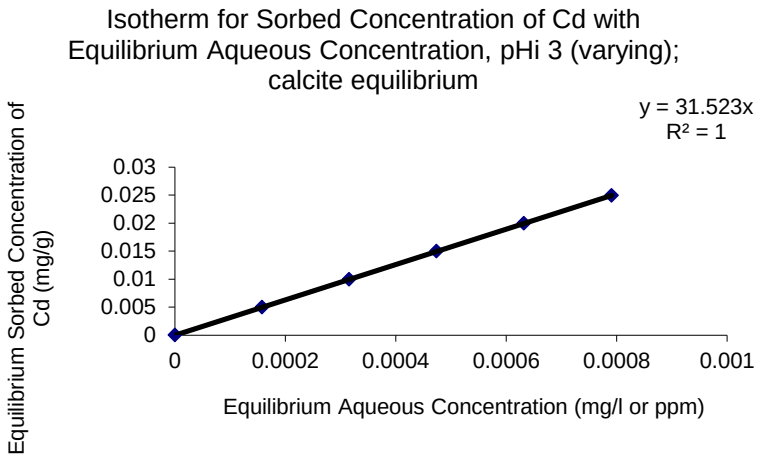

Figure 3-32: Cd sorption isotherm, pHi = 3 (varying); calcite equilibrium.

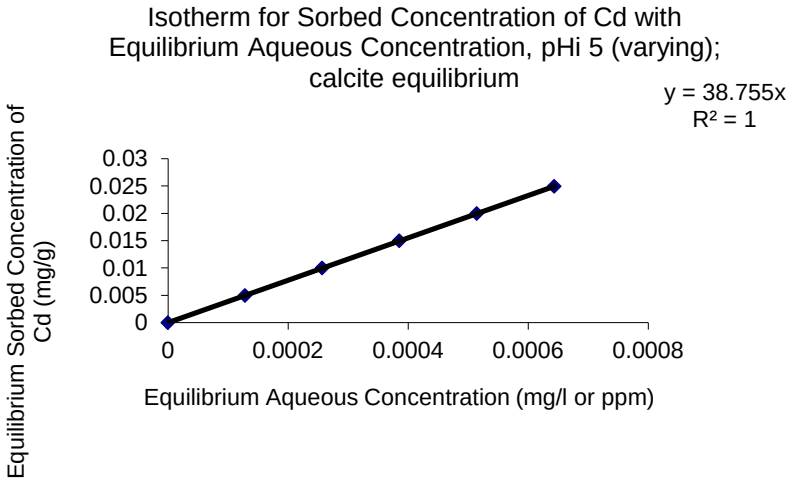

Figure 3-33: Cd sorption isotherm, pHi = 5 (varying); calcite equilibrium.

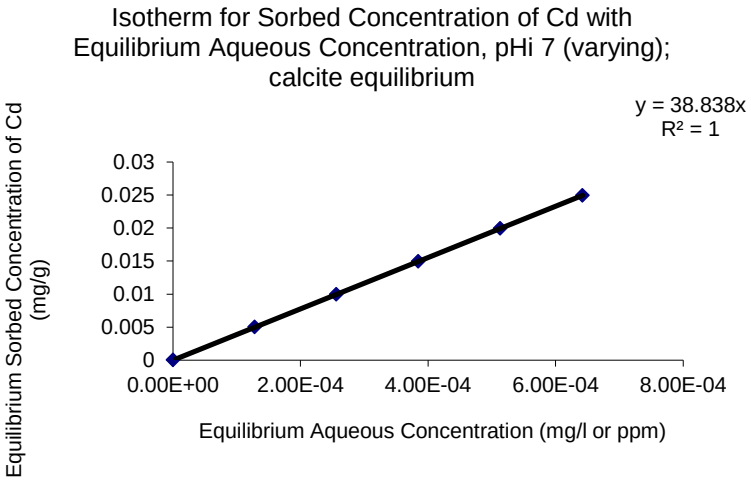

Figure 3-34: Cd sorption isotherm, pHi = 7 (varying); calcite equilibrium.

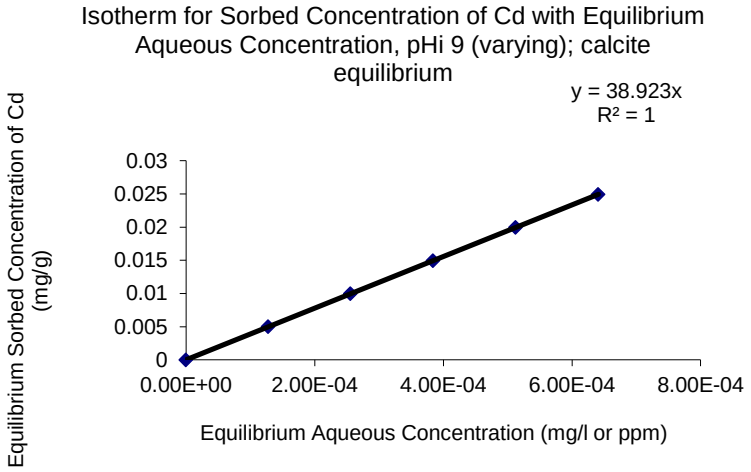

Figure 3-35: Cd sorption isotherm, pHi = 9; calcite equilibrium.

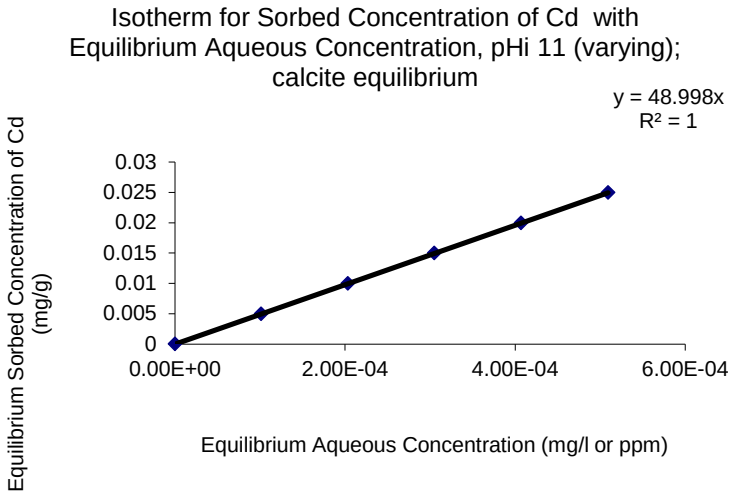

Figure 3-36: Cd sorption isotherm, pHi = 11 (varying); calcite equilibrium.

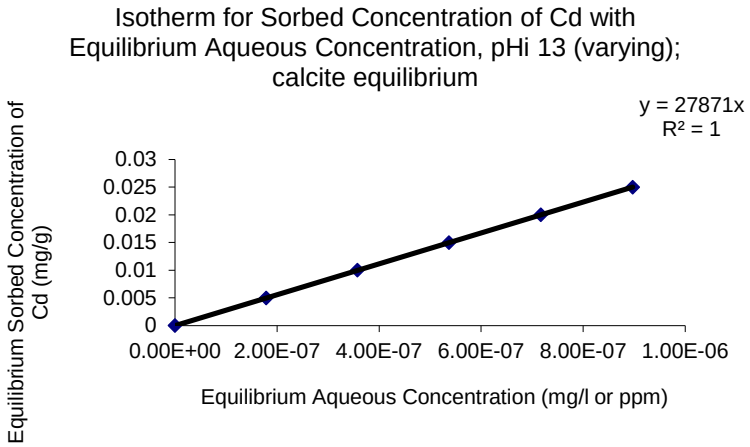

Figure 3-37: Cd sorption isotherm, pHi = 13 (varying); calcite equilibrium.

Figure 3-38 shows how tightly the equilibrium pH values are constrained by the equilibrium with calcite. Even though the equilibrium pH values are constant within field pH measurement uncertainty (~±0.1 units) between initial pH values from 3 to 11, the apparent K_d varies from about 32 to 49 l/g (Figure 3-39).

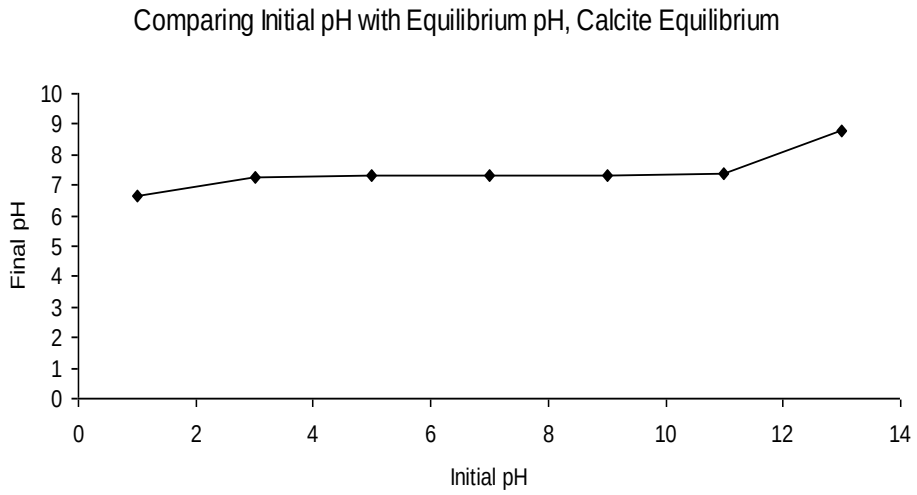

Figure 3-38: Relationship between initial pH and equilibrium pH as Cd sorbs to HFO in pure water in equilibrium with calcite

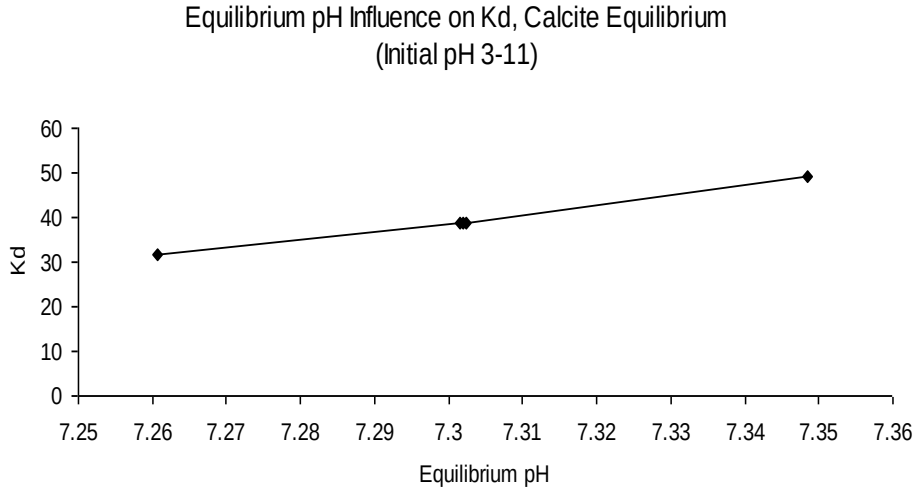

Figure 3-39: Predicted K_d / pH relationship for sorption of Cd onto HFO in pure water in equilibrium with calcite. pH allowed to vary

3.3.3.6 Comments

From the calculations undertaken using the Dzomak and Morel (1990) complexation theory as implemented in PHREEQC, the following conclusions are drawn:

1. sorption of Cd, and therefore presumably other elements of similar chemical behaviour, is very sensitive to pH, varying from effectively zero at low pH to effectively 100% at high pHs, the increase in proportion sorbed rising rapidly over a pH interval of less than 2 units (i.e. a $[H^+]$ change of less than 2 orders of magnitude);
2. isotherms are linear, except in cases where the aqueous concentrations are below usual analytical detection limits;
3. K_d values obtained from the isotherms vary strongly, as might be expected from conclusion 1, from effectively zero at low pH to infinite at high pH;
4. even when the pH is buffered to within field analytical resolution, the apparent K_d value varied from about 32 to 49 l/g;
5. the H+ sorption appears dominated by the ‘weak’ sorption sites, and the Cd by the ‘strong’ sites, when using the HFO description suggested by Dzombak and Morel (1990).

These observations confirm as expected that the K_d approach will not be viable for HFO materials.

3.4 Conclusions

This initial stage of modelling, which has used Cd as an example contaminant, suggests that the following:

1. Cd / HFO isotherms are linear over a wide range of pH values according to the surface complexation theory of Dzombak and Morel (1990) as implemented in PHREEQC;
2. however, the apparent K_d values obtained vary strongly with pH, from effectively zero to effectively infinite over a pH interval of less than two units;
3. given this sensitivity, the K_d approach seems impractical.

The numerical experimental work undertaken is in nature scoping, particularly as the relevance of the HFO complexation model of Dzombak and Morel (1990) has not been shown to be relevant for geological materials, and most of the parameter values for ion exchange and sorption models used in the experimentation are default values. Given that the numerical experimentation has indicated that sorption may play a role even in the presence of ion exchange, it is next necessary to undertake laboratory experiments to determine if Dzombak and Morel's (1990) model is appropriate, and what the parameter values should be. The numerical experimentation indicates that it is very important to consider ion exchange as well as sorption reactions in the laboratory experiments if the effects of sorption are to be determined.

3.5 Chapter Summary

This chapter has reported on the construction and results of some initial computer modelling of sorption using PHREEQC in five different systems. Whilst these were rough prototypes, the results they have generated substantiate the argument

that K_d-based predictions lack credibility, and add impetus to the need to find a better solution. The chapter also describes some scoping modelling work on transport of contaminants in the presence of surface reactions, and has shown that ion exchange and sorption must both be considered in any future investigations.

4 - CHARACTERISATION OF PERMO-TRIASSIC SANDSTONE AND DEVELOPMENT OF LABORATORY METHODS

4.1 Overview

This chapter describes the development of the laboratory experimental methods used in the project. The results of applying these methods are presented in Chapter 5, together with their interpretation using PHREEQC. Chapter 6 then uses the quantitative description developed in Chapter 5 to explore implications for site-scale contaminant transport.

The outline structure of this chapter is as follows:

- An introduction to the types of experiments used;
- Information about the sandstone used;
- Account of an initial scoping experiment to gain basic insights into the sorption behaviour of the sandstone and to give information on the likely aspects deserving more detailed study;
- Experiments and analysis designed to develop the experimental method and address the areas requiring more data;
- A summary of the main findings from these experiments;

- A final experimental method, synthesising all considerations raised by the suite of experiments.

4.2 Introduction

The initial modelling investigations (Chapter 3) appeared to show that there were several important patterns of sorption behaviour that should be investigated using laboratory data obtained from real sandstone. These patterns suggested that:

- pH is very influential in sorption behaviour;
- Both ion exchange and sorption need to be considered;
- There are competitive effects between ions such as Zn^{2+}, Ca^{2+}, and Mg^{2+};
- The chemical database used by the model was obtained using an artificially-produced, pure iron oxide under known conditions: this should be compared to the impure, 'aged' oxides contained in real rock samples.

Quantitative information about the sorption behaviour of a rock or soil sample is commonly acquired through the use of "batch experiments", which are described later. The data collected can be used to plot isotherms, in a similar manner to the outputs from the models in Chapter 3. (Indeed, the computer models in PHREEQC may be helpfully imagined as simulated batch experiments themselves.)

In the rest of this chapter, 'sorption' is used to refer to sorption to oxide surfaces, 'exchange' to refer to ion exchange processes on clays, and 'attachment' to unspecific sorption and exchange, the latter being used where a general

phenomenon is being discussed or where both sorption and exchange are likely to be occurring.

4.3 Preliminary Scoping Investigation

4.3.1 Introduction

A preliminary scoping experiment was designed to form the foundation to this stage.

The main priorities for this initial stage were to:

- demonstrate that sorption was significant;
- develop the author's competence in running batch experiments and to test ideas and techniques;
- begin to tackle any general problems arising with the laboratory work before undertaking the main suite of experiments;
- generate useful data regarding the basic behaviour of the sandstone and to plot corresponding isotherms.

If the isotherms differed markedly from a linear relationship, then this would give tentative substantiation to the reservations regarding K_d-type models and potentially indicate the areas for more comprehensive study.

4.3.2 Experiment Design Considerations

4.3.2.1 Introduction

Upon reviewing the literature and the results of the modelling studies, it seemed that the main factors to consider and control in these experiments should initially be:

- pH;
- the elements to measure;
- the solution-rock ratio;
- temperature: this should ideally be constant;
- duration: sufficient time must be allowed for the experiment to reach equilibrium, although this would have to be investigated.

These are now discussed in more detail.

4.3.2.2 pH Influence

Surface complexation theory predicts that metal cation sorption is strongly influenced by the pH of the system. When there is a high concentration of H^+ ions (i.e. low pH), they occupy the sorption sites on the surface of the oxide, thereby preventing sorption of cations. As the pH rises, their concentration decreases, and more sorption sites become available for occupation by metal ions to form surface complexes.

The initial modelling in Chapter 3, using PHREEQC, predicted that (Figure 4-1):

- between pH 1 and approximately pH 5.5, Cd will remain in solution and will not be sorbed to the oxide coating on the sandstone;
- from approximately pH 7, Cd is almost fully sorbed onto the oxide;
- between pH 5.5 and pH 7 (approximately), there is a steep gradient of increasing sorption of Cd.

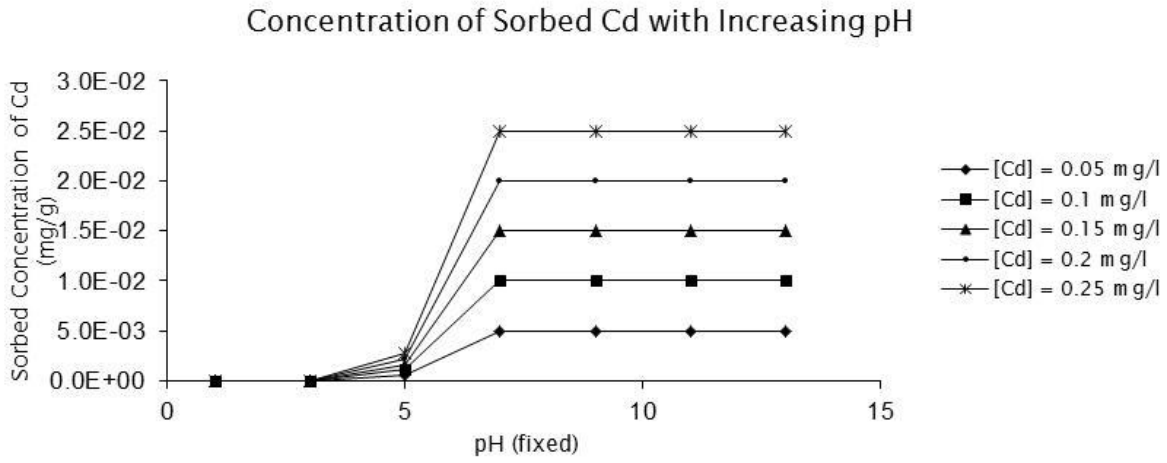

Figure 4-1: Relationship between Cd sorption on HFO and pH (pure water, pH fixed), as predicted by the Dzombak and Morel (1990) model implemented in PHREEQC

Realising that an important part of the scoping experiment would be to verify the predicted relationship between pH and sorption, a resolution was made to carefully monitor – and possibly control – the pH.

4.3.2.3 Choice of Elements

As discussed in Chapter 1, Zn was chosen as the primary metal with which to investigate sorption behaviour. Zn is a major constituent of many pollutant plumes, and can be toxic in high concentrations. However, the risks it poses in laboratory studies are much less compared to other heavy metals (e.g. Cd, Hg,

Pb, Cr), yet its chemical properties have general similarities to several other metals including Cu, Cd and Pb.

In addition to Zn as the primary metal under investigation, a number of other metals would ideally be monitored. This would give more detailed insights into sorption processes, and give further avenues of interpretation generally. Of particular interest were Ca, Sr, Mg (which may exhibit similar sorption behaviour to Zn) and Na (which may be less prone to sorption reactions though remaining very prone to ion exchange reactions).

4.3.2.4 Solution-Rock Ratio

The ratio between the volume of solution and the mass of solid sample was pragmatically established by considering the volume of the vials used for the experiments. 50 ml vials were chosen for the batch reactions as being convenient, cost-effective, and able to fit into other laboratory apparatus (such as the shaker and centrifuge). To encourage thorough mixing of the solution and the ground rock sample, 40 ml of solution was added to 1 g of solid, leaving approximately 10 cm^3 of free air volume to encourage agitation whilst on the shaker.

4.3.2.5 Temperature

Ideally, the temperature should remain constant whilst the batch reactions are running (an inherent assumption in the “isotherm” plots). After much consideration, it was found to be highly impractical to control the temperature at which these reactions were carried out. Therefore, they were carried out in the

prevailing ambient conditions in the laboratory. Temperature measurements were recorded concomitantly with pH.

4.3.2.6 Duration

Various authors have ventured a range of suggestions as to how long to leave the experiment running to allow for equilibrium (Christensen, 1985; Pang & Close, 1999; Convery, 2000). These values ranged from 6 hours to 24 hours or more. Since an unequilibrated mixture would potentially produce misleading data, it would be important to ascertain a more precise value necessary to allow for complete equilibration.

4.3.3 Purpose of the Experiment

In view of the considerations and uncertainties recognised above, the principal aims of this exploratory experiment were to:

- see what practical difficulties occurred, e.g. in not controlling temperature;
- obtain basic data on zinc attachment on real sandstone and to observe whether or not the isotherms were linear and pH-dependent;
- examine the broad pH-attachment relationship and compare it with the modelling results. The interval between approximately pH 5 and pH 7 is of particular interest due the steep gradient on the modelling plots, and so there is a desire to map this range more comprehensively using smaller pH intervals;

4.3.4 Method

4.3.4.1 Experimental Approach

In common with many investigations into the geochemical properties of rocks and soils, batch experiments are useful for these studies because they permit adsorption reactions to take place within the bounds of tightly controlled conditions. All of the batch experiments were based on a standardised approach, described later, with variations applied according to the variable(s) being investigated.

4.3.5 Materials and Material Preparation

4.3.5.1 Description of the Sandstone Samples

A sample of the UK Permo-Triassic (P-T) sandstone formation from an outcrop in Worcestershire, UK (grid reference: SO75528823), was obtained for these experiments. Red bed continental sandstones are a common aquifer type in many parts of the world (Tellam & Barker, 2006). For the purposes of this project, some other priorities that influenced this choice were:

- familiarity of this sandstone among research staff at Birmingham University, and the existence of comprehensive data sets, due to a large body of research undertaken over several decades;
- friability of this sample, which is conducive to efficient processing;
- low carbonate content, resulting from its shallow depth. This was desired so that there would be minimal buffering of pH, which would otherwise introduce additional variables into the laboratory investigations.

Thin sections of the sandstone sample were prepared and analysed to verify the main constituents. The samples were injected before sectioning with blue-dyed resin to preserve the porosity. Table 4-1 summarises the results of this analysis, and Figures 4-2 to 4-5 are photographs of the thin sections, referred to in the table. The mineralogy was estimated by point-counting.

Table 4-1: Results of thin-section analysis of the sandstone

FIG.	PLANE-POLARIZED LIGHT / CROSS-POLARS	MAG'N.	MINERALOGY (Estimated)		RANGE OF GRAINSIZE
			Mineral	% of total composition	
Figure 4-2	Plane-polarized light	100 x	Quartz Feldspar Porespace Oxide Other (e.g. Mica)	50 20 20 5 5	0.5 to 4.5 mm
Figure 4-3	Crossed polars	100 x			
Figure 4-4	Plane-polarized light	100 x	Quartz Porespace Feldspar Rock fragments Oxide Carbonate Mica	40 25 15 10 8 1 1	0.5 to 4.5 mm
Figure 4-5	Crossed polars	100 x			

Figure 4-2: (P. 80, top) Thin section in PPL 100x magnification

Figure 4-3: (P. 80, bottom) Thin section in XPL 100x magnification

Figure 4-4: (P. 81, top) Thin section in PPL 100x magnification

Figure 4-5: (P. 81, bottom) Thin section in XPL 100x magnification

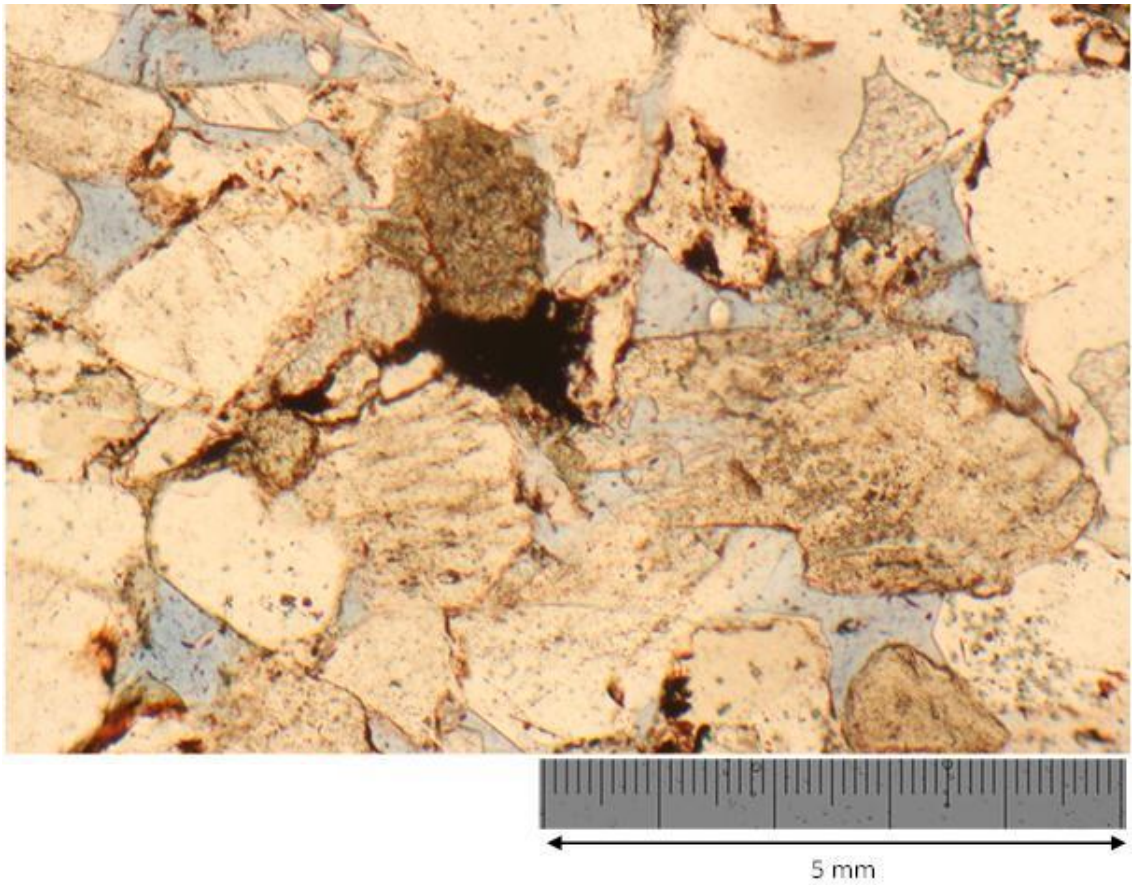
5 mm

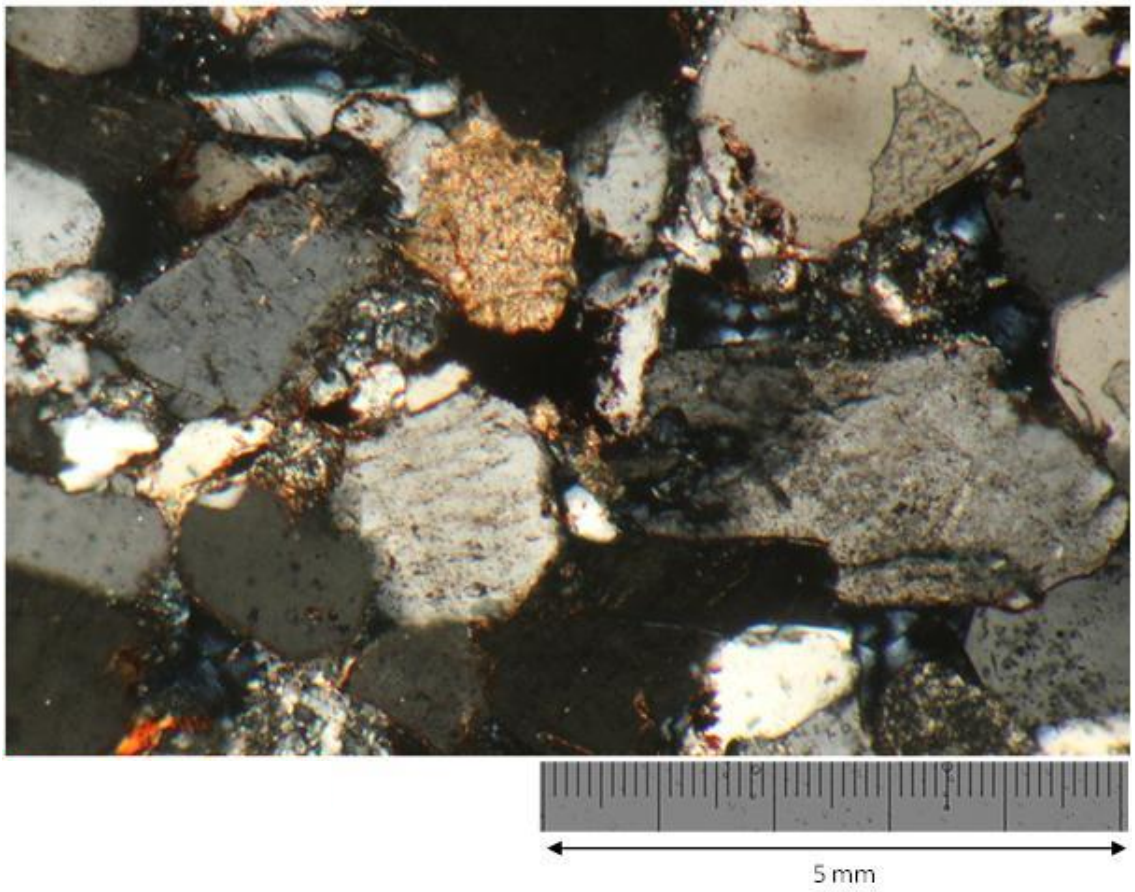
5 mm

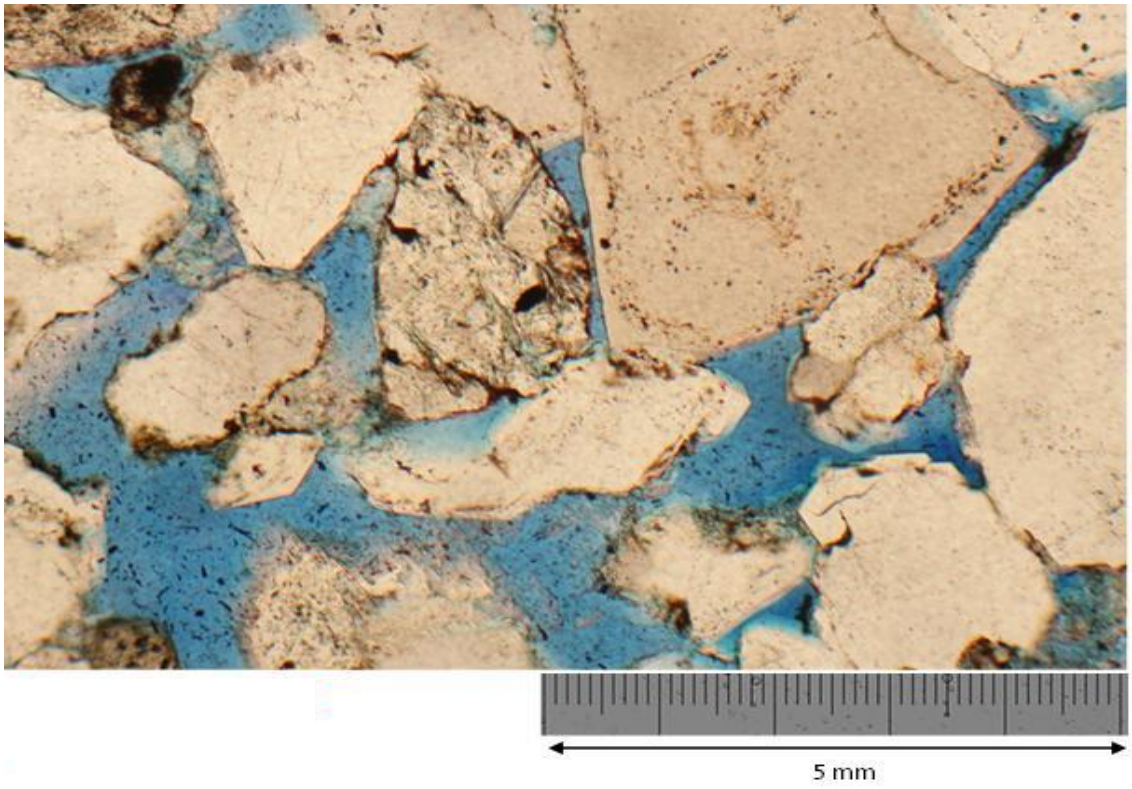
5 mm

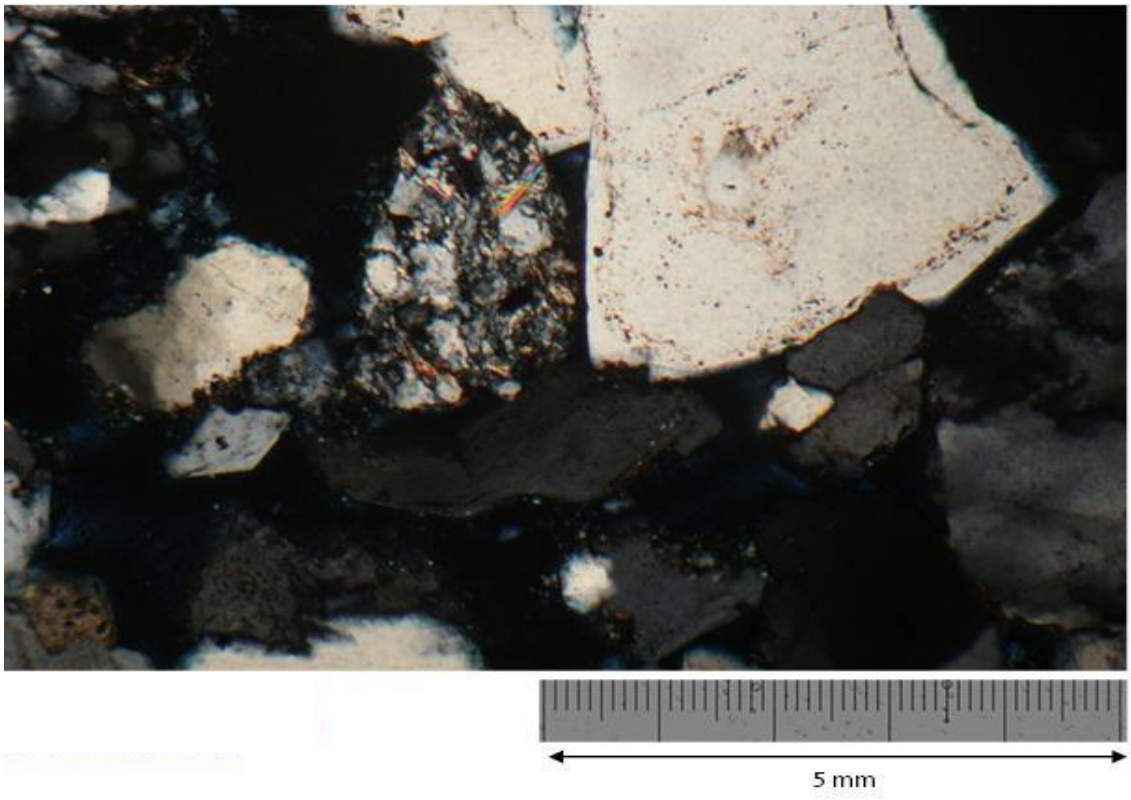
5 mm

4.3.5.2 Preparation of the Sandstone Samples

The bulk sandstone was gently disaggregated in two steps:

I. The rock was roughly broken up into smaller (approximately 1 cm^3) pieces using a rock press;

II. The smaller pieces were fully disaggregated using a mortar and pestle.

Care was taken to avoid crushing the sandstone grains, since this could increase surface area and potentially affect attachment behaviour. Once the sandstone was completely disaggregated, it was homogenised by thorough mixing by hand (wearing latex gloves) for five minutes initially and stored in sealable plastic bags in a cool cupboard. It was mixed for a further minute before each subsequent use.

4.3.5.3 Overview of Experimental Method

In a batch reaction, a known mass of a solid sample is mixed with a known volume of a solution (of known composition) in a reaction vessel. Maintaining a constant temperature, this mixture is agitated for a pre-determined amount of time to ensure thorough mixing. Ideally, a point of equilibrium is reached, wherefore any net flux of ions between the aqueous and solid phases has ceased. The final solution is then analysed and the results plotted as attachment isotherms for a particular element: the concentration of the ion sorbed onto the solid is plotted against the concentration remaining dissolved in solution. If this relationship is linear, then the slope is equal to the K_d; alternatively, it may fit a Langmuir, Freundlich, or some other isotherm model.

4.3.5.4 Experimental Design

A series of batch tests were designed to investigate the role of pH on attachment. A decision was made to use a solution containing 7 mg/l of Zn in deionised water. This concentration was settled upon after considering the WHO standards for heavy metal toxicity in drinking water, and because it fell within the expected range of concentration in pollution incidents in contaminated groundwater. The following array of pH values were chosen to investigate the influence of pH:

- pH 3; pH 5; pH 5.5; pH 6; pH 6.5; pH 7; and pH 9.

From the literature, and the modelling results, it was expected that, at pH 3 and below, there would be almost no sorption onto the solid; at pH 9 and above, almost all of the sorption sites on the solid would be occupied by the metal concerned.

4.3.5.5 Preparation

50 ml plastic centrifuge tubes with screw caps were used for all experiments; separate vials were provided for the reaction stage and for the final filtered solution. Vials for blanks (containing no sandstone, only the solution) were also prepared.

Using the prepared sandstone sample, approximately 1 g of sandstone grains were weighed into each of the vials. The exact mass of sandstone was recorded to four decimal places and taken into account in the calculations.

A stock solution of 1000 mg/l zinc nitrate hexahydrate ($Zn(NO_3)_2.6H_2O$) in deionised water was prepared in a glass flask. This was diluted to provide approximately 4 litres of a 7 mg/l Zn solution.

Dilute solutions of HNO_3 and NaOH were prepared as a means to adjust the pH of the Zn solutions (to lower or raise the pH, respectively), both before and during the experiments.

The 7 mg/l Zn solution was apportioned into seven smaller flasks (approximately 250 ml), each of which was assigned to a particular pH batch. The pH of these solutions was adjusted by drop-wise addition of either HNO_3 or NaOH, guided by a pH / temperature meter.

4.3.5.6 Execution

40 ml of the Zn solution (with the designated pH) was added to the appropriate centrifuge tubes. The initial pH in the tubes was measured, readjusted if necessary, and then the tubes were placed horizontally on a shaker, running at 100 rpm.

The experiment was scheduled to run for six hours, with pH measurements being taken every hour. If necessary, the pH in each tube was readjusted to its predetermined value using the HNO_3 or NaOH solutions.

At the end of the reaction time, the final pH and temperature values were measured in each tube. They were then centrifuged at 4,500 rpm for 10 minutes, and filtered into a fresh centrifuge tube via 0.45 µm, single-use, syringe filters.

Each experiment was repeated 3 times. Variability is indicated on the plots produced by error bars representing standard deviation.

4.3.5.7 Analysis

Prior to analysis using Flame Atomic Absorption Spectroscopy (FAAS), 0.2 ml of lanthanum chloride was added to the samples (and standard matrices) to reduce ionisation of K and Ca. Analyses were undertaken for Zn, Ca and K. These metals were previously determined to be able to give the majority of the information required to draw reasonable conclusions about the influence of pH on sorption. It would have been preferable to analyse more than three elements, but this was a prudent compromise on the basis of time constraints, given that the available apparatus demanded manual operation and could analyse only one element at a time.

4.3.6 Results

The principal results of the pH experiment are shown in Figures 4-6 and 4-7:

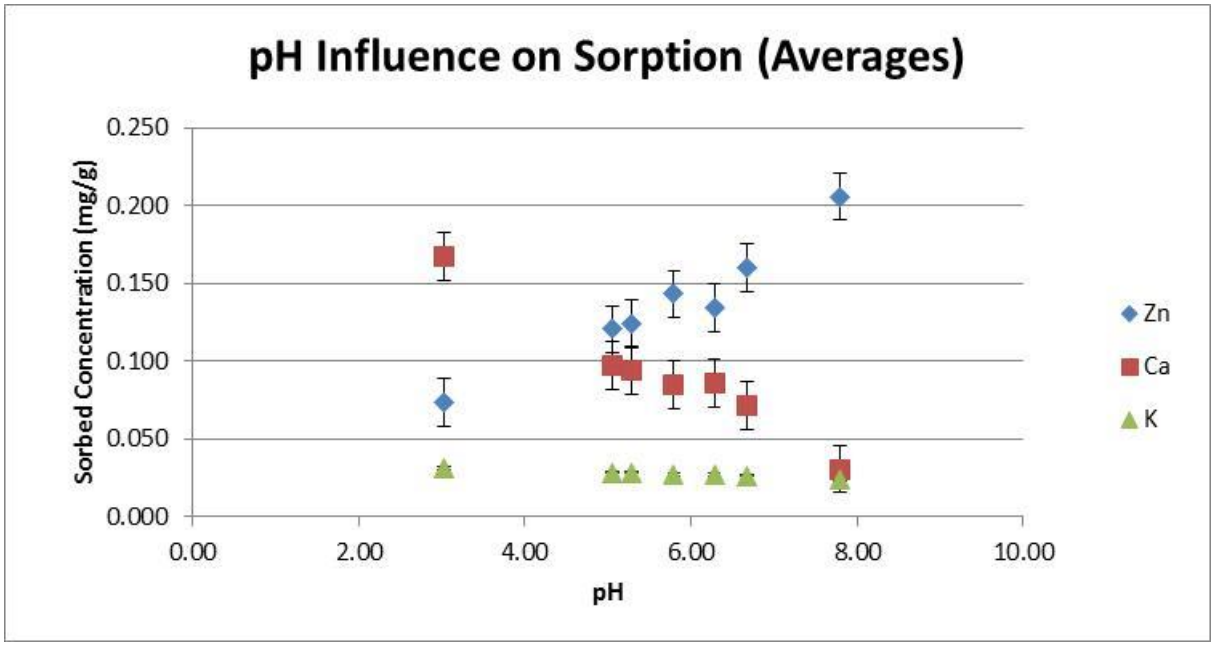

Figure 4-6: Relationship between pH and sorbed concentration of Zn, mass of Ca released per unit mass of sandstone, and mass of K released per unit mass of sandstone

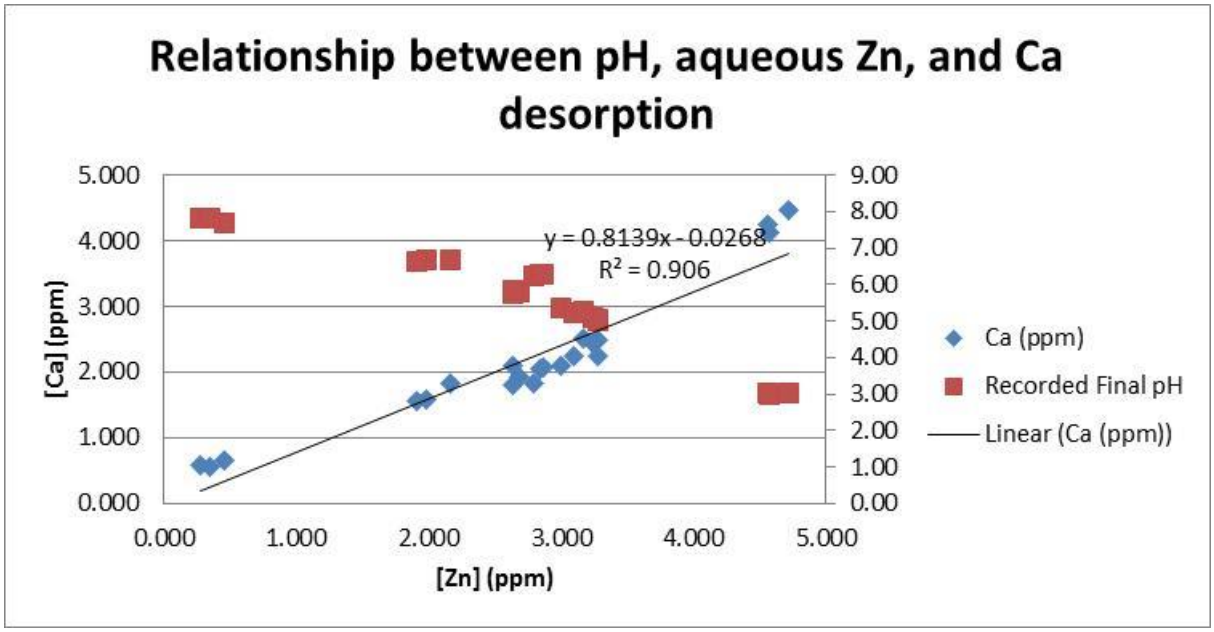

Figure 4-7: Relationship between pH and aqueous concentrations of Ca and Zn

The results show that Zn attachment is highly related to pH, with lower amounts of attachment occurring at low pH and higher amounts of attachment occurring at

higher pH. Ca exhibits a strong pH dependency also. K appears to be largely unaffected by pH or Zn attachment.

4.3.7 Discussion

The consistency between replicates in this experiment was good, suggesting that the basic protocol designed here worked well, and could form the basis of future experiments.

The results occur more-or-less as predicted: low pH conditions resulted in less Zn uptake and less Ca release. This is most likely to be occurring primarily on oxide surfaces. In contrast, K appeared to be much less sensitive to both pH changes and changes in Zn and Ca, indicating that it is mostly interacting with the surface through ion exchange reactions on clay minerals, which only have a minor dependence on environmental pH. However, contrary to the predictions made by the Dzombak and Morel models, there does not appear to be a sudden change in sorption behaviour at any particular pH value: it exhibits a more stable relationship throughout the pH range examined.

Tentatively, it is thought that at low pH (high H^+ in solution), more H^+ ions compete for sites on the sorption surfaces, and so more Ca^{2+} ions are released into the bulk solution. This then encourages more Ca^{2+} and Zn^{2+} ions to seek attachment to the exchange surfaces, but relatively low amounts of Ca is taken up as it is in competition with Zn. The ion exchange process cannot compensate for the low sorption capacity under these conditions. When there is a high solution pH, there

is increased uptake of both Ca^{2+} and Zn^{2+} ions, resulting in a lower dissolved Ca concentration.

A clear conclusion able to be drawn from these results is that any K_d value calculated for a sandstone would only apply for specific pH conditions. An overall K_d value, proposing to encompass attachment processes at a range of pH values, could not be justified, based on these results.

4.4 Development of the Experimental Method

4.4.1 Introduction

The scoping experiment clearly showed that attachment is dependent on pH. It will be assumed that this is mostly sorption on (iron) oxides, since ion exchange is less strongly influenced by pH, though will be to some extent.

Having demonstrated the pH dependency, some more questions arise:

- How fast does the system reach equilibrium? How long should these experiments run for to ensure full equilibrium?
- Is it possible to suppress the ion exchange processes and solely investigate sorption?
- The initial chemistry of the rock surface is unknown. Is it possible to either determine the initial conditions, or to artificially “set” them?

In this section, the method of performing the batch experiments is developed. Three more large experiments were undertaken to address the issues above in turn, and these are detailed below.

4.4.2 Experiment to Investigate Reaction Kinetics

4.4.2.1 Introduction

The pH-attachment experiment was run for only six hours, as a compromise between competing priorities. However, other authors have suggested durations for sorption experiments ranging from 16 hrs to over 48 hrs (Christensen, 1985; Convery, 2000; Pang & Close, 1999). For this project, it is necessary to be reasonably confident about the time it takes for the sandstone to reach equilibrium, as the real system will almost certainly be in equilibrium.

4.4.2.2 Purpose of the Experiment

The purpose of this experiment was to determine how long it takes for the sandstone sample to fully equilibrate with water. This would indicate that all ion exchange or sorption processes had reached their end-points for the particular solution, surface composition, pH, temperature, and other relevant variables, present. It was intended that the conclusions from this experiment, with regard to the time required to reach equilibrium, would be taken into account when designing the finalised protocol.

4.4.2.3 Experimental Approach

The general batch experiment method, as described in the scoping study, formed the basis of the time variance experiments, with minor adaptations. It was decided to prepare several sets of experiments, each running for predetermined time

periods. The periods were chosen to fully encompass the minimum and maximum equilibration periods accounted in the literature. The final times chosen were:

- 1 hour;
- 2 hours;
- 4 hours;
- 6 hours;
- 12 hours;
- 24 hours (1 day);
- 48 hours (2 days);
- 96 hours (4 days);
- 168 hours (7 days); and,
- 336 hours (14 days).

In order to provide enough data points to plot the attachment isotherms, four initial concentrations of Zn were used at each time period:

- 0 mg/l;
- 0.5 mg/l;
- 3 mg/l; and,
- 7 mg/l.

In addition to investigating the changes in attachment of Zn over time, other cations that may compete for sites on the iron oxide surfaces of the sandstone were also analysed for.

4.4.2.4 Materials and Methods

The method for this experiment was based on the procedure outline in the first experiment. Vials (50 ml centrifuge tubes) were prepared so that sandstone would be equilibrated with a Zn solution at each of the four Zn concentrations (0 mg/l; 0.5 mg/l; 3 mg/l; and, 7 mg/l), for each of the time periods (1 hour; 2 hours; 4 hours; 6 hours; 12 hours; 24 hours (1 day); 48 hours (2 days); 96 hours (4 days); 168 hours (7 days); and, 336 hours (14 days). Four replicates were prepared for each of these combinations.

As before, approximately 1 g of the previously-prepared sandstone was weighed into each of the reaction vials; the actual mass was recorded for later calculations. Stock solutions of zinc nitrate were prepared in deionised water to produce daughter solutions of zinc at the four concentrations specified above. 5 litres of each concentration were prepared in 10-litre white plastic buckets, carefully marked accordingly. A tight-fitting lid was kept in place at all times to prevent both contamination by dust, and evaporation. However, a further consideration was to allow enough exposure of the solutions to the atmosphere. Given that the solutions were prepared using deionised water, their limited buffering capacity was deemed a potential liability due to the sensitivity to atmospheric CO_2, which could form carbonic acid thus reducing pH. By leaving the prepared solutions in large

buckets (with a fitted lid, nevertheless) for several days, the solutions would have time to equilibrate with the atmosphere and thus be of similar starting pH. The buckets containing the solutions were opened and stirred intermittently to promote this endeavour.

The pH of each vial was measured (in triplicate, and averaged), but not adjusted in any way, at the beginning and end of the reaction time. Similarly, temperature changes were measured but not controlled. Initial Zn concentration was confirmed by analysis of the original solutions. The samples were analysed, using ICP-MS, for the following dissolved elements: Zn, B, Mg, Al, Ca, Mn, Fe, Cu, Cd, Ba.

4.4.2.5 Results

The results have been combined and summarised so as to show the relationships between time and attachment behaviour, and also the interrelations between the various ions as the experiments proceeded toward equilibrium.

Variation of Attachment with Time

Figure 4-8 shows how Zn interacted with the sandstone over time.

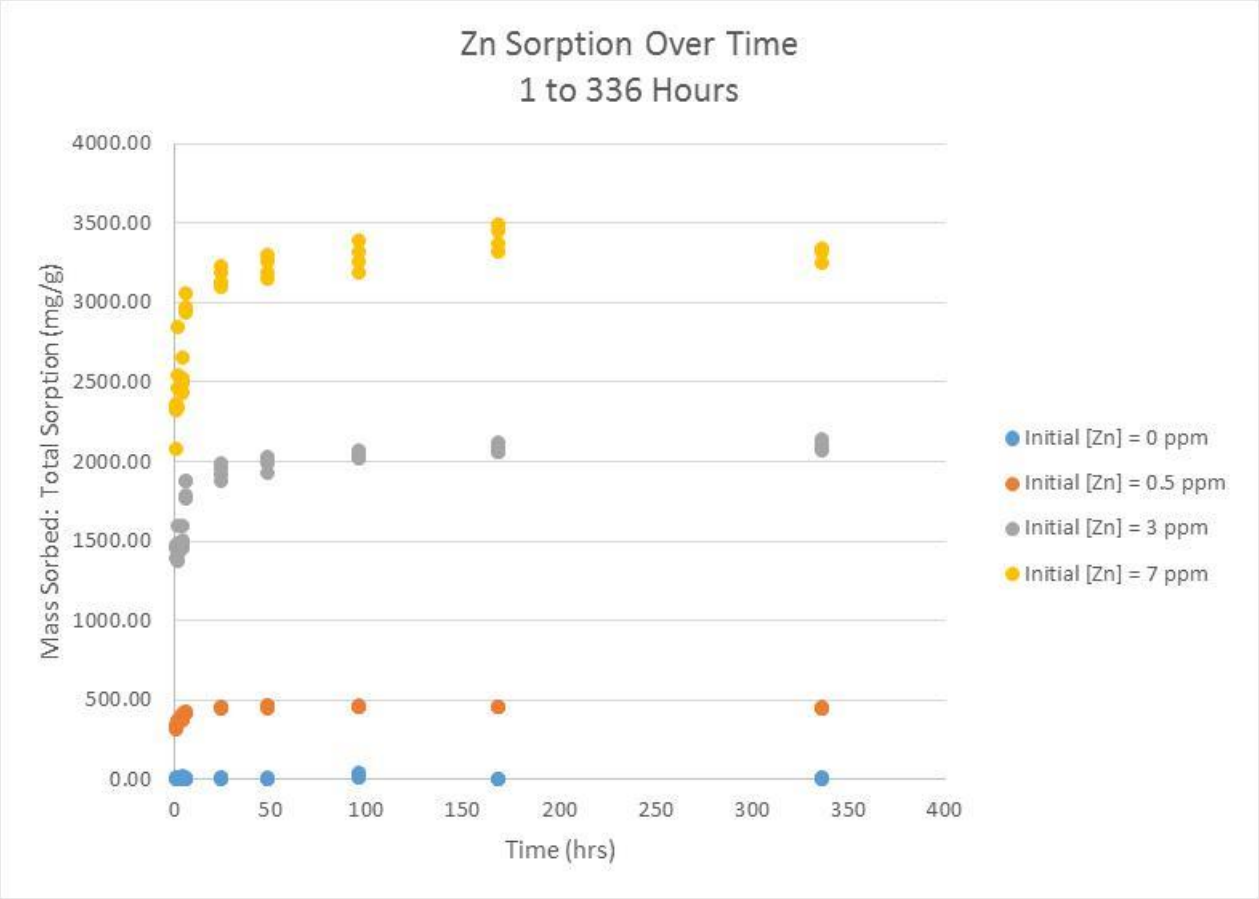

Figure 4-8: Variation of sorbed concentration with time

In all of the batches - with the exception of the 0 ppm batch - there appears to be a rapid initial phase, when most of the attachment occurs within 48 hours. After this, some degree of attachment continues, albeit at a much slower rate, until the system reaches complete equilibrium at approximately 170 hours. This “two-phase” effect seems to be more pronounced for the higher initial concentrations of Zn.

Behaviour of Competing Ions

The next aspects of interest related to how ions, presumably pre-existing upon the surface of the sandstone, would behave as the Zn sorbed to it. This is most clearly illustrated by considering the 7 ppm batch (Figure 4-9) on the next page.

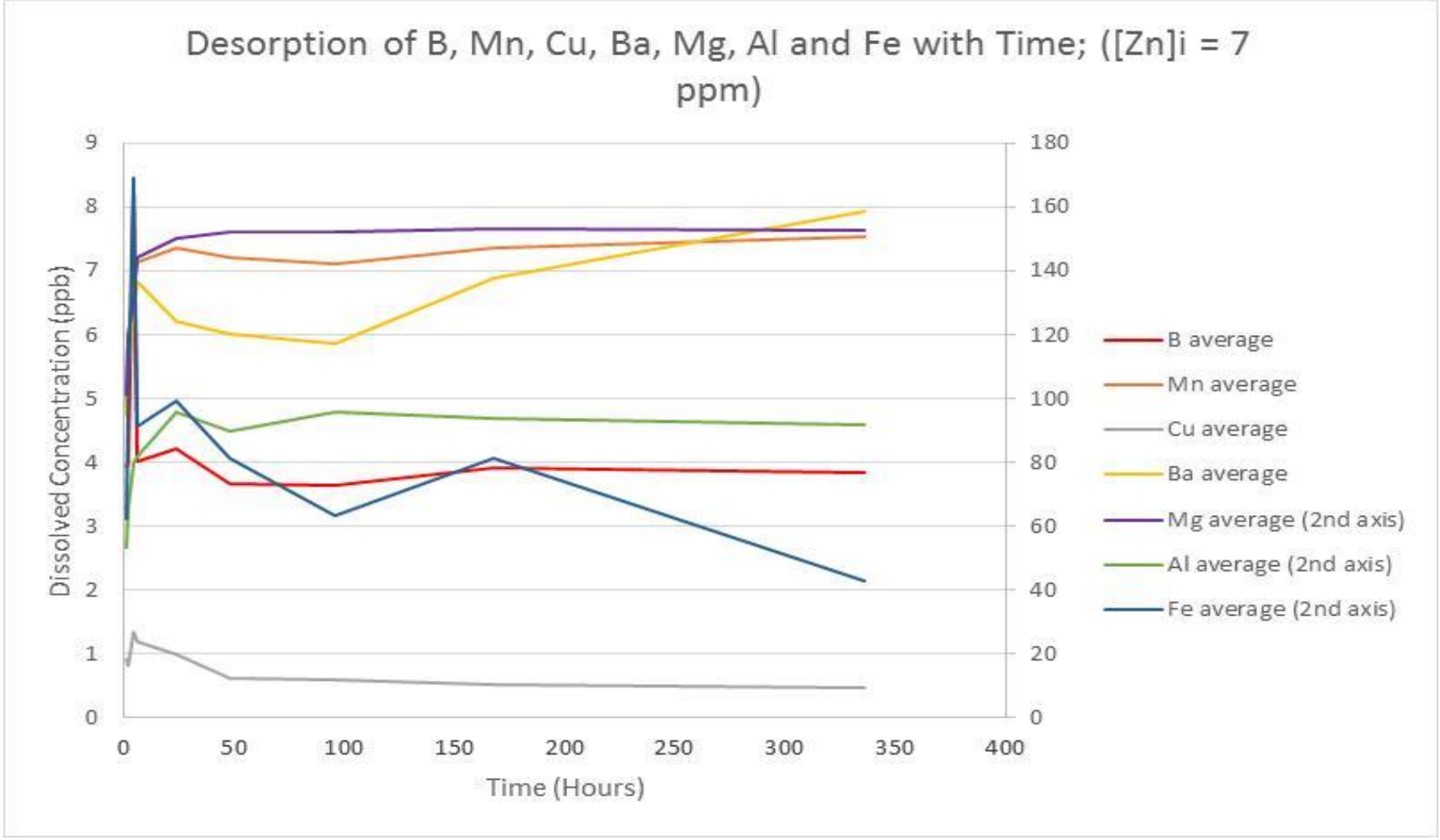

Figure 4-9: Desorption with time

Examination of the results show that Mg, Mn and Al concentrations rapidly increase within the first 24-48 hours, and steadily level off thereafter. Fe has a rather erratic pattern, but arguably exhibiting a decreasing trend, after an initial rapid increase. Cu shows a modest initial rise before levelling off. B is again somewhat erratic, but exhibits no overall trend. Mg, Fe, and Al concentrations greatly exceed those of the other elements.

Figure 4-10 now looks more closely at the relationships between Zn, Ca and Mg over time (next page).

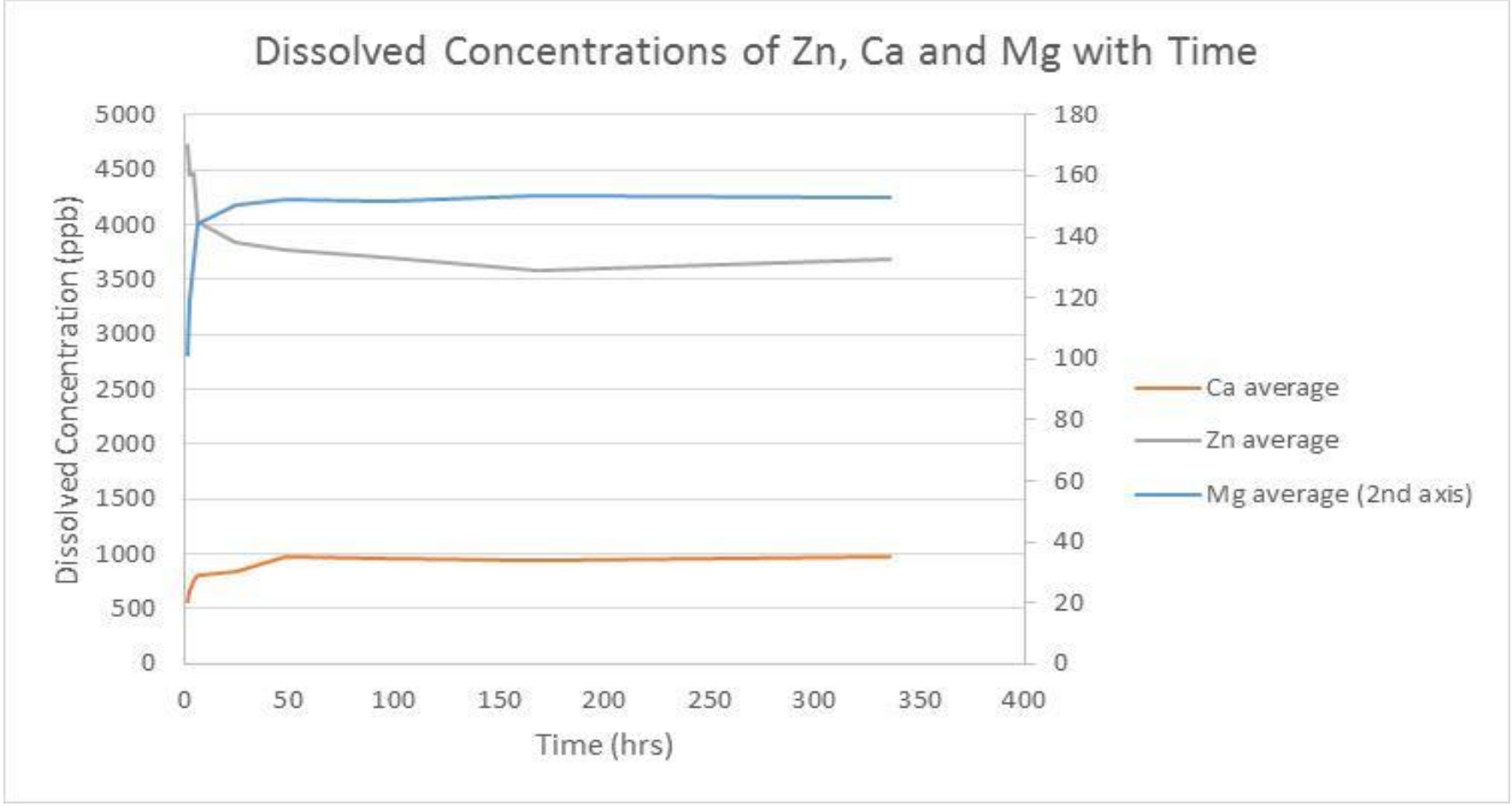

Figure 4-10: Dissolved concentrations with time

Here, as the Zn concentration falls (as attachment progresses), both Ca and Mg increase, almost in a mirror pattern. In summary, Zn is replaced from solution mainly by Ca, Mg and Al (Al may indicate the presence of particulate material (e.g. gibbsite) but for now will be assumed dissolved as the pH is low). Zn concentration drops by about 0.054 mmol/L, and Ca, Mg and Al rise by about 0.025, 0.006 and 0.034 mmol/L respectively, i.e. in total by a little more than the fall in Zn (0.065 compared with 0.055 mmol/L). However, such calculations are necessarily approximate given the absence of knowledge of other processes, and ignore pH change (see below).

pH-Temperature Relationship

Figure 4-11 suggests that there is no significant relationship between pH and temperature (e.g. via CO_2 dissolution).

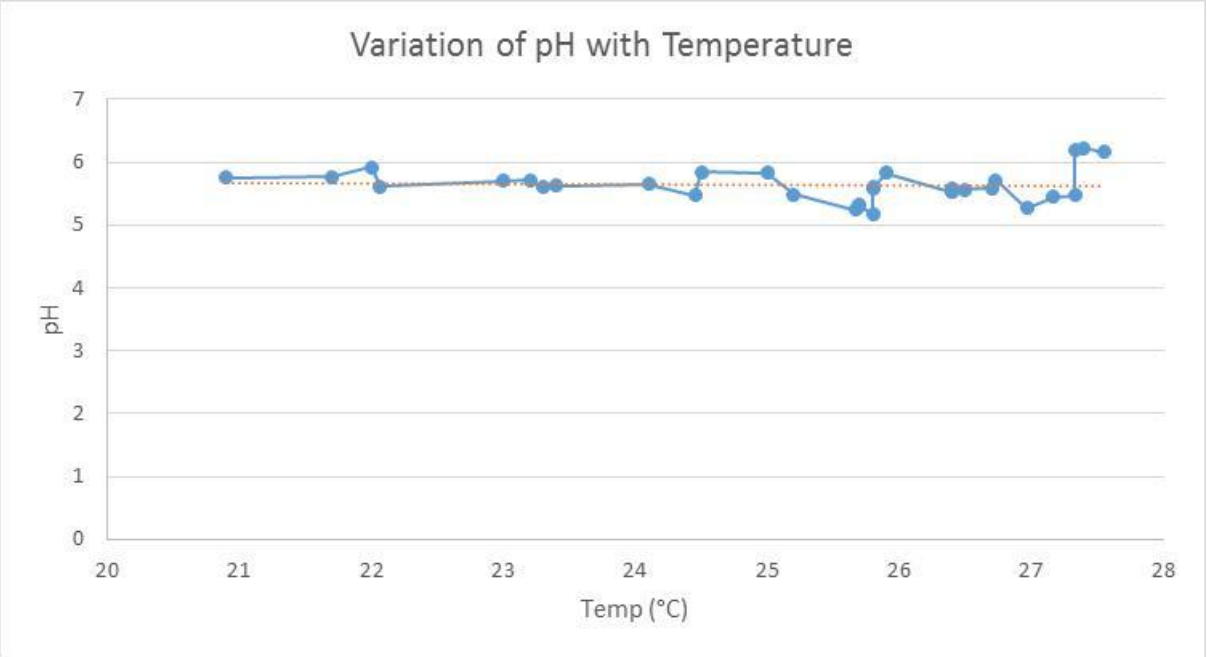

Figure 4-11: Variation of pH with temperature

pH Variation with Time

Figures 4-12 and 4-13 show how the pH of the batch experiments changed over time.

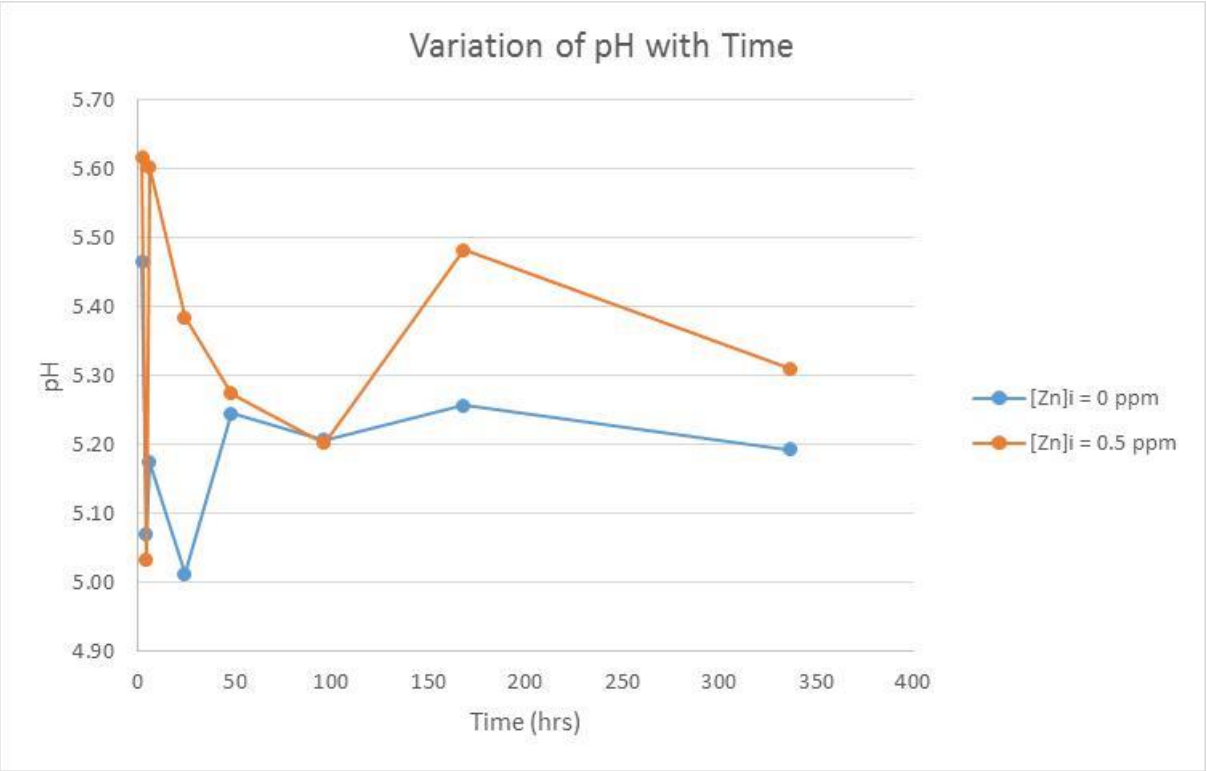

Figure 4-12: Variation of pH with time (i)

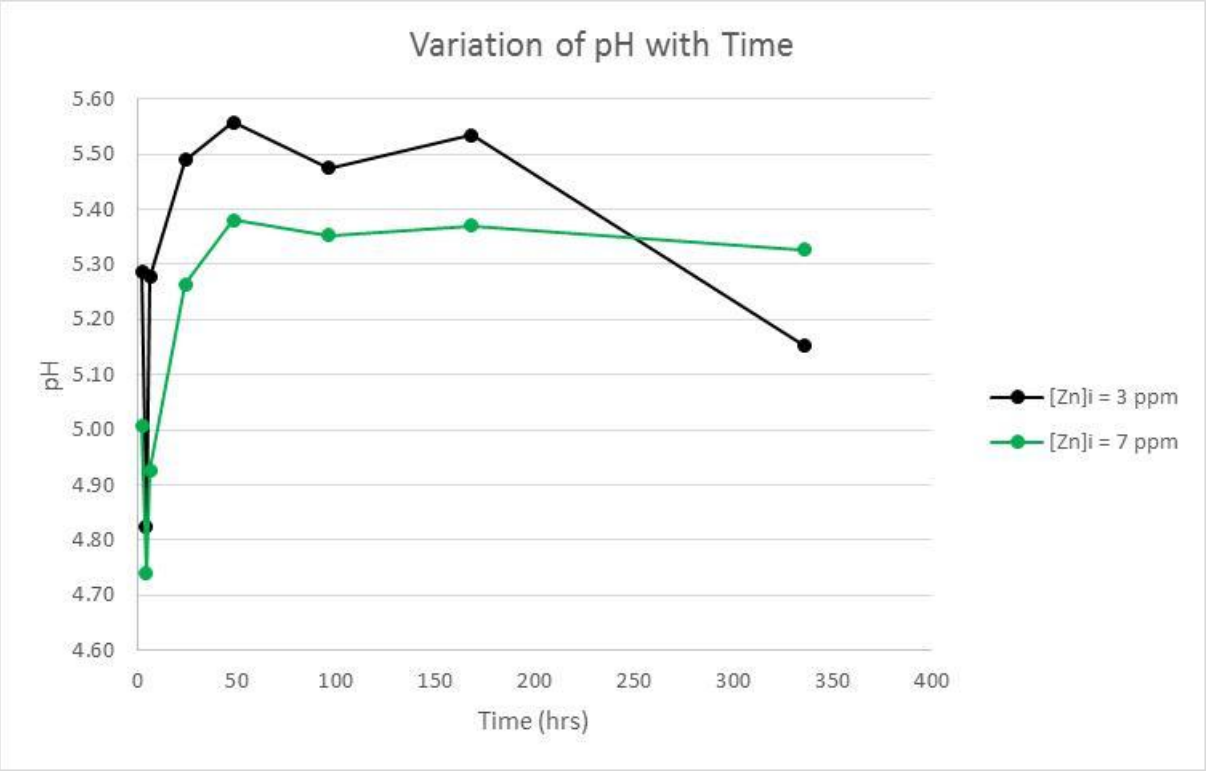

Figure 4-13: Variation of pH with time (ii)

The general pattern seems to be a significant drop in pH at 4-6 hours (compared to the pH at 1 hour), followed by steadily increasing pH up to about 48 hours. Thereafter, the pH generally became rather more stable. This pattern is more pronounced for the higher concentrations of Zn; the pattern is less clear at the lower concentrations. For the 7ppm experiments, the drop in H^+ concentration calculated from the pH change amounts to 0.016 mmol/L: the sum $[Zn] + [Ca] + [Mg] + [Al] + [H^+] = 0.055 – 0.025 – 0.006 – 0.034 + 0.016 = -0.006$ mmol/L. This is a mass balance difference of < 10% of the drop in Zn and H^+ concentrations, even ignoring other elements measured (~0.0006 mmol/L) and unmeasured.

4.4.2.6 Discussion: Implications for Subsequent Experiments

Zn Attachment over Time

The results appear to show that there are two distinct phases of attachment: a rapid phase, taking place within 48 hours, where the majority of the available Zn is sorbed, followed by a longer-lasting phase where the remaining Zn is sorbed much more slowly as the system approaches equilibrium. However, the period of time taken to reach equilibrium was much longer than anticipated, and clearly the experiment must be run for much more than six hours (as in the scoping study). The levelling-off generally began by five days.

Behaviour of Competing Ions

It is clear that Ca and Mg are markedly affected by Zn attachment. The results suggest that these ions were initially present on the surface of the sandstone grains, but were displaced by the introduction of the Zn. They could be thought of as "competing" ions, since this behaviour would imply that they were previously occupying the *sites* that the Zn ions displaced them from; it is unclear at this stage whether they were present on exchange or sorption sites. Nevertheless, it raises interesting questions as to how Zn would interact given much higher concentrations of Mg and Ca, and confirms that measures need to be taken to suppress ion exchange if sorption is to be unambiguously identified.

pH-Temperature Relationship

It is interesting to note that the results do not support the hypothesis that temperature would influence the pH of the system. This is, in fact, a helpful result

since it would complicate future experiments if temperature had to be tightly controlled.

pH Variation with Time

The pH variation over time seems to reflect the attachment-time behaviour of the main ions of interest, especially Zn. In qualitative terms the pH changes may be explainable in the following way: Precautions had been taken to ensure that the solutions were in equilibrium with the atmosphere, and hence initial pHs would have been around 5.8. On addition of the Zn, some of the oxide surfaces would be expected to sorb the Zn, replacing various ions but including H^+. This explains the low pH at early times in the experiment. However, this then would result in re-equilibration with the CO_2 content of the atmosphere (CO_2 degassing), and the pH would rise, finding an equilibrium slightly lower than the initial pH. In detail, the reactions occurring will be rather more complex, involving other ions and more than one type of surface. Further quantification has not been undertaken given the trial nature of this experiment, this being left to the final series of experiments.

4.4.2.7 Summary of the Experiment

This experiment sought to investigate the temporal influences on sorption. By running a series of batch experiments for periods of time between 1 and 336 hours, “snapshots” of the attachment process were made available for different points in time. The main conclusions were:

- There appears to be a two-phase attachment process occurring. Most attachment occurs during the “fast phase”, up to 48 hours from the start of the reaction. There is then a slower phase, continuing - albeit at a much slower rate - until the system finally reaches equilibrium at approximately 170 hours. This “two-phase” effect seems to be more pronounced for situations where there is a higher initial concentration of Zn.
- Ions such as Ca and Mg (and others, but to a lesser extent) mirror the behaviour of Zn attachment. This suggests that these ions were present on the surface prior to the start of the experiments. Such is the degree of mirroring that these ions could be thought of as *competing* for sites on the surface.

The experiment suggests the existence of pH-related impacts, as is expected, and also indicates interaction with atmospheric CO_2 is important.

4.4.3 A Study of the Initial Conditions on the Surface of the Sandstone

4.4.3.1 Introduction

A potential problem of applying the theory suggested by Dzombak and Morel (1990) is that it is built upon experiments on freshly precipitated pure ferric oxides (‘HFO’) in the simple system Fe-H_2O(-CO_2), with no other ions available for attaching to the surfaces. Of course, natural sandstone consists of a range of minerals, its oxides are aged haematite, rather than HFO, and its initial surface conditions could be complex. This was exemplified by the previous kinetic

experiments, which indicated that there were other ions pre-existing on the (oxide and clay) surfaces of the sandstone, and which were displaced as Zn ions sorbed to the surface.

4.4.3.2 Purpose of the Experiment

This experiment sought to discover a way to bring some control to this uncertainty. The main aims were to determine if the following could be achieved:

- Remove whatever ions were present on the sandstone oxide surfaces and replace them by H^+, i.e. devise a way of preparing the sorption surfaces such that initial conditions prior to any Zn sorption would be known;
- Replace exchange surface ions by one ion and maintain the dominance of that ion as other concentrations change, i.e. devise a way that during Zn sorption experiments Zn did not significantly participate in ion exchange reactions.

In effect, the experiment attempted to determine if significant exchange and sorption could be prevented from occurring: if it could be, then the techniques could be used in stopping ion exchange and limiting sorption when trying to determine Zn sorption of the sandstone oxides.

4.4.3.3 Experimental Approach

Two main steps were required to achieve the aims of this experiment.

1. The first step was designed to saturate the exchange sites with 1000 mg/l of Na (as $Na(NO_3)_2$) at a relatively low pH of ~4. The rationale for using such a high concentration of Na is that it should displace any exchangeable

ions bound to the sites; the low pH was intended to displace metals from the sorption sites due to the high concentration of H^+. The surface exchange sites should then be occupied by Na^+ ions, though these would not compete significantly with H^+ on sorption surfaces. Analysing the resultant solution for Ca, as an indicator of ions that would participate in exchange and sorption, K, as an indicator of ions that would be predominantly affected by sorption, and Zn because the presence of any background Zn needs to be known. Using Na as a displacing ion is important as it is thought not to be involved in oxide sorption (Dzombak and Morel, 1990); however, it does mean that the full composition of the exchange surfaces cannot be determined in this experiment.

2. The second step was to carry out a Zn sorption experiment whilst maintaining a high background concentration of Na to limit exchange and a low pH to limit sorption.

4.4.3.4 Materials and Methods

The experiment used the same 50 ml centrifuge tubes and prepared sandstone as in the previous experiments. There were two main steps separated by an intermediate rinse step, as follows:

Step 1: Removal of Exchangeable and Sorbed Ions; Saturation of Exchangeable Sites

1 g of prepared sandstone was weighed into 30 reaction vials; 3 blanks were also

prepared, containing no sandstone. 40 ml of 1,000 ppm $NaNO_3$ was added to each vial. The pH was measured and then adjusted by adding drops of nitric acid until the solution reached pH 4. The vials were placed on a shaker at 100 rpm and agitated for 6 hours; they were briefly interrupted at 2 hours and at 4 hours to monitor and re-adjust the pH, as necessary.

After 6 hours, the vials were removed from the shaker and centrifuged at 4,500 rpm for 5 mins. Using a 10 ml syringe, the supernatant was injected into a new vial, via a 0.45 µm disposable filter. After measuring the final pH, the solutions were acidified using 1 % HNO_3 and prepared for analysis by FAAS to determine concentrations of Zn, Ca and K.

Intermediate Step: Rinsing of Sandstone

The sandstone remaining in the reaction vials was poured onto Whatman No. 1 filter paper placed on a Büchner funnel. Approximately 100 ml of deionised water was used to rinse the sandstone. The filter paper was then removed from the Buchner funnel, folded, and placed into the appropriate reaction vial for Step 2.

Step 2: Sorption of Zn whilst maintaining saturated ion exchange sites

In the second step, the intention was to maintain a high background concentration of sodium - to keep ion exchange sites saturated – and encouraging Zn to sorb to the sorption sites. This time, two concentrations of sodium were used (250 ppm and 1000 ppm) in order to produce two markedly different ionic strengths. Zinc

solutions were prepared using zinc nitrate hexahydrate to give zinc at the following concentrations: 0 ppm, 0.5 ppm, 1 ppm, 3 ppm and 7 ppm.

The sandstone was fully rinsed off the filter paper and into the reaction vial using a 10 ml syringe filled with the new $Zn(NO_3)_2$ / $NaNO_3$ solution. This action continued until the required 40 ml of the solution had been added. The filter paper was removed from the vial and the pH of the solution measured (but not adjusted). The vials were placed on the shaker at 100 rpm for 12 hours (overnight).

At the end of the experiment, the final pH was recorded, and the solutions centrifuged, filtered and acidified, as before, in preparation for analysis by FAAS, again to determine the concentrations of Zn, Ca and K.

4.4.3.5 Results

4.4.3.5.1 Results for Step 1

The results for step 1 are shown below (Figure 4-14 and Table 4-2):

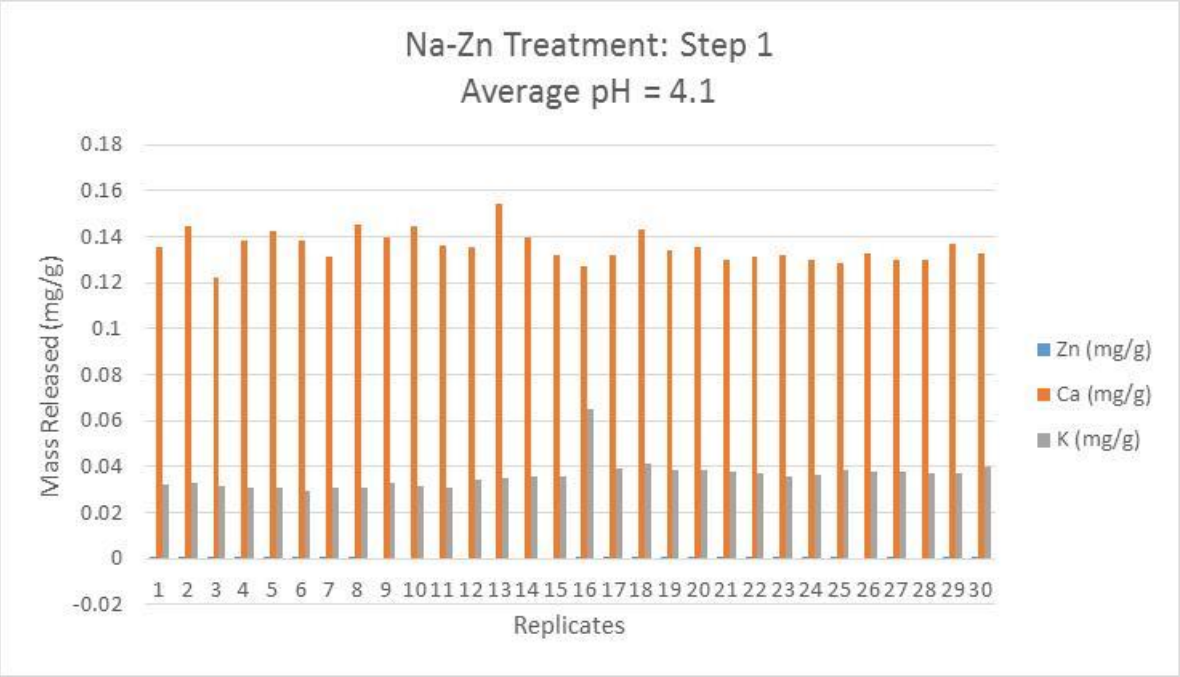

Figure 4-14: Na-Zn treatment: step 1

Table 4-2: Results of FAAS analysis for all vials after Step 1 of the experiment: treatment with 1000 ppm Na

Average Masses of Ions Released			Equilibrium pH
Zn (mg/g)	Ca (mg/g)	K (mg/g)	
<DL	0.136	0.036	4.1

The data from the first step of the experiment show that, upon addition of 1000 ppm Na (as $NaNO_3$) and reduction of pH to approximately 4.1, both Ca and K were released from the sandstone, with Ca exhibiting a higher concentration than K by an order of magnitude. Zn mass released, as expected, was very small in comparison with Ca and K.

4.4.3.5.2 Results for Step 2

Figures 4-15 and 4-16 show the equilibrium surface concentrations of Zn, and the mass of Ca and K released per unit sandstone mass, and also the pH, in relation to the initial Zn concentration that was added. The plots are divided to separately show the results for the situations where there was a background Na concentration of 250 ppm and 1000 ppm, respectively.

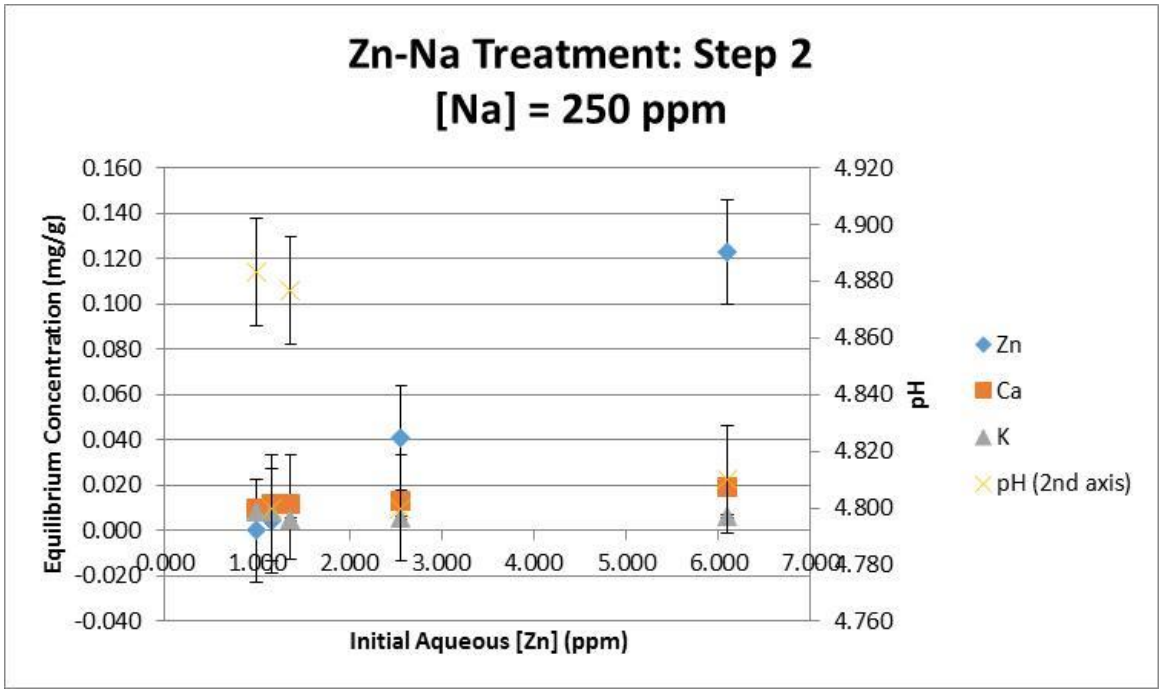

Figure 4-15: the sorbed concentration of Zn and the mass of Ca and K released per unit mass of sandstone as a function of the initial Zn concentration for the experiments involving 250 ppm Na in step 2

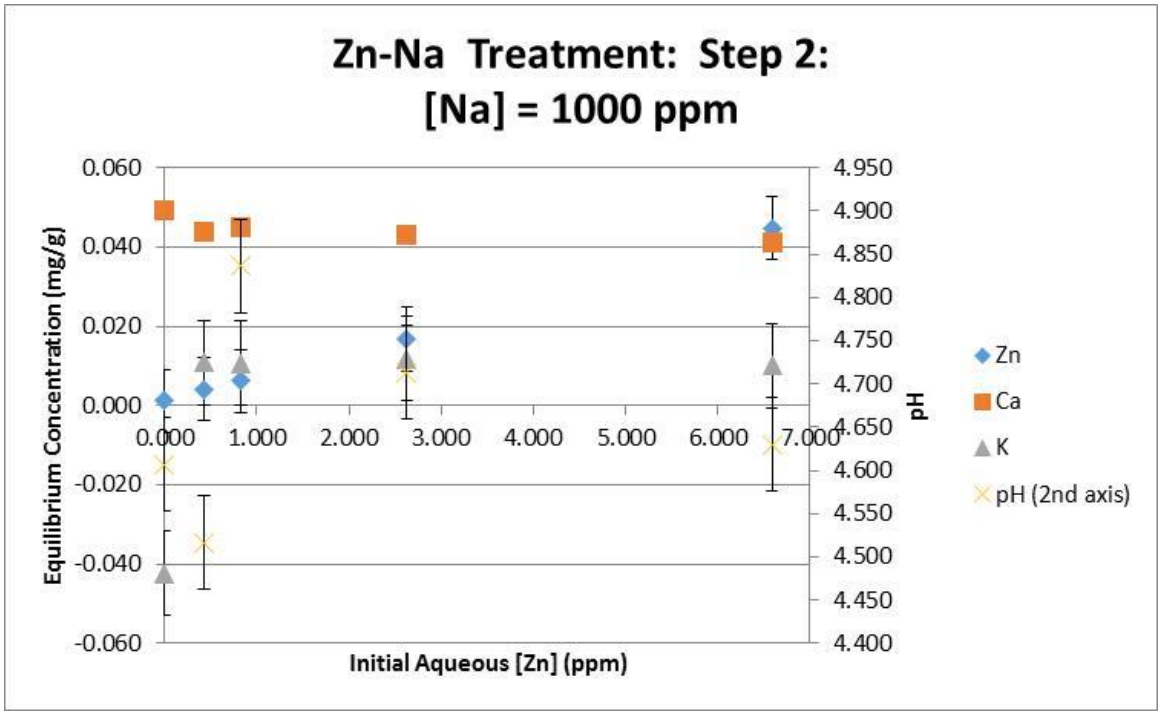

Figure 4-16: The sorbed concentration of Zn and the mass of Ca and K released per unit mass of sandstone as a function of the initial Zn concentration for the experiments involving 1000 ppm Na in step 2.

Here, Ca and K do not change much as the Zn concentration increases, but the overall release of both is somewhat higher when the Na concentration is higher. The pH exhibits only mild fluctuations as the Zn concentration increases.

The next two figures (Figures 4-17 and 4-18) show isotherms for the Zn for the two different Na concentrations. They exhibit an almost exactly linear sorption isotherm, with markedly similar "K_d" values of approximately 0.039 L/g.

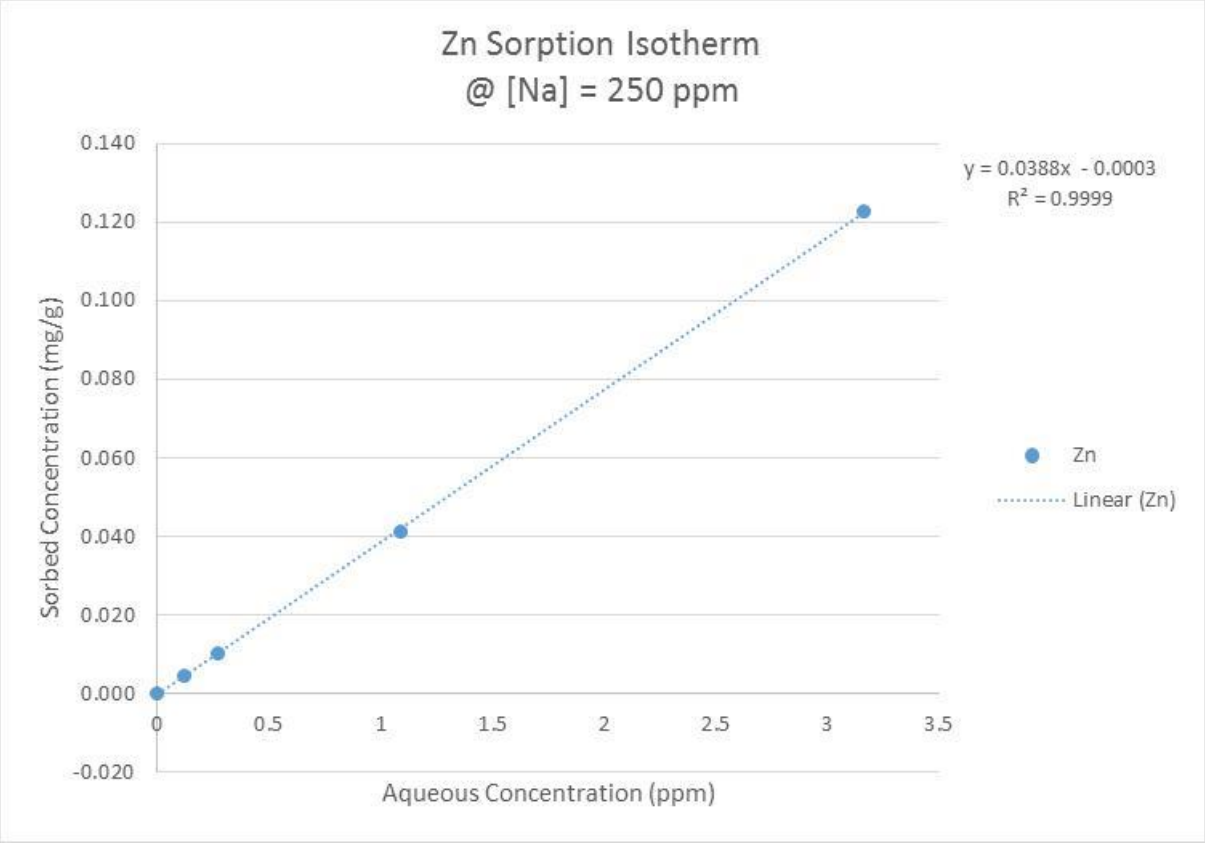

Figure 4-17: Zn attachment isotherm for the experiments involving 250 ppm Na in step 2

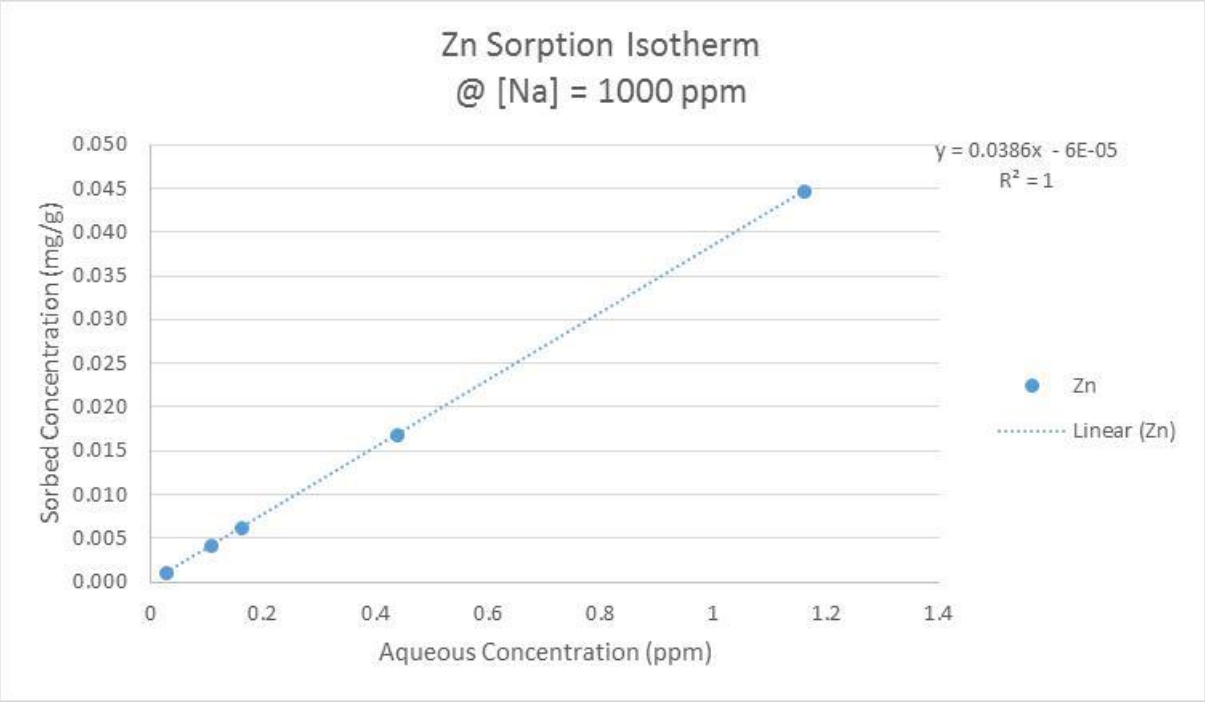

Figure 4-18: Zn attachment isotherm for the experiments involving 1000 ppm Na in step 2

4.4.3.6 Discussion

The experiment produced credible data in that there was good consistency between replicates, and good correlation between the two batches, with almost identical, linear isotherms produced for Zn sorption in step 2. (The results for Step 2 of the experiment must be treated with some caution due to a possible minor systematic experimental error in producing the initial solutions. This may explain some of the difference in the absolute Zn concentration values between the two sets of data.)

It is clear from the results (Figures 4-15 and 4-16) that the low pH and very high Na concentrations used have not stopped attachment of Zn. The small Ca and K concentrations are independent of the Zn concentrations but are dependent on the

Na concentration. These observations would be explained by the low masses of both Ca and K being released from exchange sites by displacement by Na: the Na/Ca and Na/K concentration ratios when the Na was added in stage 2 would have been rather greater than the ratios at the end of stage 1, as the stage 1 solutions contained Ca and K that had been displaced from the exchange surfaces. The pH remained approximately the same in both stages of the experiment, so release of Ca from sorption sites seems unlikely, and this is consistent with Ca behaving very similarly to K (both approximately double their concentrations as Na rises). Dissolution may be a contributing factor for both Ca and K concentrations, but the dependence on Na concentration suggests that it is not the dominant process. The Zn concentrations are not a function of the Na concentrations. Zn may be sorbing to oxides but, if so, the pH would be expected to have changed; it seems more likely that the Zn is mainly exchanging with Na. The linear isotherms can be explained by recognising that the ratio of Na concentrations in solution to that on exchange sites is effectively constant, and the selectivity coefficient equation collapses to a K_d equation. The idea that ion exchange is dominant is given more weight by observing that the Dzombak and Morel (1990) theory suggests that at pH 4.75, the amount of Zn sorption on HFO would be limited to less than 10% of the Zn mass, which is in contrast to this experimental result showing that more than 80% of the Zn is sorbed / exchanged. In summary, the results are consistent with sorption being limited by low pH and ion exchange by high Na concentrations, but that the latter do not reduce ion exchange of Ca, K, or Zn to insignificant levels.

The implications of this experiment are therefore that:

- ion exchange cannot be made insignificant by use of high Na concentrations; use of even higher Na concentrations will take the experiments outside the range of fresh groundwater ionic strengths;
- the presence of Ca and K suggest that it is difficult to completely eliminate the presence of other ions;
- high concentrations of Na mean that ion exchange for low concentrations of other ions are rendered simpler – in this case linear isotherms – and competition between Zn and other exchanged ions looks to be very limited.

It is concluded that use of a high Na background is useful, but that any interpretation of sorption experiments it will be necessary to model ion exchange as well as sorption.

4.4.3.7 Summary of the Experiment

This experiment was designed to offer a way of controlling the otherwise-uncertain initial chemical conditions of the sandstone surfaces, before carrying out sorption experiments using Zn.

A two-step protocol was designed, whereby the sandstone was first treated with high Na (1000 ppm) at a pH of 4. The intention of this was to displace exchangeable ions from their sites by Na, and sorbed cations from their sites by H^+ ions. By the end of this operation, the initial conditions on the surface sites could be expected to consist of almost only Na on the exchange sites, and almost only H^+ ions on the sorption sites. The second step of the experiment involved

maintaining the high background Na levels and low pH, whilst introducing increasing concentrations of Zn.

The first step of the experiment showed that Ca and K were important components on the surfaces initially. Once these were removed and Zn was introduced to the system, it was found that Zn attached with a linear isotherm. Though Ca and K were also present in small amounts, their concentrations were independent of Zn concentrations, though were dependent on Na concentrations. These observations are consistent with ion exchange involving all four elements.

The implications of these findings are that ion exchange cannot be controlled as effectively as sorption and, if excessively high Na concentrations are to be avoided, it will be necessary to include representation of ion exchange in the interpretation of any sorption experiment data. Nevertheless, the low pH / high Na concentration conditioning of the sandstone would help make initial conditions simpler and probably facilitate interpretation.

4.4.4 Experiment to Distinguish Ion Exchange and Sorption Processes

4.4.4.1 Introduction

From the results of the previous experiment, it is clear that it is essential to be able to distinguish between sorption and ion exchange and to quantify their respective

contributions. The experiment described in this section was the first attempt at achieving this.

4.4.4.2 Purpose of the Experiment

The objectives of this experiment were to:

- distinguish between the ion exchange and sorption processes operating between the sandstone surface and the aqueous phase;
- quantify and compare the contribution of each process.

4.4.4.3 Experimental Approach

The basic necessity was to find a way to separate the sorption and ion exchange processes. One way to do this was to suppress the ion exchange component and proceed with a sorption-only reaction, and *vice versa*. This would require treating the sandstone in two comparative ways:

- First, introducing agents that would bind to the surface almost exclusively by ion exchange, for example ammonium (Appelo & Postma, 2007);
- Second, introducing agents that would bind to the surface almost exclusively by sorption.

By presenting the agents in sufficiently-high concentrations, they may completely saturate the respective sites, causing ions that were previously present on the surface to be displaced and become free ions in solution. These could then be measured using FAAS.

The experiment was divided into two steps:

1. The first step was to flush the exchange sites with a high concentration of an ion that would not be present on the exchange surfaces of the sandstone. The ion chosen was ammonium (as ammonium nitrate).
    - Ammonium does not specifically sorb (Dzombak and Morel, 1990), but it will participate in exchange reactions, potentially with ions that would otherwise sorb – for instance, calcium. It was assumed that ammonium would *not* bind to any sorption sites.
    - Using a high concentration could be expected to ensure that ammonium would dominate the exchange sites, thus displacing any existing ions bound to the exchange sites.
    - Analysing for these ions then gives an approximate measure of what exchangeable ions were present on the sandstone initially.
    - However, it is possible that the relative concentrations of the ions displaced from the exchange surfaces into solution will be modified by sorption, but this cannot be avoided: if the pH remains the same, the total amount of attached ions should remain almost constant.

2. The second step was to displace ions from the sorption sites.
    - In a manner similar to the first step, a high concentration of strontium (as strontium nitrate) ions were used: strontium ions will not be present in significant amounts on the sandstone.
    - These were assumed to bind to both the sorption sites and the ion exchange sites, but by measuring ion concentrations other than NH_4^+, a measure of sorbed ions would be obtained.

- To ensure that the strontium was present in excess, two concentrations were used: 250 mg/l and 300 mg/l. If present in excess, it would be expected that the results of the analysis for both of these concentrations would be the same. If the results were different, then the strontium was not present in excess, and the results would be less certain.

4.4.4.4 Materials and Methods

4.4.4.4.1 Introduction

This experiment used the general batch method outlined in the first experiment, and used the prepared sandstone sample described there. Adaptations to the general batch method are now described.

4.4.4.4.2 Preparation

A solution of 1000 mg/l ammonium (as ammonium nitrate) was prepared for the first step of the experiment, to saturate the exchange sites. For the second step – saturation of the sorption sites – a stock solution of 1000 mg/l strontium nitrate was prepared, along with daughter solutions of 250 mg/l and 300 mg/l.

50 ml centrifuge tubes were again used as the reaction vessels, prepared in triplicate for each batch reaction. Approximately 1 g of sandstone (exact mass recorded for later calculations) was weighed into each centrifuge tube, except for those designated as controls.

The concentrations of NH_4 and Sr solutions were such that the mass of NH_4 and Sr greatly exceeded the expected total cation exchange capacity of the sandstone.

4.4.4.4.3 Execution

Table 4-3 summarises the scheme of treatments applied to the sandstone.

Table 4-3: Summary of the treatments as applied to the sandstone to distinguish the respective contributions of ion exchange and sorption

STAGE 1 TREATMENT	STAGE 2 TREATMENT
NH_4NO_3 (1000 ppm) for 24 hrs	$Sr(NO_3)_2$ (250 ppm) for 5 days
	$Sr(NO_3)_2$ (300 ppm) for 5 days
NH_4NO_3 (1000 ppm) for 5 days	$Sr(NO_3)_2$ (250 ppm) for 5 days
	$Sr(NO_3)_2$ (300 ppm) for 5 days
$Sr(NO_3)_2$ (250 ppm) for 24 hrs	N / A [END]
$Sr(NO_3)_2$ (300 ppm) for 24 hrs	N / A [END]

4.4.4.4.4 Stage 1 – Extraction of Exchangeable Ions

40 ml of NH_4NO_3 was added to each of the reaction vials containing sandstone (and to the blanks containing no sandstone). The vials were placed on a shaker at 100 rpm and left for the duration detailed in Table 4-3. The pH was measured at the start of the experiment, but was not controlled. At the end of the required time,

the vials were removed from the shaker and centrifuged at 4,500 rpm for 5 mins. The supernatant was then filtered, using a 0.45 µm disposable syringe filter, into a new vial. The final pH was recorded. Finally, this solution was acidified using 1% HNO_3; a 2% LaCL buffer added (to reduce interference), and analysed by FAAS for the concentrations of Zn, Ca, Sr, Mg, K, Na, and Mn.

4.4.4.4.5 Intermediate Rinse Step

The sandstone remaining in the reaction vials from Step 1 was transferred onto Whatman No. 1 filter paper placed on a Büchner funnel. A fresh filter paper[2] was used for each replicate, identified with a simple numbering scheme. The sandstone was then thoroughly rinsed with approximately 50 ml of deionised water under the influence of a mild vacuum. Upon conclusion of rinsing, the filter paper was removed from the Büchner funnel, folded, and placed into a designated new reaction vial in preparation for the next stage.

4.4.4.4.6 Stage 2 – Extraction of Sorbed Ions

In the new vials, a 10 ml syringe was used repeatedly to add 40 ml of the new strontium nitrate solution, directing the nozzle at the filter papers to dislodge the rinsed sandstone grains from the filter papers into the vials. The filter papers were removed from the vial and retained. The "initial" pH was measured, and the vials replaced on the shaker at 100 rpm for the required time (see Table 4-3). On

[2] The filter papers were weighed before use; after use, they were oven-dried at 60°C for 48 hrs and weighed again. Any increase in mass was assumed to indicate that fine sandstone, clay or other particles were retained on the filter paper. The average mass involved was 0.04 g (approx. 3.8 % of the original mass of sandstone.) This difference was later subtracted from the known mass of sandstone in the calculations for Part 2.

completion of shaking, they were centrifuged and filtered using the same method as Step 1. After recording the final pH, the solutions were prepared for, and analysed by, FAAS, in the same way as Step 1.

4.4.4.5 Results

Figure 4-19 shows the release of ions (as milligrammes per gramme of solid) of Zn, Ca, Mg, K, Na and Mn, for each treatment of the sandstone. Figure 4-20 shows the final pH. In Figure 4-19, recounting from left to right:

- groups i-iv relate to “Stage 1” of the experiment;
- groups v-viii relate to “Stage 2”.

The results from Stage 1 will now be discussed. Groups i and ii (treated with 1000 mg/l NH_4NO_3) show very little difference in the concentrations of ions released with respect to time, and the pH is stable at approximately 4.65. The main ions released are Na, Ca, K and Mn, in descending order of magnitude. This is unusual as Ca is normally dominant on exchange sites in the sandstone (e.g. Carlyle et al., 2004): however, this sandstone contains negligible carbonate, and hence Ca concentrations in its groundwaters are expected to be low. Groups iii and iv (treated with either 250 or 300 mg/l $Sr(NO_3)_2$) exhibit a very similar pattern of ion release to the NH_4NO_3 groups, but with marginally higher concentrations of Na, Ca and K. There appears to be a slight difference between the two concentrations of $Sr(NO_3)_2$, with the 300 ppm treatment showing slightly higher release of Na and Ca than the 250 ppm treatment.

The description now turns to the results of Stage 2. Groups v to viii exhibit interrelated patterns of minimal release of Ca, Na and K. Upon treatment with $Sr(NO_3)_2$, the two groups which had been previously treated with NH_4NO_3 for 5 days showed slightly less release of ions than did the groups that had been previously treated with NH_4NO_3 for 24 hrs. Table 4-4 lists the masses released.

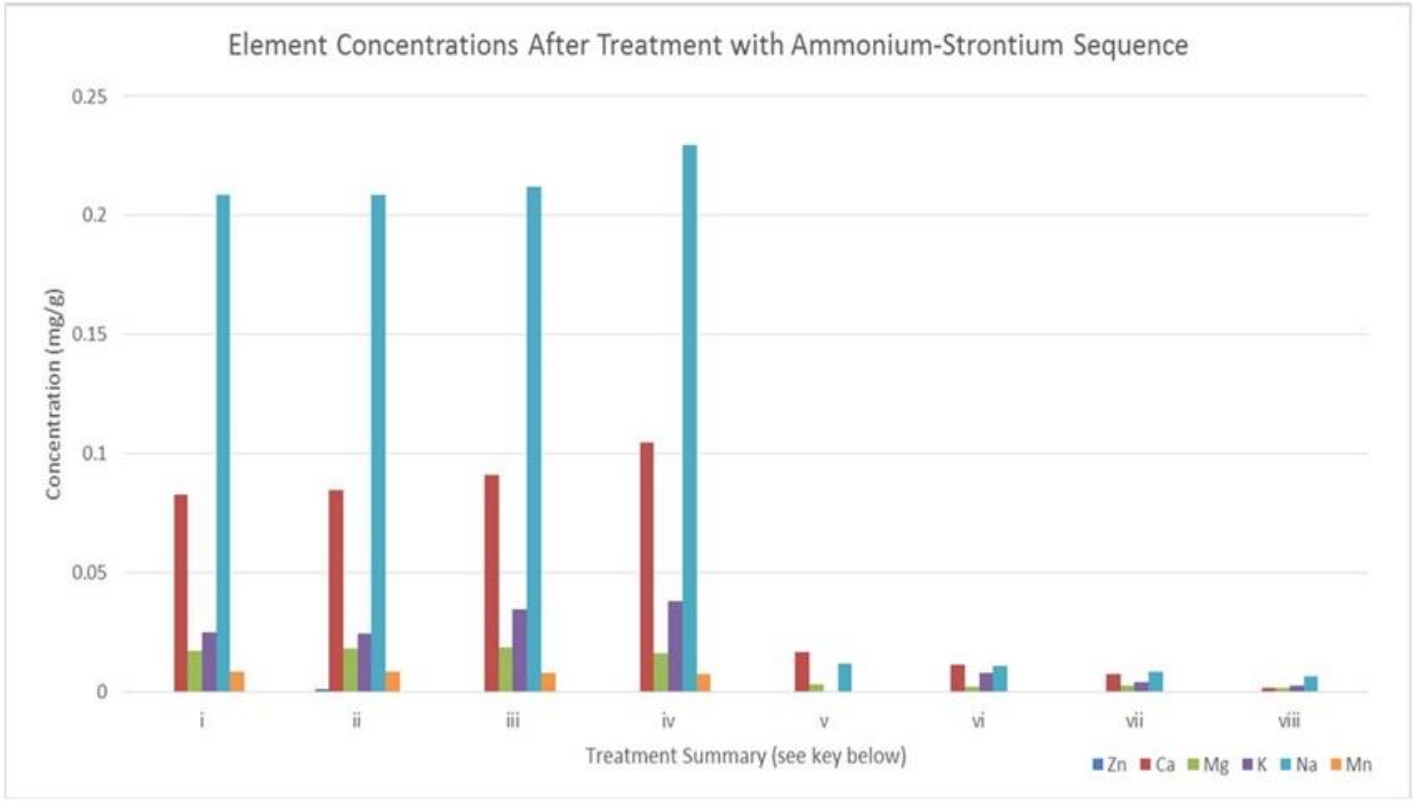

Figure 4-19: Element concentrations emanating from the sandstone after ammonium-strontium treatment

The treatment stages are summarised in Table 4-3; the key is as follows: i: 1000 ppm NH_4NO_3 for 24 hrs; ii: 1000 ppm NH_4NO_3 for 5 days; iii: 250 ppm $Sr(NO_3)_2$ for 24 hrs; iv: 300 ppm $Sr(NO_3)_2$ for 24 hrs; v: 1000 ppm NH_4NO_3 for 24 hrs, followed by 250 ppm $Sr(NO_3)_2$ for 5 days; vi: 1000 ppm NH_4NO_3 for 24 hrs, followed by 300 ppm $Sr(NO_3)_2$ for 5 days; vii: 1000 ppm NH_4NO_3 for 5 days followed by 250 ppm $Sr(NO_3)_2$ for 5 days; viii: 1000 ppm NH_4NO_3 for 5 days, followed by 300 ppm $Sr(NO_3)_2$ for 5 days.

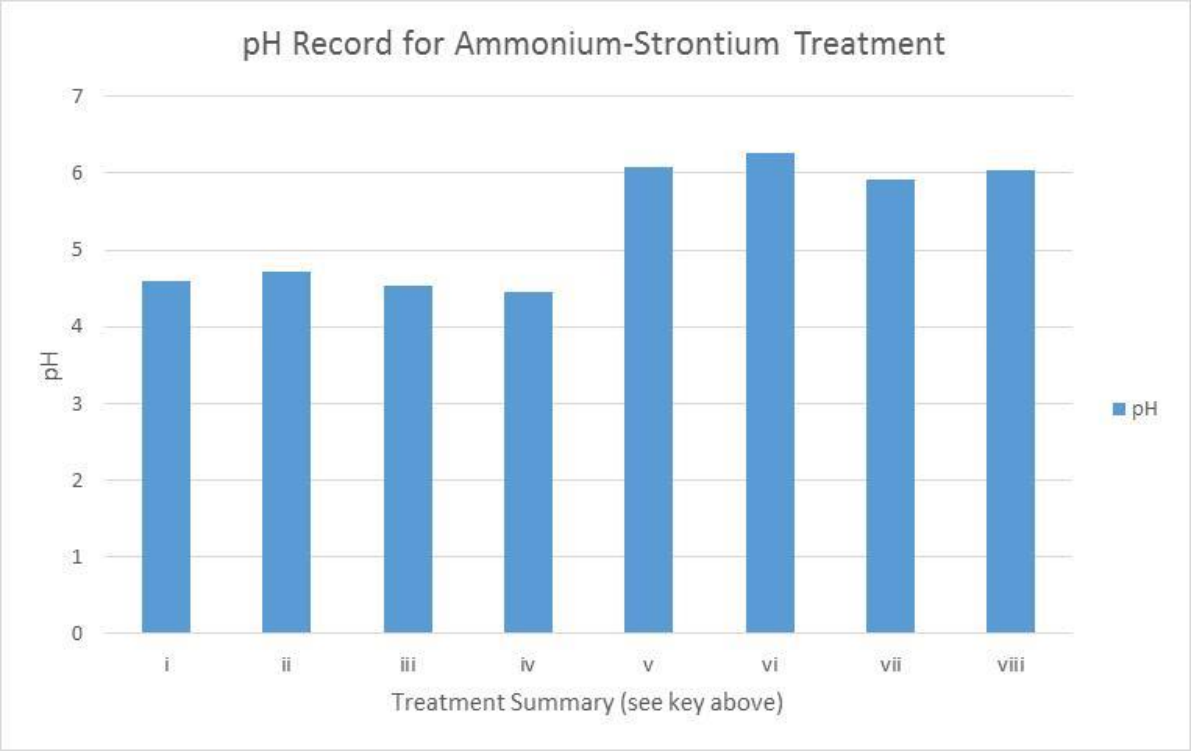

Figure 4-20: Final pH readings after the treatment of sandstone with the ammonium-strontium sequences. Key is as for previous figure.

Table 4-4: Summary of ions released by the ammonium-strontium treatments

STEP	TREATMENT SUMMARY	Average Mass released per gram of sandstone (mg/g)							pH (average)
		Zn	Ca	Sr	Mg	K	Na	Mn	
STEP 1	(i) 1000 ppm NH_4NO_3 for 24 hrs	0.00	0.08	0.00	0.02	0.03	0.21	0.01	4.60
	(ii) 1000 ppm NH_4NO_3 for 5 days	0.00	0.08	0.00	0.02	0.02	0.21	0.01	4.72
	(iii) 250 ppm $Sr(NO_3)_2$ for 24 hrs	0.00	0.09	0.00	0.02	0.03	0.21	0.01	4.53
	(iv) 300 ppm $Sr(NO_3)_2$ for 24 hrs	0.00	0.10	0.00	0.02	0.04	0.23	0.01	4.46
STEP 2	(v) (ex-NH_4NO_3) 250 ppm $Sr(NO_3)_2$ for 5 days	0.00	0.017	N / A	0.003	0.000	0.012	0.000	6.09
	(vi) (ex-NH_4NO_3) 300 ppm $Sr(NO_3)_2$ for 5 days	0.00	0.012	N / A	0.002	0.008	0.011	0.000	6.27
	(vii) (ex-NH_4NO_3) 250 ppm $Sr(NO_3)_2$ for 5 days	0.00	0.008	N / A	0.003	0.004	0.008	0.000	5.91
	(viii) (ex-NH_4NO_3) 300 ppm $Sr(NO_3)_2$ for 5 days	0.00	0.002	N / A	0.002	0.003	0.007	0.000	6.03

4.4.4.6 Discussion

Groups i and ii could be interpreted as quantifying the release, principally, of *exchanged* species, since the sandstone had been treated with NH_4NO_3. Groups

iii and iv may be interpreted as quantifying the release of both *exchanged* and *sorbed* species, since the sandstone had been treated with $Sr(NO_3)_2$; this is based on the assumption that Sr may undergo both exchange and sorption processes. Groups v to viii, in "Step 2" of the experiment, had been pre-treated with NH_4NO_3 with the intention of removing most of the exchangeable species, leaving just species that would be expected to sorb. Upon subsequent treatment with $Sr(NO_3)_2$, it could be interpreted that the Sr would undergo mainly sorption, and so the four last groups are quantifying the release of *sorbed* ions only – or, an approximation of the maximum sorption for the surface. However, it should be noted that pH for groups i to iv is around 4.5, suggesting that there may have been some desorbing in these groups too.

It is possible to better estimate the contribution of the various processes by calculating the milliequivalents of the species released. These are summarised in Figure 4-21 and in Table 4-5.

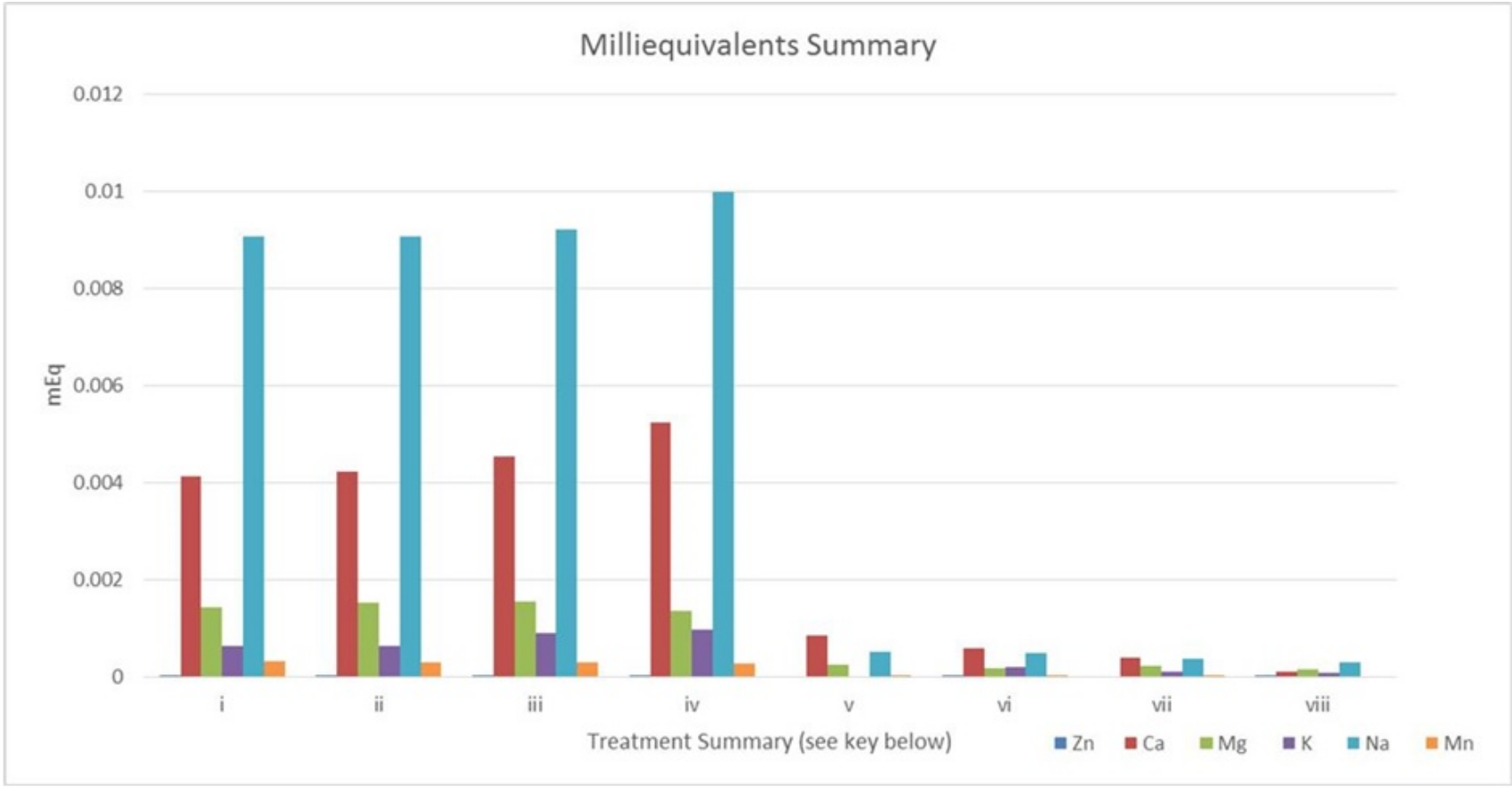

Figure 4-21: Milliequivalents analysis of the ions emanating from the sandstone after ammonium-strontium treatment

The treatment stages are summarised in Table 4-3; the key is as follows: i: 1000 ppm NH_4NO_3 for 24 hrs; ii: 1000 ppm NH_4NO_3 for 5 days; iii: 250 ppm $Sr(NO_3)_2$ for 24 hrs; iv: 300 ppm $Sr(NO_3)_2$ for 24 hrs; v: 1000 ppm NH_4NO_3 for 24 hrs, followed by 250 ppm $Sr(NO_3)_2$ for 5 days; vi: 1000 ppm NH_4NO_3 for 24 hrs, followed by 300 ppm $Sr(NO_3)_2$ for 5 days; vii: 1000 ppm NH_4NO_3 for 5 days followed by 250 ppm $Sr(NO_3)_2$ for 5 days; viii: 1000 ppm NH_4NO_3 for 5 days, followed by 300 ppm $Sr(NO_3)_2$ for 5 days.

Table 4-5: Summary of milliequivalents

STEP	TREATMENT SUMMARY	MilliEquivalents (mEq / 100g)							TOTAL mEq
		Zn	Ca	Sr	Mg	K	Na	Mn	
STEP 1	1000 ppm NH_4NO_3 for 24 hrs	0.0007	0.4141	0.0000	0.1430	0.0640	0.9080	0.0315	1.5614
	1000 ppm NH_4NO_3 for 5 days	0.0036	0.4228	0.0000	0.1526	0.0630	0.9068	0.0309	1.5798
	250 ppm $Sr(NO_3)_2$ for 24 hrs	0.0007	0.4545	0.0000	0.1563	0.0895	0.9223	0.0293	1.6527
	300 ppm $Sr(NO_3)_2$ for 24 hrs	0.0017	0.5230	0.0000	0.1356	0.0979	0.9991	0.0282	1.7855
STEP 2	(ex-NH_4NO_3) 250 ppm $Sr(NO_3)_2$ for 5 days	0.0000	0.0843	N / A	0.0264	0.0000	0.0525	0.0009	0.1641
	(ex-NH_4NO_3) 300 ppm $Sr(NO_3)_2$ for 5 days	0.0014	0.0580	N / A	0.0189	0.0212	0.0492	0.0001	0.1488
	(ex-NH_4NO_3) 250 ppm $Sr(NO_3)_2$ for 5 days	0.0000	0.0390	N / A	0.0220	0.0111	0.0368	0.0004	0.1094
	(ex-NH_4NO_3) 300 ppm $Sr(NO_3)_2$ for 5 days	0.0010	0.0100	N / A	0.0151	0.0072	0.0294	0.0000	0.0627

Using these results, the separate and combined contributions of ion exchange and sorption to the overall process was calculated and is given in Table 4-6:

Table 4-6: Calculations to distinguish the separate and combined contributions of ion exchange and sorption

<table>
<tr><th>STEP</th><th>TREATMENT SUMMARY</th><th>TOTAL mEq</th><th colspan="2">SORPTION PROCESS</th><th>DIFFERENCE IN SORPTION BETWEEN PROCESSES</th><th>AVERAGE SORPTION</th></tr>
<tr><td rowspan="4">STEP 1</td><td>1000 ppm NH_4NO for 24 hrs</td><td>1.5614</td><td rowspan="2"><u>Ion Exchange ‘Only’:</u>

1.5706 mEq / 100g</td><td rowspan="4">Sorption (= "ion exchange + sorption" - "ion exchange ‘only’")

0.1485 mEq / 100g</td><td rowspan="8">0.0273 mEq / 100g</td><td rowspan="8">0.1349 mEq / 100g</td></tr>
<tr><td>1000 ppm NH_4NO_3 for 5 days</td><td>1.5798</td></tr>
<tr><td>250 ppm $Sr(NO_3)_2$ for 24 hrs</td><td>1.6527</td><td rowspan="2"><u>Ion Exchange + Sorption</u>

1.7191 mEq / 100g</td></tr>
<tr><td>300 ppm $Sr(NO_3)_2$ for 24 hrs</td><td>1.7855</td></tr>
<tr><td rowspan="4">STEP 2</td><td>(ex-NH_4NO_3) 250 ppm $Sr(NO_3)_2$ for 5 days</td><td>0.1641</td><td colspan="2" rowspan="4"><u>Sorption ‘Only’</u>

0.1212 mEq / 100g</td></tr>
<tr><td>(ex-NH_4NO_3) 300 ppm $Sr(NO_3)_2$ for 5 days</td><td>0.1488</td></tr>
<tr><td>(ex-NH_4NO_3) 250 ppm $Sr(NO_3)_2$ for 5 days</td><td>0.1094</td></tr>
<tr><td>(ex-NH_4NO_3) 300 ppm $Sr(NO_3)_2$ for 5 days</td><td>0.0627</td></tr>
</table>

Analysis of the ions released by milliequivalents shows that sorption processes account for 0.1349 mEq / 100g, in comparison to ion exchange processes, which appear to be the dominant process, at 1.5706 mEq / 100 g, an order of magnitude greater. However, because the pH is relatively low in the NH_4 stage of the experiment, this estimate is likely to underestimate the total sorption contribution.

Thus the values in Table 4-6 for sorption are minimum bounding values. Taken at face value, the data suggest that Na and K are involved in sorption. However, the Na experiment described in Section 4.4 showed that not quite all the attached ions are removed by high flushing ion concentrations, and additionally as pointed out above, there will be equilibrium between the exchange surfaces and the sorption surfaces: thus the exact ion ratios of the exchange and sorption surfaces cannot be determined precisely, even if the totals of both are determined. The total sorption values estimated here are very similar to those determined by Carlyle et al. (2004).

4.4.4.7 Summary of the Experiment

This experiment used a two-step protocol employing ammonium and strontium solutions to displace ions on exchange and sorption sites, respectively. Analysing the resulting equilibrated solutions for the concentrations of Zn, Ca, Sr, Mg, K, Na and Mn ions gave semi-quantitative indications of the contribution of ion exchange and sorption to the overall sorption processes. The results indicated that ion exchange processes dominate over sorption by at most a factor of an order of magnitude.

4.5 Conclusions arising from the Method Development

The experiments reported here show the evolution of techniques intended to gain a semi-quantitative appreciation of the attachment behaviour of the sandstones prior to developing a final method. Here, a summary of the conclusions arising from these scoping studies is presented. Attention then turns to the design of a finalised, large-scale experiment, intended to generate data that will allow

comparison of the behaviour of the real sandstone to the predictions generated by the pure-HFO PHREEQC representation.

As discussed at the opening of this chapter, the main thrust of the preliminary experimental work was intended to provide data in the following areas, arising from the predictions made by the initial modelling work:

- pH is very influential in sorption behaviour;
- Sorption and exchange reactions are both expected to occur;
- Sorption and ion exchange reactions, though rapid, are not instantaneous, and therefore time should be considered;
- There are competitive effects between ions such as Zn^{2+}, Ca^{2+}, Mg^{2+}, and others;

Insights on these questions obtained from the preliminary experiments are now considered.

- attachment of Zn on the sandstone is pH dependent (Section 4.3), suggesting that there is a measurable component of sorption as ion exchange reactions are generally much less pH dependent. It is probable that ion exchange dominates over sorption (Section 4.6), but that Zn will participate in both types of reaction.
- Attachment reactions in the sandstone samples take a significant amount of time to occur (Section 4.4). Up to 48 hours after the start of the reaction, a relatively rapid rate of sorption occurs, accounting for the majority (>85 %)

of the total sorption. Thereafter, the rate slows down considerably, approaching equilibrium by approximately 170 hours. This “two-phase” effect seems to be more pronounced when there is a higher initial concentration of Zn.

- Ions such as Ca and Mg were shown to mirror the sorption behaviour of Zn to such an extent that they could be thought of as *competing* with Zn for a presence on the surface (Section 4.4). These ions were most likely to be present on the sandstone prior to the experiments, and their presence must be taken into account.
- Minimizing, though not completely removing, the effects of competing ions and the defining of initial surface conditions can be undertaken by conditioning the sandstone using elevated concentrations of appropriately chosen ion solutions (Sections 4.5 and 4.6).
- Because ion exchange reactions cannot practicably be eliminated, the final experiments will have to be interpreted using a modelling approach including representation of both ion exchange and sorption.

These conclusions inform the priorities for the finalised experiment. The next section describes the synthesis of these results, along with the best of the techniques evolved thereby, into a final, large-scale experiment designed to characterise the sorption behaviour of the sandstone.

4.6 Chapter Summary

This chapter has been concerned with describing a set of preliminary laboratory experiments, and with their use in developing a final protocol for determining sorption properties of the sandstone being investigated. Using zinc as a representative heavy metal, a suite of experiments sought to investigate the sorption behaviour of the sandstone, and to appreciate the important factors influencing it. An array of techniques therefore evolved, and these were incorporated into a final, large-scale experiment designed to generate data to use in subsequent stages of the project. This experiment and its results and interpretation are presented in Chapter 5.

5 - RESULTS AND INTERPRETATION OF SORPTION EXPERIMENTS

5.1 Overview

In this chapter, the results of the finalized experiment from Chapter 4 are presented and discussed. Then, these results are interpreted by way of PHREEQC models, by attempting to fit a computer model to the data generated in the laboratory. The Chapter closes with an assessment of the success of this venture, drawing conclusions regarding the model's behaviour in comparison to the evidence furnished by the real sandstone system, the implications for the sorption characteristics of the rock and the suitability of the derived model for predicting the effects of pH-dependent sorption on contaminant transport.

5.2 Introduction

Chapter 4 recounted the development of experimental methods intended to generate data on a number of properties of a sample of Triassic sandstone. Choosing Zn as an exemplar heavy metal, batch experiments were undertaken to observe the sorption and ion exchange processes taking place and the key influences acting upon them. The theoretical and technical evolution of these prototypic experiments constitutes the design of a large-scale trial, presented here.

5.3 Finalised Method

5.3.1 Introduction

This experiment represented the conclusion in the evolution of the preliminary experiments, and was intended to produce isotherms and other data giving information about the sorption of zinc on the sandstone samples. This was intended to provide evidence as to the applicability of the Dzombak and Morel (1990) HFO model.

5.3.2 Purpose of the Experiment

The conclusions drawn from the method development stage spearheaded the design of this experiment. As far as appropriate and possible, it sought to incorporate the following main factors:

- The influence of pH on sorption behaviour: whilst ion exchange is, at most, mildly affected by environmental pH, sorption processes are very sensitive. The design endeavoured to control this tightly to define fully the relationship.
- Sorption reaction rates and time to equilibrium: the design had to assert a compromise on the observed two-phase nature of the sorption processes, balancing the need for (at least) near-equilibrium with the time restrictions for completing the experiment.
- Competitive ions: the design had to take into account the likelihood of pre-existing ions (such as Ca and Mg) competing with Zn on the sorption sites.

- Initial conditions on the sandstone surfaces: the design had to improve upon the uncertainty of the initial conditions of the natural sandstone surface by pre-treating the sandstone prior to undertaking sorption measurements.

5.3.3 Experimental Approach

Step 1: Set-up of initial conditions and saturation of exchange sites

The first step was designed to flush the exchange sites with 1000 ppm Na. The use of a high concentration of Na was to encourage Na to dominate the exchange sites, displacing any ions that were bound to the exchange sites. Na is preferred over NH_4, as the latter has a pH buffering capacity. Analysing for these ions then gives an approximate measure of what exchangeable ions, other than Na, were present on the sandstone initially, and also decreases uncertainty regarding the initial composition of the exchange sites. This step of the experiment could be run for 6 hours (fast phase process), with pH controlled to pH 4 to force desorption.

Step 2: Intermediate Rinse

It was thought necessary to rinse the sandstone after the first step, to remove any ions that were displaced from the ion exchange sites by the Na.

Step 3: Promotion of Zn sorption under pH control

The third step was to produce sorption isotherms for Zn at different pH values, so as to provide data on the pH influence of sorption, among other things. Meanwhile, maintaining a high background concentration of Na was deemed prudent to minimise the participation of Zn in ion exchange reactions. The third step of the experiment would be run for 168 hours (7 days), in keeping with the "slow" phase of the sorption processes.

5.3.4 Materials and Methods

Step 1: Set-Up of Initial Conditions and Saturation of Exchange Sites

Whatman No. 1 filter papers were thoroughly dried for 2 days at 60°C in a convection oven. They were identified with a simple numbering system, weighed, and set aside. (Their recorded masses were used later in the experiment.)

As in previous experiments, 50 ml centrifuge tubes were prepared: 30 reaction vials and 3 blanks were prepared. 1 g of sandstone was weighed into each reaction vial, followed by 40 ml of 1,000 ppm Na (as $NaNO_3$). The initial pH was measured and adjusted to pH 4 using nitric acid. The vials were placed on a shaker at 100 rpm for a total of 6 hours. At 2-hour intervals, they were briefly removed from the shaker in order to monitor and maintain the pH at pH 4.

At 6 hours, the vials were removed from the shaker and centrifuged at 4,500 rpm for 10 mins. The supernatant was filtered through a 0.45 µm disposable syringe

filter into a new vial, and the final pH was measured. The solutions were acidified and prepared for analysis by FAAS for the presence of Zn, Ca and K.

Step 2: Intermediate Rinse

The sandstone remaining in the vials after Step 1 was transferred (individually) onto the oven-dried filter papers, which were placed on a Büchner funnel. Under a mild vacuum, the sandstone was rinsed thoroughly with approximately 100 ml deionised water. The filter papers were then removed from the Büchner funnel, folded, and placed into the appropriate reaction vial in preparation for Step 3.

Step 3: Promotion of Zn sorption under pH control

The array of solutions listed in Table 5-1 were prepared, using $Zn(NO_3)_2$, all with a matrix of 1000 ppm $NaNO_3$:

Table 5-1: The array of Zn solutions prepared for Step 3

[Zn]	pH
0 ppm Zn	3
	5
	6
	7
	9
0.5 ppm Zn	3
	5
	6
	7
	9
3 ppm Zn	3
	5
	6
	7
	9
7 ppm Zn	3
	5
	6
	7
	9

The sandstone was carefully and thoroughly washed off the filter papers and into their assigned vials using a 10 ml syringe filled with $Zn(NO_3)_2$ / $NaNO_3$ solution designated for it (see Table 5-1, above). 40 ml of this solution was added in total. The filter papers were removed and set aside.

The pH was measured and adjusted for the required pH value (Table 5-1) using very dilute NaOH or HNO_3, added drop-wise using a 1 ml syringe. The vials were manual shaken briefly, and then placed on a shaker set to 100 rpm for 168 hours (7 days). Every 24 hours, the experiment was briefly interrupted to monitor and

re-adjust the pH, as necessary.

Whilst the experiment was ongoing, the used filter papers were again dried in a convection oven, using the same procedure as before. They were again weighed, and their masses recorded. Any gain in mass was assumed to correspond to fine sandstone particles retained on the filter papers; this difference was used to calculate the actual mass of sandstone present in Step 2. (Measurements showed that the average mass lost was 0.04 g – approximately 3.7 % of the initial sandstone mass.)

At the end of the experiment, the vials were centrifuged at 4,500 rpm for 10 minutes. They were filtered as before, and the final pH recorded. Finally, the solutions were acidified and further prepared for analysis by FAAS. They were separated into two batches as follows:

- Batch 1: Zn, Ca, K, Mg, Mn, Sr (in 1000 ppm Na matrix; LaCl buffer)
- Batch 2: Na (only LaCl buffer)

5.4 Results of Final Laboratory Experiment

5.4.1 Introduction

This experiment is intended to produce isotherms of the sorption of zinc on sandstone which may then be interpreted, using PHREEQC, to investigate their consistency with the surface complexation model. It draws on the results and

experience of all the previous experiments looking at various properties of the sandstone. There are two steps to this experiment.

5.4.2 Results of Step 1

The first step is designed to flush the exchange sites with 1000 ppm sodium (as sodium nitrate). Using such a high concentration should ensure that sodium dominates the exchange sites, and so any ions that were bound to exchange sites should be replaced by sodium, and thus become free ions in solution. Analyzing for these ions then gives an approximate measure of what exchangeable ions were present on the sandstone initially. The experiment was run for 6 hours, with pH controlled to pH 4.

The sandstone was then rinsed with $NaNO_3$ to remove any ions that were displaced from the ion exchange sites by the Na. This is to reduce the possibility that they may later sorb onto the oxide phases of the sandstone.

The results of Step 1 of the experiment are shown in Figure 5-1 and Table 5-2. The dominant ion on the exchange sites, other than Na which cannot be determined using the Na flush technique used here, is Ca, followed by K and Mg.

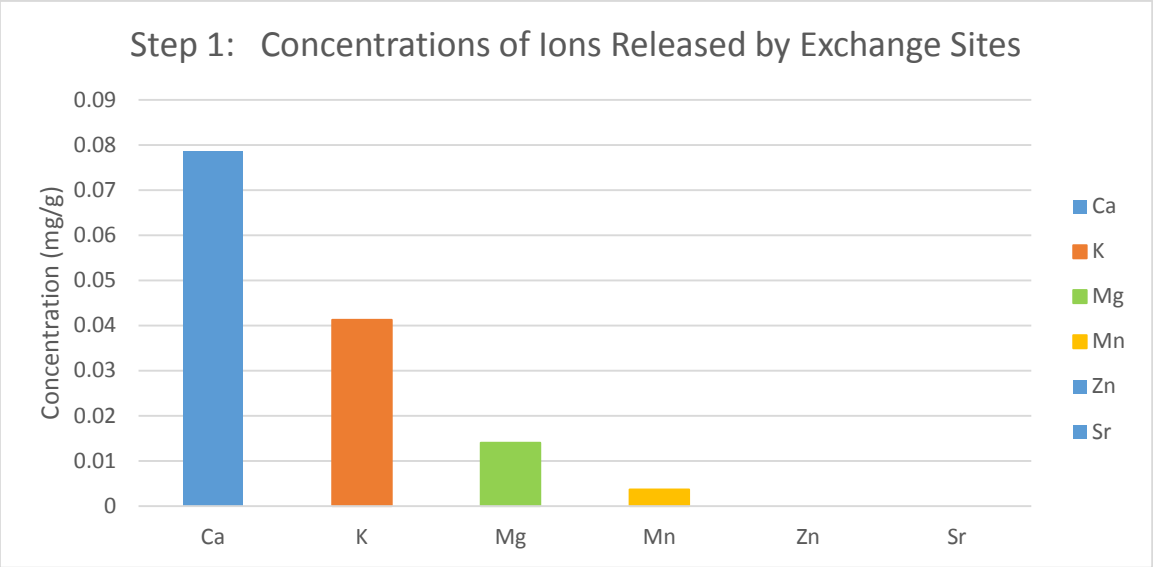

Figure 5-1: The release of ions resulting from the contact with 1000 ppm Na solution

Table 5-2: Summary of Concentrations of Ions Released by Exchange Sites (mg/g)

pH	Ca	K	Mg	Mn	Zn	Sr
4.24	0.078	0.041	0.014	0.004	<DL	<DL

5.4.3 Results of Step 2

The second step is to introduce Zn at varying concentrations to the sandstone at different pH values, so as to look at how pH influences sorption, and also to plot sorption isotherms for Zn. A high background concentration of Na was maintained to ensure that the ion exchange sites remained saturated.

Figure 5-2 presents the results of Step 2 in terms of isotherms at each of the 5 pHs studied. It is clear that the isotherms are not linear and that the responses are very pH-dependent.

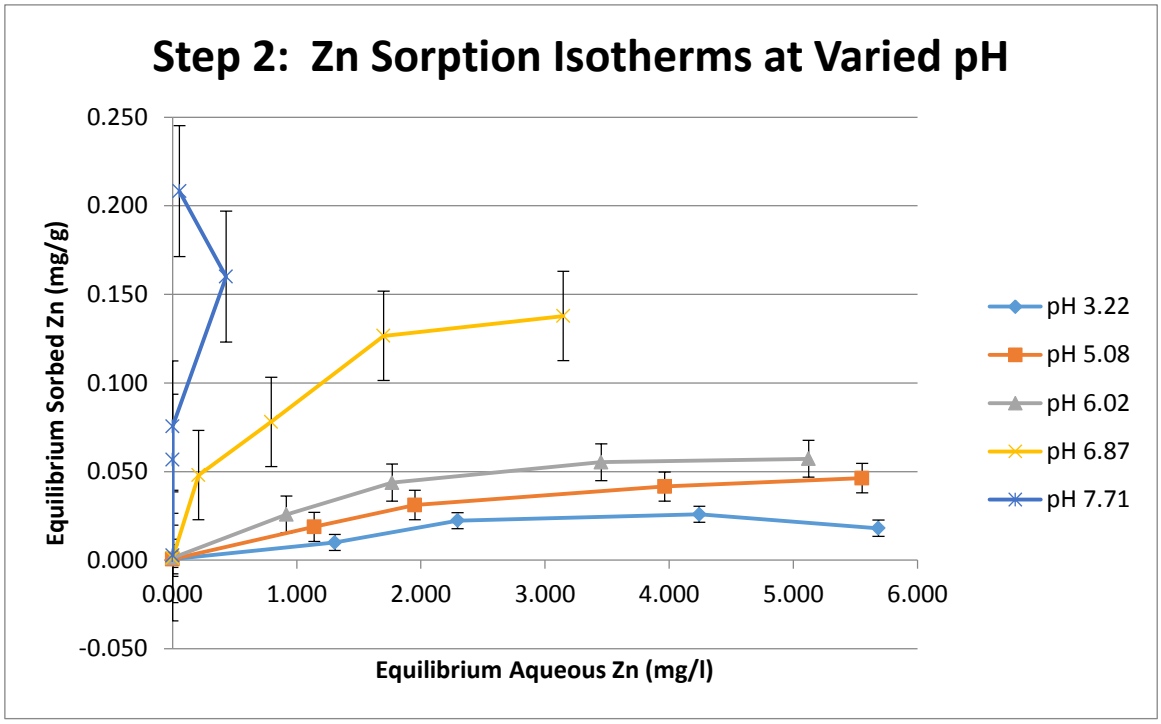

Figure 5-2: Isotherms for Zn at pHs from 3.22 to 7.71.

Figure 5-3 shows the amount of sorption as a function of pH for each of the initial concentrations (in effect masses) added to the reactors. As also implied by Figure 5-2, the sorption increases rapidly as pH rises, in keeping with the numerical experiments outlined in Chapter 3.

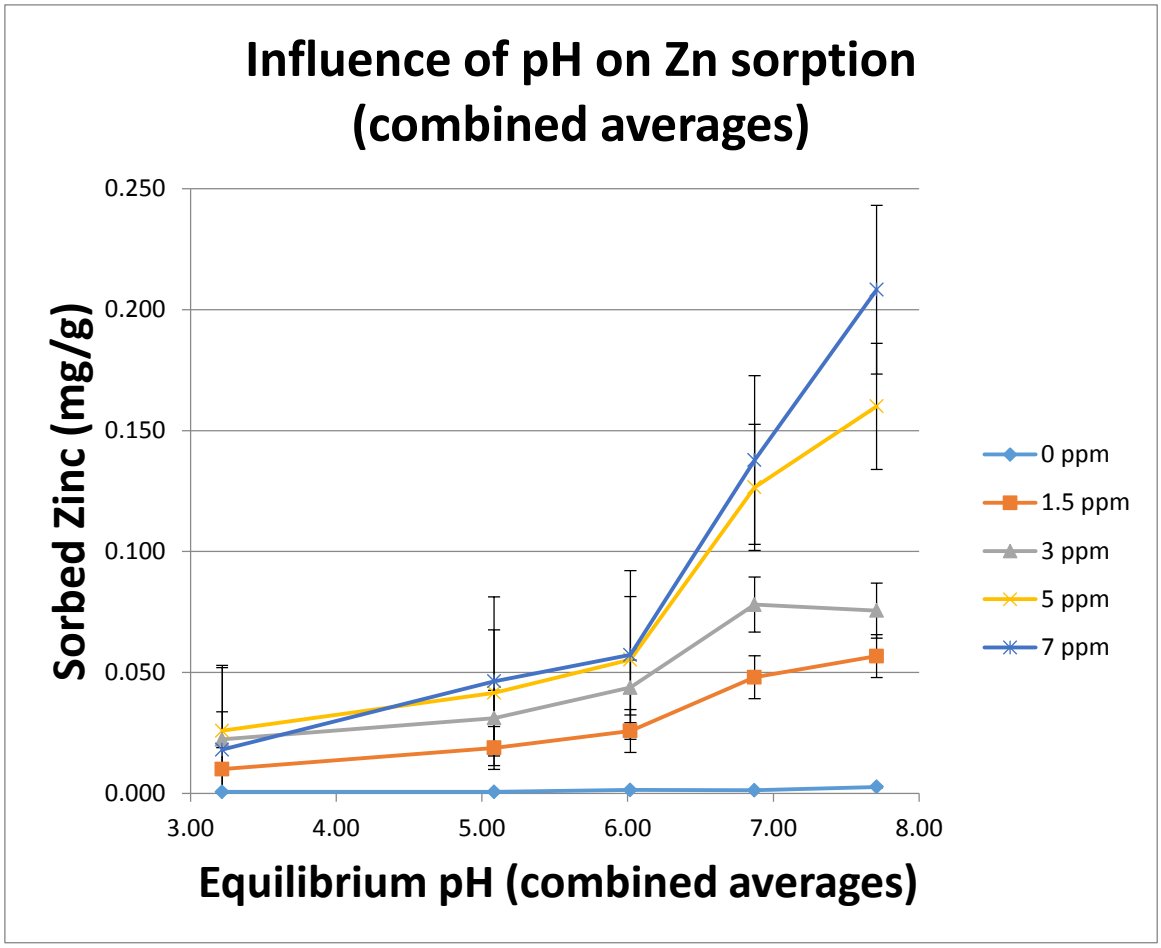

Figure 5-3: Sorption of Zn as a function of pH for each initial concentration of Zn.

Figures 5-4 and 5-5 show the release of other ions accompanying the sorption of Zn. Mn and Sr concentrations were undetectable. The correlations between the concentrations of Zn sorbed and other ions released is weak. In fact, there appears to be at least as much correlation between the concentrations of these other ions as with Zn release. All the concentrations of these ions are low, and they do not increase with pH. K^+, an ion expected to sorb much less than Ca, increases at least as much as Ca. All these observations suggest that Ca, K and Mg concentrations are not dominated by desorption in response to Zn sorption,

either via ion exchange or ‘true’ sorption, and presumably are present through dissolution.

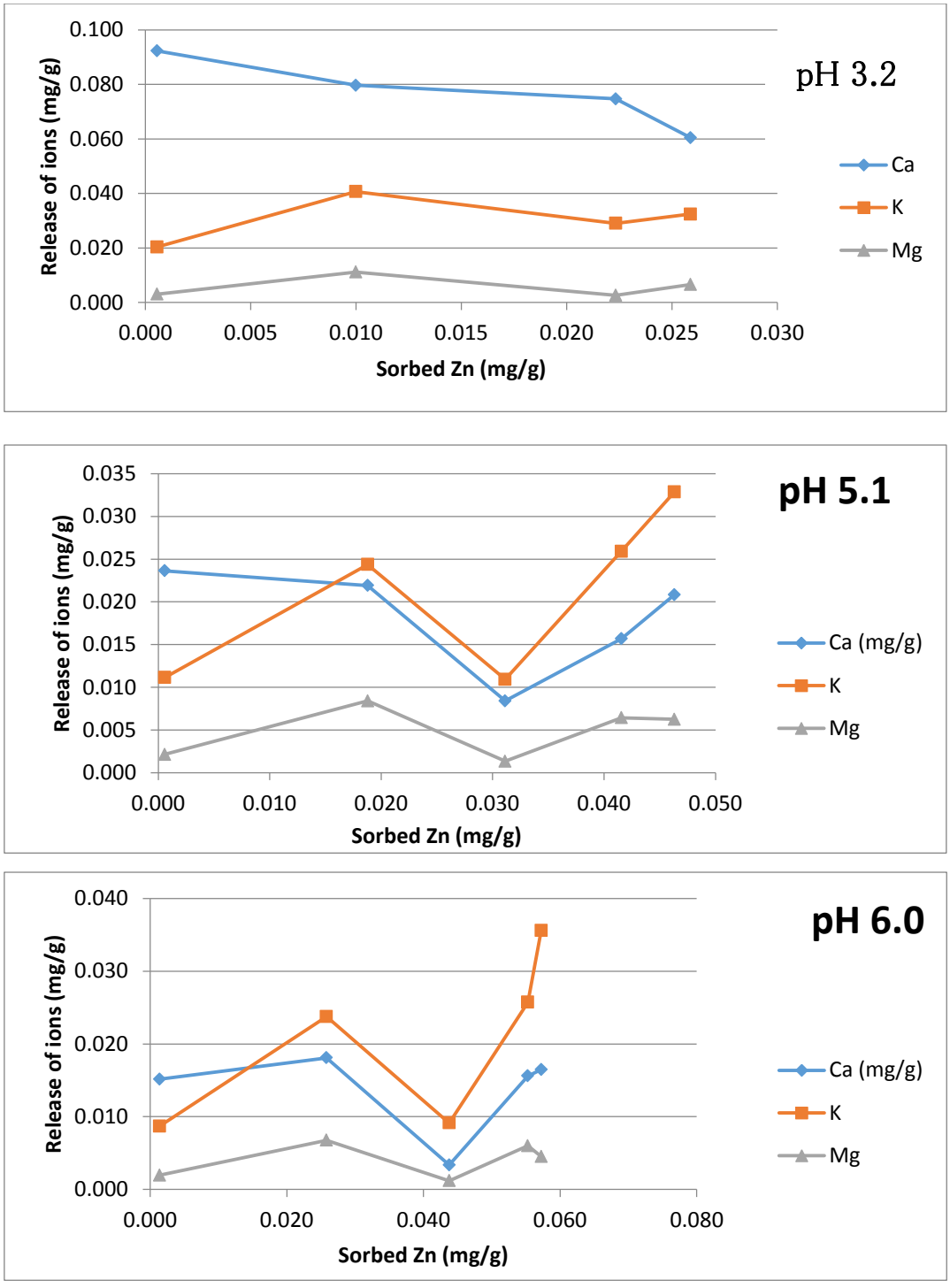

Figure 5-4: Concentrations of other ions released during Zn sorption experiments at pHs of approx. 3, 5 and 6.

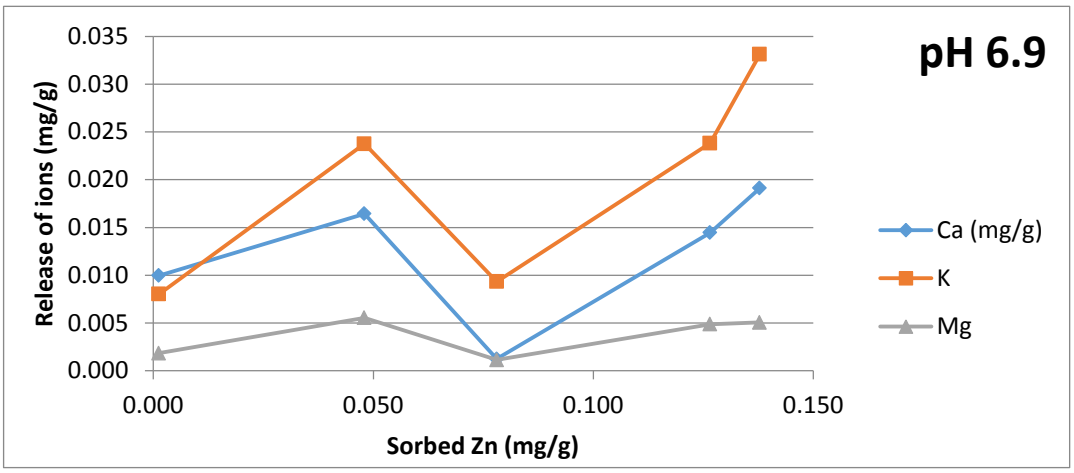

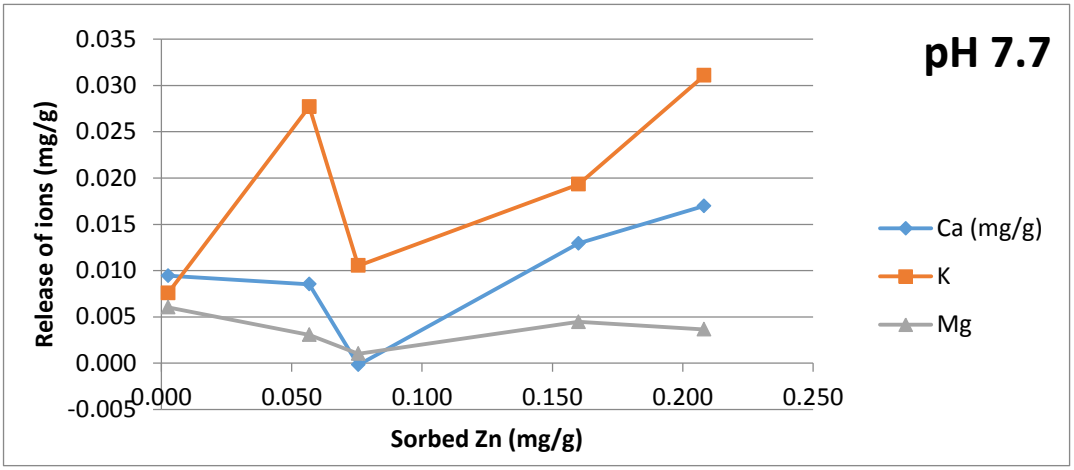

Figure 5-5: Concentrations of other ions released during Zn sorption experiments at pHs of approx. 7 and 8.

5.4.4 Discussion of Results

The lack of obvious correlation of sorbed Zn concentration and release of other ions into solution (Figures 5-4 and 5-5) suggests that the high-Na, low-pH flush has limited the presence of other ions on the attachment sites. Comparing the masses per gramme released from the Step 1 high-Na, low-pH flush with those from the Zn sorption phase in Step 2 indicates that the former is much greater than the latter, reinforcing the conclusion that the Step 1 flush was successful.

These results are consistent with sorption being dominant over exchange, and sorption involving H^+ as the other, potentially competing ions have been displaced by the previous low-pH flush.

The non-linear, pH-dependent sorption isotherms (Figure 5-2) and the sorption / pH relationships (Figure 5-3) indicate that a K_d approach is inappropriate, and are consistent qualitatively with the surface complexation model described in Chapter 3. This could represent specific sorption on oxide surfaces or on clay mineral edges.

5.5 Interim Conclusions

It is concluded that the data are such that an interpretation of the data using the surface complexation approach is warranted.

5.6 Interpretation

5.6.1 Purpose

The aim of this section is to determine if the Dzombak and Morel (1990) complexation theory (Chapter 2) is consistent quantitatively with the results of the experiments. If this is found to be the case, then a means is provided whereby sorption can be predicted for the sandstones. Just because Zn sorption experiments can be described quantitatively does not prove that the complexation theory is correct for all metals, or even for Zn, but it is a necessary condition. If complexation theory can be successfully used, the importance of sorption for

solute migration in the presence of other reactions can then be investigated, and the validity of the K_d concept examined.

5.6.2 Discussion of Approach

For the reasons explained in Chapter 2, PHREEQC was chosen as the code to be used to model the experimental data. Though the experiments were designed to reduce the effect of ion exchange and to establish known initial conditions on the surfaces, it was thought prudent to represent not just sorption in the final Step of the experiment but also to represent initial conditions and ion exchange processes explicitly.

In its conception, it was envisaged that the numerical model would need to include three successive stages:

1) The first stage represented the pre-existing, natural environment. Recalling that the rock sampled for the laboratory work had been carefully chosen for its lack of carbonate minerals, the first stage of the computer modelling represented the rock in contact with a low-carbonate groundwater solution, thus setting up the rock exchange and sorption surfaces to be in equilibrium with the expected ionic composition of the in situ groundwater. The model was calibrated against the results from Step 1 of the final laboratory experiment, which indicated the initial composition of the sandstone surface, and hence the initial groundwater with which it had equilibrated.

2) The second stage was to introduce a high-Na, low-pH solution, as used in Step 1 of the laboratory experiment, to encourage displacement of exchangeable and sorbed ions.
3) The third stage represented the introduction of the Zn and the control of the pH as undertaken in Step 2 of the experiments. Like the laboratory experiments, this final solution would additionally contain a high-Na background, to reduce the likelihood of metals attaching by way of exchange sites.

Whilst the laboratory experiments were carried out with 1 g of rock sample in 40 ml of solution, the model was up-scaled to 25 g in 1 ltr of solution.

Within the bounds of this general three-stage structure, there were many factors that were able to be adjusted. These comprised:

- Solution composition:
    - Each of the three solutions consisted of a separate composition, and each of the elemental concentrations could be adjusted;
    - pH: initial pH, and also potential for maintaining a fixed pH by addition of an acid or base as required;
- Properties of the surface
    - Coefficients related to the exchangeable ions;
    - Total quantity of exchange sites;

    - Specifications of the sorption sites, divided into weak and strong sites;
    - Coefficients related to the affinity of these sites for certain ions, and their speciation;
    - Specifications of the complexes able to be formed by these interactions;
    - The specific surface area per gramme;
    - The total mass of 'HFO' available.
- Specifying whether precipitates may form, and in particular Smithsonite and Zn hydroxides.

A detailed log was kept of the calibration runs, including all conditions, sensitivities and result summaries. 472 trials were undertaken before the final model was produced. Calibration involved matching the evidence from Step 1 before continuing to Step 2, but returning to Step 1 if necessary. Matching was judged by eye rather than using any optimization scheme, as this was judged simpler and allowed direct user involvement in the process. Once a reasonable Step 1 fit was obtained, an attempt was made to fit one of the isotherms, including examining wide ranges of parameter values. Dzombak and Morel (1990) provide an indication of parameter values, but investigation included values outside the ranges they suggest as the rock sorption surfaces are potentially very different from synthetic HFO. Ion exchange was modelled using the Gaines-Thomas convention as this has been shown for Triassic sandstone to provide a reasonable description over small ranges of exchange compositions (Carlyle, et al., 2004): parameter values were based on value ranges suggested by Carlyle et al. (2004)

and Appelo and Postma (2007). Once one isotherm had been adequately described, others were examined. Frequently, failure to match more than one isotherm resulted in returning to find a new description of the first isotherm, and then repeating the process. The difficulty of finding a consistent model to describe all five isotherms suggests that despite the number of parameters available, there may be only a limited amount of equivalence, though any success in fitting the experimental data does not prove that the process is adequately described by surface complexation theory or that the 'correct' set of parameter values has been identified.

5.6.3 Input Code

The finalized PHREEQC input for Trial 459 (pH 6.08[3]) is given below in Table 5-3. This was then adjusted to give the other pH values to match the average pH values recorded at equilibrium in the laboratory experiments, that is, 3.22, 5.08, 6.87, and 7.71.

Table 5-3 (a) describes the setting up of the initial conditions on the rock surface using a groundwater composition that is consistent with near surface groundwater in Triassic sandstone. The composition is broadly modelled on that from a borehole at Haydock Park racecourse in Lancashire (Tellam, 2013, pers. comm.). The effects of the exact composition of this water were investigated, but the final results are insensitive to moderate changes. At the end of this part of the

[3] A minor inputting error was discovered after this modelling phase had been completed: pH 6.08 was entered instead of 6.02.

simulation the sorption and ion exchange surfaces are in equilibrium with the input water chemistry, and this set of surfaces is stored for the next part of the simulation.

Table 5-3 (b) describes the conditioning of the sandstone using low-pH, high-Na solutions. This results in the modification of the compositions of the exchange and sorption surfaces, and release of ions that could then be compared with the release of ions in the experiments. Again, finalizing this stage was an iterative process, with apparently successful simulations that then led onto unsuccessful attempts at fitting isotherms. This resulted in modifications of the exchange and sorption parameters in this stage, and then returning to attempting to fit the isotherms.

Table 5-3 (c) describes the simulation of Step 2, the addition of Zn under controlled pH conditions. The results from this simulation were recalculated as isotherms and compared with the experimental isotherms.

Table 5-3: PHREEQC input code for Trial 459 (pH 6.08), and used also for Trials 460 (pH 7.71), 461 (pH 6.87), 462 (pH 5.08), and 463 (pH 3.22).

[(a) Setting up the rock surfaces in equilibrium with groundwater]

```
TITLE  Model for lab expts: 1g in 0.04L, but upscaled to 1L, i.e. 25g in 1L
SOLUTION 1 Natural gw
        pH      7.0
        pe     8
        temp    25.0
        units mg/l
        Na      23
        K       5.00
        Ca      20
```

```
        Mg      10.00
        Zn      0.0001
        Mn      0.01
        C(+4)   5
        S(6)    86
        N(+5)   5
        Cl      35


EXCHANGE_SPECIES

K+ + X- = KX                    #Gaines-Thomas format
log_k  0.9
-gamma      3.5     0.015
delta_h  -4.3 # Jardine & Sparks, 1984

Zn+2 + 2X- = ZnX2
log_k 0.1
-gamma 5.0 0.0

Na+ + X- = NaX
log_k  0.0
-gamma      4.0     0.075

Ca+2 + 2X- = CaX2
log_k   0.4
-gamma      5.0     0.165
delta_h  7.2   # Van Bladel & Gheyl, 1980

Mg+2 + 2X- = MgX2
log_k   0.4
-gamma      5.5     0.2
delta_h  7.4   # Laudelout et al., 1968

Mn+2 + 2X- = MnX2
log_k  0.52
-gamma      6.0     0.0


EXCHANGE 1

X-  6.25e-4
#       cec ~ 2.5 mmol/100g = 25 mmol/kg;for 1g therefore = 2.5e-5 mol;
#       used 0.04L in expt; so if use 1L in calc, then 2.5e-5/0.04L = 6.25e-4mol
        -equilibrate 1

SURFACE_SPECIES
```

```
Hfo_sOH + H+ = Hfo_sOH2+
log_k 8.18
Hfo_sOH = Hfo_sO- + H+
log_k -10.82
Hfo_sOH + Zn+2 = Hfo_sOZn+ + H+
log_k 0.66
Hfo_sOH + Ca+2 = Hfo_sOHCa+2
log_k 0.15
Hfo_sOH + Mg+2 = Hfo_sOMg+ + H+
log_k 0.15


Hfo_wOH + H+ = Hfo_wOH2+
log_k 8.18
Hfo_wOH = Hfo_wO- + H+
log_k -8.82
Hfo_wOH + Zn+2 = Hfo_wOZn+ + H+
log_k -2.32
Hfo_wOH + Ca+2 = Hfo_wOCa+ + H+
log_k -2.32
Hfo_wOH + Mg+2 = Hfo_wOMg+ + H+
log_k -2.32


SURFACE 1
 -equilibrate with solution 1

 Hfo_sOH 3.0e-4 6 0.119

# Hfo_sOH 0.00214285714285714 600 38.1428571428571
# Dz&M used 0.2mol weak sites / mol Fe and 0.005 mol strong sites / mol Fe
# From Jaweesh (2014, pers comm), we have ~ 3mgFe/g sst, so with 1g we
have 0.2 x 3/56000 mol;
# for up scaling to 1L from 0.04L, we have 0.2 x 3/56000/0.04 = 2.68e-4 mol
# for strong sites, 2.68e-4/.2 x 0.005 = 6.70e-6 mol
# for mass of sorber, 3 Fe mg/g sst = 3/56000 mol Fe/g sst
# = 3/56000 x 89g HFO / g = 3/56000 x 89 / 0.04 g HFO in contact with 1L
# i.e. 0.119 g (Dz&M have 89gHFO/mol Fe; also 600m2/g)
# Hfo_wOH 0.0857142857142857

 Hfo_wOH 2.68e-8

# Hfo_sOH 5e-6 600. 0.09
# Hfo_wOH 2e-4


EQUILIBRIUM_PHASES 1
       Smithsonite   0.0    0.0
```

```
        Zn(OH)2(e)    0.0    0.0


SAVE surface 1
SAVE exchange 1

END
```

[(b) Step 1: Conditioning with 1000ppm Na]

```
SOLUTION 2 Conditioning
        pH      4.0
        pe     8
        temp    25.0
        units mg/l
        Na   1000
        K    0.01
        Ca   0.01
        Mg   0.01
        Zn   0.0001
        Mn    0.01
        Cl   15.43
        C    .01 as HCO3

USE exchange 1
USE surface 1


EQUILIBRIUM_PHASES 2

        Smithsonite   0.0    0.0
        Zn(OH)2(e)    0.0    0.0


SELECTED_OUTPUT

-file   PRO TRL Zn 7 pH 3_459A.sel
-totals Zn Ca K Mg Mn Sr

SAVE surface 2
SAVE exchange 2


EXCHANGE_SPECIES

K+ + X- = KX
log_k  0.9
-gamma        3.5      0.015
```

```
delta_h  -4.3  # Jardine & Sparks, 1984

Zn+2 + 2X- = ZnX2
log_k 0.1
-gamma 5.0 0.0

Na+ + X- = NaX
log_k  0.0
-gamma        4.0      0.075

Ca+2 + 2X- = CaX2
log_k   0.4
-gamma        5.0      0.165
delta_h  7.2   # Van Bladel & Gheyl, 1980

Mg+2 + 2X- = MgX2
log_k   0.4
-gamma        5.5      0.2
delta_h  7.4   # Laudelout et al., 1968

Mn+2 + 2X- = MnX2
log_k  0.52
-gamma        6.0      0.0


END
                                [(c) Step 2:  Zn addition]

PHASES
                Fix_H+
                H+ = H+
                log_k 0.0


SOLUTION 3 Zn test

pH      6.08
pe     8
temp    25.0
units mg/l
Na   1000
K    .01
Ca   .01
Mg   .01
Cl   15.43
C    .01 as HCO3
Zn    0.0001
```

```
USE exchange 2
USE surface 2


EXCHANGE_SPECIES

K+ + X- = KX
log_k  0.9
-gamma        3.5      0.015
delta_h  -4.3  # Jardine & Sparks, 1984

Zn+2 + 2X- = ZnX2
log_k 0.1
-gamma 5.0 0.0

Na+ + X- = NaX
log_k  0.0
-gamma        4.0      0.075

Ca+2 + 2X- = CaX2
log_k   0.4
-gamma        5.0      0.165
delta_h  7.2   # Van Bladel & Gheyl, 1980

Mg+2 + 2X- = MgX2
log_k   0.4
-gamma        5.5      0.2
delta_h  7.4   # Laudelout et al., 1968

Mn+2 + 2X- = MnX2
log_k  0.52
-gamma        6.0      0.0


EQUILIBRIUM_PHASES 3

Fix_H+                  -6.08   NaOH           100.0

CO2(g)  -3.5  10
Smithsonite   0.0    0.0
Zn(OH)2(e)    0.0    0.0


reaction
          Zn
           0.0  0.0000231 0.00004615  .0000769       .0001077
```

```
SELECTED_OUTPUT
       -file   PRD TRL Zn 7 pH 3_459B.sel
#exchange sites:
 -molalities ZnX2 #CaX2 MgX2 KX AlOHX2 AlX3 FeX2
#strong sites:
 -molalities Hfo_sOZn+ #Hfo_sOH    Hfo_sOHCa+2 Hfo_sOH2+ Hfo_sO-
Hfo_sOFe+
#weak sites:
 -molalities Hfo_wOZn+ #Hfo_wOH Hfo_wOH2+ Hfo_wO-  Hfo_wOCa+
 -totals Zn

END
```

5.6.4 Model Results

Figure 5-5 compares the Step 1 (Na, low pH conditioning) experimental and simulation results, and Figure 5-6 the experimental and simulated isotherms.

The Step 1 results (Figure 5-5) indicate that the model produces a reasonable simulation of the release of Ca, Mg, and K.

Figure 5-6 shows that the broad patterns of the isotherm variation with pH are reproduced by the model, with very high sorption occurring at pH of 7.7, and decreasing, non-linear, sorption isotherms at the lower pHs. The closest simulations were for the higher pHs, where sorption was greatest. At the lowest pHs, 5.08 and 3.22, the model predicts almost identical isotherms, but the experimental data suggest a difference, albeit it rather small when the uncertainty is considered. The lower pH experimental isotherms also appear to have a greater curvature than those of the simulation, despite extensive attempts to

reproduce the curvature during the calibration. This suggests that apparent sorption capacity is decreasing with pH at a greater rate than the model predicts.

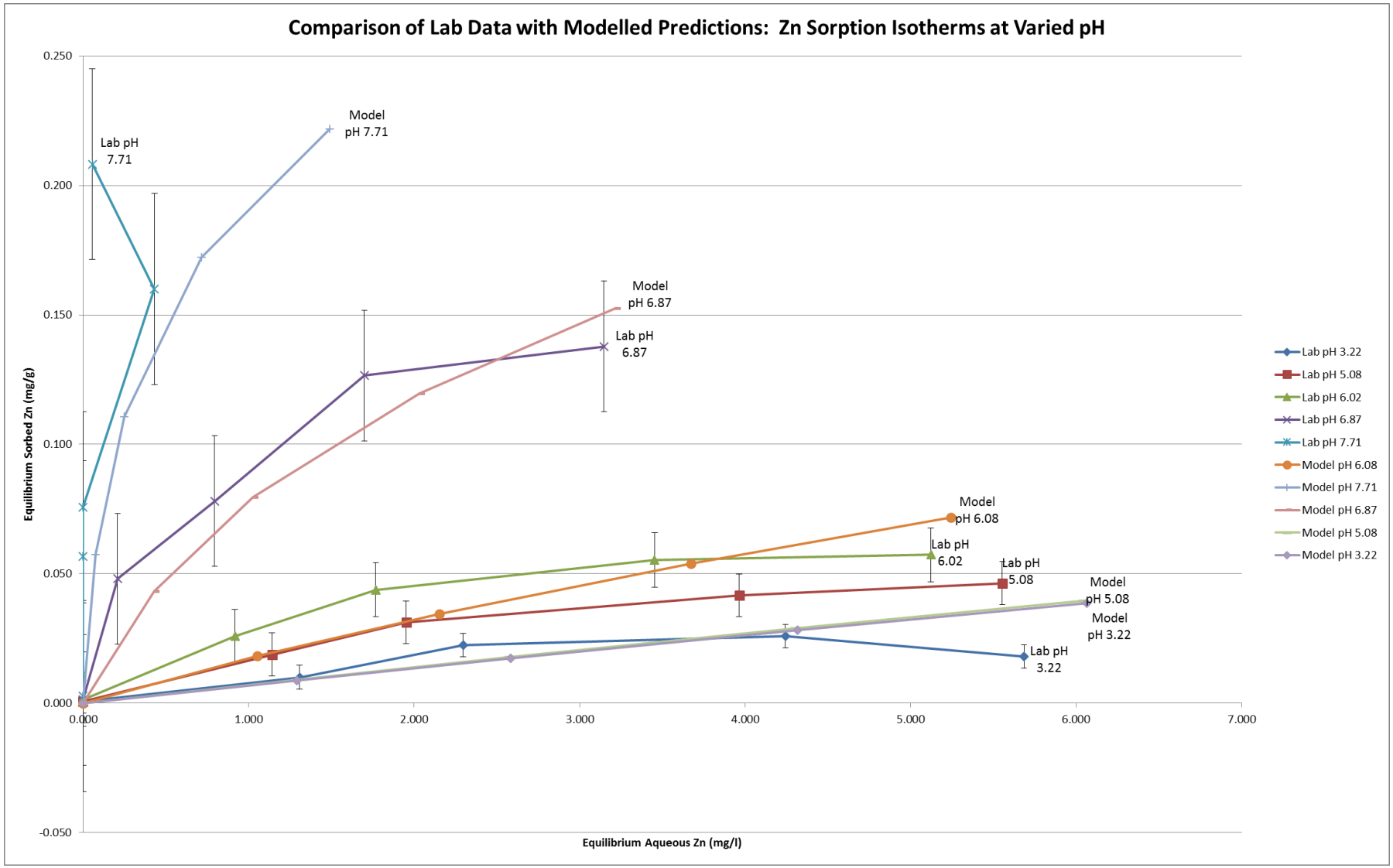

Figure 5-6: Simulation of the isotherms

5.6.5 Discussion

Given the complexity of the system and the impossibility of completely removing the presence of ion exchange reactions, it is suggested that the simulations presented in Figure 5-6 are reasonable. It is possible that the discrepancies seen are due to non-sorption processes rather than sorption processes, but the work undertaken here cannot demonstrate this. In addition, some of the pH-dependence could arise from clay edge sites.

The difficulty with which the calibration shown in Figure 5-6 was obtained, taking nearly 500 simulations, suggests that even though there are many parameter values to vary, there are very few sets of parameter values that can describe the data if the model is correct.

The final model parameter values are as listed in Table 5-4.

Table 5-4: Final parameter values for Trials 459-463

DATA BLOCK GROUP	PARAMETER			INPUT VALUE	REMARKS
SURFACE PROPERTIES	**General Surface Properties**		Specific Surface Area (m2/g)	6.00	
			Mass (g)	0.119	
	Strong sites	Number of Strong Sites (mols)		3.00E-04	
		Surface Species (log_k)	Hfo_sOH + H+ = Hfo_sOH2+	8.18	Default = 7.18
			Hfo_sOH = Hfo_sO- + H+	-10.82	Default = -8.82
			Hfo_sOH + Zn+2 = Hfo_sOZn+ + H+	0.66	Default = 0.66
			Hfo_sOH + Ca+2 = Hfo_sOCa+ + H+	0.15	Default = 4.97
			Hfo_sOH + Mg+2 = Hfo_sOMg+ + H+	0.15	Default unknown
	Weak sites	Number of Weak Sites (mols)		2.68E-08	
		Surface Species (log_k)	Hfo_wOH + H+ = Hfo_wOH2+	8.18	Default = 7.18
			Hfo_wOH = Hfo_wO- + H+	-8.82	Default = -8.82
			Hfo_wOH + Zn+2 = Hfo_wOZn+ + H+	-2.32	Default = -1.99
			Hfo_wOH + Ca+2 = Hfo_wOCa+ + H+	-2.32	Default = -5.85
			Hfo_wOH + Mg+2 = Hfo_wOMg+ + H+	-2.32	Default = -4.6
EXCHANGE PROPERTIES	**X (Quantity of exchange sites) (moles)**		6.25E-04		
	Exchange Species (log_k)		Zn+2 + 2X- = ZnX2	0.10	Default = 0.8
			Na+ + X- = NaX	0.00	Default = 0.0
			K+ + X- = KX	0.90	Default = 0.7
			Ca+2 + 2X- = CaX2	0.4	Default = 0.8
			Mg+2 + 2X- = MgX2	0.4	Default = 0.6
			Mn+2 + 2X- = MnX2	0.52	Default = 0.52

DATA BLOCK GROUP	PARAMETER		IMPUT VALUE	REMARKS
INITIAL SOLUTION COMPOSITIONS	Solution 1 (mg/l)	Na	23	
		K	5	
		Ca	20	
		Mg	10	
		Zn	0.0001	
		Mn	0.01	
		HCO3-	5	
		SO4[2-]	86	
		NO3-	5	
		Cl-	35	
	Solution 2 (mg/l)	Na	1000	
		K	0.01	
		Ca	0.01	
		Mg	0.01	
		Zn	0.0001	
		Mn	0.01	
	pH	Initial pH	6.08	Varied: see Trials 459-463
		pH fix?	Y	
		pH fixed using…	NaOH	NaOH or HCl

5.7 Conclusions

The experimental procedure developed in Chapter 4 has worked well, allowing the effects of pH-dependent sorption to be seen clearly despite the potentially dominant presence of ion exchange reactions.

The results of the experiments show sorption, with non-linear isotherms, increasing sharply as pH values rise, qualitatively as expected from the Dzombak and Morel (1990) model.

This result means that K_d-based approaches are likely to be inappropriate from two points of view: the non-linearity of the isotherms, and the pH dependence.

Simulation of the results of the experiments proved difficult, but eventually a description that reproduced the main features of the experimental isotherms was produced. The difficulty of producing this description suggested that equivalence was limited.

The fact that the sorption is pH-dependent could in principle arise not just from oxide sorption, but from sorption on clay edge sites. The experimental work undertake here cannot distinguish between these two possibilities.

The final simulation was least successful in reproducing the curvature of the isotherms to constant sorbed Zn concentrations at higher dissolved concentrations. This may mean that use of the model may over-predict sorption at lower pHs (<5) and higher Zn concentrations (> about 4 ppm).

Nevertheless, it is suggested that the simulation produced is suitable for tentative use in investigating the importance of pH-dependent sorption in contaminant transport, and this will be undertaken in Chapter 6.

5.8 Summary

Successful Zn isotherms were produced using the two step experimental procedure developed in Chapter 4. These were then simulated using PHREEQC, accounting for both experimental stages. The simulations proved difficult, but eventually a reasonable fit with the experimental data was obtained. The least successful aspect of the final simulations were the over-prediction of sorption at pHs less than 5 at Zn concentrations above about 4 ppm. The final parameter values used suggested that the rock sorption surfaces are rather less reactive than HFO, as expected. It is suggested that the simulation produced is appropriate for tentative use in investigating the importance of pH-dependent sorption in contaminant transport.

6 - USING THE LABORATORY RESULTS TO INVESTIGATE FIELD SCALE SYSTEM BEHAVIOUR

6.1 Overview

This chapter uses a slightly modified version of the model developed in Chapter 5 to investigate the fate of a Zn-contaminated plume in a field-scale aquifer.

6.2 Introduction

Chapter 5 showed that it had been possible to develop a numerical model representation of the sorption of the P-T sandstone, using simulated batch reactions. This Chapter reports on Stage 4 of the project, as initially outlined in Chapter 1. Here, the objective was to incorporate the model developed in Chapter 5 (Stage 3) into a field-scale contaminant transport model by which to explore the implications of the project's findings in predicting metal mobility in the field.

6.2.1 Scope

A PHREEQC solute transport model was conceptualised with the following specifications:

- The model was intended to represent the migration of a contaminant plume in an aquifer - as may be found, for instance, in an industrial area. Therefore, it was important to model a realistically-dimensioned cross-section of an aquifer.
- It was desirable for the model to predict both the migration and the elution phases of a pollutant plume, thus being of relevance to both the invasion and flushout phases of a pollution incident. Therefore, the model needed to represent a pulsed influx of Zn (chosen to be 7 ppm to fit with the laboratory results) to give both breakthrough and recovery curves, and to allow comparison with Bethke & Brady (2000(b)).
- Central to the model was the incorporation of the surface properties as deduced in Chapter 5 as part of the interpretation of the laboratory results.
- The model would be required to plot the breakthrough curves for the main elements under review and the pH.

6.3 Approach and Methods

In order for the model to predict the behaviour of Zn and other elements in both the up-take and elution phases, a three-step structure for the model was designed:

i. In Step 1, the HFO surfaces were equilibrated with the initial groundwater;
ii. Step 2 involved the introduction of a pulse of Zn-contaminated groundwater, which was then transported through the system; the composition of this solution only differed from that of the background groundwater in the presence of Zn;

iii. In Step 3, the original, Zn-free groundwater was re-introduced, flushing the system as it was transported through the column.

This process is summarised in the schematic illustration in Figure 6-1.

.

STEP 1: The HFO and exchange surfaces equilibrate with the groundwater.

STEP 2: A pulse of Zn-contaminated water is transported through the system.

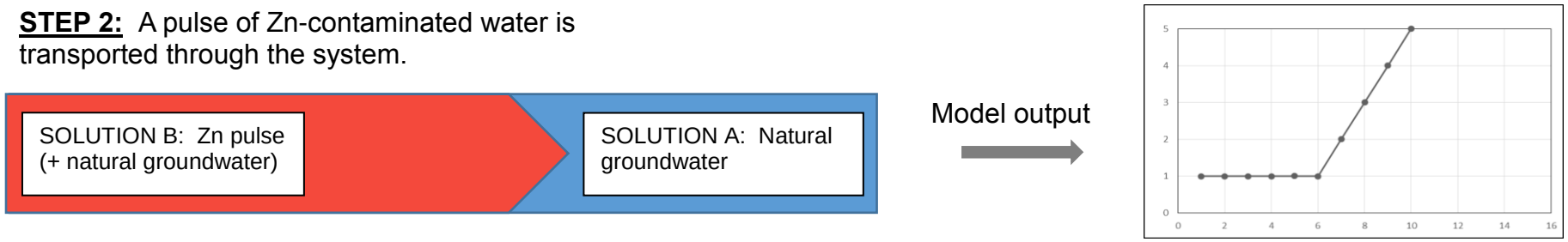

STEP 3: Zn-free groundwater is re-introduced and transported through the system.

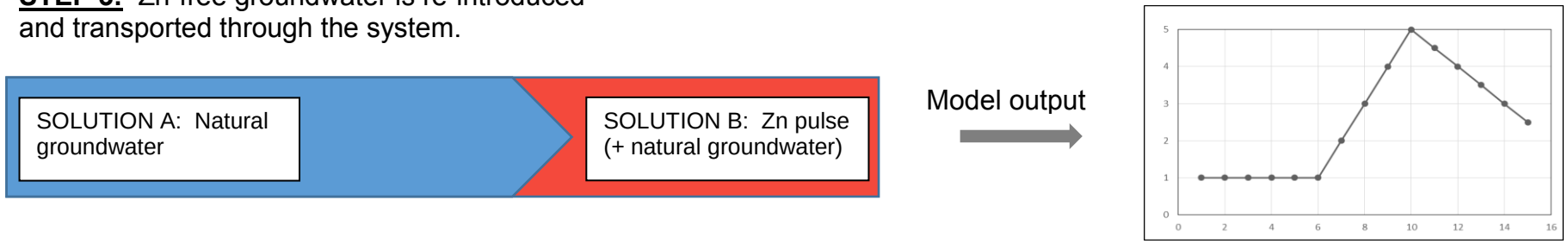

Figure 6-1: A schematic representation of the simulations undertaken. In all cases, the x-axes represent time and the y-axes represent concentration.

This new PHREEQC model incorporated the finalised input code from the 'best fit' model runs in Chapter 5. The code from Chapter 5 was adapted to produce a transport model, and the generic code used as the basis of all of the simulations in this chapter is given in Appendix 9.3.1. At the end of each of the three steps in the overall structure, the model outputted the composition of the surface and the solution. These outputs were combined during processing to produce the entire sequence of pre-contamination, contamination and elution phases.

The compositions of the different solutions used in these simulations are given in Table 6-1. In all calculations, Smithsonite ($ZnCO_3$) and $Zn(OH)_2$ were allowed to precipitate if they became oversaturated, and any precipitated material was subsequently allowed to re-dissolve.

Table 6-1: Compositions of solutions used in numerical transport experiments

Species	Background and eluting solution (mg/l unless otherwise indicated)	Zn-containing solution (mg/l unless otherwise indicated)
pH	5 (-)	5 (-)
Temp	298 K	298 K
Na	23	23
K	5	5
Ca	20	20
Mg	10	10
Zn	0.0001	7
Mn	0.01	0.01
HCO_3	100	25
SO_4	86	86
NO_3	5	5
Br	0	17
Cl	35	35

An initial array of nine simulations were run. Calcite equilibrium was not controlled, and all three solutions – the initial groundwater, the Zn pulse, and the elution water – were given the same pH, which was incrementally increased in each of the nine runs as follows:

5.0; 5.5; 6.0; 6.5; 7.0; 7.5; 8.0; 8.5; 9.0.

The results of these are now presented and discussed.

6.4 Results and Discussion

6.4.1 Main Simulation Results

Appendix 9.3.2 reproduces the entire suite of individual results from the nine simulations; summary plots and specific aspects are reported and discussed here. Figure 6-2 shows the resulting aqueous concentrations of Zn and Br for the solutions as the Zn pulse proceeds through the system. Br was included as a conservative element, to act as a 'control': it was not expected to interact with the HFO, and the results show this to be the case.

The Zn breakthrough curves show marked differences as the pH changes. The lowest pH runs exhibit a 'lag', as might be expected from some attachment, in this case ion exchange. As the pH rises, however, the breakthrough of the Zn is more delayed and the curve shallower. Up to pH 7.5, the concentration does eventually reach that of the lower pHs, before falling in the elution phase; for pH 8.0 and above, the concentration does not reach that of the lower pH. At elution, for higher pHs the sorbed Zn is released quite slowly, causing significant tailing. At

lower pHs, this tailing is much shorter, almost disappearing by pH 6. However, the behaviour is quite complex, as for lower pHs the aqueous concentration is higher, then falls suddenly (see pH 6.5) whereas for the still higher pHs the aqueous concentrations are less, presumably because the release is slower and the tailing much longer (well beyond the experimental time frame). These results reinforces earlier observations, that at lower pH, there is very little sorption, and at higher pHs, almost all of the Zn is attached to the surface.

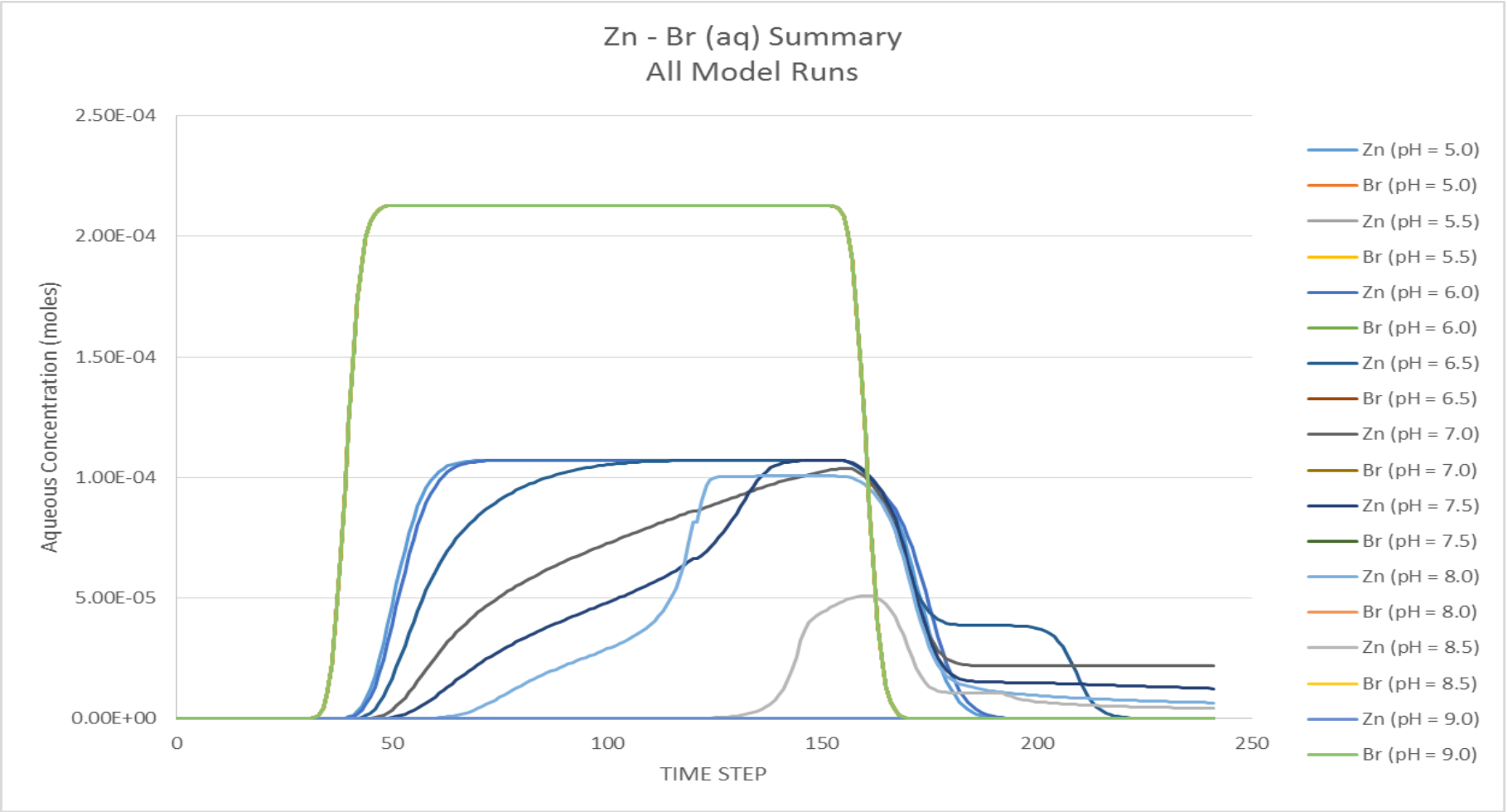

Figure 6-2: Modelled breakthrough curves for Zn and Br

Figure 6-3 shows in more detail how the pH fluctuates as the Zn enters and leaves the system. For the lower pH systems (pH 5.0-6.0), there is very little fluctuation in pH, but for the higher initial pH systems, there is a considerable fluctuation (except for pH 9.0).

Given that in all of these systems, the initial pH of the Zn pulse was the same as that of the initial and elution waters, it is clear that there is a relationship between the pH and the Zn sorption. The most likely process is (Equation 6-1):

$$\equiv OH_2^+ + Zn^{2+} \rightarrow \equiv OZn^+ 2H^+ \qquad \text{(Equation 6-1)}$$

Here, it follows that where there is a drop in pH, H^+ is released, allowing more sites to become available for sorption.

However, the degree to which this process operates varies when comparing the contamination and elution phases of the system. This is illustrated in Figure 6-4, which shows a clear hysteretic pattern in the relationship of pH and Zn concentration. This pattern becomes more pronounced above 6 (with the exception of pH 9 where attachment is effectively 100% throughout). On this plot, pure ion exchange is represented by a vertical line, and the spread laterally in the pH direction is the influence of (pH-dependent) sorption. Taking the pH 8 run as an example, the initial displacement to the right along the pH axis represents the period where attachment is effectively 100%, with H^+ being released from the sorption sites which are taking up Zn^{2+} (Equation 6-1). As Zn breakthrough

occurs, the Zn concentration increases and pH rises; the final part of the curve represents the point where the Zn is being eluted.

From the results presented in Figures 6-2, 6-3 and 6-4, it can be concluded that Zn / pH relationship is complex and non-unique, as might be expected. This was now the focus for further investigation.

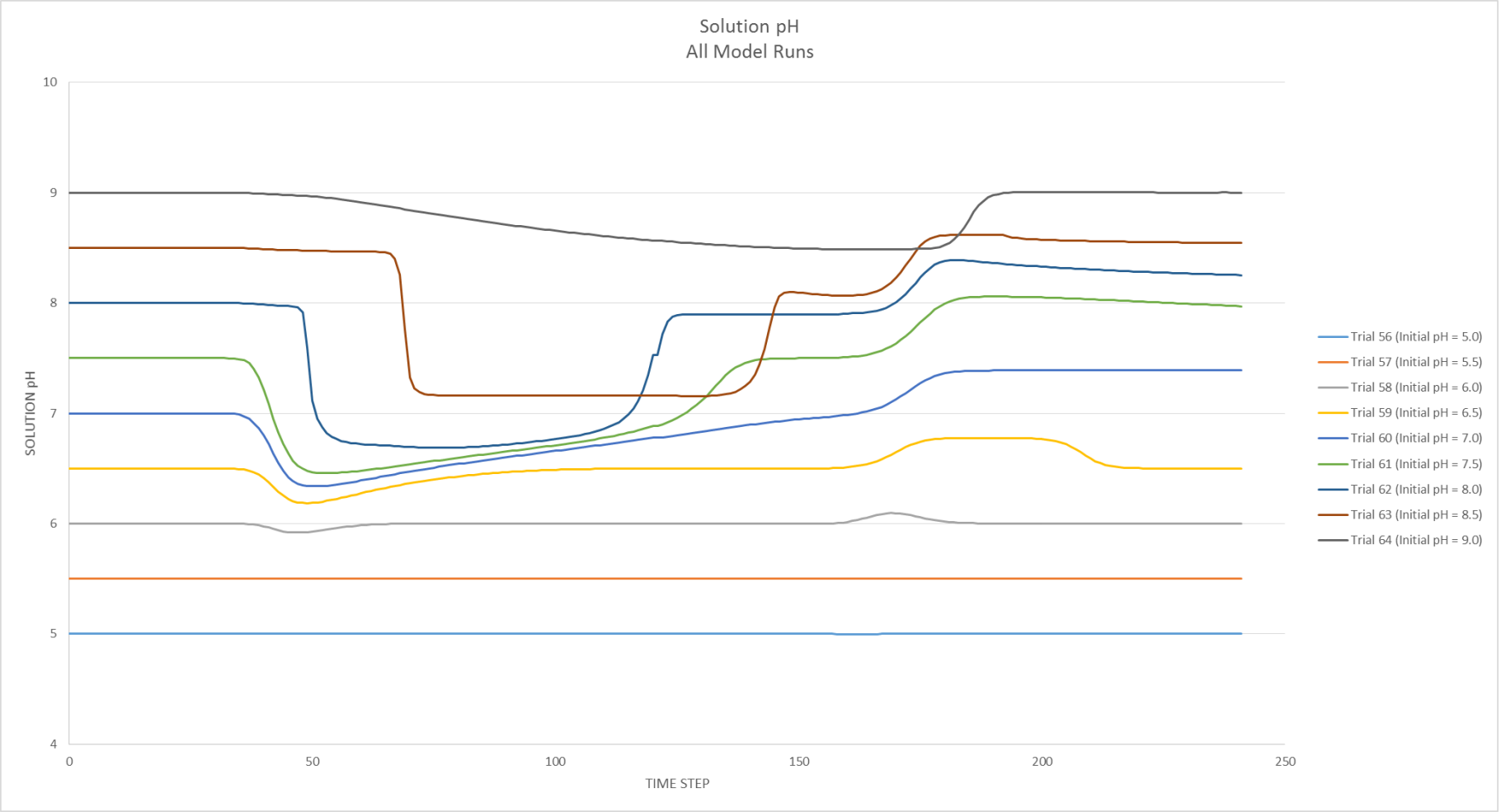

Figure 6-3: Summary of pH fluctuation

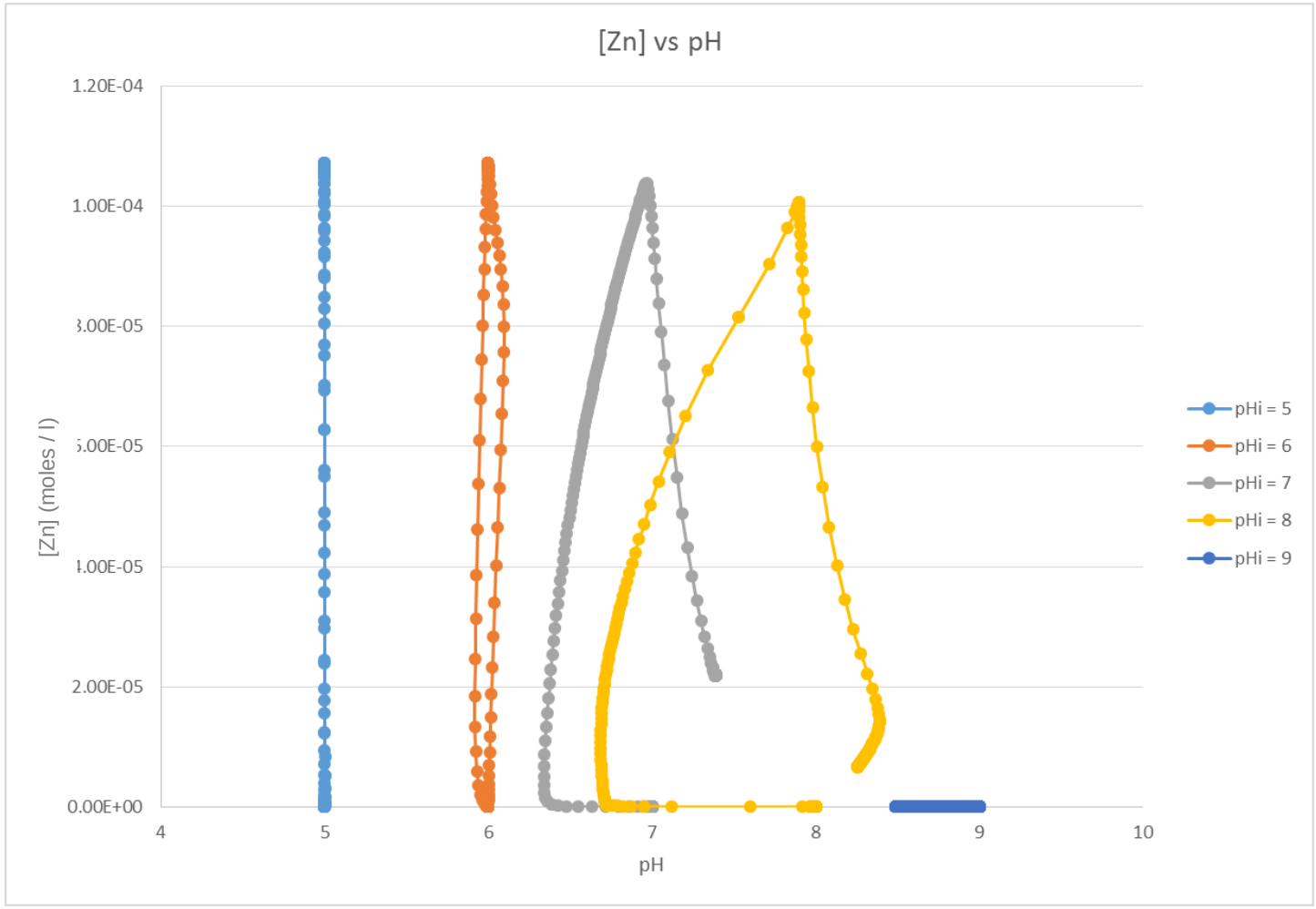

Figure 6-4: Zn concentrations as a function of pH for runs of different initial pH

The laboratory stage informed the work that ion exchange was a very important process in the attachment of Zn to the sandstone surface. It was possible to use the model to separate these processes and to look at their interrelationship. Figure 6-5 shows the ratio of exchange site Zn concentration to sorption site Zn concentration as the Zn plumes migrate through the system. In this summary plot, an increase in the ratio means that there is more exchange occurring; a lower value implies more sorption. It is clear that at pH 5 to 6, ion exchange processes are more dominant, whereas at pH values above 6, sorption becomes important. In most cases, there is an abrupt change in the ratio at the point at which Zn enters the system, then a stabilisation, then another (much more gentle) change, in the opposite direction, as the elution phase begins. The initial sharper (positive and negative) peaks on the onset of breakthrough and elution are due to ion exchange occurring.

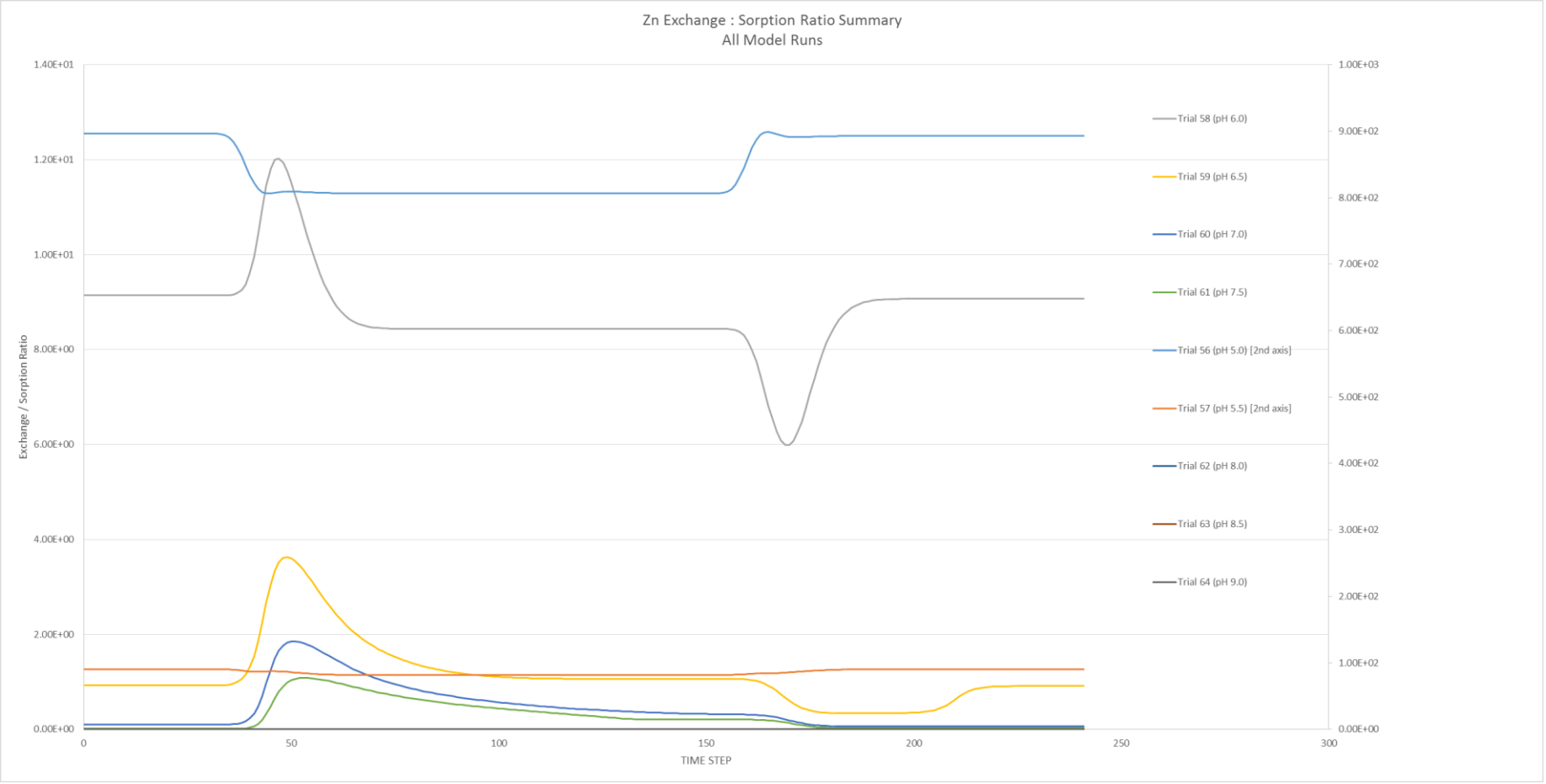

Figure 6-5: Ratio of exchange site concentration to sorption site concentration as a function of time for solutions initially at the pHs indicated passing through the column

Looking more closely at this relationship by referring to the individual outputs from the pH 5, pH 7 and pH 8.5 simulations, there is a clear evolution of the exchange : sorption ratio. At pH 5 (Figure 6-6), the system is initially mostly exhibiting exchange processes, but as Zn enters and the pH changes, it abruptly magnifies its sorption processes, though still with ion exchange predominant, before reverting, again abruptly, to mostly ion exchange in the elution phase.

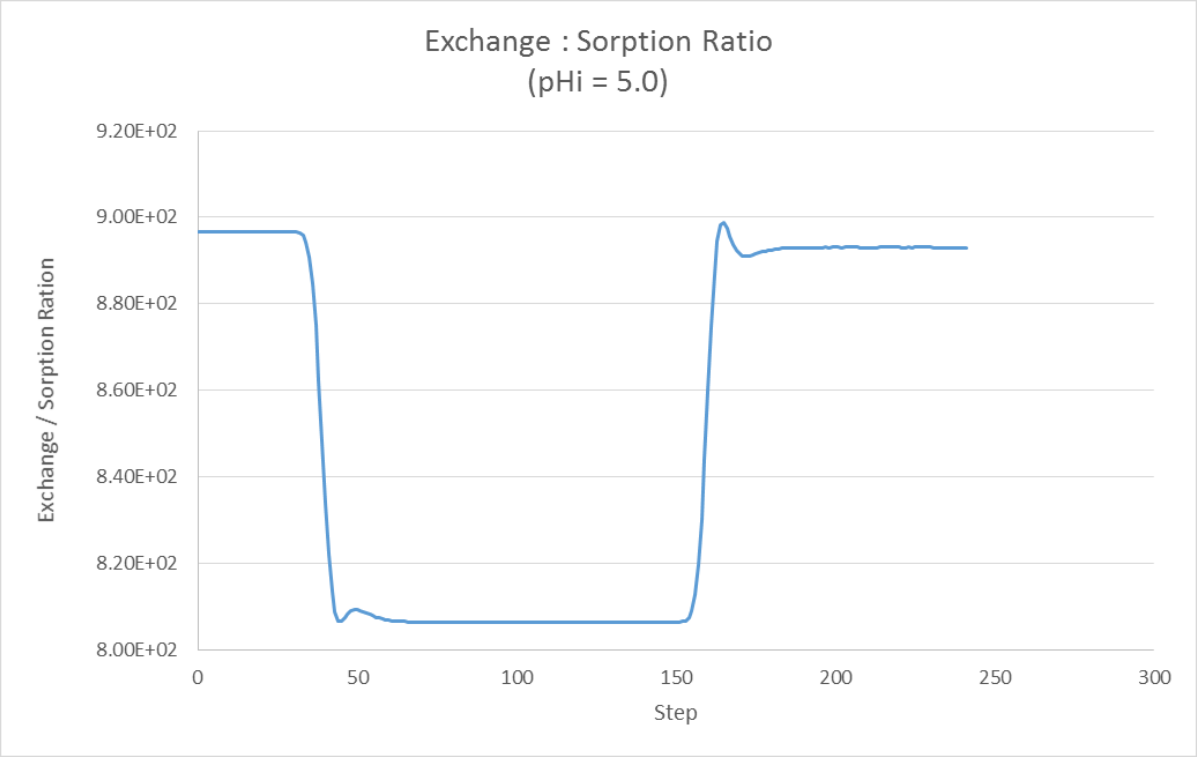

Figure 6-6: The ratio of Zn exchange site concentration to sorption site concentration as a function of time for an initial pH of 5

At pH 7 (Figure 6-7), the Zn system is initially more sorption-based; ion exchange briefly becomes more important as Zn enters the system, but it quickly reverts to a sorption-based system.

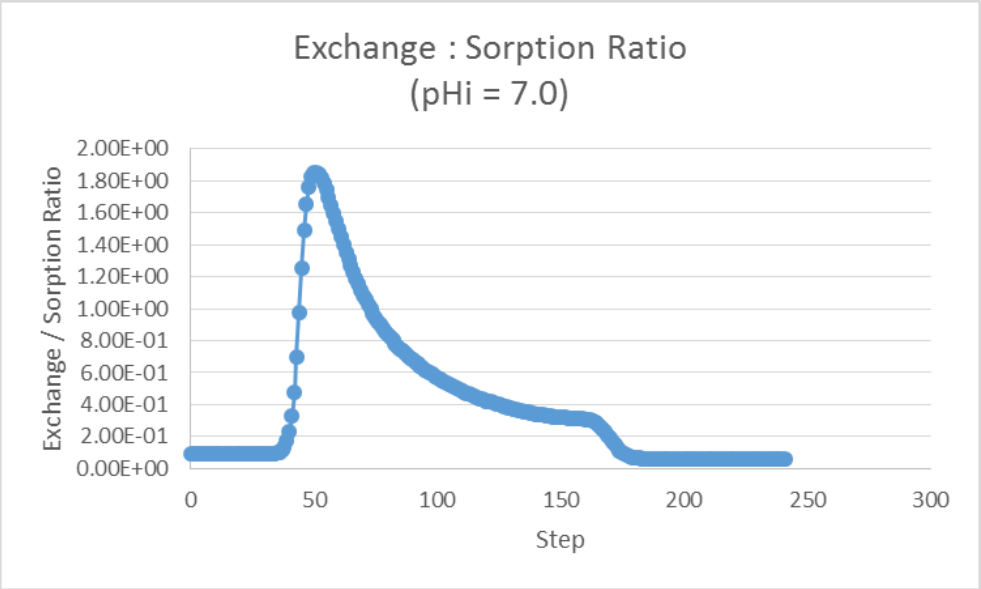

Figure 6-7: Zn exchange site concentration : sorption site concentration against time for run with initial pH of 7.

By pH 8.5 (Figure 6-8), the system is strongly sorbing. Whilst the ratio of exchange : sorption appears to be a reflection of the system at pH 5, the contribution of exchange processes to total attachment of Zn is very small.

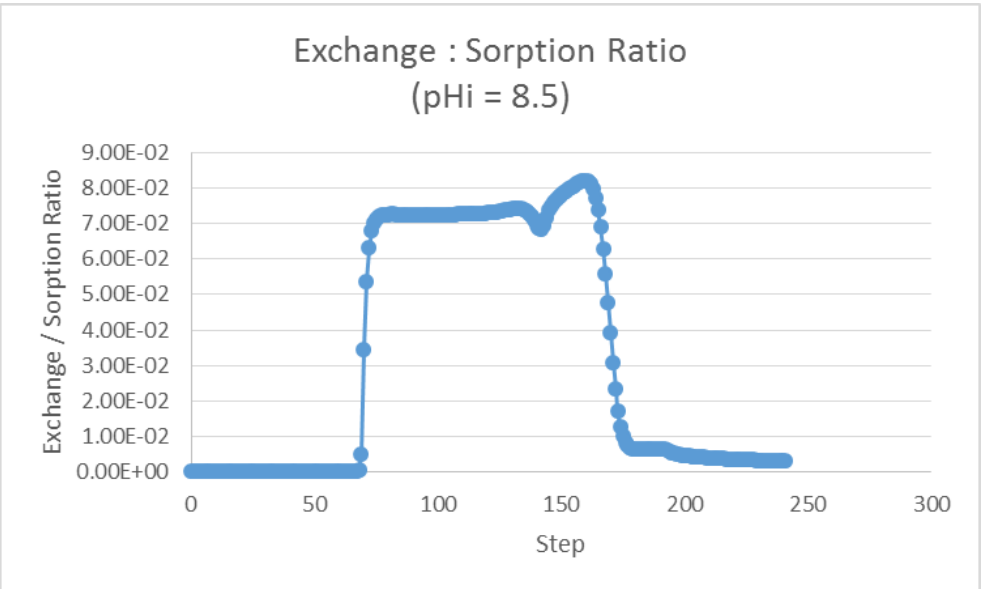

Figure 6-8: Zn exchange site concentration : sorption site concentration against time for run with initial pH of 8.5

Figures 6-9, 6-10 and 6-11 provide more insight into this result, by considering the relationship between aqueous and attached concentrations (apparent isotherms) for sorption, exchange, and sorption plus exchange at different pH values. At pH 5 (Figure 6-9), there is little difference between the ion exchange-only and sorption-only results, suggesting that the sorption sites are only weakly involved. However, the outcomes for both the pH 7 and pH 8.5 systems show considerable differences between the sorption-only and ion exchange-only results, suggesting that the sorption sites become increasingly more important as the pH increases. The relationships are apparent isotherms only, as pH is not constant throughout the experiments. The lack of 'closure' of the apparent isotherms is due to there still being considerable sorbed Zn at the end of the experiment for the higher pH cases. As noted above, the release of Zn is quicker for the runs at lower initial pH, but slower and therefore at lower concentrations but for longer for the cases where pH is highest. It is clear that at any point in the system the apparent isotherms do not correspond well with the K_d approach.

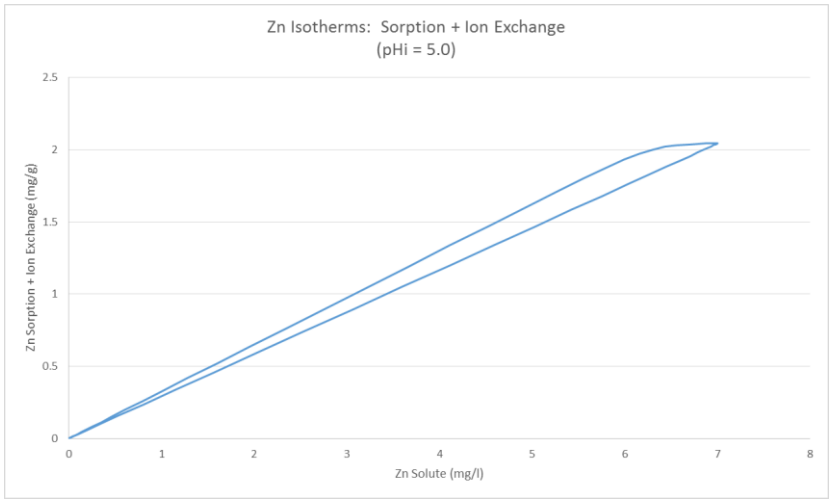

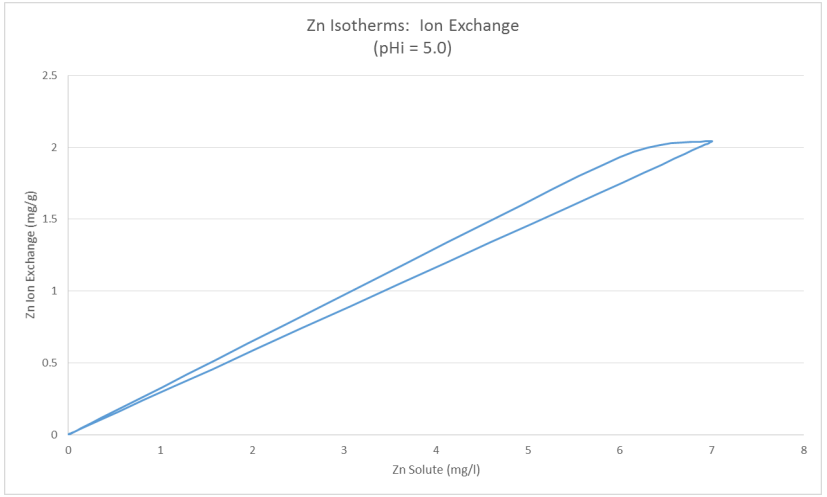

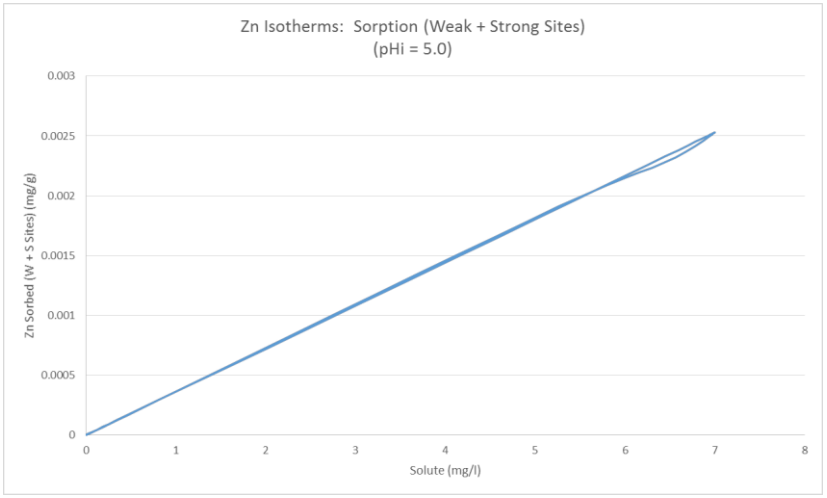

Figure 6-9: Isotherms for sorption + ion exchange, ion exchange alone, and sorption alone at an initial pH of 5

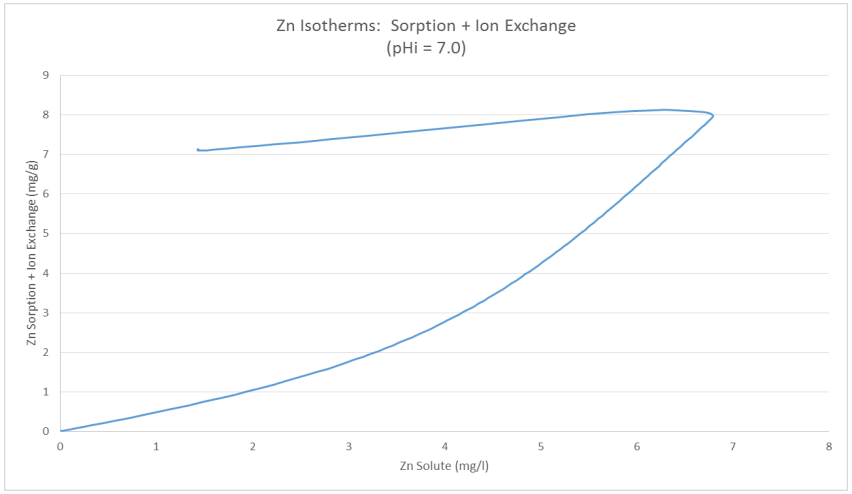

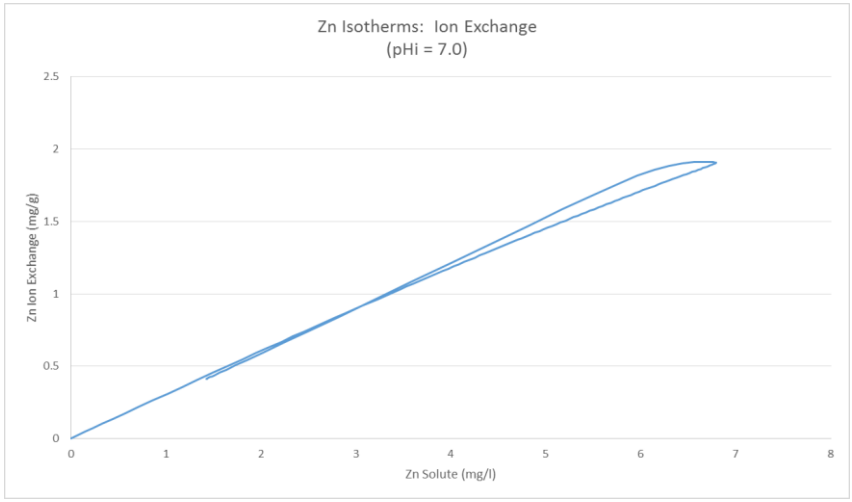

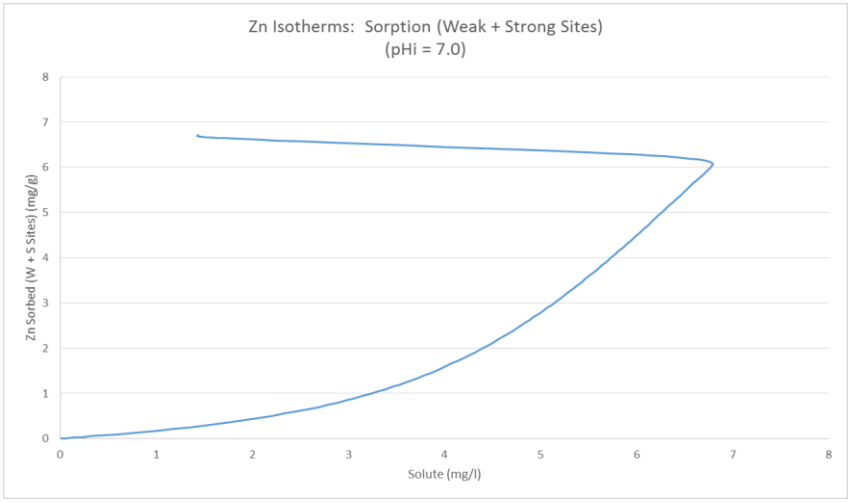

Figure 6-10: Isotherms for sorption + ion exchange, ion exchange alone, and sorption alone at an initial pH of 7.

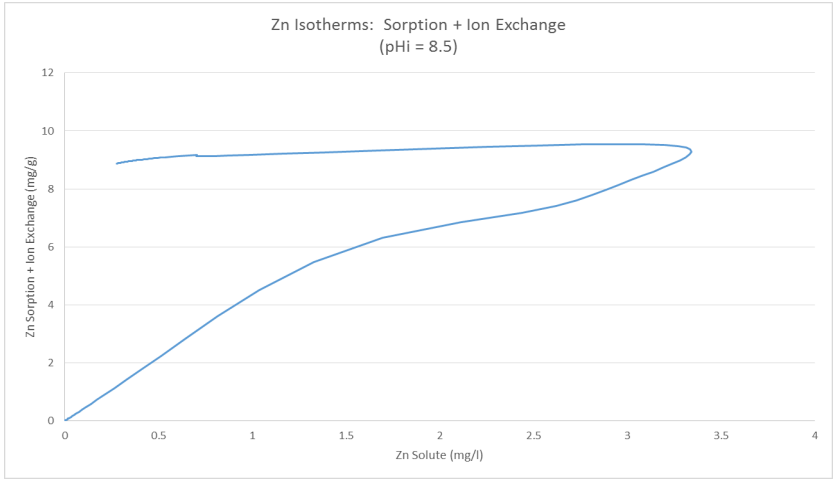

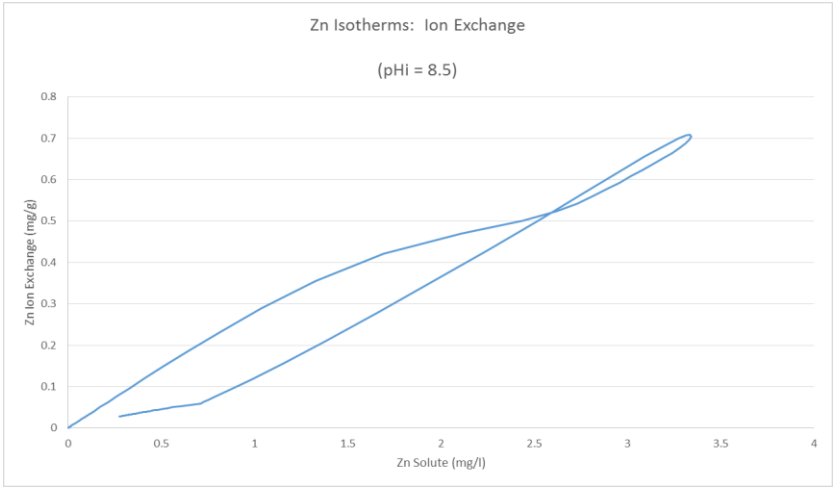

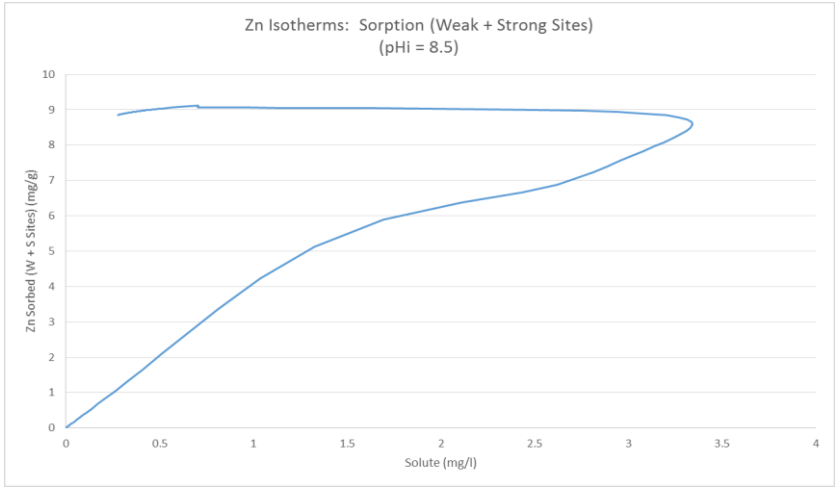

Figure 6-11: Isotherms for sorption + ion exchange, ion exchange alone, and sorption alone at an initial pH of 8.5

Figure 6-12 shows the results of a plot of the ratio of the attached (“sorbed”) and aqueous concentrations of Zn as the plume migrated. This analysis shows eloquently the variation in aqueous:sorbed concentrations in this scenario, with a continuously evolving outcome as the plume proceeds, and changing by orders of magnitude within the range of pH shown here. (More results for other pH values are available in Appendix 9.3.2)

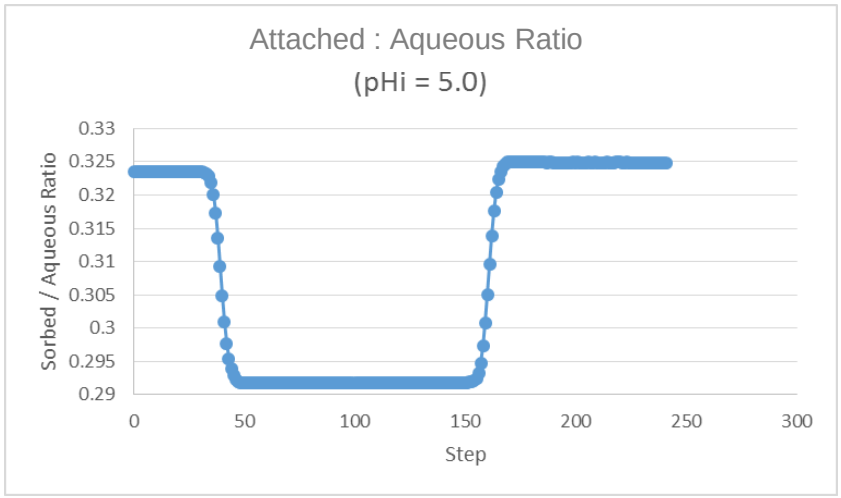

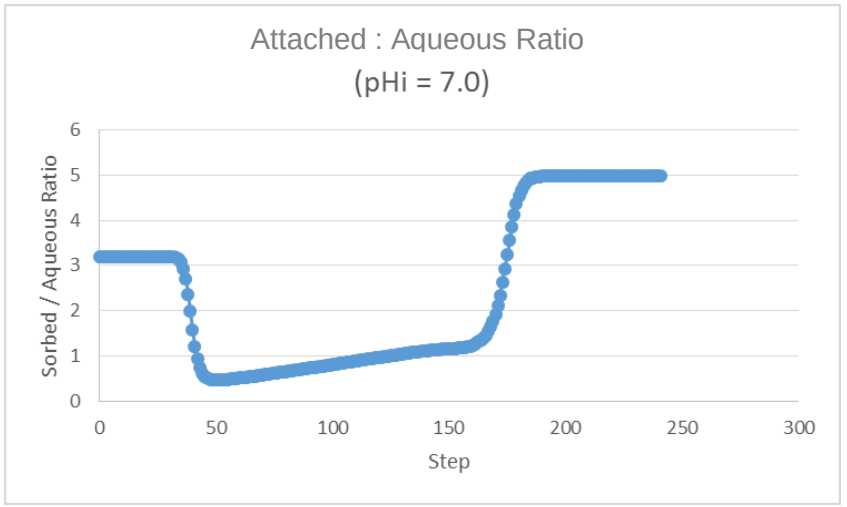

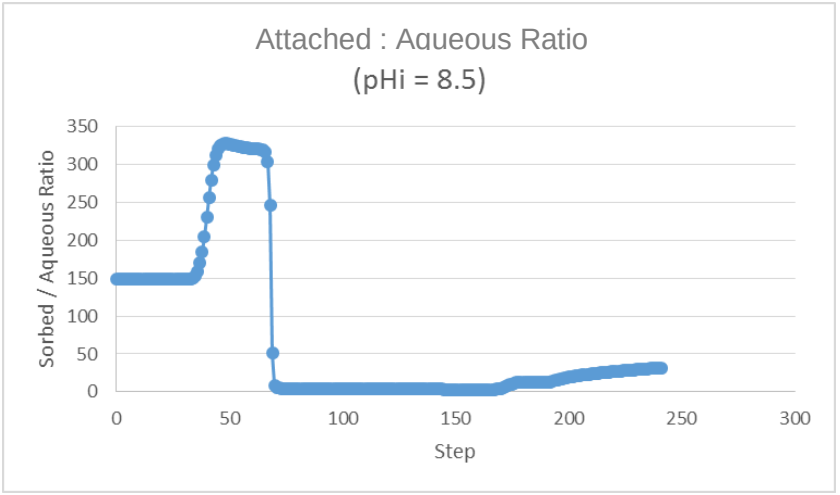

Figure 6-12: The variation in attached concentration to aqueous concentration with time

As an interpretative summary:

- At pH 5, the system flushes the Zn so that the elution waters quickly return to the composition of the initial waters.
- At pH 7, there is a slower release of Zn from the sorbed phase, meaning that Zn is likely to remain detectable in the elution waters for longer.
- In the range of pH 8.5, Zn is reluctant to leave the system, instead remaining sorbed. The elution waters retain a low, but persistent, long trailing concentration of Zn as flushing continues.
- The movement is complex, involving both exchange and sorption, the latter dependent on pH and both processes involving competition with other ions.

6.4.2 Variation: K_d-type breakthroughs

A variation on the model was performed, with three simulations undertaken where all sorption reactions were disabled, thus permitting only ion exchange reactions to take place. This, it was hypothesised, would result in a series of "K_d-type" breakthrough curves, which may be the result if one ignored the variable effects of sorption (as the K_d concept does). A perfect partitioning relationship is expected with ion exchange is the ion of interest has a vanishingly small concentration compared with the concentrations of the other exchanging ions. Though Zn has a small concentration compared with the other ions, it is not vanishingly small, and so this representation is not quite a perfect partitioning relationship.

These simulations were based on the code for the pH 5 run in the series just described. In addition to all surface-relevant interactions being disabled, the exchange capacity was increased by an order of magnitude (from $6.25e^{-4}$ to $6.25e^{-3}$ mol), and the log_k values for Zn exchange were changed to 0.05, 0.4 and 0.8, respectively, to give low, medium and high values, within a reasonable range.

The results are given in Figure 6-13 to 6-15.

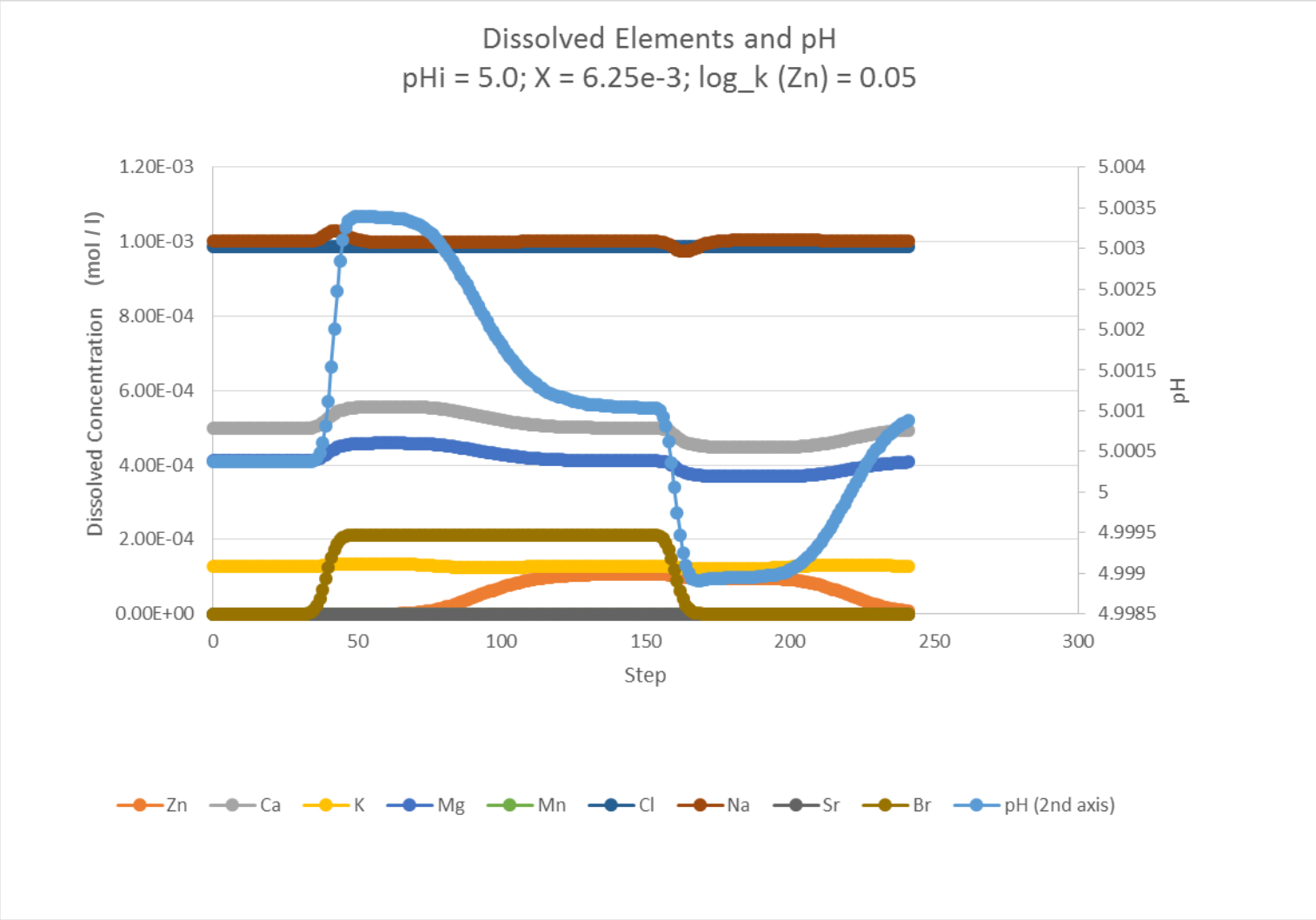

Figure 6-13: Breakthrough curves for ion exchange only simulations for low Zn exchange selectivity

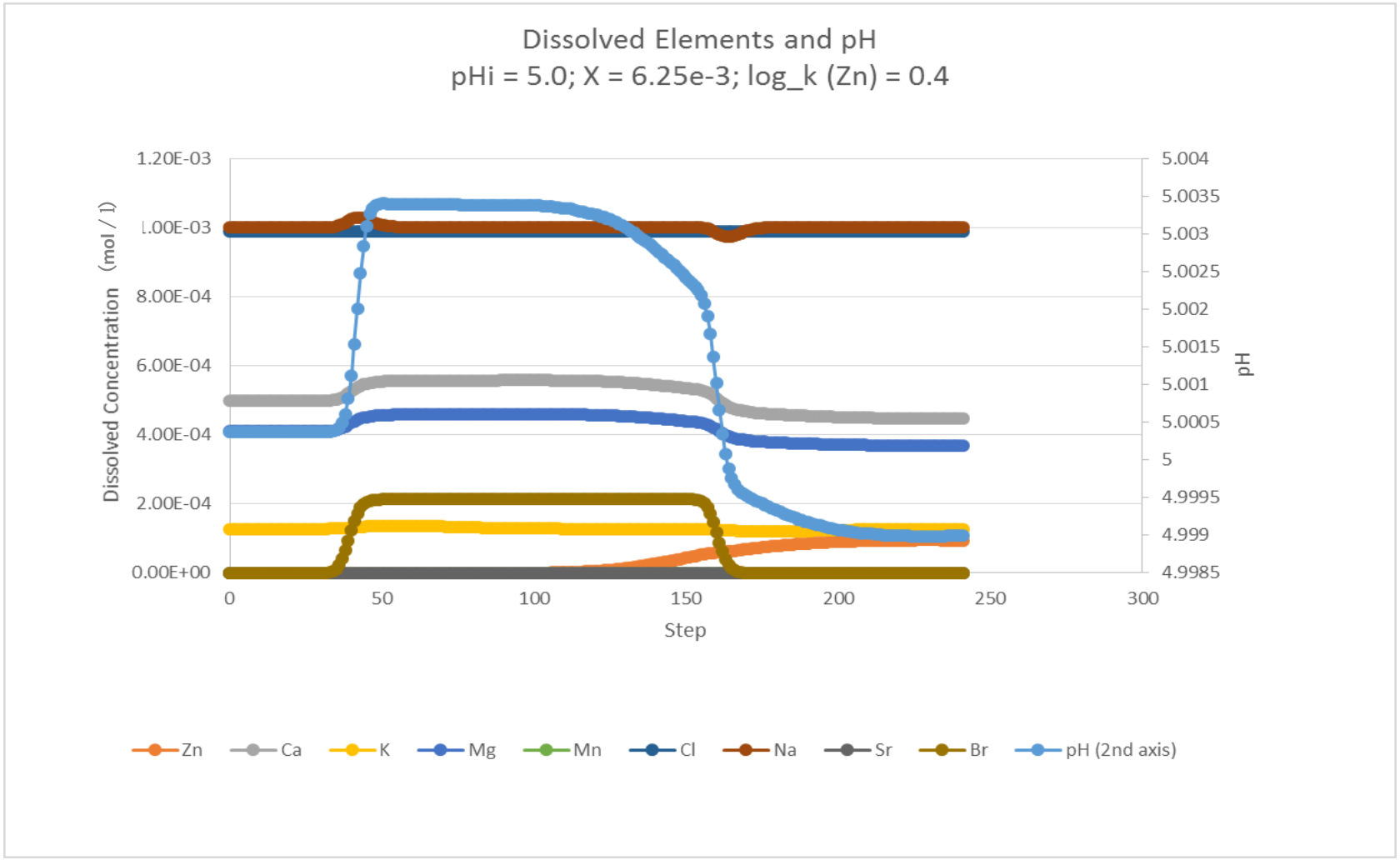

Figure 6-14: Breakthrough curves for ion exchange only simulations for moderate Zn exchange selectivity

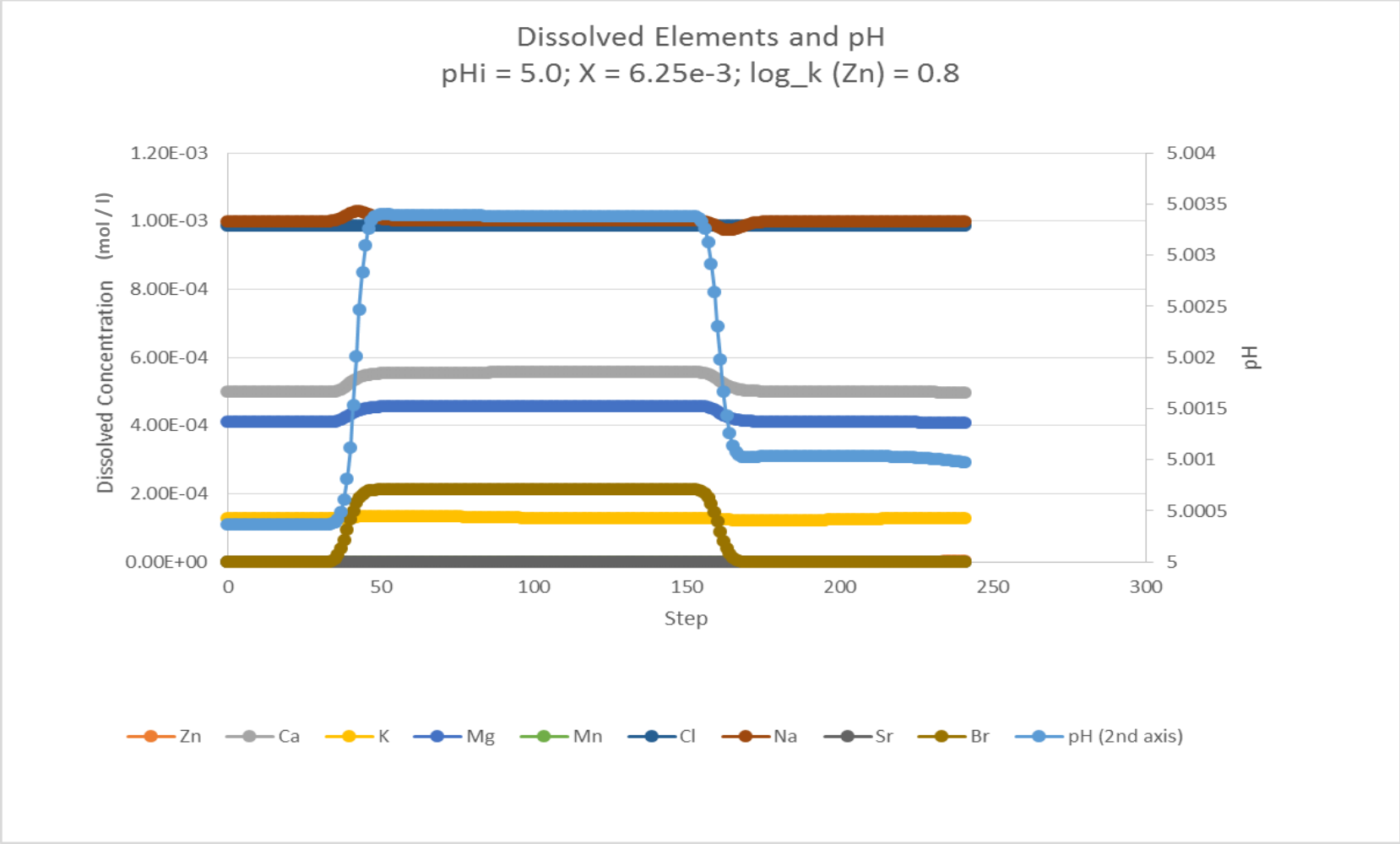

Figure 6-15: Breakthrough curves for ion exchange only simulations for high Zn exchange selectivity

In examining these results, pH change is small (note the scale on the secondary axis), but has been included as there is a variation related to the speciation of the dissolved phases. Of more interest is the change in Zn. Where the log_k value is 0.05 – i.e. weakly held by the exchange sites - it portrays a likeness to the lower-pH scenarios in the main set of simulations, with a fairly abrupt increase, a stable portion as the Zn pulse continues, and then an equally abrupt reduction as the elution phase takes hold. For the situation where the log_k is a mid-range value of 0.4 (which is the same as for the nine main simulations in this chapter), delay in breakthrough is very significant, and much Zn is still retained at the end of the run. For the highest log_k value (0.8), there is very little dissolved Zn, presumably entirely taken up by the surface. This suggests that the relative roles of exchange and sorption may well be significantly affected by the selectivity coefficient for Zn on the exchange sites.

The selectivity coefficient value changes can make the difference between negligible breakthrough and significant breakthrough. Appelo and Postma (2007) give a range for Zn selectivity coefficients equivalent to log k = 0.44 to 1.0, with 0.8 as the most common: however, from the laboratory experiments, a value of 0.4 was found to fit the data best. Taking the values from Appelo and Postma (2007) to be an indication of Zn exchange in many systems, the case of log k = 0.05 (Figure 6-13) is unlikely (exchange uptake of Zn very weak), the case of log k = 0.4 (Figure 6-14) is possible, the case of log k = 0.8 (Figure 6-15) is the most likely, and a case where log k might reach 1.0 is possible: however, the log k = 0.4 value is what appears to operate in the sandstone samples examined in the

current study. It is clear from comparing the breakthrough curves for ion exchange only with those for ion exchange with sorption that the latter are much more complex, as would be expected.

6.4.3 Variation: pH_i (Groundwater) = 8.0; pH_i (Zn pulse) = 5.0

So far, the modelling simulations have all used the same initial pH for both the initial and elution waters, and the Zn pulse. This was a deliberate choice in order to help discern the processes taking place – but it is arguably unrealistic. The final part of this chapter is to add a little more realism to the model by changing the pH of the Zn pulse, whilst keeping the other factors the same. Thus, it was decided to introduce a Zn pulse at pH 5 into groundwater at pH 8, and flushed by similar groundwater at pH 8. Both sorption and ion exchange were simulated. An overview of the results is given in Figures 6-16 to 6-18.

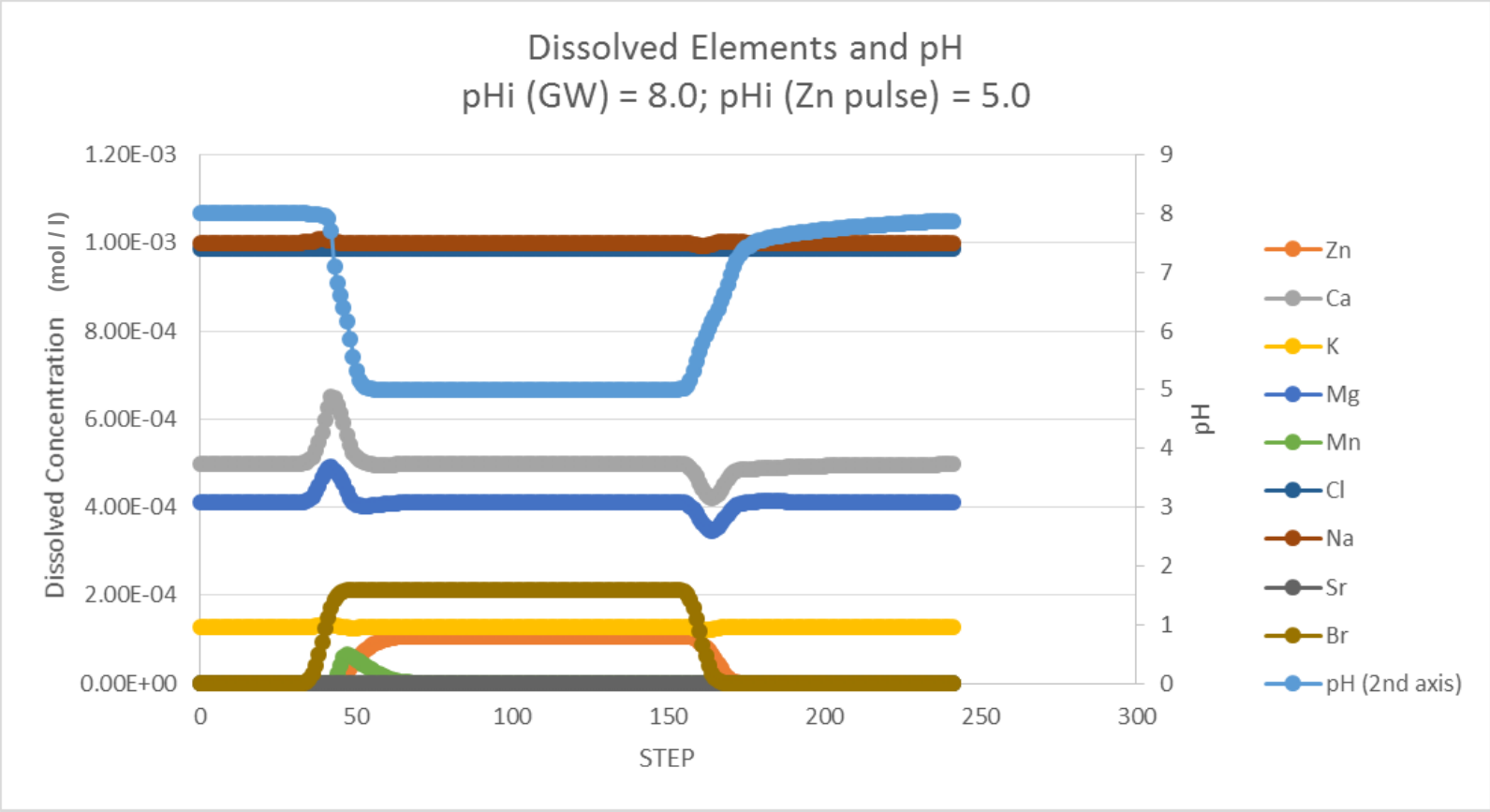

Figure 6-16: Breakthrough curves for experiments where the initial and eluting groundwater compositions have a pH of 8, and the Zn solution has a pH of 5

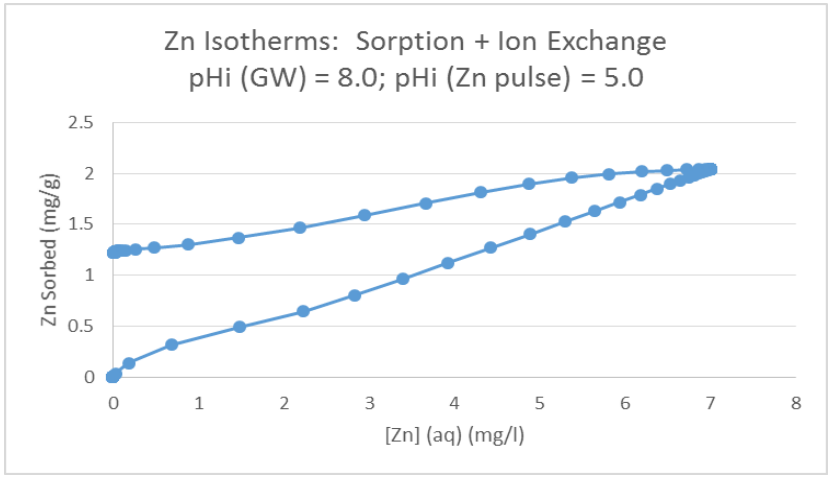

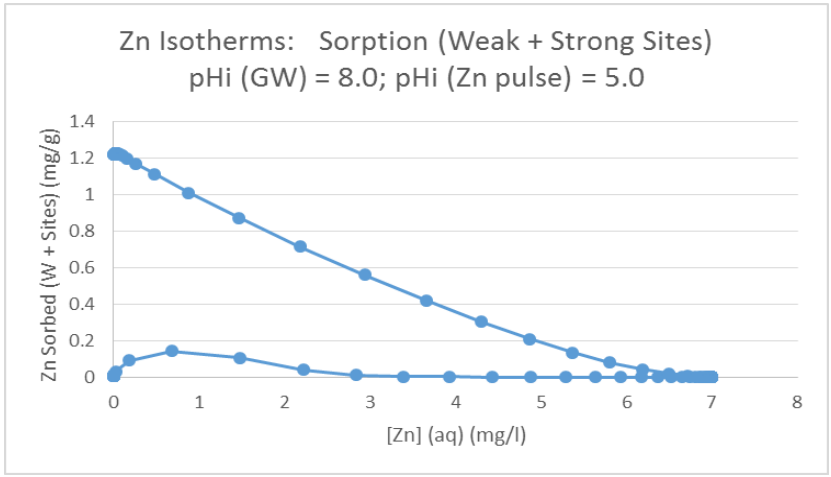

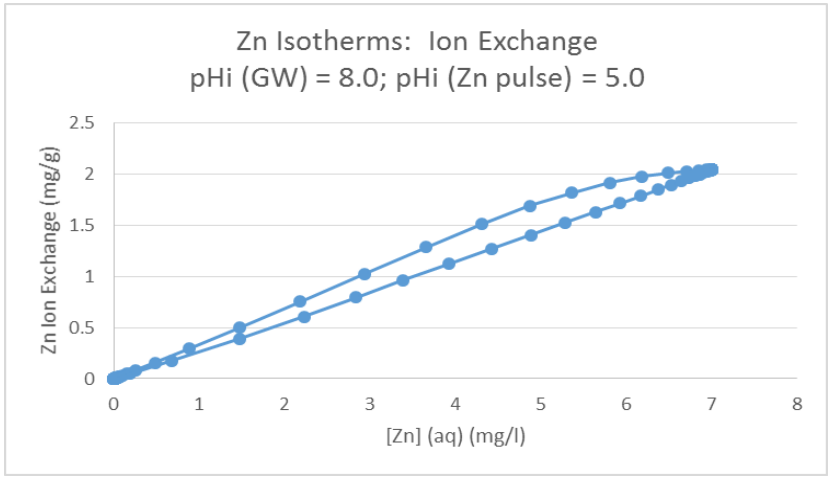

Figure 6-17: Apparent isotherms for experiments where the initial and eluting groundwater compositions have a pH of 8, and the Zn solution has a pH of 5

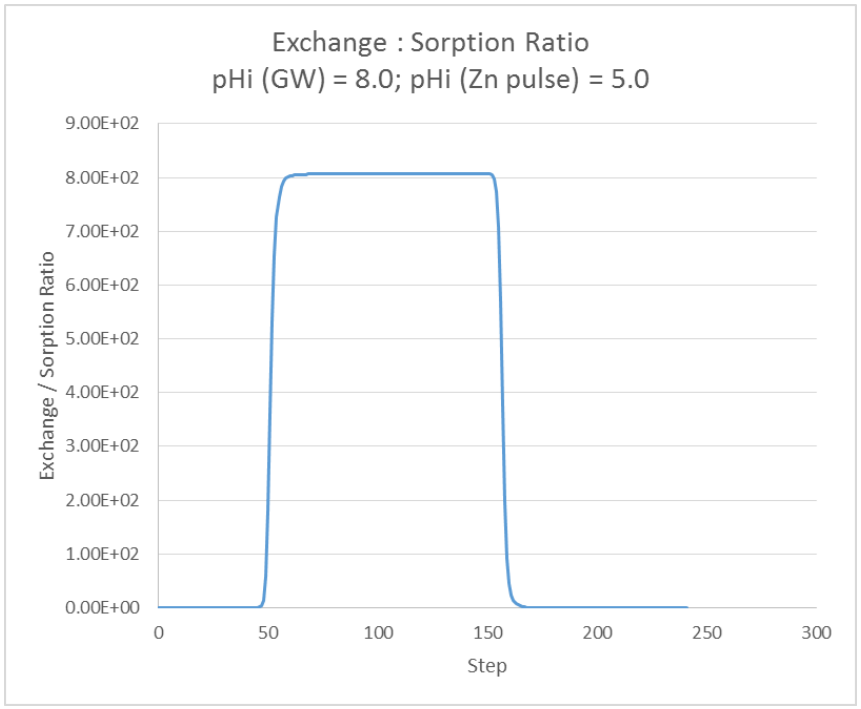

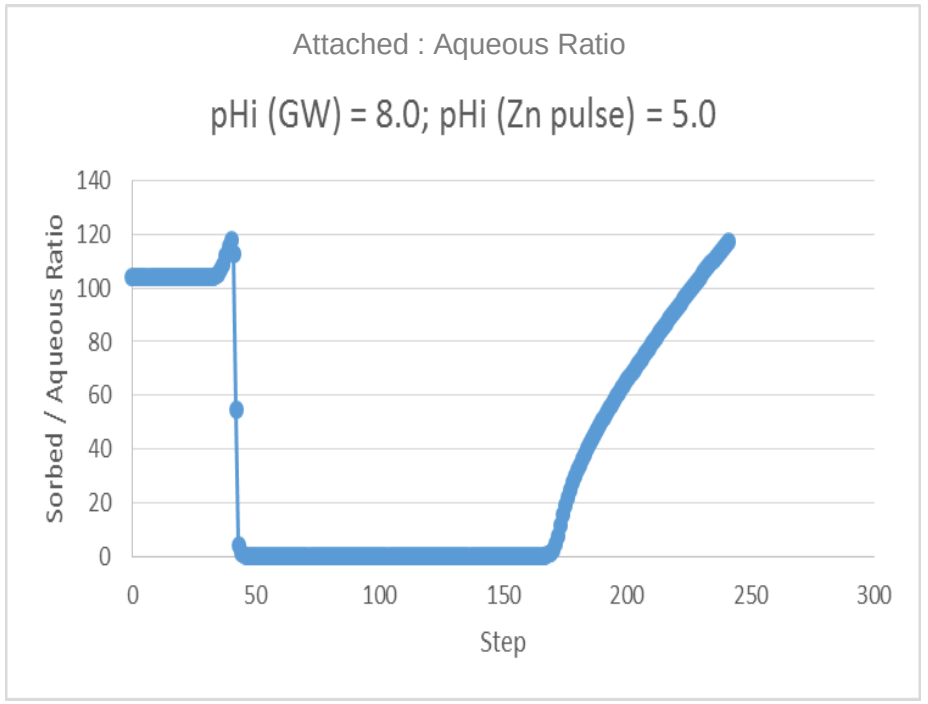

Figure 6-18: Exchange site concentration : sorption site concentration and attached concentration to aqueous concentration ratios for experiments where the initial and eluting groundwater compositions have a pH of 8, and the Zn solution has a pH of 5

Figure 6-16 shows how the pH changed from pH 8 to pH 5, and back to pH 8. The Zn concentration appears to bear much similarity to the lower pH scenarios in the main set of simulations (Figure 6-2), even though the initial and elution phases are of much higher pH, presumably because the pH rapidly adjusted to 5 during the injection phase. Nevertheless, examination of the contributions of sorption and ion exchange does confirm that both processes are operating, but their dominance swaps, as before, as the plume migrates.

6.5 Conclusions

The modelling work reported in this chapter has, overall, underlined the main issues and conclusions raised in the earlier stages of the project. These could be summarised as:

- There is considerable interplay of ion exchange and sorption processes governing the migration of a Zn-laden contamination plume in groundwater.
- For the sandstones investigated, ion exchange processes are more dominant where pH is below 6.5, whereas sorption becomes more important above pH 6.5.
- The value of the selectivity coefficient of Zn is an important factor, and in other systems, ion exchange could be more dominant.
- The variability of Zn concentration is much more complex than could be credibly predicted used a K_d-type approach. This is because the ratio of sorbed : dissolved Zn in the system is extremely variable as a migration plume proceeds.

- Tailing effects are of increasing importance as the pH of the system increases.

Overall, the model was successful in that it showed that it is possible to model a reasonably complex system with far greater detail than a simple K_d-type calculation, with far more precise predictions of concentration and speciation at a given point and local chemistry. Ignoring such factors may risk wrongly predicting local concentrations of contaminants by up to a factor of 10 or more.

7 - CONCLUSIONS AND FURTHER WORK

7.1 Introduction

For many years, hydrogeologists working to remediate contaminated groundwater have expressed concerns about their dependency on the K_d approach for quantifying the sorption behaviour of heavy metals. These concerns focused mostly on its lack of account of the complex geochemical processes predicted by surface complexation theory, and the consequent possibilities of misinformed judgement regarding clean-up recommendations.

This project was initiated in response to these concerns. The principal aims had been:

- To determine the validity of the K_d approach for the Permo-Triassic sandstone – a common aquifer type worldwide.
- Depending on the results of the first aim, to suggest another, practical, way of quantifying sorption.

A four-stage approach was devised to investigate this, the results of which are now reviewed below.

7.2 Synopsis

7.2.1 Stage 1: Initial Investigations of Sorption Theory Regarding Metal Mobility in Groundwater

In Chapter 3, some initial, exploratory computer simulations were undertaken using the geochemical code PHREEQC. Using Cd as a case study, in batch reaction simulations, these focussed particularly on the effects of varying pH, different input concentrations of Cd, and the water chemistry, among other factors.

The principal conclusions resulting from this work were that pH is highly influential on sorption, and also that pH variability is itself strongly controlled by the chemistry of the system, with very little sorption at low pH, and almost 100 % sorption above pH 7. The apparent K_d for a system thus could range between effectively zero and infinity over a pH interval of about 2 pH units. In most cases, however, at a given pH the predicted isotherms were linear. Later, the models were adapted in order to simulate the transport of Cd, K, Na, Mg, Ca, and Cl in a system as different concentrations of Cd were injected, and with ion exchange or sorption processes operating in various combinations.

The results suggested that there is considerable interplay between the different elements as they are influenced by the differing Cd concentrations and the attachment processes operating. Perhaps the most significant finding was that these interactions, and the resulting sorption result for Cd, is extremely difficult to

predict, and certainly not possible by considering Cd alone, which the K_d approach attempts to do.

7.2.2 Stage 2: Characterisation of Permo-Triassic Sandstone and Development of Laboratory Methods

Given that the PHREEQC models were based on synthetic HFO, it was clear that the code would be of limited value unless it could be shown to be valid for a real system. Therefore, a sample of sandstone from an outcrop of suitable Permo-Triassic sandstone was retrieved and subjected to a series of laboratory batch experiments, each extracting geochemical data to inform particular aspects of its composition. Using Zn instead of Cd for safety reasons, the main conclusions from these investigations were:

- Attachment of Zn on the sandstone is pH dependent suggesting that there is a measurable component of sorption.
- It is probable that ion exchange dominates over sorption
- Attachment reactions in the sandstone samples take a significant amount of time to occur, exhibiting a “two-phase” effect, with full equilibrium reached by approximately 170 hours.
- Ions such as Ca and Mg, most likely initially present on the surface before any contact with the contaminating species, must be taken into account, as they were shown to affect the sorption behaviour of Zn significantly. It was possible to minimize – though not completely remove – the effects of

competing ions by conditioning the sandstone surface with high concentrations of suitable ion solutions. In doing so, the initial conditions on the surface also become more controllable.

- Though pH dependence of attachment was demonstrated, the experimental data do not prove that the pH-dependence is due entirely to oxide surfaces. It is possible that at least a component of the pH-dependence is due to clay edge sites.

All of the techniques and lessons learned were synthesised into a large-scale experiment to conclude the laboratory stage. The data that this generated were then interpreted in Stage 3.

7.2.3 Stage 3: Appraisal of the Theoretical Model

In Chapter 5, the data generated by the final experiment in Chapter 4 was interpreted using PHREEQC. By representing both ion exchange and sorption, and performing over 400 trial simulations of batch reactions, trialling different values and combinations of factors, it was eventually possible to fit modelled Zn isotherms to the Zn isotherms from the laboratory data. The difficulty in achieving the match instilled a degree of confidence that there were few possible combinations of the model parameters that satisfactorily fitted the data. The model also gave further information regarding the sorption and exchange properties of the sandstone.

7.2.4 Stage 4: Applying the Model to Investigate the Implications of the Understanding Developed

Chapter 6 recounted how the PHREEQC simulations used to interpret the laboratory data were adapted in order to simulate transport of Zn through an aquifer. Using the same set of factors deduced during the model development, the transport model was used to predict both the migration and the elution phases of a pulsed influx of Zn (at 7 ppm) in an 800-metre-long aquifer.

The transport model reiterated and emphasised the observations and conclusions raised in the earlier stages of the project, particularly that:

- There is considerable interplay of ion exchange and sorption processes governing the migration of a Zn-laden contamination plume in groundwater.
- Ion exchange processes are more dominant where pH is below 6.5, whereas sorption becomes more important above pH 6.5.
- The variability of Zn concentration is much more complex than could be credibly predicted used a K_d-type approach. This is because of the interplay of H^+ and other competing ions in particular.
- Tailing effects are of increasing importance as the pH of the system increases.
- The impact of 'sorption' (i.e. pH-dependent attachment) is very dependent on pH and the ion exchange selectivity coefficients of the contaminant concerned.

7.3 Overall Conclusions

This project commenced with two principal aims:

- To determine the validity of the K_d approach for the Permo-Triassic sandstone – a common aquifer type worldwide.
- Depending on the results of the first aim, to suggest another, practical, way of quantifying sorption.

The project has comprehensively substantiated the existing reservations regarding the use of the K_d approach to represent sorption processes. It can be expected that the degree of attachment would vary widely as a contaminant plume migrates through a system, influenced by a number of factors - especially pH, the concentration of the heavy metal, and the overall chemistry of the system. Such a system is extremely sensitive to minor perturbations in any of these factors, and, except, perhaps, for very low metal concentrations, will not withstand the degree of simplification inherent in the K_d approach.

Having arrived at this conclusion, the project then focused on the second aim, and was able to demonstrate a better way of quantifying sorption in a way accessible to practising hydrogeologists. Using a finely-calibrated PHREEQC transport model representing real sandstone, the full complexity of the system was clearly portrayed in a manner that could, in principle, be used to inform decision making regarding remediation strategies. Particularly notable features of the model included the representation of tailing effects, when this would not otherwise be predicted by a K_d-type calculation; the widely varying aqueous / dissolved ratio of

the heavy metal as the plume migrated; and the variation in the ratio of ion exchange and sorption processes.

The author commends the results of this research as offering a more precise delineation of where the partition coefficient approach may or may not be used with confidence for cadmium, zinc and related metals in the Permo-Triassic redbed sandstone, and has shown that an alternative, much more comprehensive method is available. Whilst this is arguably more labour-intensive than the partition coefficient approach, the long-term benefits of a more reliable prediction method may outweigh the short term labour savings, which may otherwise risk an incorrect remediation strategy being undertaken.

7.4 Recommendations for Further Work

Notably, this project did not provide any laboratory data regarding the interaction of the sandstone with a synthetic groundwater solution, i.e. one that included at least all the major ions. Attempts to accomplish this during the project failed due to a late-stage experimental error, and the attempt was abandoned due to time constraints. Therefore, repetition of the final laboratory experiment (at the very least), using a groundwater solution without carbonate, would be a high priority.

Data from laboratory column experiments were also a desirable outcome, but it was not possible to undertake these in the time available. Such experiments

would undoubtedly prove extremely useful to further test the performance of the PHREEQC transport models in Chapter 6.

The work undertaken has not determined unambiguously the source of the pH-dependent sorption. Questions remain as to how much pH dependent sorption can be ascribed to clay edge sites, or indeed to Mn oxides. An investigation using sequential stripping and 'pure' clay samples may help answer this question.

The work presented here is only applicable for shallow-surface Permo-Triassic sandstone. An obvious extension would be to repeat the rock characterisation and model interpretation on other parts of the UK Permo-Triassic sandstone, particularly where carbonates feature more prominently. To determine the wider applicability of the work, it would be necessary to apply the methods to other redbed sandstones, and subsequently to other non-redbed clastic sequences.

8 - REFERENCES

Abbas, A. A. et al., 2009. Review on landfill leachate treatments. *Journal of Applied Sciences Research,* 5(5), pp. 534-545.

Ainsworth, C. C., Pilon, J. L., Gassman, P. L. & Van Der Sluys, W. G., 1994. Cobalt, cadmium, and lead sorption to hydrous iron oxide: Residence time effect. *Soil Science Society of America Journal,* 58(6), pp. 1615-1623.

Allen, D. J. et al., 1997. *The physical properties of major aquifers in England and Wales. Technical Report WD/97/34,* Nottingham: British Geological Survey.

Altin, O., Ozbelge, O. H. & Dogu, T., 1999. Effect of pH, flow rate and concentration on the sorption of Pb and Cd on montmorillonite: I. Experimental. *J. Chem. Technol. Biotechnol.,* Volume 74, pp. 1131-1138.

Appel, C. & Ma, L., 2002. Concentration, pH, and Surface Charge Effects on Cadmium and Lead Sorption in Three Tropical Soils. *J. Environ. Qual.,* Volume 31, pp. 581-589.

Appelo, C. A. J. & Postma, D., 2007. *Geochemistry, Groundwater and Pollution, 2nd Edition.* s.l.:A. A. Balkema.

Balistrieri, L. S. & Murray, J. W., 1982. The adsorption of Cu, Pb, Zn, and Cd on goethite from major ion seawater. *Geochim. Cosmochim. Acta,* Volume 46, pp. 1253-1265.

Baun, D. L. & Christensen, T. H., 2004. Speciation of Heavy Metals in Landfill Leachate: A Review. *Waste Management & Research,* 22(1), pp. 3-23.

BBC, 2014. *Report: One fifth of China's soil contaminated.* [Online]
Available at: http://www.bbc.co.uk/news/world-asia-china-27076645
[Accessed 11 February 2016].

Bethke, C. M. & Brady, P. V., 2000(a). Beyond the Kd Approach. *Groundwater ,* 38(3), pp. 321-322.

Bethke, C. M. & Brady, P. V., 2000(b). How the Kd approach undermines ground water cleanup. *Groundwater,* 38(3), pp. 435-443.

Bibak, A., 1994. Cobalt, copper, and manganese adsorption by aluminium- and iron-oxides and humic acid. *Commun. Soil. Sci. Plant Anal.,* Volume 25, pp. 3229-3239.

Blacksmith Institute, 2012. *Blacksmith Institute's Global Inventory Project,* s.l.: Available at

http://www.blacksmithinstitute.org/files/FileUpload/files/GIP%20Short%20Description.pdf.

Boethling, R. & Mackay, D., 2000. *Handbook of Property Estimation Methods for Chemicals.* s.l.:Lewis Publishing.

Bohdziewicz, J. & Kwarciak, A., 2008. The application of hybrid system UASB reactor-RO in landfill leachate treatment. *Desalination,* 222(1-3), pp. 128-134.

Bond, W. J., 1995. On the Rothmund-Kornfeld description of cation-exchange.. *Soil Science Society of America Journal, 59(2).,* pp. 436-443.

Brassington, R., 1998. *Field Hydrogeology.* 2nd edition ed. Chichester: John Wiley & Sons.

Brown, J. G., Bassett, R. L. & Glynn, P. D., 1998. Analysis and simulation of reactive transport of metal contaminants in ground water in Pinal Creek Basin, Arizona. *Journal of Hydrology,* 209(1-4), pp. 225-250.

Bruemmer, G. W., Gerth, J. & Tiller, K. G., 1988. Reaction kinetics of the adsorption and desorption of nickel, zinc, and cadmium by goethite. I. Adsorption and diffusion of metals.. *J. Soil Sci.,* Volume 39, pp. 37-52.

Brusseau, M. L., 1994. Transport of reactive contaminants in heterogeneous porous media. *Review of Geophysics,* 32(3), pp. 285-313.

BSI, 1990. *BS 1377-1 (1990): Methods of test for soils for civil engineering purposes - Part 1: General requirements and sample preparation.,* London: British Standards Institution.

BSI, 2004. *BS ISO 17294-2 (2004): Water quality - Application of Inductively-Coupled Plasma Mass Spectrometry (ICP-MS) - Part 2: Determination of 62 elements,* London: British Standards Institution.

BSI, 2008. *BS ISO 19730 (2008): Soil quality - Extraction of trace elements from soil using ammonium nitrate solution,* London: British Standards Institution.

Carlyle, H. F., Tellam, J. H. & Parker, K. E., 2004. The use of laboratory-determined ion exchange parameters in the prediction of field-scale major cation migration over a 40 year period.. *Journal of Contaminant Hydrology, 68.,* pp. 55-81.

Carriere, P. P. E., Reed, B. & Cline, S. R., 1995. Retention and release of lead by a silty loam and a fine sand loam. II. Kinetics. *Separation Science and Technology,* 30(18), pp. 3471-3487.

Cederberg, G. A., Street, R. I. & Leckie, J. O., 1985. A groundwater mass transport and equilibrium chemistry model for multicomponent systems. *Water Resources Research,* 21(8), pp. 1095-1104.

Cheng, S., 2003. Heavy metal pollution in China: origin, pattern and control. *Environ Sci Pollut Res Int,* 10(3), pp. 192-198.

Christensen, 1985. Cadmium Soil Sorption at Low Concentrations IV: Effect of Waste Leachates on Distribution Coefficients.. *Water, Air and Soil Pollution 26,* pp. 265-274.

Christensen, T. H., Kjeldsen, P. & Kjeldsen, P., 2001. Biogeochemistry of landfill leachate plumes. *Applied Geochemistry,* 16(7-8), pp. 659-718.

Comans, R. N. J. & Middleburg, J. J., 1987. Sorption of trace metals on calcite: Applicability of the surface precipitation model. *Geochimica et Cosmochimica Acta,* 51(9), pp. 2587-2591.

Convery, M. E., 2000. *An Investigation into the Solubility and Sorption of Cadmium. MSc Hydrogeology Thesis,* s.l.: School of Earth Sciences, University of Birmingham.

de Marsily, G., 1986. *Quantitative Hydrogeology - Groundwater Hydrology for Engineers..* s.l.:Academic Press, Inc. .

Downing, R. A., 1998. *Groundwater - our hidden asset.* s.l.:British Geological Survey.

Dzombak, D. A. & Morel, F. M. M., 1990. *Surface Complexation Modelling - Hydrous Ferric Oxide. 393 pp..* Chichester: Wiley.

EA, 2000. *CEC and Kd determination in landfill performance evaluation. Environment Agency R&D Technical Report P340,* Bristol: Environment Agency.

EA, 2003(a). *Hydrogeological risk assessment for landfills and the derivation of groundwater control and trigger levels. Environment Agency report LFTGN01,* Bristol: Environment Agency.

EA, 2003(b). *LandSim release 2.5: groundwater risk assessment tool for landfill design. National Groundwater & Contaminated Land Centre Report GW/03/09,* Bristol: Environment Agency.

EEA, 2014. *European Environment Agency: Progress in management of contaminated sites.* [Online]
Available at: http://www.eea.europa.eu/data-and-maps/indicators/progress-in-management-of-contaminated-sites-3/assessment
[Accessed 11 February 2016].

Environment Agency, 2005(a). *Indicators for Land Contamination,* s.l.: Environment Agency. Available at https://www.gov.uk/government/uploads/system/uploads/attachment_data/file/290711/scho0805bjmd-e-e.pdf.

Environment Agency, 2005(b). *Guide to Good Practice for the Development of*

Conceptual Models and the Selection and Application of Mathematical Models of Contaminant Transport Processes in the Subsurface., s.l.: Environment Agency. Available at https://www.gov.uk/government/uploads/system/uploads/attachment_data/file/290422/scho0701bitr-e-e.pdf.

Environment Agency, 2009(a). *Human health toxicological assessment of contaminants in soil (SR2),* s.l.: Environment Agency, available at https://www.gov.uk/government/uploads/system/uploads/attachment_data/file/291011/scho0508bnqy-e-e.pdf.

Environment Agency, 2009(b). *Dealing with contaminated land in England and Wales: A review of progress from 2000-2007 with Part 2A of the Environmental Protection Act,* s.l.: Environment Agency.

Environment Agency, 2010. *GPLC1 - Guiding principles for land contamination,* s.l.: Environment Agency. Available at https://www.gov.uk/government/uploads/system/uploads/attachment_data/file/297450/geho1109brgy-e-e.pdf.

Environment Agency, 2013. *Groundwater Protection: Principles and practice (GP3), Version 1.1,* s.l.: Environment Agency.

Environment Agency, 2014. *Model Procedures for the Management of Land Contamination (CLR11) - full report,* s.l.: Environment Agency. Available at https://www.gov.uk/government/uploads/system/uploads/attachment_data/file/297401/scho0804bibr-e-e.pdf.

EPM, 2014. *Ministry of Environmental Protection and the Ministry of land publish national survey of soil pollution bulletin [translated from Chinese].* [Online] Available at: http://www.mep.gov.cn/gkml/hbb/qt/201404/t20140417_270670.htm [Accessed 10 February 2016].

Erickson, B., 2011. *Common global pollution issues: Blacksmith Institute's experience. Presentation to the 10th meeting of the International Committee on Contaminated Land, Washington, DC, 4-6 October 2011.* s.l., s.n.

Erskine, A. D., 2000. Transport of ammonium in aquifers: retardation and degradation.. *Quarterly Journal of Engineering Geology and Hydrogeology, 33.,* pp. 161-170.

Essington, M. E., 2004. *Soil and Water Chemistry.* s.l.:CRC Press.

Evanko, C. R. & Dzombak, D. A., 1999. *Remediation of Metals-Contaminated Soils and Groundwater,* s.l.: Ground-Water Remediation Technologies Analysis Center, 1997 (cited November 1999). Available at https://clu-in.org/download/toolkit/metals.pdf.

Evans, A. M., 2005. *Ore Geology and Industrial Minerals: An Introduction.* s.l.:Blackwell Science.

Fetter, C. W., 2000. *Applied Hydrogeology.* 4th edition ed. s.l.:Prentice Hall.

Forbes, E. A., Posner, A. M. & Quirk, J. P., 1976. The specific adsorption of divalent Cd, Co, Cu, Pb, and Zn on goethite. *J. Soil Sci.,* Volume 27, pp. 154-166.

Fowler, R., 2007. *Site contamination law and policy in Europe, North America and Australia - trends and challenges. Paper presented to the 8th meeting of the International Committee on Contaminated Land, Stockholm, 10-11 September 2007..* s.l., s.n.

Gapon, E. N., 1933. On the theory of exchange adsorption in soil (Abstract in Chemical Abstract, 28:4149).. *Journal of General Chemistry (USSR), 3.,* pp. 144-163.

Gibbs, J. W., 1876. On the equilibrium of heterogeneous substances Part I. *Trans. Conn. Acad. Arts Sci.,* Volume 3, pp. 108-248.

Gibbs, J. W., 1878. On the equilibrium of heterogeneous substances Part II. *Trans. Conn. Acad. Arts Sci,* Volume 3, pp. 343-524.

Glynn, P. & Brown, J., 1996. Reactive transport modeling of acidic metal-contaminated ground water at a site with sparse spatial information. *In Reactive Transport in Porous Media, ed. P.C. Lichtner, C.I. Steefel, and E.H. Olkers: Mineralogical Society of America, Reviews in Mineralogy,* Volume 34, pp. 377-438.

Golder, 2006. *LandSim 2.5,* s.l.: Golder Associates, www.landsim.co.uk.

Golder, 2009. *ConSim 2.5,* s.l.: Golder Associates, www.consim.co.uk.

Halim, C. E. et al., 2005. Modelling the leaching of Pb, Cd, As, and Cr from cementitious waste using PHREEQC. *J. Hazard Mater.,* 125(1-3), pp. 45-61.

Hara, T., 2013. *Electric Double Layer.* [Online]
Available at: http://img.webme.com/pic/t/toruhara/electric-double-layer.jpg

Hellferich, F. G., 1995. *Ion Exchange, New Edition.* s.l.:Dover Publication Inc..

Henry, W., 1803. Experiments on the quantity of gases absorbed by water, at different temperatures and different pressures. *Philos. Trans. R. Soc. London,* Volume 93, pp. 29-46.

Hiscock, K. M., 2005. *Hydrogeology - Principles and Practice.* s.l.:Blackwell.

Hooda, P. S. & Alloway, B. J., 1998. Cadmium and lead sorption behaviour of selected English and Indian soils. *Geoderma ,* Volume 84, pp. 121-134.

Hubbard, A. T., 2002. *Encyclopedia of Surface and Colloid Science, Vol. 1.* s.l.:Marcel Dekker Inc.

Hu, P. & Dai, W., 2013. Computer Modeling of Leaching of Heavy Metal from

Cementitious Waste. *Research Journal of Applied Sciences, Engineering and Technology,* 6(11), pp. 2083-2085.

Jennings, A. A., Kirkner, D. J. & Thies, T., 1982. Multicomponent equilibrium chemistry in groundwater quality models. *Water Resources Research,* 18(4), pp. 1089-1096.

Jung, M. C. & Thornton, I., 1997. Environmental contamination and seasonal variation of metals in soils, plants and waters in the paddy fields around a Pb-Zn mine in Korea. *Sci Total Environ,* 198(2), pp. 105-121.

Kao, J., 2004. Groundwater cleanup in developing countries. *Pract Periodical Hazard Toxic Radioact Waste Manage,* 8(2), p. 66.

Kent, D. B., Davis, J. A., Anderson, L. C. D. & Rea, B. A., 1995. Transport of chromium and selenium in a pristine sand and gravel aquifer: Role of adsorption processes. *Water Resources Research,* 31(4), pp. 1041-1050.

Kipton, H., Powell, J. & Town, R. M., 1992. Solubility and fractionation of humic acid: effect of pH and ionic edium. *Anal. Chim. Acta.,* Volume 267, pp. 47-54.

Kirk, G. J. D., 2004. *The biogeochemistry of submerged soil.* s.l.:Wiley Blackwell.

Kohler, M., Curtis, G. P., Kent, D. B. & Davis, J. A., 1996. Experimental investigation and modeling of uranium (VI) transport under variable chemical conditions. *Water Resources Research,* 32(12), pp. 3539-3551.

Kuo, S., Lai, M. S. & Lin, C. W., 2006. Influence of solution acidity and CaCl2 concentration on the removal of heavy metals from metal-contaminated rice soils. *Environ Pollut,* 144(3), pp. 918-925.

Lee, S.-Z.et al., 1996. Predicting Soil-Water Partition Coefficients for Cadmium. *Environ. Sci. Technol.,* 30(12), pp. 3418-3424.

Lenntech B.V., 2016. *Heavy Metals.* [Online]
Available at: http://www.lenntech.com/processes/heavy/heavy-metals/heavy-metals.htm
[Accessed 11 February 2016].

Lewis, G. N., 1901. The law of physic-chemical change. *Proc. Am. Acad. Arts Sci,* 37(3), pp. 49-69.

Li, H., Ellis, D. & Mackay, D., 2007. Measurement of low air-water partition coefficients of organic acids by evaporation from a water surface.. *J. Chem. Eng. Data,* Volume 52, pp. 1580-1584.

Liu, H., Probst, A. & Liao, B., 2005. Metal contamination of soils and crops affected by the Chenzhou lead/zinc mine spill (Hunan, China). *Sci Total Environ,* 339(1-3), pp. 153-166.

Lyman, W. J. & Reehl, W. F., 1982. *Handbook of chemical property estimation methods.* s.l.:McGraw-Hill Book Company.

Mackay, D., Celsie, A. K. D. & Parnis, J. M., 2016. The evolution and future of environmental partition coefficients. *Environ. Rev.,* Volume 24, pp. 1-13.

Mackay, D., Shiu, W. Y., Ma, K. C. & Lee, S. C., 2006. *Physical chemical properties and environmental fate for organic chemicals.* Boca Raton: Taylor and Francis publishing, CRC group.

Margat, J. & van der Gun, J., 2013. *Groundwater around the World: A Geographic Synopsis.* s.l.:CRC Press.

Markiewicz-Patkowska, J., Hursthouse, A. & Przybyla-Kij, H., 2005. The interaction of heavy metals with urban soils: sorption behaviour of Cd, Cu, Cr, Pb and Zn with a typical mixed brownfield deposit. *Environ. Int.,* 31(4), pp. 513-521.

McMahon, A. C. M. H. J. &. E. A., 2001. *Guidance on the Assessment and Interrogation of Subsurface ANalytical Contaminant Fate and Transport Models, Report NC/99/38/1,* s.l.: National Groundwater and Contaminated Land Centre, Environment Agency.

Meyer, H. H., 1899. Zur Theorie der Alkoholnarkose. *Arch. Exp. Pathol. Pharmacol.,* Volume 42, pp. 109-118.

Mostbauer, P., 2003. Criteria selection for landfills: do we need a limitation on inorganic total content?. *Waste Management, 23(6),* pp. 547-554.

Nernst, W., 1891. Distribution of a substance between two solvents, etc.. *J. Chem. Soc.,* Volume 8, pp. 110-139.

NGWA, 2016. *Facts About Global Groundwater Usage,* Westerville, OH, USA: National Ground Water Association.

OSHA(a), 2013. *Occupational Safety & Health Administration: Safety and Health Topics - Cadmium.* [Online]
Available at: https://www.osha.gov/SLTC/cadmium/index.html
[Accessed 12 February 2016].

OSHA(b), 2014. *Occupational Safety & Health Administration: Safety and Health Topics: Lead.* [Online]
Available at: https://www.osha.gov/SLTC/lead/
[Accessed 12 February 2016].

OSHA(c), 2012. *Occupational Safety & Health Administration: Safety and Health Topics - Mercury.* [Online]
Available at: https://www.osha.gov/SLTC/mercury/index.html
[Accessed 12 February 2016].

Overton, C. E., 1901. *Studien uber die Narkose zugleich ein Bertrag zur*

allgemeinen Pharmakologie. Jena, Switzerland: Gustav Fischer.

Pang, L. & Close, M. E., 1999. Non-Equilibrium Transport of Cd in Alluvial Gravels. *Journal of Contaminant Hydrology,* Volume 36, pp. 185-206.

Pankow, J. et al., 1997. Conversion of nicotine in tobacco smoke to its volatile and available free-base form through the action of gaseous ammonia. *Environ. Sci. Technol.,* Volume 31, pp. 2428-2433.

Parkhurst, D. L. & Appelo, C. A. J., 1999. *User's Guide to PHREEQC (Version 2) - A Computer Program for Speciation, Batch-Reaction, One-Dimensional Transport, and Inverse Geochemical Calculations.,* s.l.: United States Geological Survey.

Parkhurst, D. L. & Appelo, C. A. J., 2015. *PHREEQC - A Computer Program for Speciation, Batch-Reaction, One-Dimensional Transport, and Inverse Geochemical Calculations.,* s.l.: USGS: http://wwwbrr.cr.usgs.gov/projects/GWC_coupled/phreeqc/ (1998-2015).

Pauley, J. L., 1953. Prediction of cation-exchange equilibria.. *Journal of American Chemical Society, 76.,* pp. 1422-1425.

Payne, T. E., Davis, J. A. & Waite, T. D., 1994. Uranium retention by weathered schists - the role of iron minerals. *Radiochimica Acta,* 66(7), pp. 301-307.

Puls, R. W., Powell, R. M., Clark, D. & Eldrid, C. J., 1991. Effects of pH, solid/solution ratio, ionic strength, and organic acids on Pb and Cd sorption on kaolinite. *Water Air Soil Pollut.,* 57-58(423-430).

Randall, S. R., Sherman, D. M., Ragnarsdottir, K. V. & Collins, C. R., 1999. The mechanism of cadmium surface complexation on iron oxyhydroxide minerals. *Geochim. Cosmochim. Acta,* Volume 63, pp. 2971-2987.

Reddy, K. R., 2008. *Overexploitation and Contamination of Shared Groundwater Resources, Chapter 12 (pp. 257-274). Darnault, C. J. G. (Ed.).* s.l.:Springer Science.

Reed, B. E., Moore, R. E. & Cline, S. R., 1995. Soil flushing of a sandy loam contaminated with Pb(II), PbSO4(s), PbCO3 (3), or Pb-naphthalene: Column results. *Journal of Soil Contamination,* 4(3), pp. 1-25.

Rose, C., 2004. *An Introduction to the Environmental Physics of Soil, Water and Watersheds.* s.l.:Cambridge University Press.

Rothmund, V. & Kornfeld, G., 1919. The base exchange in permutite II.. *Zeitschrift Fur Anorganische Une Allgemeine Chemie, 108(3),* pp. 215-225.

Ruddiman, W. F., 2002. *Earth's Climate - Past and Future.* New York: W. H. Freeman and Company.

Runkel, R. L., Kimball, B. A., McKnight, D. M. & Bencala, K. E., 1999. Reactive

solute transport in streams: a surface complexation approach for trace metal sorption. *Water Resour. Res.,* Volume 35, pp. 3829-3840.

Santos, A., Alonso, E., Callejon, M. & Jimenez, J. C., 2002. Heavy metal content and speciation in groundwater of the Guadiamar river basin. *Chemosphere,* 48(3), pp. 279-285.

Selim, H. M., Buchter, B., Hinz, C. & Ma, L., 1992. Modeling the transport and retention of cadmium in soils: Multireaction and multi-component approaches.. *Soil Science Society of America Journal,* 56(4), pp. 1004-1015.

Stollenwerk, K. G., 1994. Geochemical interactions between constituents in acidic groundwater and alluvium in an aquifer near Globe, Arizona. *Appl. Geochem,* Volume 9, pp. 353-369.

Stollenwerk, K. G., 1995. Modeling the effects of variable groundwater chemistry on adsorption of molybdate. *Water Resources Research,* 31(2), pp. 347-357.

Stumm, W., 1992. *Chemistry of the Solid-Water Interface.* New York: Wiley.

Tamunobereton-ari, I., Omubo-Pepple, V. B. & Tamunobereton-ari, N. A., 2011. Speciation of heavy metals (Cu, Pb, Ni) pollutants and the vulnerability of groundwater resource in Okrika of Rivers State, Nigeria. *American Journal of Scientific and Industrial Research,* 2(1), pp. 69-77.

Tatsi, A. A. & Zouboulis, A. I., 2002. A field investigation of the quantity and quality of leachate from a municipal solid waste landfill in a Mediterranean climate (Thessaloniki, Greece). *Advances in Environmental Research,* 6(3), pp. 207-219.

Taylor, R. G. et al., 2013. Ground water and climate change. *Nature Climate Change,* Issue 3, pp. 322-329.

Tellam, J. H., 2013. *Composition of groundwater observed at Haydock Park. Personal communication* [Interview] 2013.

Tellam, J. H. & Barker, R. D., 2006. *Fluid Flow and Solute Movement in Sandstones: The Onshore UK Permo-Triassic Red Bed Sequence.* London: Geological Society.

Troeh, F. R. & Thompson, L. M., 2005. *Soils and Soil Fertility, 6th Edition.* s.l.:Wiley-Blackwell.

Tuin, B. J. W. & Tels, M., 1990. Extraction kinetics of six heavy metals from contaminated clay soils. *Environmental Technology,* 11(6), pp. 541-554.

Twardowska, I. & Kyziol, J., 2003. Sorption of metals onto natural organic matter as a function of complexation and adsorbent-adsorbate contact mode. *Environ. Int.,* 28(8), pp. 783-791.

Umar, M., Aziz, H. A. & Yusoff, M. S., 2010. Variability of Parameters Involved in

Leachate Pollution Index and Determination of LPI from Four Landfills in Malaysia. *International Journal of Chemical Engineering,* Volume 2010, pp. 6 pages, Article ID 747953.

UNEP, 2002. *GEO-3: Global environment outlook,* s.l.: Available at www.unep.org/geo/geo3/english/153.htm.

USEPA, 2013. *Protecting and restoring land: Making a visible difference in communities: OSWER FY13 end of year accomplishments report.* [Online] Available at: http://www2.epa.gov/sites/production/files/2014-03/documents/oswer_fy13_accomplishment.pdf [Accessed 11 February 2016].

USGS, 1998-2015. *Example 13--1D Transport in a Dual Porosity Column with Cation Exchange.* [Online] Available at: wwwbrr.cr.usgs.gov/projects/GWC_coupled/phreeqc/phreeqc3-html/phreeqc3-68.htm#586914680_pgfId-1565361

USGS, 2016(a). *United States Geological Survey: Mineral Commodity Summaries - Cadmium,* s.l.: United States Geological Survey.

USGS, 2016(b). *United States Geological Survey: Mineral Commodity Summaries: Lead,* s.l.: Available at http://minerals.usgs.gov/minerals/pubs/commodity/lead/mcs-2016-lead.pdf.

USGS, 2016(c). *United States Geological Survey: Mineral Commodity Summaries - Mercury,* s.l.: United States Geological Survey.

USITC, 2004. *Remediation and nature and landscape protection services: an examination of US and foreign markets,* s.l.: United States International Trade Commission.

van der Lee, J., 1997. *Modelisation du comportement geochimique et du transport des radionucleides en presence de colloides. PhD thesis,* Fontainebleau, France: Centre d'Informatique Geologique, Ecole Nationale Superieure des Mines de Paris.

Vanselow, A. P., 1932. Equilibria of base-exchange reactions of bentonites, permutites, solid colloids, and zeolites. *Soil Science,* Volume 33, pp. 95-113.

W.H.O., 2011. *Guidelines for drinking water quality, 4th edition.,* s.l.: World Health Organisation.

Wang, F. Y., Chen, J. S. & Forsling, W., 1997. Modeling sorption of trace metals on natural sediments by surface complexation model. *Env. Sci. Technol.,* Volume 31, pp. 448-453.

Wen, X., Du, Q. & Tang, H., 1998. Surface complexation model for the heavy metal adsorption on natural sediment. *Environmental Science and Technology,* 32(7), pp. 870-875.

Yeh, G. T. & Tripathi, V. S., 1990. *HYDROGEOCHEM: A coupled model of HYDROlogic transport and GEOCHEMical equilibria in reactive multicomponent systems. Report ORNK-6371,* Oak Ridge, Tennessee: Oak Ridge National Laboratory.

Zachara, J. M. & Smith, S. C., 1994. Edge complexation reactions of cadmium on specimen an soil-derived smectite. *Soil Science Society of American Journal,* 58(3), pp. 762-769.

Zechmeister, L. & Cholnoky, L., 1941. *Principles and Practice of Chromatography.* s.l.:Chapman and Hall.

Zhang, K., Pereira, A. S. & Martin, J. W., 2015. Estimates of octanol-water partitioning for thousands of dissolved organic species in oil sands process-affected water.. *Environ. Sci. Technol.,* 49(14), pp. 8907-8913.

Zhuang, P. et al., 2009. Health risk from heavy metals via consumption of food crops in the vicinity of Dabaoshan mine, South China. *Sci Total Environ,* 407(5), pp. 1551-1561.

9 - APPENDICES

9.1 Appendix 1 – Chapter 3 Appendices

9.1.1 PHREEQC example input code for System 1: H_20-Cd-HFO; fixed pH

Table 9-1: PHREEQC example input code for System 1

```
PHASES
        Fix_H+
        H+ = H+
        log_k 0.0

SOLUTION 1
    Temp        25
    pH          3
    pe          4
    redox       pe
    units       ppm
    density     1
    Cd          0.0
    Cl          10.0 charge
    #N(5)  100.
    -water      0.1 # kg


SURFACE 1
    Hfo_sOH  0.000055   600     1
    Hfo_wOH  0.0022

EQUILIBRIUM_PHASES
        Fix_H+      -3.0    HCl     50.0


SELECTED_OUTPUT
        file c3ph3fixchargebal.sel
        molalities    Cd+2   Hfo_wOCd+     Hfo_sOCd+

END


PHASES
```

```
                Fix_H+
                H+ = H+
                log_k 0.0

SOLUTION 2
        Temp            25
        pH              3
        pe              4
        redox           pe
        units           ppm
        density         1
        Cd              0.05
        Cl              10.0 charge
        #N(5)   100.
        -water          0.1 # kg


SURFACE 2
        Hfo_sOH  0.000055   600     1
        Hfo_wOH  0.0022

EQUILIBRIUM_PHASES
                Fix_H+          -3.0    HCl     10.0

END

PHASES
                Fix_H+
                H+ = H+
                log_k 0.0

SOLUTION 3
        Temp            25
        pH              3
        pe              4
        redox           pe
        units           ppm
        density         1
        Cd              0.1
        Cl              10.0 charge
        #N(5)   100.
        -water          0.1 # kg


SURFACE 3
        Hfo_sOH  0.000055   600     1
        Hfo_wOH  0.0022

EQUILIBRIUM_PHASES
                Fix_H+          -3.0    HCl     1.0

END
```

```
PHASES
        Fix_H+
        H+ = H+
        log_k 0.0


SOLUTION 4
    Temp        25
    pH          3
    pe          4
    redox       pe
    units       ppm
    density     1
    Cd          0.15
    Cl          10.0 charge
    #N(5)  100.
    -water      0.1 # kg


SURFACE 4
    Hfo_sOH  0.000055   600     1
    Hfo_wOH  0.0022

EQUILIBRIUM_PHASES
        Fix_H+      -3.0    HCl     10.0

END

PHASES
        Fix_H+
        H+ = H+
        log_k 0.0

SOLUTION 5
    Temp        25
    pH          3
    pe          4
    redox       pe
    units       ppm
    density     1
    Cd          0.2
    Cl          10.0 charge
    #N(5)  100.
    -water      0.1 # kg


SURFACE 5
    Hfo_sOH  0.000055   600     1
    Hfo_wOH  0.0022

EQUILIBRIUM_PHASES
        Fix_H+      -3.0    HCl     10.0
```

```
END


PHASES
                Fix_H+
                H+ = H+
                log_k 0.0

SOLUTION 6
        Temp            25
        pH              3
        pe              4
        redox           pe
        units           ppm
        density         1
        Cd              0.25
        Cl              10.0 charge
        #N(5)   100.
        -water          0.1 # kg


SURFACE 6
        Hfo_sOH  0.000055    600     1
        Hfo_wOH  0.0022

EQUILIBRIUM_PHASES
                Fix_H+          -3.0    HCl     10.0

END
```

9.1.2 PHREEQC example input code for System 2: Groundwater-Cd-HFO; fixed pH

Table 9-2: PHREEQC example input code for System 2

```
PHASES
                Fix_H+
                H+ = H+
                log_k 0.0


SOLUTION 1
        Temp            25
        pH              3
        pe              4
```

```
        redox           pe
        units           ppm
        density         1
        Cd              0.0
        Cl              54.4
        S(6)    151.3
        N(+5)   33.4
        Ca              97.3
        Mg              33.1
        Na              32.3
        K               4.9
        Fe              0.03
        Zn              0.11
        Mn              0.02
        Cu              0.1
        Pb              0.2
        #Ni             0.03
        Ba              0.1
        #Cr             0.02
        #Cd             0.03
        Si              5.7
        -water          0.1 # kg

SURFACE 1
        Hfo_sOH  0.000055      600     1
        Hfo_wOH  0.0022

EQUILIBRIUM_PHASES
                Fix_H+          -3.0    HCl     50.0

SELECTED_OUTPUT
    -file [filename].sel
    -molalities   Cd+2   Hfo_wOCd+    Hfo_sOCd+

END

PHASES
                Fix_H+
                H+ = H+
                log_k 0.0

SOLUTION 2
        Temp            25
        pH              3
        pe              4
        redox           pe
        units           ppm
        density         1
        Cd              0.05
```

```
        Cl              54.4
        S(6)    151.3
        N(+5)   33.4
        Ca              97.3
        Mg              33.1
        Na              32.3
        K               4.9
        Fe              0.03
        Zn              0.11
        Mn              0.02
        Cu              0.1
        Pb              0.2
        #Ni             0.03
        Ba              0.1
        #Cr             0.02
        #Cd             0.03
        Si              5.7
        -water          0.1 # kg


SURFACE 2
        Hfo_sOH  0.000055      600     1
        Hfo_wOH  0.0022

EQUILIBRIUM_PHASES
                Fix_H+          -3.0    HCl     50.0

END

PHASES
                Fix_H+
                H+ = H+
                log_k 0.0

SOLUTION 3
        Temp            25
        pH              3
        pe              4
        redox           pe
        units           ppm
        density         1
        Cd              0.1
  Cl            54.4
        S(6)    151.3
        N(+5)   33.4
        Ca              97.3
        Mg              33.1
        Na              32.3
        K               4.9
```

```
        Fe              0.03
        Zn              0.11
        Mn              0.02
        Cu              0.1
        Pb              0.2
        #Ni             0.03
        Ba              0.1
        #Cr             0.02
        #Cd             0.03
        Si              5.7
        -water          0.1 # kg


SURFACE 3
        Hfo_sOH  0.000055      600     1
        Hfo_wOH  0.0022

EQUILIBRIUM_PHASES
                Fix_H+          -3.0    HCl     50.0

END

PHASES
                Fix_H+
                H+ = H+
                log_k 0.0

SOLUTION 4
        Temp            25
        pH              3
        pe              4
        redox           pe
        units           ppm
        density         1
        Cd              0.15
        Cl              54.4
        S(6)    151.3
        N(+5)   33.4
        Ca              97.3
        Mg              33.1
        Na              32.3
        K               4.9
        Fe              0.03
        Zn              0.11
        Mn              0.02
        Cu              0.1
        Pb              0.2
        #Ni             0.03
        Ba              0.1
```

```
        #Cr             0.02
        #Cd             0.03
        Si              5.7
        -water          0.1 # kg


SURFACE 4
        Hfo_sOH  0.000055       600     1
        Hfo_wOH  0.0022

EQUILIBRIUM_PHASES
                Fix_H+          -3.0    HCl     50.0

END

PHASES
                Fix_H+
                H+ = H+
                log_k 0.0

SOLUTION 5
        Temp            25
        pH              3
        pe              4
        redox           pe
        units           ppm
        density         1
        Cd              0.2
        Cl              54.4
        S(6)    151.3
        N(+5)   33.4
        Ca              97.3
        Mg              33.1
        Na              32.3
        K               4.9
        Fe              0.03
        Zn              0.11
        Mn              0.02
        Cu              0.1
        Pb              0.2
        #Ni             0.03
        Ba              0.1
        #Cr             0.02
        #Cd             0.03
        Si              5.7
        -water          0.1 # kg


SURFACE 5
```

```
        Hfo_sOH  0.000055      600     1
        Hfo_wOH  0.0022

EQUILIBRIUM_PHASES
                Fix_H+          -3.0    HCl     50.0

END

PHASES
                Fix_H+
                H+ = H+
                log_k 0.0

SOLUTION 6
        Temp            25
        pH              3
        pe              4
        redox           pe
        units           ppm
        density         1
        Cd              0.25
        Cl              54.4
        S(6)    151.3
        N(+5)   33.4
        Ca              97.3
        Mg              33.1
        Na              32.3
        K               4.9
        Fe              0.03
        Zn              0.11
        Mn              0.02
        Cu              0.1
        Pb              0.2
        #Ni             0.03
        Ba              0.1
        #Cr             0.02
        #Cd             0.03
        Si              5.7
        -water          0.1 # kg


SURFACE 6
        Hfo_sOH  0.000055      600     1
        Hfo_wOH  0.0022

EQUILIBRIUM_PHASES
                Fix_H+          -3.0    HCl     50.0

END
```

9.1.3 PHREEQC input code for System 3: H_20-Cd-HFO; varying pH

Table 9-3: PHREEQC example input code for System 3

```
SOLUTION 1
        Temp            25
        pH              3
        pe              4
        redox           pe
        units           ppm
        density                 1
        Cd              0.0
        -water          0.1 # kg

SURFACE 1
        Hfo_sOH  0.000055 600     1
        Hfo_wOH  0.0022

SELECTED_OUTPUT
      -file [filename].sel
      -molalities     Cd+2    Hfo_wOCd+       Hfo_sOCd+

END

SOLUTION 2
        Temp            25
        pH              3
        pe              4
        redox           pe
        units           ppm
        density                 1
        Cd              0.05
        -water          0.1 # kg


SURFACE 2
        Hfo_sOH  0.000055 600     1
        Hfo_wOH  0.0022

END
```

```
SOLUTION 3
        Temp            25
        pH              3
        pe              4
        redox           pe
        units           ppm
        density                 1
        Cd              0.1
        -water          0.1 # kg


SURFACE 3
        Hfo_sOH  0.000055 600    1
        Hfo_wOH  0.0022

END

SOLUTION 4
        Temp            25
        pH              3
        pe              4
        redox           pe
        units           ppm
        density                 1
        Cd              0.15
        -water          0.1 # kg


SURFACE 4
        Hfo_sOH  0.000055 600    1
        Hfo_wOH  0.0022

END

SOLUTION 5
        Temp            25
        pH              3
        pe              4
        redox           pe
        units           ppm
        density                 1
        Cd              0.2
        -water          0.1 # kg


SURFACE 5
        Hfo_sOH  0.000055 600    1
        Hfo_wOH  0.0022
```

```
END

SOLUTION 6
        Temp            25
        pH              3
        pe              4
        redox           pe
        units           ppm
        density                 1
        Cd              0.25
        -water          0.1 # kg


SURFACE 6
        Hfo_sOH  0.000055 600     1
        Hfo_wOH  0.0022

END
```

9.1.4 System 4: Groundwater-Cd-HFO; varying pH

Table 9-4: PHREEQC example input code for System 4

```
SOLUTION 1
        Temp            25
        pH              3
        pe              4
        redox           pe
        units           ppm
        density                 1
        Cd              0.0
        Cl              54.4
        S(6)    151.3
        N(+5)  33.4
        Ca              97.3
        Mg              33.1
        Na              32.3
        K               4.9
        Fe              0.03
        Zn              0.11
        Mn              0.02
        Cu              0.1
        Pb              0.2
        #Ni             0.03
```

```
        Ba              0.1
        #Cr             0.02
        #Cd             0.03
        Si              5.7
        -water          0.1 # kg

SURFACE 1
        Hfo_sOH  0.000055 600    1
        Hfo_wOH  0.0022

SELECTED_OUTPUT
      -file [filename].sel
      -molalities    Cd+2    Hfo_wOCd+      Hfo_sOCd+

END

SOLUTION 2
        Temp            25
        pH              3
        pe              4
        redox           pe
        units           ppm
        density                 1
        Cd              0.05
        Cl              54.4
        S(6)    151.3
        N(+5)  33.4
        Ca              97.3
        Mg              33.1
        Na              32.3
        K               4.9
        Fe              0.03
        Zn              0.11
        Mn              0.02
        Cu              0.1
        Pb              0.2
        #Ni             0.03
        Ba              0.1
        #Cr             0.02
        #Cd             0.03
        Si              5.7
        -water          0.1 # kg


SURFACE 2
        Hfo_sOH  0.000055 600    1
        Hfo_wOH  0.0022
```

```
END

SOLUTION 3
        Temp            25
        pH              3
        pe              4
        redox           pe
        units           ppm
        density                 1
        Cd              0.1
   Cl           54.4
        S(6)    151.3
        N(+5)   33.4
        Ca              97.3
        Mg              33.1
        Na              32.3
        K               4.9
        Fe              0.03
        Zn              0.11
        Mn              0.02
        Cu              0.1
        Pb              0.2
        #Ni             0.03
        Ba              0.1
        #Cr             0.02
        #Cd             0.03
        Si              5.7
        -water          0.1 # kg


SURFACE 3
        Hfo_sOH  0.000055 600     1
        Hfo_wOH  0.0022

END

SOLUTION 4
        Temp            25
        pH              3
        pe              4
        redox           pe
        units           ppm
        density                 1
        Cd              0.15
        Cl              54.4
        S(6)    151.3
        N(+5)   33.4
        Ca              97.3
```

```
        Mg              33.1
        Na              32.3
        K               4.9
        Fe              0.03
        Zn              0.11
        Mn              0.02
        Cu              0.1
        Pb              0.2
        #Ni             0.03
        Ba              0.1
        #Cr             0.02
        #Cd             0.03
        Si              5.7
        -water          0.1 # kg


SURFACE 4
        Hfo_sOH  0.000055 600     1
        Hfo_wOH  0.0022

END

SOLUTION 5
        Temp            25
        pH              3
        pe              4
        redox           pe
        units           ppm
        density                 1
        Cd              0.2
        Cl              54.4
        S(6)    151.3
        N(+5)  33.4
        Ca              97.3
        Mg              33.1
        Na              32.3
        K               4.9
        Fe              0.03
        Zn              0.11
        Mn              0.02
        Cu              0.1
        Pb              0.2
        #Ni             0.03
        Ba              0.1
        #Cr             0.02
        #Cd             0.03
        Si              5.7
        -water          0.1 # kg
```

```
SURFACE 5
        Hfo_sOH  0.000055 600     1
        Hfo_wOH  0.0022

END

SOLUTION 6
        Temp            25
        pH              3
        pe              4
        redox           pe
        units           ppm
        density                 1
        Cd              0.25
        Cl              54.4
        S(6)    151.3
        N(+5)  33.4
        Ca              97.3
        Mg              33.1
        Na              32.3
        K               4.9
        Fe              0.03
        Zn              0.11
        Mn              0.02
        Cu              0.1
        Pb              0.2
        #Ni             0.03
        Ba              0.1
        #Cr             0.02
        #Cd             0.03
        Si              5.7
        -water          0.1 # kg


SURFACE 6
        Hfo_sOH  0.000055 600     1
        Hfo_wOH  0.0022

END
```

9.1.5 System 5: H_20-Cd-HFO in equilibrium with calcite

Table 9-5: PHREEQC example input code for System 5

```
SOLUTION 1
        Temp            25
        pH              3
        pe              4
        redox           pe
        units           ppm
        density                 1
        Cd              0.0
        -water          0.1 # kg

EQUILIBRIUM_PHASES

CO2(g)          -2.0
Calcite         0.0

SURFACE 1
        Hfo_sOH  0.000055 600     1
        Hfo_wOH  0.0022

SELECTED_OUTPUT
      -file [filename].sel
      -molalities     Cd+2    Hfo_wOCd+       Hfo_sOCd+

END

SOLUTION 2
        Temp            25
        pH              3
        pe              4
        redox           pe
        units           ppm
        density                 1
        Cd              0.05
        -water          0.1 # kg

EQUILIBRIUM_PHASES

CO2(g)          -2.0
Calcite         0.0

SURFACE 2
        Hfo_sOH  0.000055 600     1
```

```
        Hfo_wOH  0.0022

END

SOLUTION 3
        Temp            25
        pH              3
        pe              4
        redox           pe
        units           ppm
        density                 1
        Cd              0.1
        -water          0.1 # kg

EQUILIBRIUM_PHASES

CO2(g)          -2.0
Calcite         0.0

SURFACE 3
        Hfo_sOH  0.000055 600     1
        Hfo_wOH  0.0022

END

SOLUTION 4
        Temp            25
        pH              3
        pe              4
        redox           pe
        units           ppm
        density                 1
        Cd              0.15
        -water          0.1 # kg

EQUILIBRIUM_PHASES

CO2(g)          -2.0
Calcite         0.0

SURFACE 4
        Hfo_sOH  0.000055 600     1
        Hfo_wOH  0.0022

END

SOLUTION 5
        Temp            25
```

```
        pH              3
        pe              4
        redox           pe
        units           ppm
        density                 1
        Cd              0.2
        -water          0.1 # kg

EQUILIBRIUM_PHASES

CO2(g)      -2.0
Calcite     0.0

SURFACE 5
        Hfo_sOH  0.000055 600    1
        Hfo_wOH  0.0022

END

SOLUTION 6
        Temp            25
        pH              3
        pe              4
        redox           pe
        units           ppm
        density                 1
        Cd              0.25
        -water          0.1 # kg

EQUILIBRIUM_PHASES

CO2(g)      -2.0
Calcite     0.0

SURFACE 6
        Hfo_sOH  0.000055 600    1
        Hfo_wOH  0.0022

END
```

9.2 Appendix 2 – Chapter 5 appendices

9.2.1 PHREEQC input code for simulation of laboratory-derived isotherms in Chapter 5.

Table 9-6: PHREEQC input code for simulation of laboratory-derived isotherms in Chapter 5

```
TITLE  Model for lab expts: 1g in 0.04L, but upscaled to 1L, i.e. 25g in 1L
SOLUTION 1 Natural gw
      pH      7.0
                  pe     8
      temp    25.0
                  units mg/l
                  Na          23
                  K           5.00
      Ca          20
      Mg          10.00
                  Zn          0.0001
      Mn          0.01
                  C(+4)   5           # = HCO3- i.e. bicarbonate [I THINK!  TBC]
      S(6)    86          # = SO4-2 i.e. sulphate [TBC]
                  N(+5)   5           # = NO3- i.e. nitrate [TBC]
      Cl   35           # = Cl-

#                 S(6) 48
#      C    366 as HCO3
#                 Cu    0.001
#                 Cd    0.001
#                 B    0.9
#                 Al    0.001
#                 Si    .1
#                 Fe    0.01


#                 Hg    0.01
#                 Sb    0.1
#      Ni    0.01
#      As    0.01

EXCHANGE_SPECIES

K+ + X- = KX                    #Gaines-Thomas format
log_k    0.9
-gamma          3.5        0.015
```

```
delta_h  -4.3      # Jardine & Sparks, 1984

Zn+2 + 2X- = ZnX2
log_k 0.1
-gamma 5.0 0.0

Na+ + X- = NaX
log_k    0.0
-gamma          4.0       0.075

Ca+2 + 2X- = CaX2
log_k   0.4
-gamma          5.0       0.165
delta_h  7.2       # Van Bladel & Gheyl, 1980

Mg+2 + 2X- = MgX2
log_k   0.4
-gamma          5.5       0.2
delta_h  7.4       # Laudelout et al., 1968

Mn+2 + 2X- = MnX2
log_k    0.52
-gamma          6.0       0.0




EXCHANGE 1
#          X-  0.2
           X-  6.25e-4
# cec ~ 2.5 mmol/100g = 25 mmol/kg;for 1g therefore = 2.5e-5 mol;
# used 0.04L in expt; so if use 1L in calc, then 2.5e-5/0.04L = 6.25e-4mol
#          CaX2  0.08
#          MgX2  0.08
#    KX    0.01
#          NaX   0.03
           -equilibrate 1




SURFACE_SPECIES
Hfo_sOH + H+ = Hfo_sOH2+
log_k 8.18
Hfo_sOH = Hfo_sO- + H+
log_k -10.82
Hfo_sOH + Zn+2 = Hfo_sOZn+ + H+
```

```
log_k 0.66
Hfo_sOH + Ca+2 = Hfo_sOHCa+2
log_k 0.15
Hfo_sOH + Mg+2 = Hfo_sOMg+ + H+
log_k 0.15


Hfo_wOH + H+ = Hfo_wOH2+
log_k 8.18
Hfo_wOH = Hfo_wO- + H+
log_k -8.82
Hfo_wOH + Zn+2 = Hfo_wOZn+ + H+
log_k -2.32
Hfo_wOH + Ca+2 = Hfo_wOCa+ + H+
log_k -2.32
Hfo_wOH + Mg+2 = Hfo_wOMg+ + H+
log_k -2.32

SURFACE 1
 -equilibrate with solution 1

 Hfo_sOH 3.0e-4 6 0.119

# Hfo_sOH 0.00214285714285714 600 38.1428571428571
# Dz&M used 0.2mol weak sites / mol Fe and 0.005 mol strong sites / mol Fe
# From Mahmoud, we have ~ 3mgFe/g sst, so with 1g we have 0.2 x 3/56000 mol;
# for up scaling to 1L from 0.04L, we have 0.2 x 3/56000/0.04 = 2.68e-4 mol
# for strong sites, 2.68e-4/.2 x 0.005 = 6.70e-6 mol
# for mass of sorber, 3 Fe mg/g sst = 3/56000 mol Fe/g sst
# = 3/56000 x 89g HFO / g = 3/56000 x 89 / 0.04 g HFO in contact with 1L
# i.e. 0.119 g (Dz&M have 89gHFO/mol Fe; also 600m2/g)
# Hfo_wOH 0.0857142857142857

 Hfo_wOH 2.68e-8

# Hfo_sOH 5e-6 600. 0.09
# Hfo_wOH 2e-4


EQUILIBRIUM_PHASES 1
#       Calcite         0.0     10.9
#       Dolomite        0.0     1.0
#       Barite
#       Quartz          0.0     47.5
#       Kaolinite
#       K-feldspar      0.0     5.24
#       Albite          0.0     0.547
#       Anorthite       0.0     0.524
#       Chlorite(14A)
```

```
#       Ca-Montmorillonite
#       Illite
#       Hematite        0.0    0.75
#       Goethite
#       Fe(OH)3(a)
#       Pyrolusite
#       Hausmannite
#       Manganite
#       Pyrochroite
#       CO2(g)
      Smithsonite   0.0    0.0
      Zn(OH)2(e)    0.0    0.0
#       Cd(OH)2
#       Otavite 315
#       CdSiO3      328
#       CdSO4       329

SAVE surface 1
SAVE exchange 1

END


SOLUTION 2 Conditioning
      pH      4.0
                  pe     8
      temp    25.0
                  units mg/l
                  Na   1000
                  K    0.01
                  Ca   0.01
                  Mg   0.01
      Zn   0.0001
      Mn    0.01

                  Cl   15.43

#                 S(6) .1
      C    .01 as HCO3
#                 Cu    0.001
#                 Cd    0.001
#                 B     0.9
#                 Al    0.001
#                 Si    .1
#                 Fe    0.01
#                 Hg    0.01
#                 Sb    0.1
#      Ni    0.01
#      As    0.01
```

```
USE exchange 1
USE surface 1


EQUILIBRIUM_PHASES 2
#       Calcite         0.0     10.9
#       Dolomite        0.0     1.0
#       Barite
#       Quartz          0.0     47.5
#       Kaolinite
#       K-feldspar      0.0     5.24
#       Albite          0.0     0.547
#       Anorthite       0.0     0.524
#       Chlorite(14A)
#       Ca-Montmorillonite
#       Illite
#       Hematite        0.0     0.75
#       Goethite
#       Fe(OH)3(a)
#       Pyrolusite
#       Hausmannite
#       Manganite
#       Pyrochroite
#       CO2(g)
        Smithsonite     0.0     0.0
        Zn(OH)2(e)      0.0     0.0
#       Cd(OH)2
#       Otavite 315
#       CdSiO3      328
#       CdSO4       329


SELECTED_OUTPUT
        -file   PRO TRL Zn 7 pH 3_459A.sel
# -molalities ZnX2 #CaX2 MgX2 KX AlOHX2 AlX3 FeX2
# -molalities Hfo_sOZn+ #Hfo_sOH  #Hfo_sOHCa+2 Hfo_sOH2+ Hfo_sO- Hfo_sOFe+
# -molalities Hfo_wOZn+ #Hfo_wOH Hfo_wOH2+ Hfo_wO-  #Hfo_wOCa+
 -totals Zn Ca K Mg Mn Sr
# -molalities Hfo_wHCO3 Hfo_wCO3- Hfo_wOHSO4-2
# -molalities Hfo_wSO4- Hfo_wOMg+ Hfo_wOFe+ Hfo_wOFeOH
# -species Zn(OH)2 Zn(OH)3- Zn(OH)4-2 ZnOH+ Zn(CO3)2-2 ZnCO3 Zn+2 ZnCl+ ZnHCO3+ ZnCl2
ZnCl3- ZnCl4-2
#       -si     calcite dolomite quartz k-feldspar albite anorthite
#                       -si     Chlorite(14A)  Ca-Montmorillonite Illite
#                       -si     Hematite  Goethite Fe(OH)3(a)
```

```
SAVE surface 2
SAVE exchange 2

EXCHANGE_SPECIES
K+ + X- = KX
log_k    0.9
-gamma          3.5       0.015
delta_h  -4.3     # Jardine & Sparks, 1984

Zn+2 + 2X- = ZnX2
log_k 0.1
-gamma 5.0 0.0

Na+ + X- = NaX
log_k    0.0
-gamma          4.0       0.075

Ca+2 + 2X- = CaX2
log_k   0.4
-gamma          5.0       0.165
delta_h  7.2      # Van Bladel & Gheyl, 1980

Mg+2 + 2X- = MgX2
log_k   0.4
-gamma          5.5       0.2
delta_h  7.4      # Laudelout et al., 1968

Mn+2 + 2X- = MnX2
log_k    0.52
-gamma          6.0       0.0



END

PHASES
                  Fix_H+
                  H+ = H+
                  log_k 0.0


 SOLUTION 3 Zn test
     pH     6.08
                  pe    8
     temp    25.0
                  units mg/l
                  Na   1000
#                 Na   3.125
                  K    .01
```

```
                    Ca   .01
                    Mg   .01
#                   Cl   4.82
                    Cl   15.43
#                   S(6) .1
     C    .01 as HCO3
#                   Cu    0.001
#                   Cd    0.001
#                   B    0.9
#                   Al    0.001
#                   Si    .1
#                   Fe    0.01
#                   Mn    0.01
                    Zn    0.0001
#                   Hg    0.01
#                   Sb    0.1
#      Ni    0.01
#      As    0.01

USE exchange 2
USE surface 2

EXCHANGE_SPECIES
K+ + X- = KX
log_k    0.9
-gamma          3.5       0.015
delta_h  -4.3     # Jardine & Sparks, 1984

Zn+2 + 2X- = ZnX2
log_k 0.1
-gamma 5.0 0.0

Na+ + X- = NaX
log_k    0.0
-gamma          4.0       0.075

Ca+2 + 2X- = CaX2
log_k   0.4
-gamma          5.0       0.165
delta_h  7.2      # Van Bladel & Gheyl, 1980

Mg+2 + 2X- = MgX2
log_k   0.4
-gamma          5.5       0.2
delta_h  7.4      # Laudelout et al., 1968

Mn+2 + 2X- = MnX2
log_k    0.52
-gamma          6.0       0.0
```

```
EQUILIBRIUM_PHASES 3

                    Fix_H+              -6.08     NaOH    100.0



#       Calcite         0.0     10.9
#       Dolomite        0.0     1.0
#       Barite
#       Quartz          0.0     47.5
#       Kaolinite
#       K-feldspar      0.0     5.24
#       Albite          0.0     0.547
#       Anorthite       0.0     0.524
#       Chlorite(14A)
#       Ca-Montmorillonite
#       Illite
#       Hematite        0.0     0.75
#       Goethite
#       Fe(OH)3(a)
#       Pyrolusite
#       Hausmannite
#       Manganite
#       Pyrochroite
      CO2(g)  -3.5  10
      Smithsonite   0.0     0.0
      Zn(OH)2(e)    0.0     0.0
#       Cd(OH)2
#       Otavite 315
#       CdSiO3      328
#       CdSO4       329


reaction
           Zn
            0.0  0.0000231 0.00004615  .0000769      .0001077

SELECTED_OUTPUT
       -file   PRD TRL Zn 7 pH 3_459B.sel
 -molalities ZnX2 #CaX2 MgX2 KX AlOHX2 AlX3 FeX2                          #EXCHANGE SITES
 -molalities Hfo_sOZn+ #Hfo_sOH    Hfo_sOHCa+2 Hfo_sOH2+ Hfo_sO- Hfo_sOFe+      #STRONG
SITES
 -molalities Hfo_wOZn+ #Hfo_wOH Hfo_wOH2+ Hfo_wO-  Hfo_wOCa+                #WEAK SITES
 -totals Zn
# -molalities #Hfo_wHCO3 Hfo_wCO3- Hfo_wOHSO4-2
```

```
# -molalities #Hfo_wSO4- Hfo_wOMg+ Hfo_wOFe+ Hfo_wOFeOH
#       -si     calcite dolomite quartz k-feldspar albite anorthite
#                       -si     Chlorite(14A)  Ca-Montmorillonite Illite
#                       -si     Hematite  Goethite Fe(OH)3(a)
END
```

9.3 Appendix 3 – Chapter 6 Appendices

9.3.1 PHREEQC input code for transport simulations in Chapter 6

Table 9-7: PHREEQC input code for transport simulations in Chapter 6

```
TITLE  Model for lab expts: 1g in 0.04L, but upscaled to 1L, i.e. 25g in 1L



SOLUTION 0   #Zn pulse
        pH     5.0
        pe     8
        temp    25.0
        units mg/l
        Na         23
        K          5.00
        Ca         20
        Mg         10.00
        Mn         0.01
        C(+4)   25            # = HCO3- i.e. bicarbonate
        S(6)    86            # = SO4-2 i.e. sulphate
        N(+5)   5             # = NO3- i.e. nitrate
        Cl         35           # = Cl-
        Zn      7            #MIXING AND REACTION
        Br      17           #marker/tracer element JUST MIXING



EQUILIBRIUM_PHASES 0

#       Calcite      0.0    0.0
        Smithsonite   0.0    0.0
        Zn(OH)2(e)    0.0    0.0
#       CO2(g)  -3.5  10

END

SOLUTION 1-40 #Natural gw
        pH     5.0
        pe     8
        temp    25.0
        units mg/l
        Na         23
        K          5.00
        Ca         20
        Mg         10.00
        Zn         0.0001
        Mn         0.01
```

```
        C(+4)   100             # = HCO3- i.e. bicarbonate
        S(6)    86              # = SO4-2 i.e. sulphate
        N(+5)   5               # = NO3- i.e. nitrate
        Cl      35              # = Cl-

EQUILIBRIUM_PHASES  1-40
#       Calcite     0.0    0.0
        Smithsonite   0.0    0.0
        Zn(OH)2(e)    0.0    0.0
#       CO2(g)  -3.5  10

EXCHANGE_SPECIES   1-40

K+ + X- = KX                    #Gaines-Thomas format
log_k    0.9
-gamma          3.5     0.015
delta_h  -4.3    # Jardine & Sparks, 1984

Zn+2 + 2X- = ZnX2
log_k 0.4
-gamma 5.0 0.0

Na+ + X- = NaX
log_k    0.0
-gamma          4.0     0.075

Ca+2 + 2X- = CaX2
log_k   0.4
-gamma          5.0     0.165
delta_h  7.2     # Van Bladel & Gheyl, 1980

Mg+2 + 2X- = MgX2
log_k   0.4
-gamma          5.5     0.2
delta_h  7.4     # Laudelout et al., 1968

Mn+2 + 2X- = MnX2
log_k    0.52
-gamma          6.0     0.0

EXCHANGE   1-40

        X-  6.25e-4
# cec ~ 2.5 mmol/100g = 25 mmol/kg;for 1g therefore = 2.5e-5 mol;
# used 0.04L in expt; so if use 1L in calc, then 2.5e-5/0.04L = 6.25e-4mol
 -equilibrate 1-40

SURFACE_SPECIES    1-40
Hfo_sOH + H+ = Hfo_sOH2+
```

```
log_k 9.18
Hfo_sOH = Hfo_sO- + H+
log_k -8.82
Hfo_sOH + Zn+2 = Hfo_sOZn+ + H+
log_k -0.15
Hfo_wOH + H+ = Hfo_wOH2+
log_k 8.18
Hfo_wOH = Hfo_wO- + H+
log_k -8.82
Hfo_wOH + Zn+2 = Hfo_wOZn+ + H+
log_k -2.32

SURFACE 1-40
                    Hfo_sOH  3.0e-4 6 0.119        #[TO BE CHECKED]
                    Hfo_wOH  2.68e-8
 -equilibrate  1-40

# Hfo_sOH 0.00214285714285714 600 38.1428571428571
# Dz&M used 0.2mol weak sites / mol Fe and 0.005 mol strong sites / mol Fe
# From Mahmoud, we have ~ 3mgFe/g sst, so with 1g we have 0.2 x 3/56000 mol;
# for up scaling to 1L from 0.04L, we have 0.2 x 3/56000/0.04 = 2.68e-4 mol
# for strong sites, 2.68e-4/.2 x 0.005 = 6.70e-6 mol
# for mass of sorber, 3 Fe mg/g sst = 3/56000 mol Fe/g sst
# = 3/56000 x 89g HFO / g = 3/56000 x 89 / 0.04 g HFO in contact with 1L
# i.e. 0.119 g (Dz&M have 89gHFO/mol Fe; also 600m2/g)
# Hfo_wOH 0.0857142857142857

SAVE surface  1-40
SAVE exchange 1-40

SELECTED_OUTPUT
      -file   T56a.sel            # [REVISIT]
 -molalities ZnX2 CaX2 MgX2 KX NaX
 -molalities Hfo_sOZn+ Hfo_sOH  Hfo_sOHCa+2 Hfo_sOH2+ Hfo_sO-
 -molalities Hfo_wOZn+ Hfo_wOH  Hfo_wOCa+   Hfo_wOH2+ Hfo_wO-  Hfo_wOMg+
 -totals         Zn Ca K Mg Mn  Cl  Na Sr Br
 -pH
 -si     Smithsonite  Zn(OH)2(e)

# -molalities Hfo_wHCO3 Hfo_wCO3- Hfo_wOHSO4-2
# -molalities Hfo_wSO4-  Hfo_wOFe+ Hfo_wOFeOH
# -species Zn(OH)2 Zn(OH)3- Zn(OH)4-2 ZnOH+ Zn(CO3)2-2 ZnCO3 Zn+2 ZnCl+ ZnHCO3+ ZnCl2
ZnCl3- ZnCl4-2
#          -si    calcite dolomite quartz k-feldspar albite anorthite
#          -si    Chlorite(14A)  Ca-Montmorillonite Illite
#          -si    Hematite  Goethite Fe(OH)3(a)

END
```

```
TRANSPORT
      -cells         40
      -length         20
      -shifts         120
      -time_step      7200000.0
      -flow_direction  forward
      -boundary_cond   flux    flux
      -diffc          0.0e-9
      -dispersivity    2
      -correct_disp    true
      -punch          40
      -punch_frequency 1
      -print          40
      -print_frequency 20

SELECTED_OUTPUT
      -file           T56b.sel
      -reset          false
      -step

 -molalities ZnX2 CaX2 MgX2 KX NaX
 -molalities Hfo_sOZn+ Hfo_sOH  Hfo_sOHCa+2 Hfo_sOH2+ Hfo_sO-
 -molalities Hfo_wOZn+ Hfo_wOH  Hfo_wOCa+   Hfo_wOH2+ Hfo_wO-  Hfo_wOMg+
 -totals         Zn Ca K Mg Mn  Cl  Na Sr Br
 -pH
 -si    Smithsonite  Zn(OH)2(e)

END

SOLUTION 0  #Natural gw
          pH     5.0
          pe     8
          temp    25.0
          units mg/l
          Na         23
          K          5.00
          Ca         20
          Mg         10.00
          Zn         0.0001
          Mn         0.01
          C(+4)   25            # = HCO3- i.e. bicarbonate
          S(6)    86           # = SO4-2 i.e. sulphate
          N(+5)   5             # = NO3- i.e. nitrate
          Cl         35           # = Cl-

EQUILIBRIUM_PHASES  0
#         Calcite      0.0   0.0
          Smithsonite   0.0    0.0
          Zn(OH)2(e)    0.0    0.0
```

```
#          CO2(g)  -3.5  10

 TRANSPORT
      -cells          40
      -length         20
      -shifts         120
      -time_step      7200000.0
      -flow_direction  forward
      -boundary_cond   flux    flux
      -diffc          0.0e-9
      -dispersivity    2
      -correct_disp    true
      -punch          40
      -punch_frequency 1
      -print          40
      -print_frequency 20
SELECTED_OUTPUT
      -file           T56c.sel
      -reset          false
      -step
           -molalities ZnX2 CaX2 MgX2 KX NaX
           -molalities Hfo_sOZn+ Hfo_sOH  Hfo_sOHCa+2 Hfo_sOH2+ Hfo_sO-
           -molalities Hfo_wOZn+ Hfo_wOH  Hfo_wOCa+   Hfo_wOH2+ Hfo_wO-  Hfo_wOMg+
           -totals         Zn Ca K Mg Mn  Cl  Na Sr Br
  -pH
           -si     Smithsonite  Zn(OH)2(e)
END
```

9.3.2 Individual Simulation Results for Trials 64-73

pH 5.0

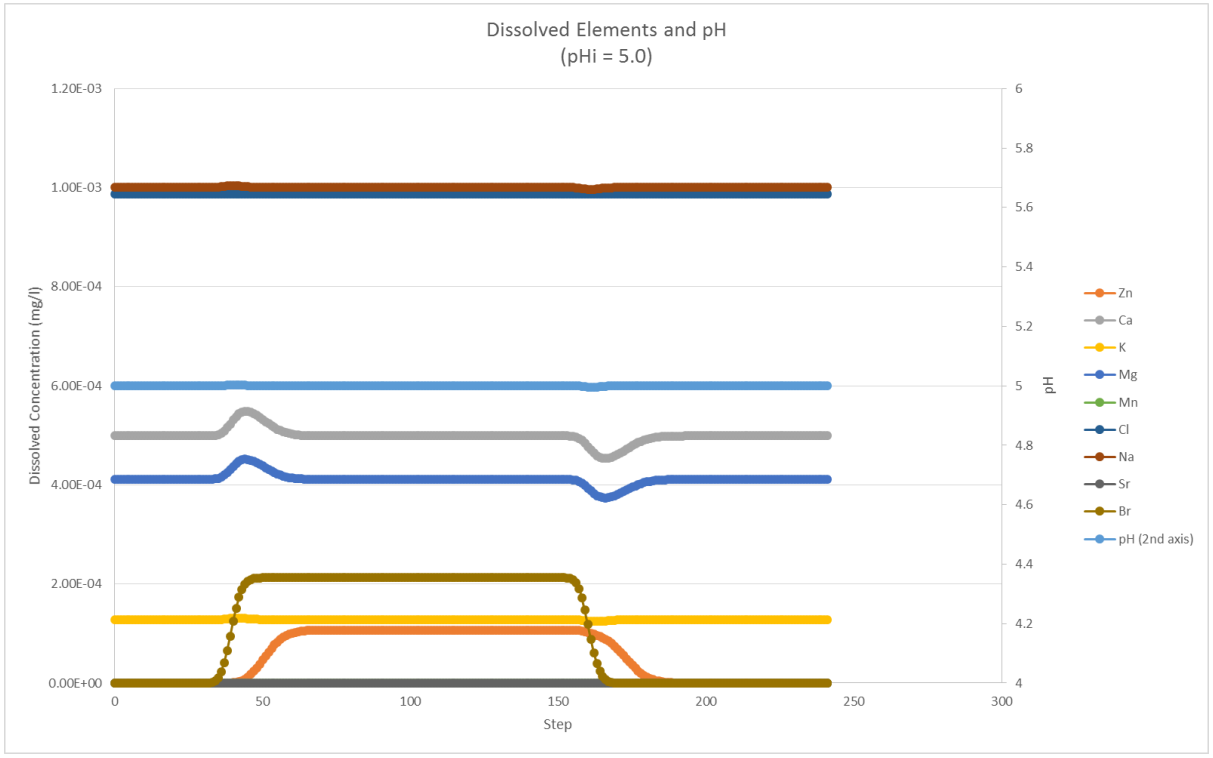

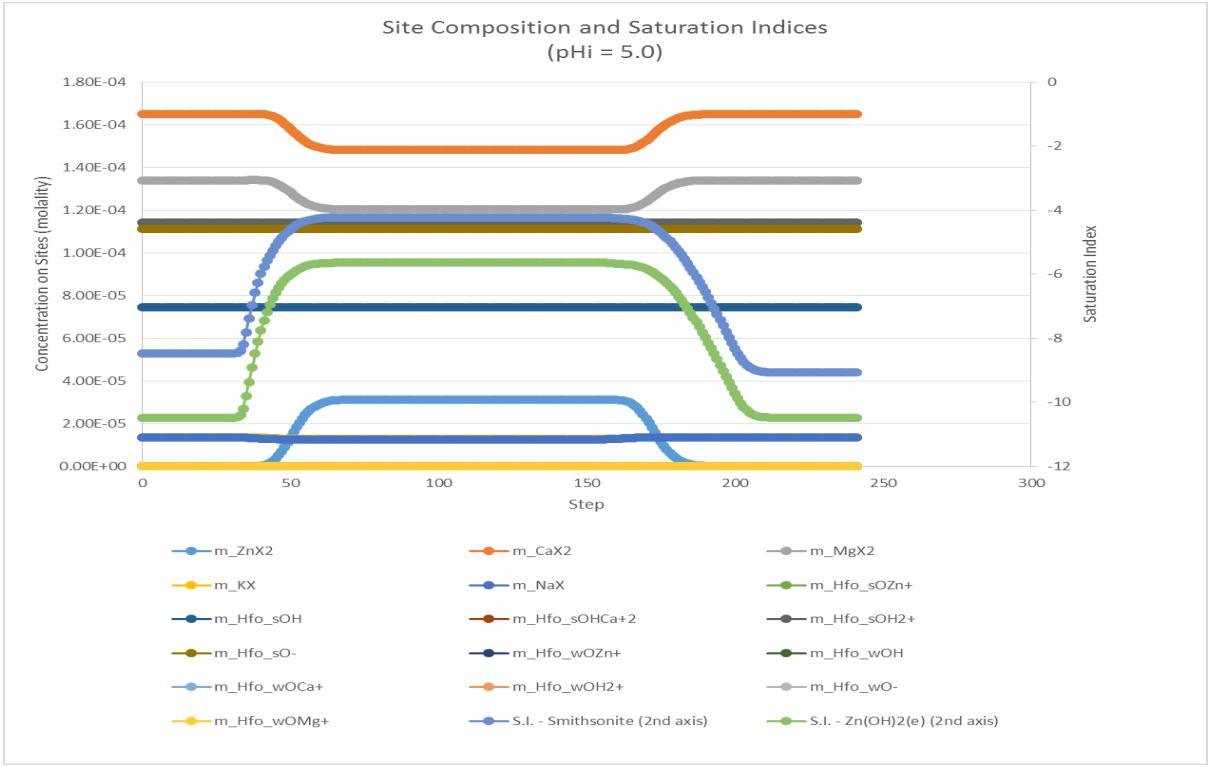
Site Composition and Saturation Indices
(pHi = 5.0)
Concentration on Sites (molality)
Saturation Index
Step
1.80E-04
1.60E-04
1.40E-04
1.20E-04
1.00E-04
8.00E-05
6.00E-05
4.00E-05
2.00E-05
0.00E+00
0
-2
-4
-6
-8
-10
-12
0
50
100
150
200
250
300
m_ZnX2
m_CaX2
m_MgX2
m_KX
m_NaX
m_Hfo_sOZn+
m_Hfo_sOH
m_Hfo_sOHCa+2
m_Hfo_sOH2+
m_Hfo_sO-
m_Hfo_wOZn+
m_Hfo_wOH
m_Hfo_wOCa+
m_Hfo_wOH2+
m_Hfo_wO-
m_Hfo_wOMg+
S.I. - Smithsonite (2nd axis)
S.I. - Zn(OH)2(e) (2nd axis)

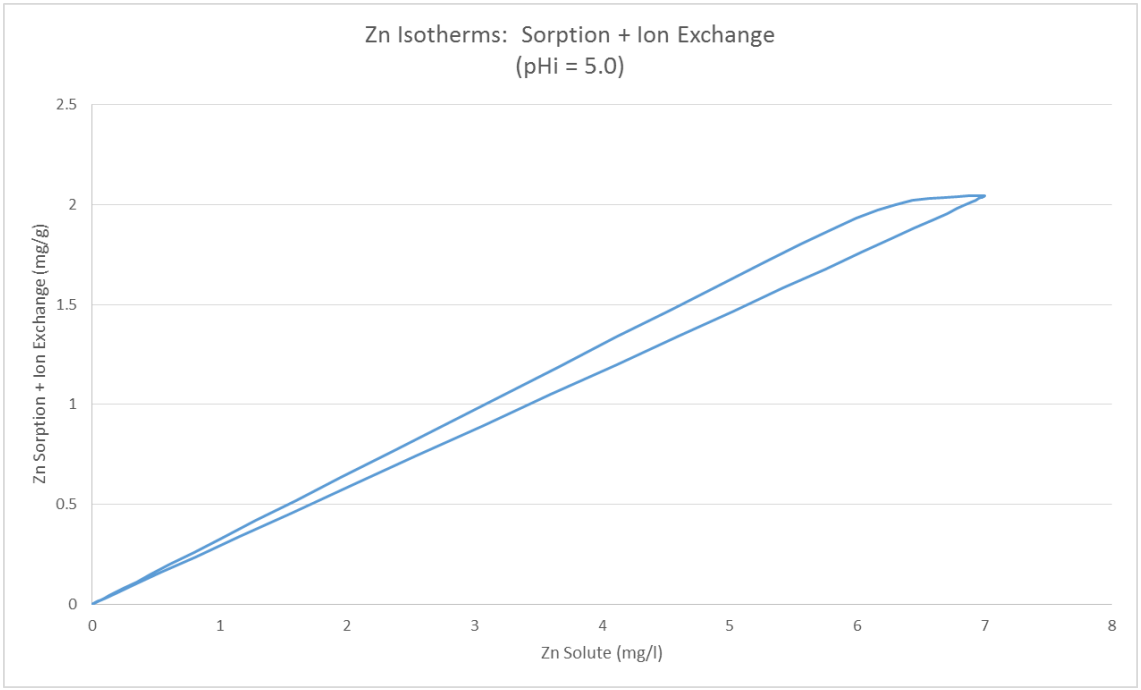
Zn Isotherms: Sorption + Ion Exchange
(pHi = 5.0)
Zn Sorption + Ion Exchange (mg/g)
2.5
2
1.5
1
0.5
0
0
1
2
3
4
5
6
7
8
Zn Solute (mg/l)

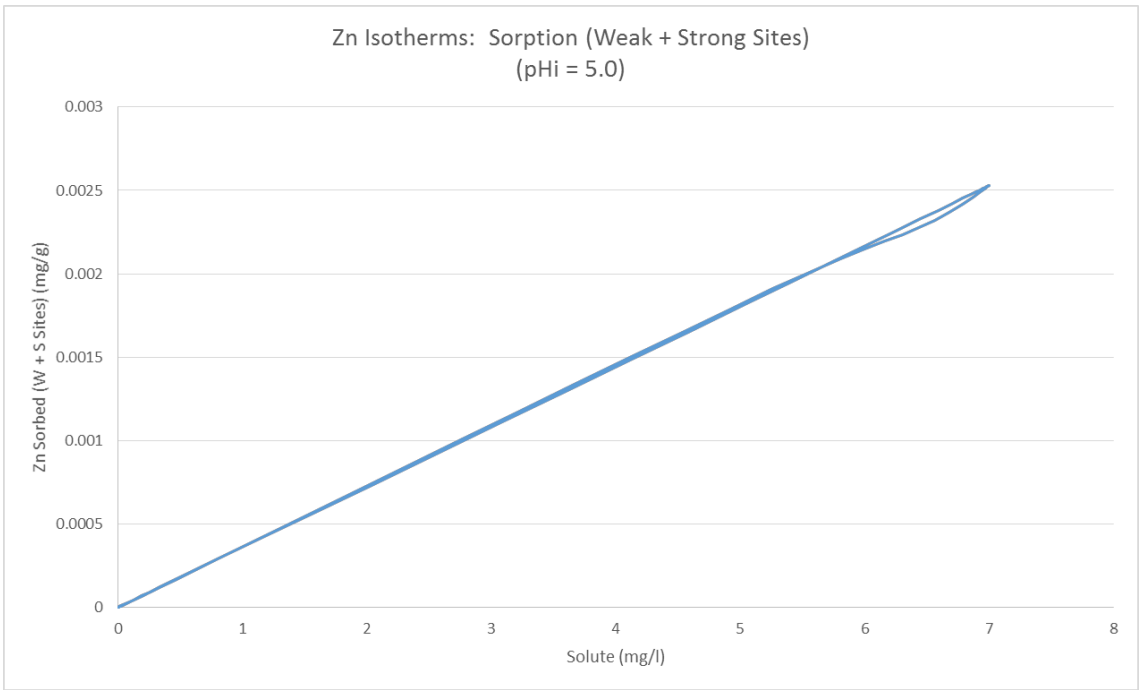
Zn Isotherms: Sorption (Weak + Strong Sites)
(pHi = 5.0)
Zn Sorbed (W + S Sites) (mg/g)
0.003
0.0025
0.002
0.0015
0.001
0.0005
0
0
1
2
3
4
5
6
7
8
Solute (mg/l)

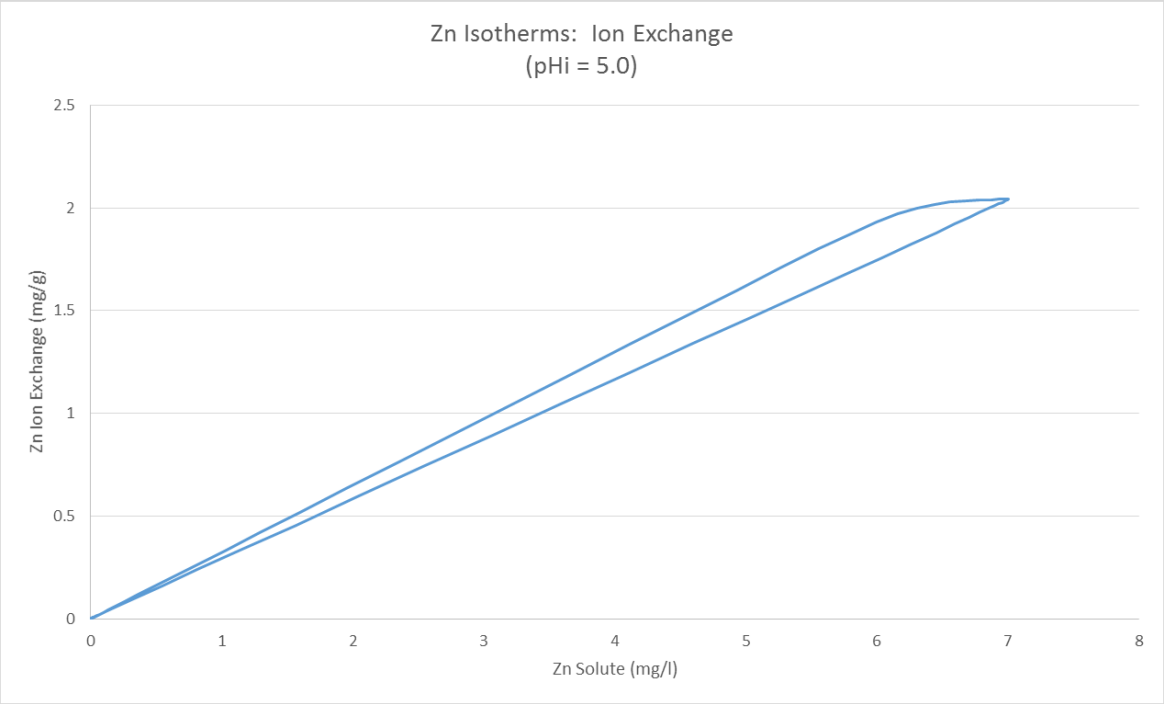
Zn Isotherms: Ion Exchange
(pHi = 5.0)
Zn Ion Exchange (mg/g)
2.5
2
1.5
1
0.5
0
0
1
2
3
4
5
6
7
8
Zn Solute (mg/l)

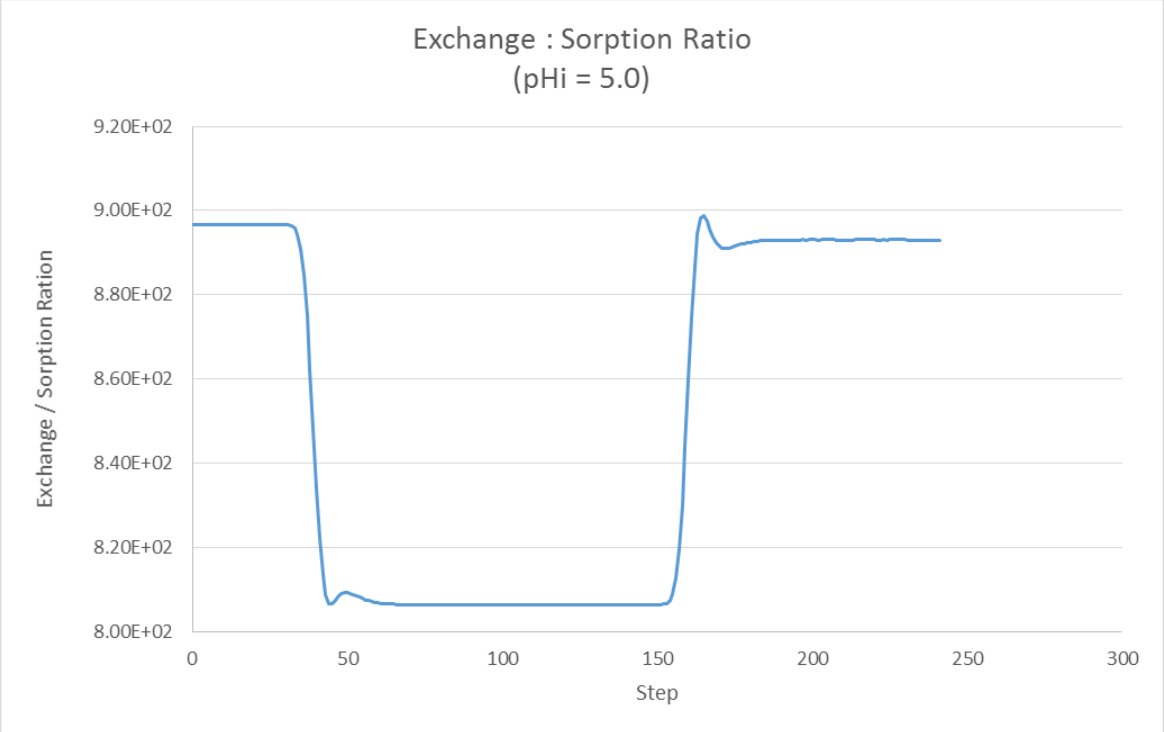
Exchange : Sorption Ratio
(pHi = 5.0)
Exchange / Sorption Ration
9.20E+02
9.00E+02
8.80E+02
8.60E+02
8.40E+02
8.20E+02
8.00E+02
0
50
100
150
200
250
300
Step

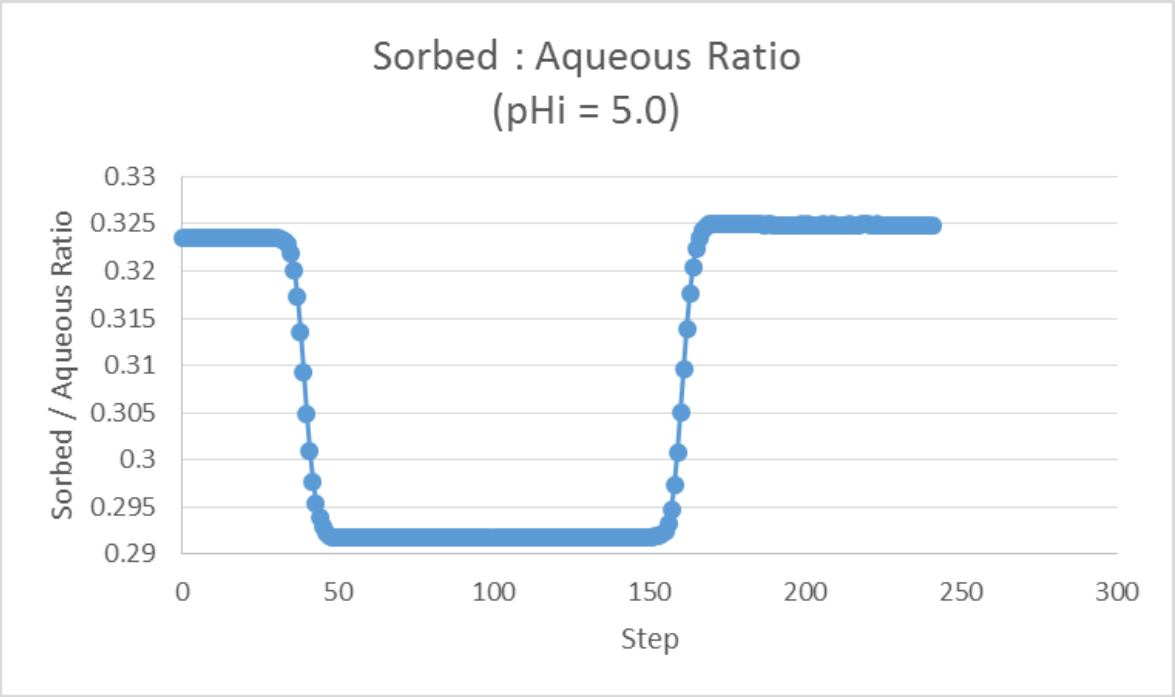
Sorbed : Aqueous Ratio
(pHi = 5.0)
Sorbed / Aqueous Ratio
0.33
0.325
0.32
0.315
0.31
0.305
0.3
0.295
0.29
0
50
100
150
200
250
300
Step

pH 5.5

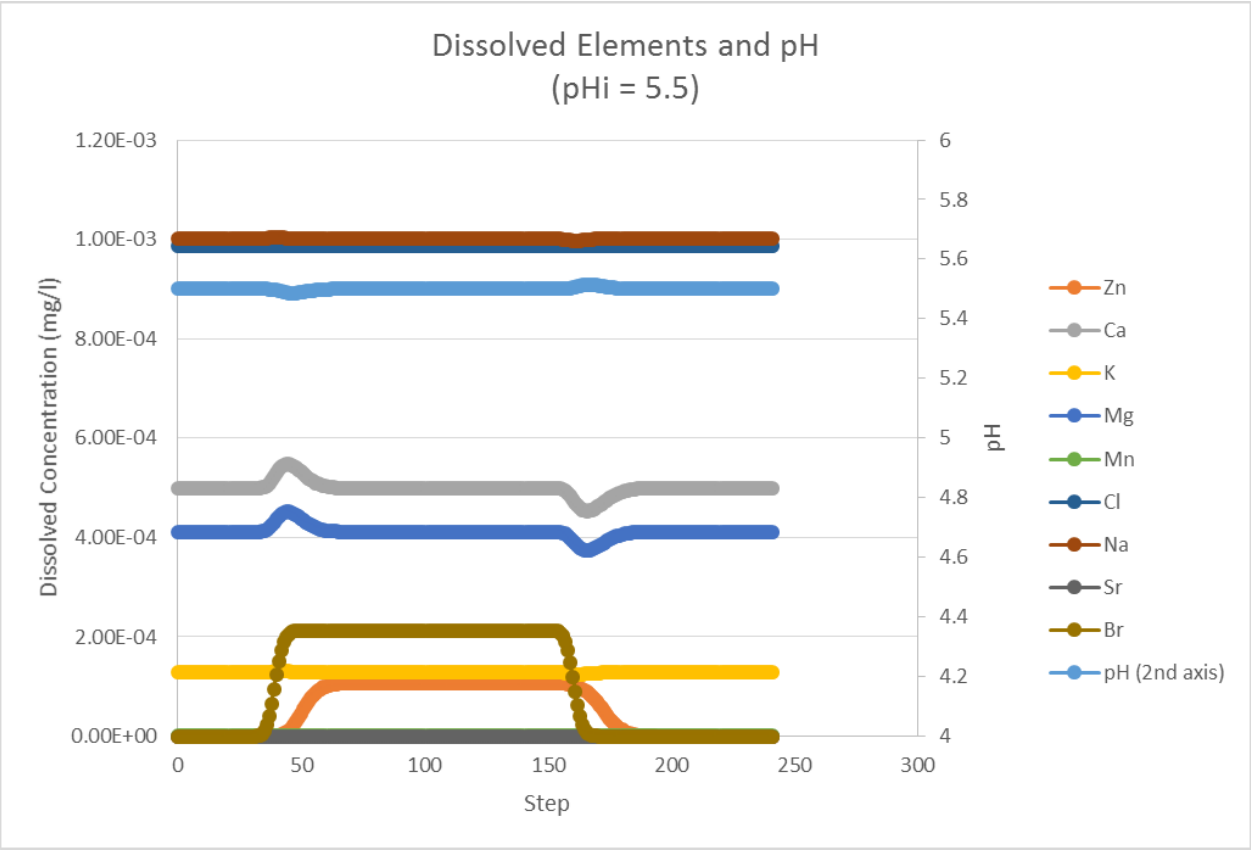
Dissolved Elements and pH
(pHi = 5.5)
Dissolved Concentration (mg/l)
1.20E-03
1.00E-03
8.00E-04
6.00E-04
4.00E-04
2.00E-04
0.00E+00
0
50
100
150
200
250
300
Step
6
5.8
5.6
5.4
5.2
5
4.8
4.6
4.4
4.2
4
pH
Zn
Ca
K
Mg
Mn
Cl
Na
Sr
Br
pH (2nd axis)

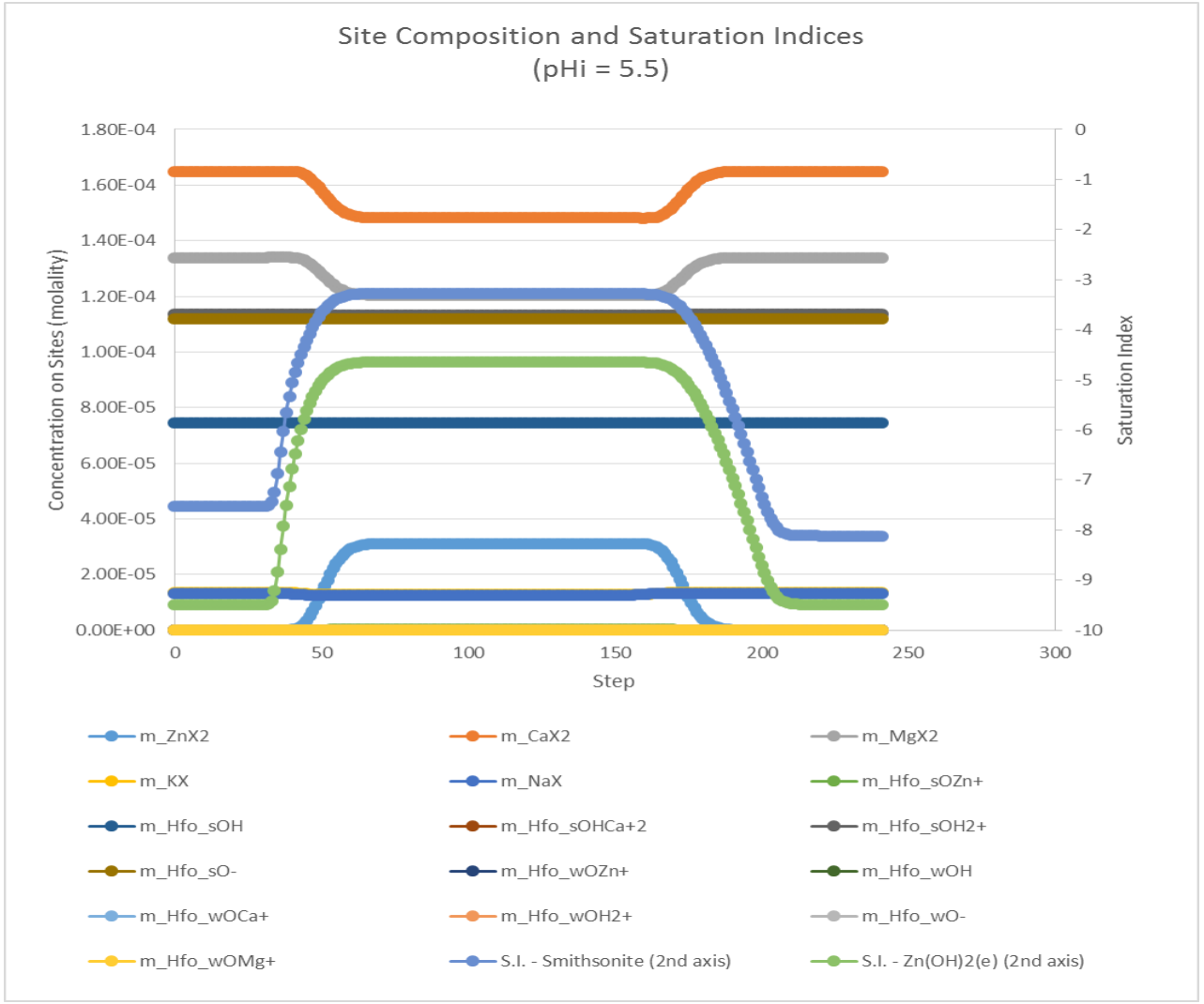
Site Composition and Saturation Indices
(pHi = 5.5)
Concentration on Sites (molality)
Saturation Index
Step
1.80E-04
1.60E-04
1.40E-04
1.20E-04
1.00E-04
8.00E-05
6.00E-05
4.00E-05
2.00E-05
0.00E+00
0
-1
-2
-3
-4
-5
-6
-7
-8
-9
-10
0
50
100
150
200
250
300
m_ZnX2
m_CaX2
m_MgX2
m_KX
m_NaX
m_Hfo_sOZn+
m_Hfo_sOH
m_Hfo_sOHCa+2
m_Hfo_sOH2+
m_Hfo_sO-
m_Hfo_wOZn+
m_Hfo_wOH
m_Hfo_wOCa+
m_Hfo_wOH2+
m_Hfo_wO-
m_Hfo_wOMg+
S.I. - Smithsonite (2nd axis)
S.I. - Zn(OH)2(e) (2nd axis)

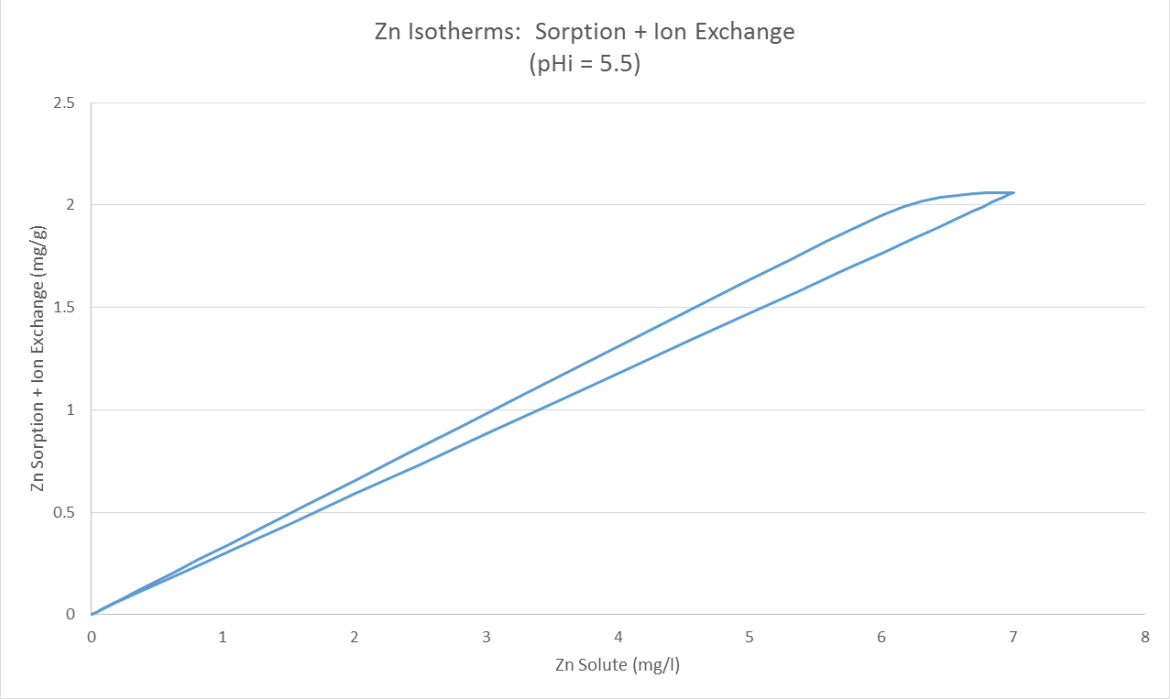
Zn Isotherms: Sorption + Ion Exchange
(pHi = 5.5)
Zn Sorption + Ion Exchange (mg/g)
2.5
2
1.5
1
0.5
0
0
1
2
3
4
5
6
7
8
Zn Solute (mg/l)

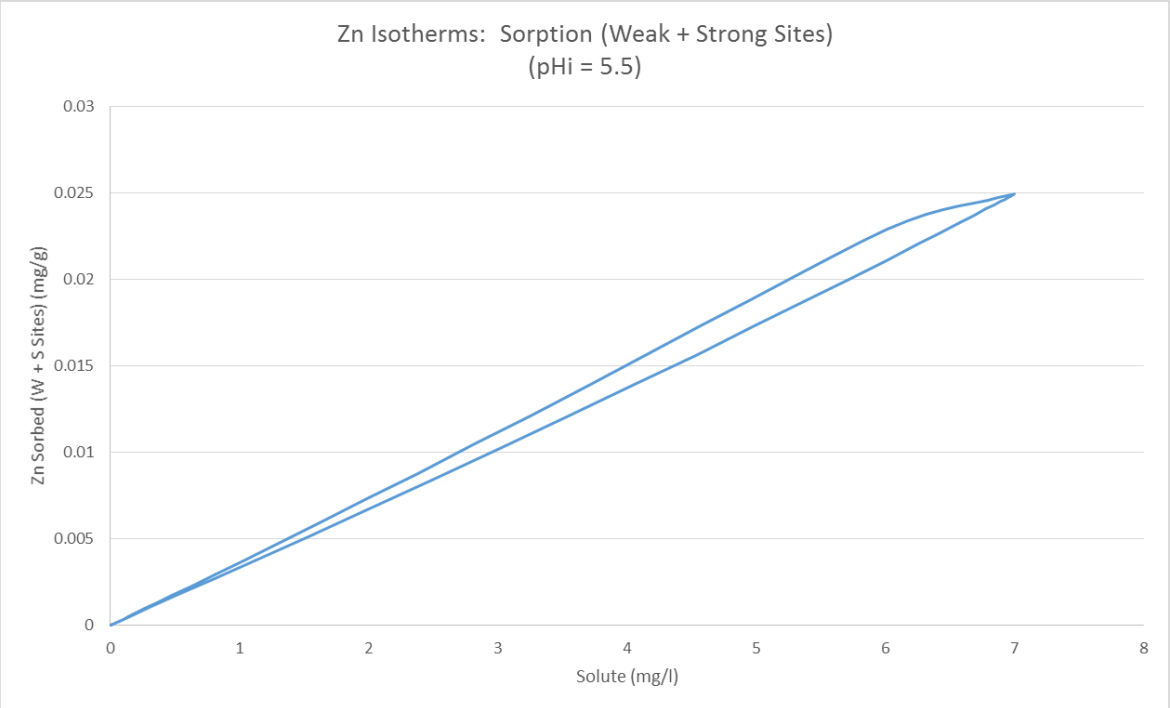
Zn Isotherms: Sorption (Weak + Strong Sites)
(pHi = 5.5)
Zn Sorbed (W + S Sites) (mg/g)
0.03
0.025
0.02
0.015
0.01
0.005
0
0
1
2
3
4
5
6
7
8
Solute (mg/l)

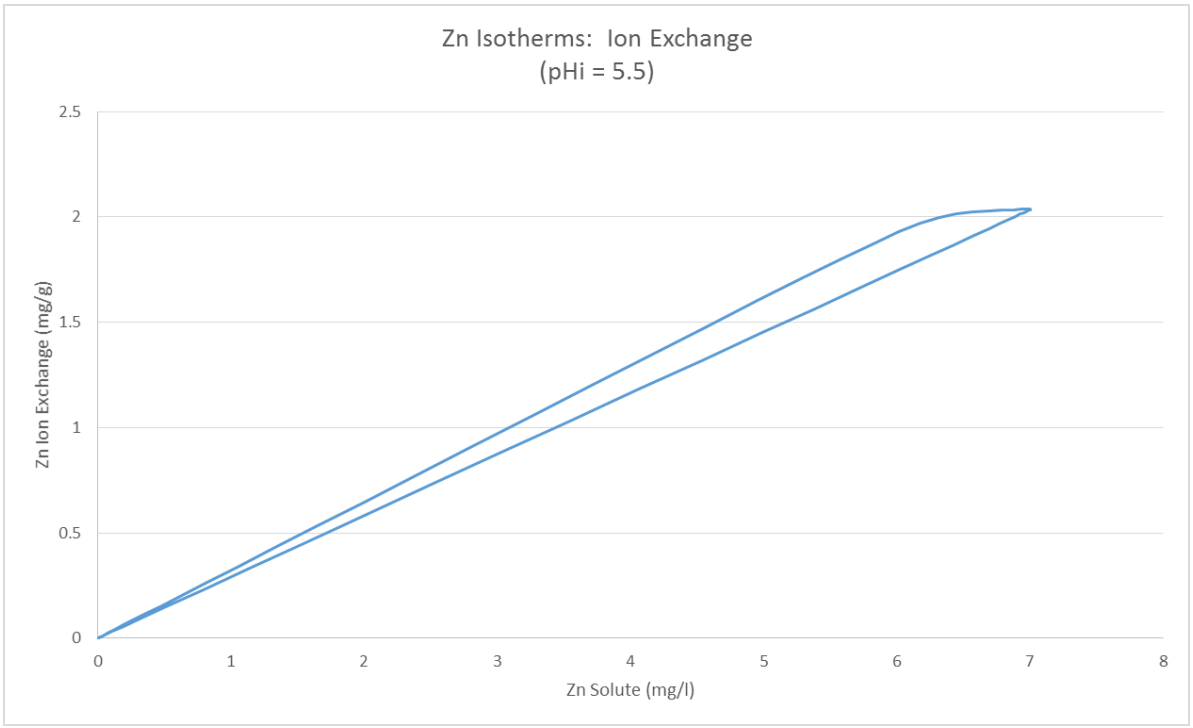
Zn Isotherms: Ion Exchange
(pHi = 5.5)
Zn Ion Exchange (mg/g)
2.5
2
1.5
1
0.5
0
0
1
2
3
4
5
6
7
8
Zn Solute (mg/l)

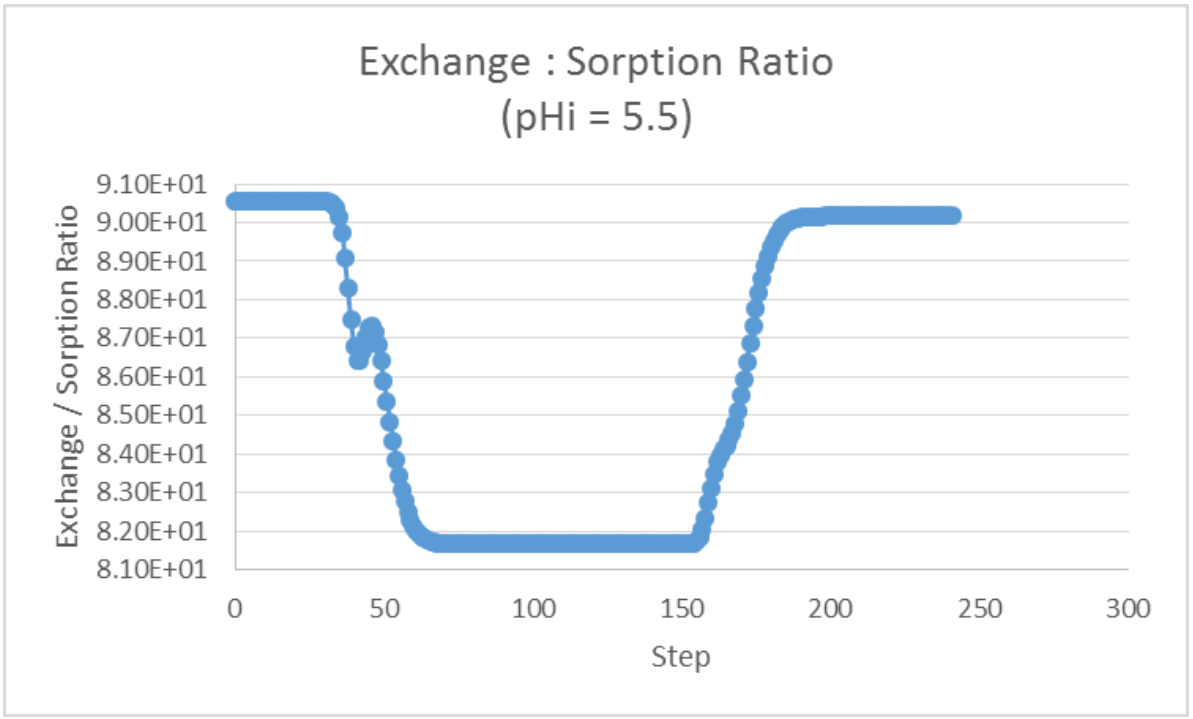
Exchange : Sorption Ratio
(pHi = 5.5)
Exchange / Sorption Ratio
9.10E+01
9.00E+01
8.90E+01
8.80E+01
8.70E+01
8.60E+01
8.50E+01
8.40E+01
8.30E+01
8.20E+01
8.10E+01
0
50
100
150
200
250
300
Step

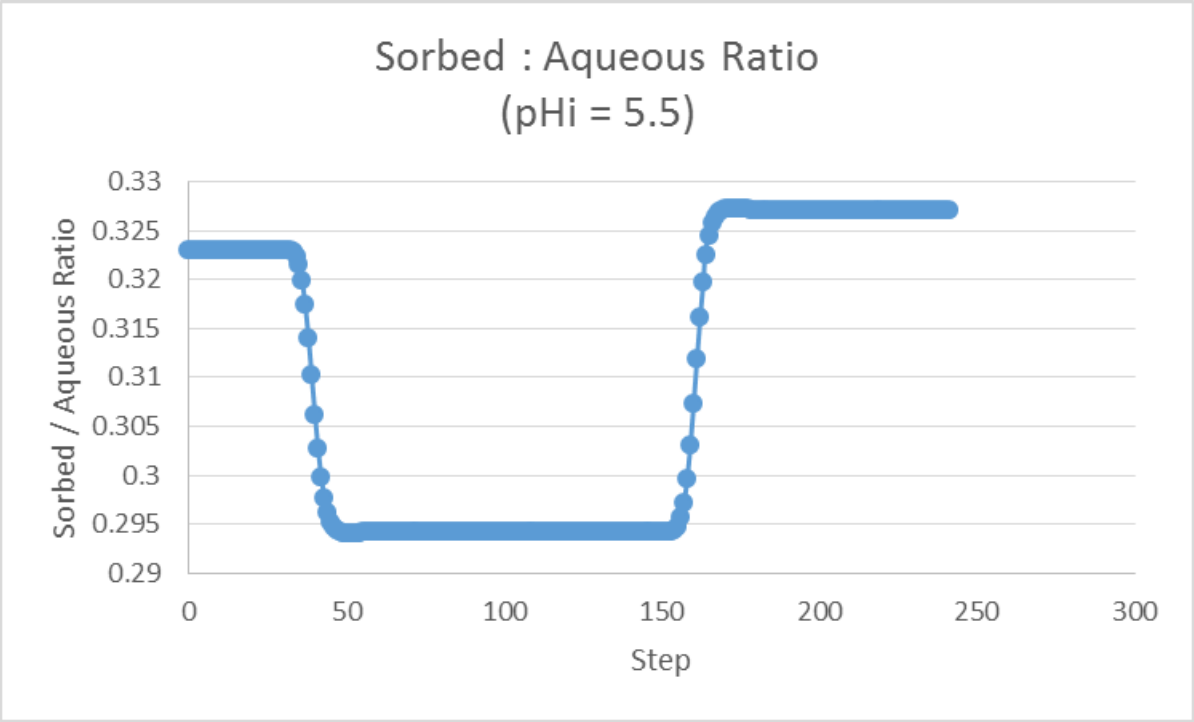
Sorbed : Aqueous Ratio
(pHi = 5.5)
Sorbed / Aqueous Ratio
0.33
0.325
0.32
0.315
0.31
0.305
0.3
0.295
0.29
0
50
100
150
200
250
300
Step

pH 6.0

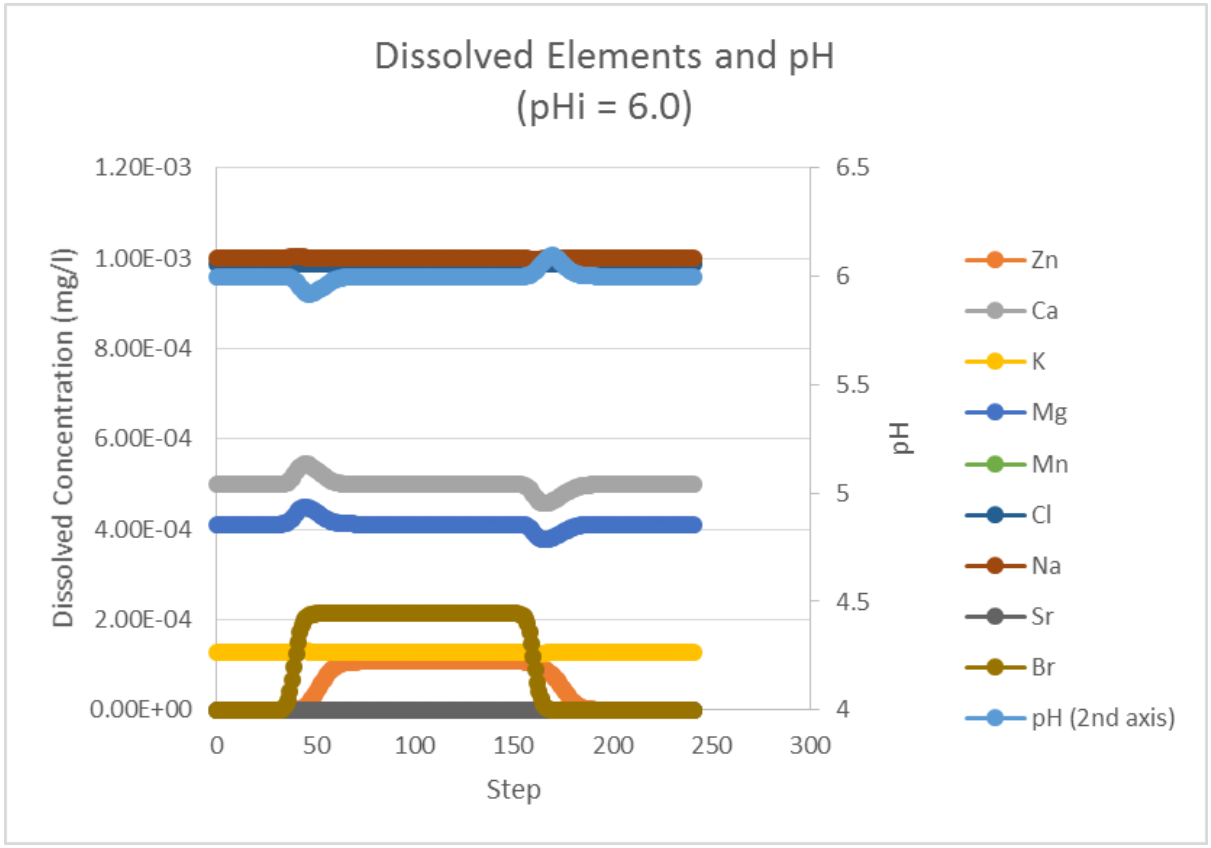
Dissolved Elements and pH
(pHi = 6.0)
Dissolved Concentration (mg/l)
1.20E-03
1.00E-03
8.00E-04
6.00E-04
4.00E-04
2.00E-04
0.00E+00
0
50
100
150
200
250
300
Step
6.5
6
5.5
5
4.5
4
pH
Zn
Ca
K
Mg
Mn
Cl
Na
Sr
Br
pH (2nd axis)

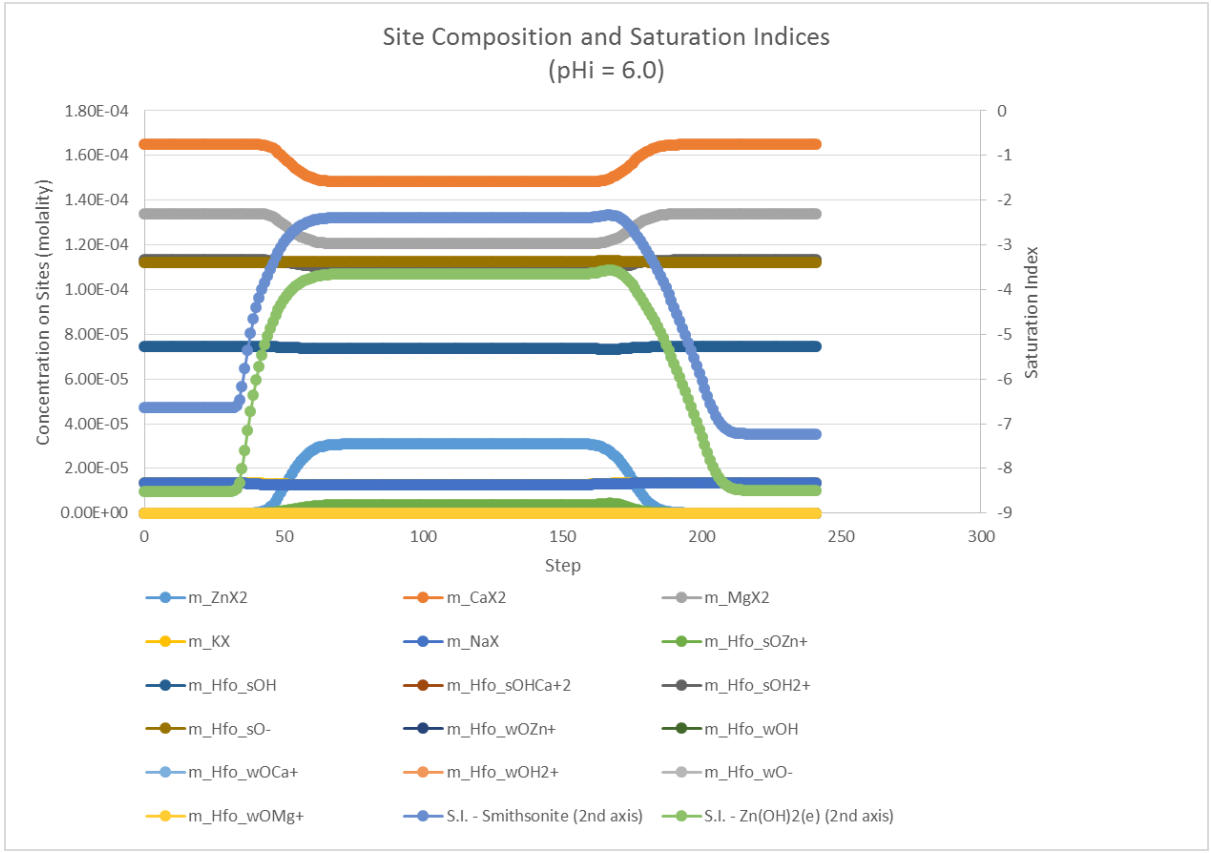
Site Composition and Saturation Indices
(pHi = 6.0)
Concentration on Sites (molality)
Saturation Index
Step
1.80E-04
1.60E-04
1.40E-04
1.20E-04
1.00E-04
8.00E-05
6.00E-05
4.00E-05
2.00E-05
0.00E+00
0
-1
-2
-3
-4
-5
-6
-7
-8
-9
0
50
100
150
200
250
300
m_ZnX2
m_CaX2
m_MgX2
m_KX
m_NaX
m_Hfo_sOZn+
m_Hfo_sOH
m_Hfo_sOHCa+2
m_Hfo_sOH2+
m_Hfo_sO-
m_Hfo_wOZn+
m_Hfo_wOH
m_Hfo_wOCa+
m_Hfo_wOH2+
m_Hfo_wO-
m_Hfo_wOMg+
S.I. - Smithsonite (2nd axis)
S.I. - Zn(OH)2(e) (2nd axis)

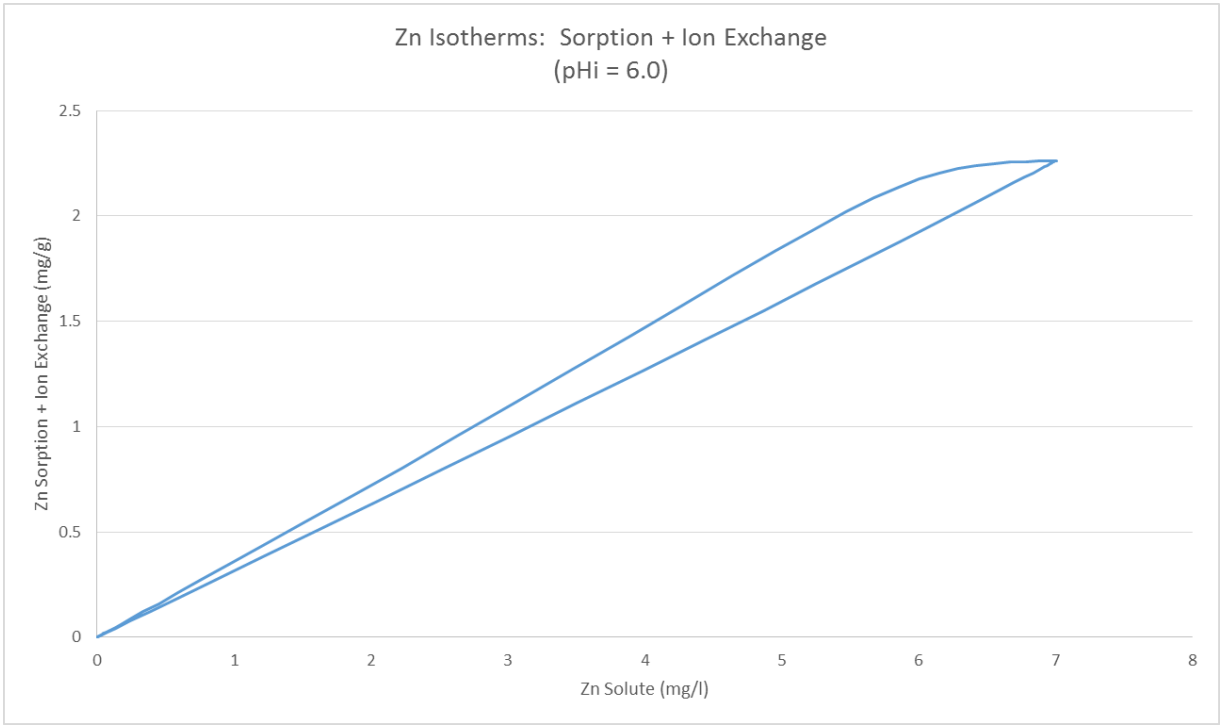
Zn Isotherms: Sorption + Ion Exchange
(pHi = 6.0)
Zn Sorption + Ion Exchange (mg/g)
2.5
2
1.5
1
0.5
0
0
1
2
3
4
5
6
7
8
Zn Solute (mg/l)

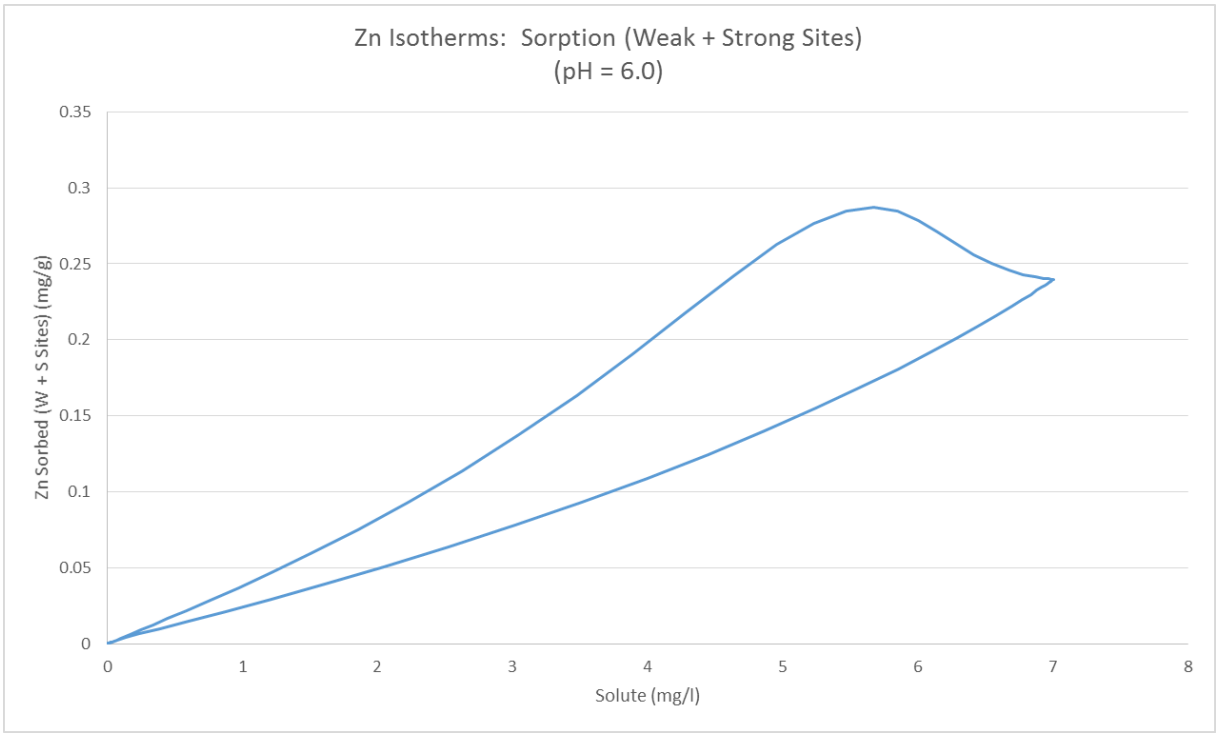
Zn Isotherms: Sorption (Weak + Strong Sites)
(pH = 6.0)
Zn Sorbed (W + S Sites) (mg/g)
0.35
0.3
0.25
0.2
0.15
0.1
0.05
0
0
1
2
3
4
5
6
7
8
Solute (mg/l)

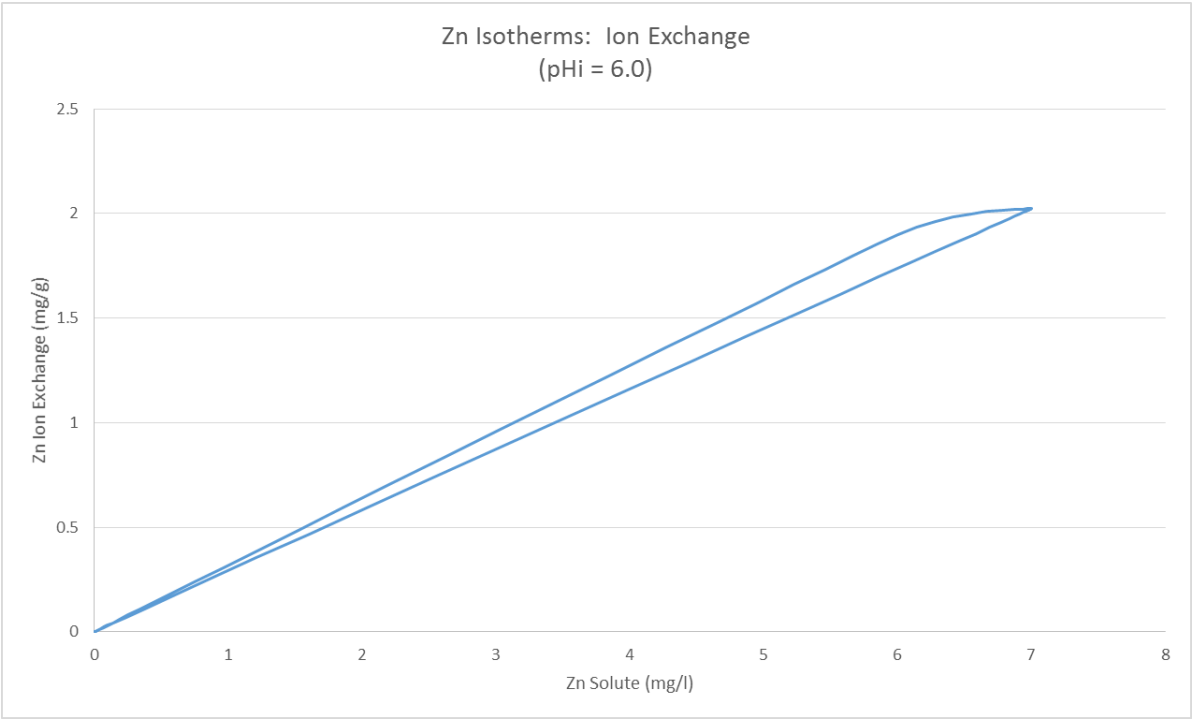
Zn Isotherms: Ion Exchange
(pHi = 6.0)
Zn Ion Exchange (mg/g)
2.5
2
1.5
1
0.5
0
0
1
2
3
4
5
6
7
8
Zn Solute (mg/l)

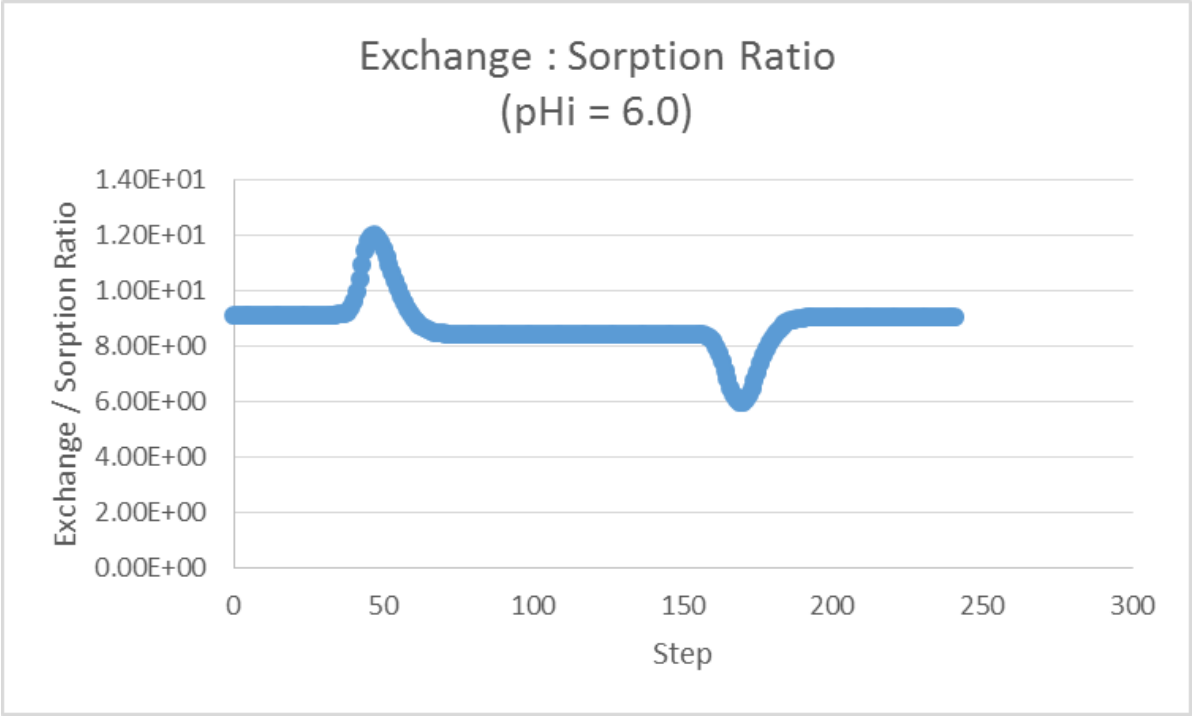
Exchange : Sorption Ratio
(pHi = 6.0)
Exchange / Sorption Ratio
1.40E+01
1.20E+01
1.00E+01
8.00E+00
6.00E+00
4.00E+00
2.00E+00
0.00E+00
0
50
100
150
200
250
300
Step

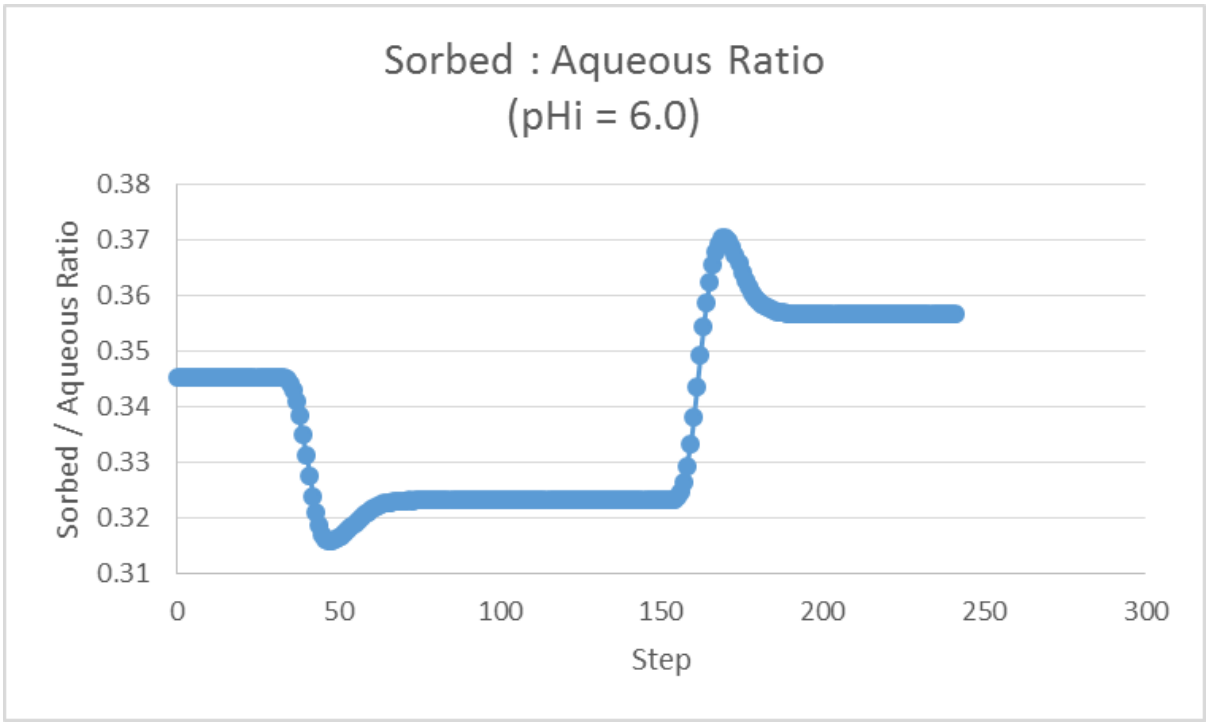
Sorbed : Aqueous Ratio
(pHi = 6.0)
Sorbed / Aqueous Ratio
0.38
0.37
0.36
0.35
0.34
0.33
0.32
0.31
0
50
100
150
200
250
300
Step

pH 6.5

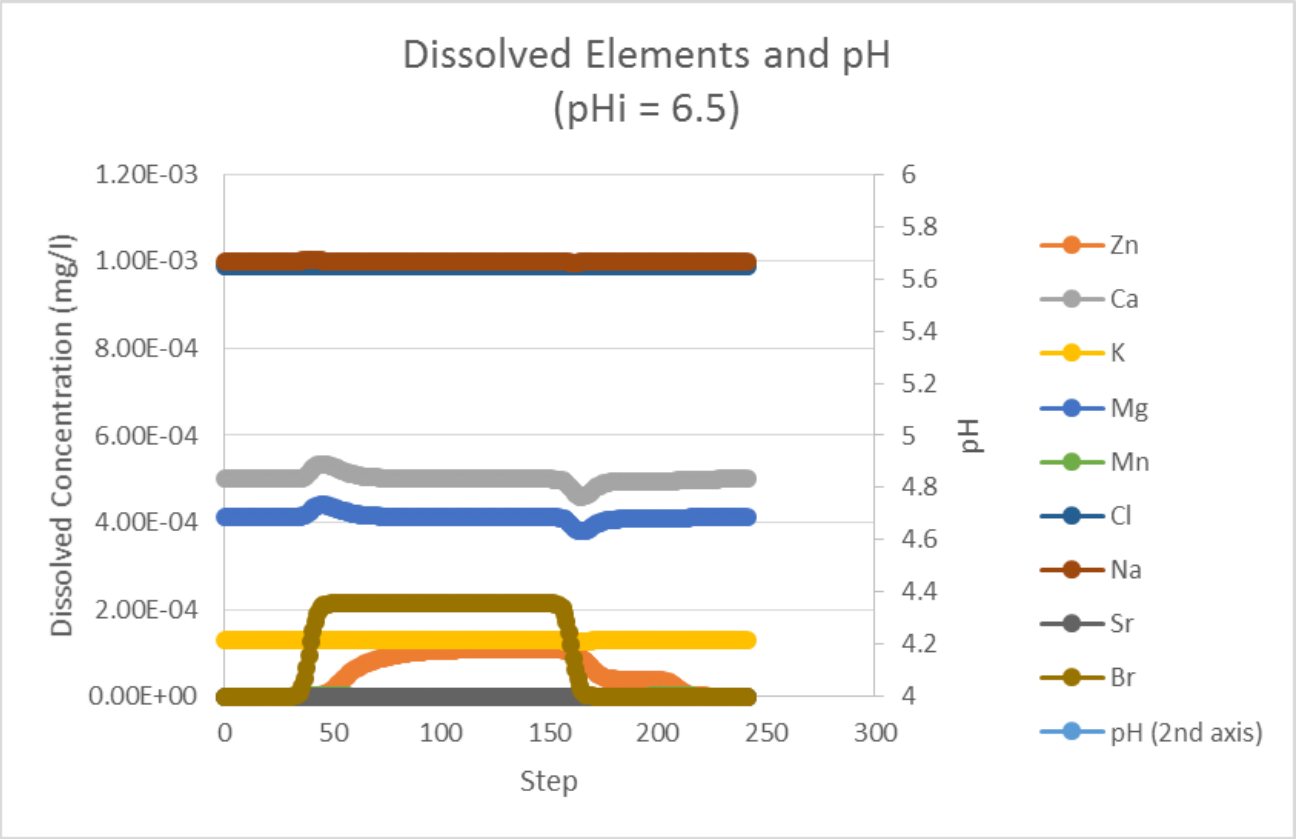
Dissolved Elements and pH
(pHi = 6.5)
Dissolved Concentration (mg/l)
1.20E-03
1.00E-03
8.00E-04
6.00E-04
4.00E-04
2.00E-04
0.00E+00
0
50
100
150
200
250
300
Step
6
5.8
5.6
5.4
5.2
5
4.8
4.6
4.4
4.2
4
pH
Zn
Ca
K
Mg
Mn
Cl
Na
Sr
Br
pH (2nd axis)

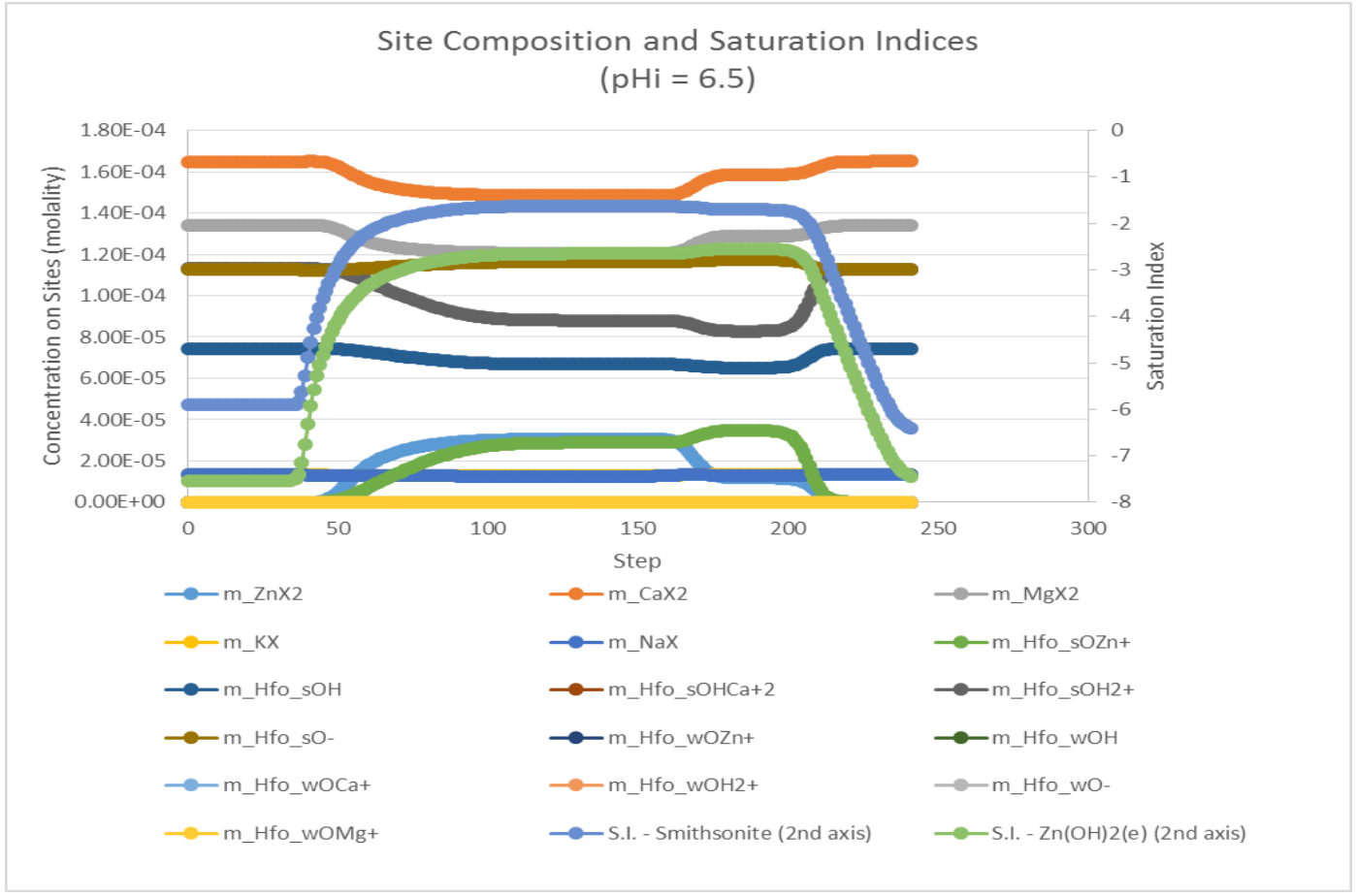
Site Composition and Saturation Indices
(pHi = 6.5)
Concentration on Sites (molality)
1.80E-04
1.60E-04
1.40E-04
1.20E-04
1.00E-04
8.00E-05
6.00E-05
4.00E-05
2.00E-05
0.00E+00
Saturation Index
0
-1
-2
-3
-4
-5
-6
-7
-8
0
50
100
150
200
250
300
Step
m_ZnX2
m_CaX2
m_MgX2
m_KX
m_NaX
m_Hfo_sOZn+
m_Hfo_sOH
m_Hfo_sOHCa+2
m_Hfo_sOH2+
m_Hfo_sO-
m_Hfo_wOZn+
m_Hfo_wOH
m_Hfo_wOCa+
m_Hfo_wOH2+
m_Hfo_wO-
m_Hfo_wOMg+
S.I. - Smithsonite (2nd axis)
S.I. - Zn(OH)2(e) (2nd axis)

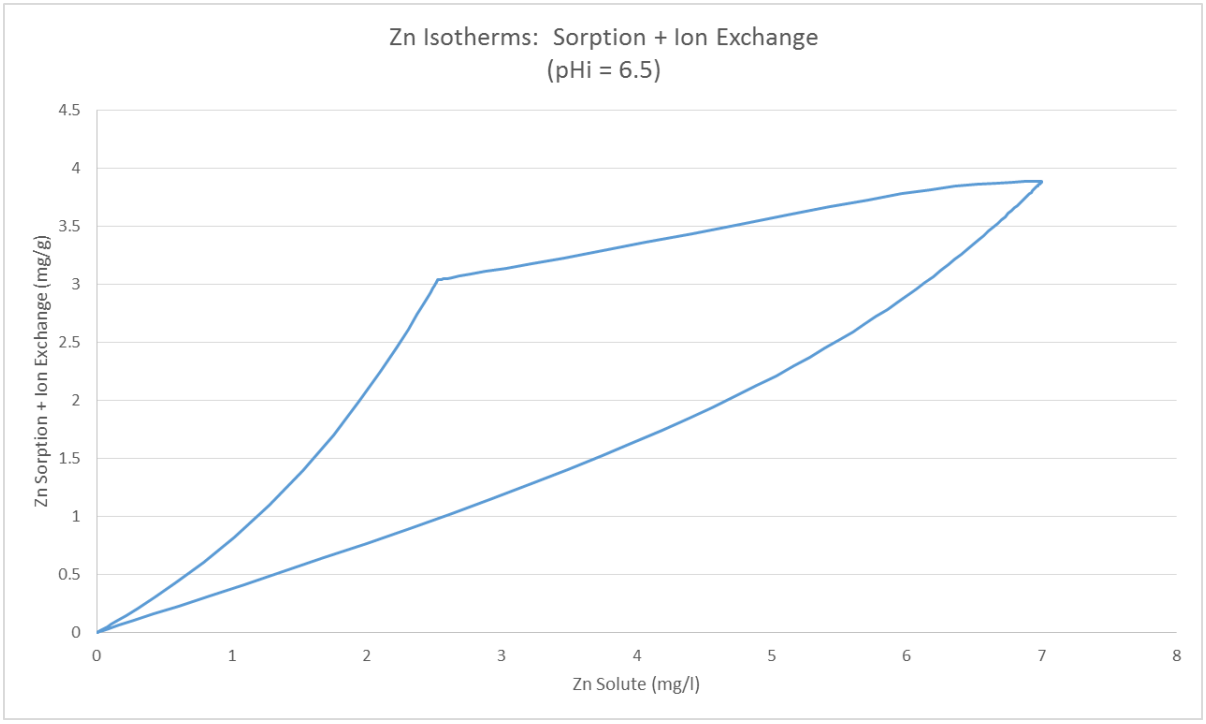
Zn Isotherms: Sorption + Ion Exchange
(pHi = 6.5)
Zn Sorption + Ion Exchange (mg/g)
Zn Solute (mg/l)
0
0.5
1
1.5
2
2.5
3
3.5
4
4.5
0
1
2
3
4
5
6
7
8

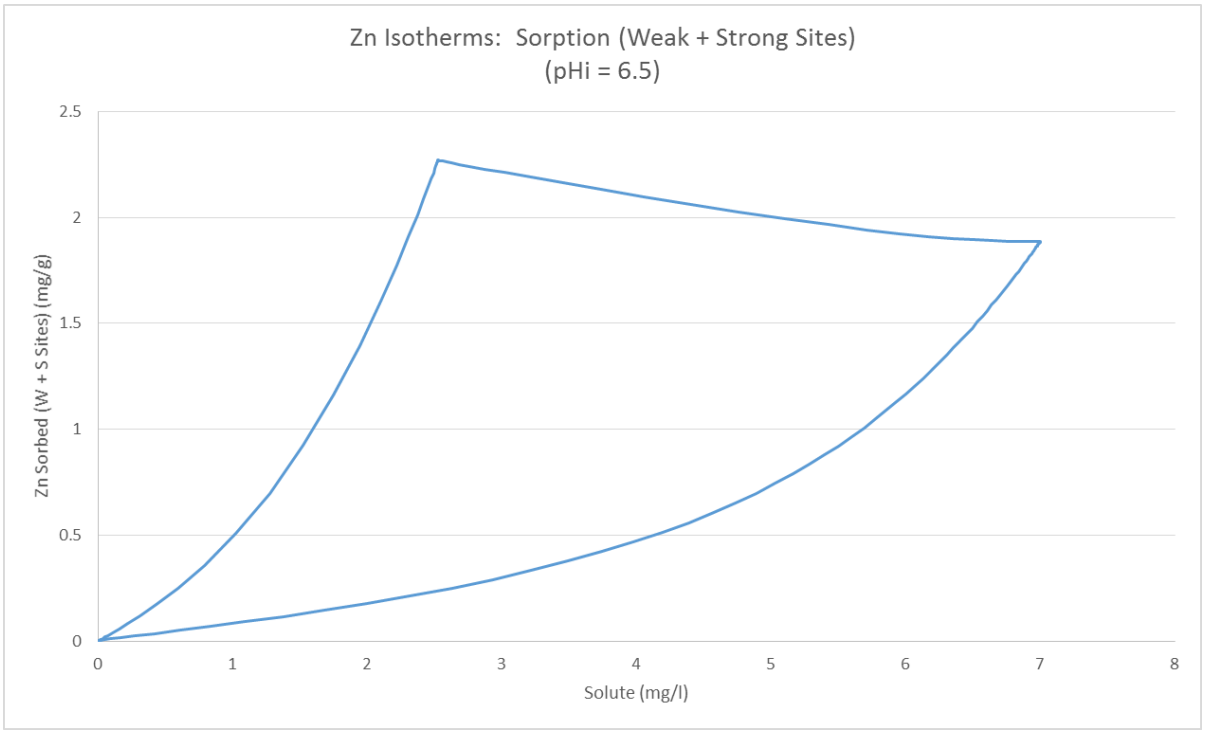
Zn Isotherms: Sorption (Weak + Strong Sites)
(pHi = 6.5)
Zn Sorbed (W + S Sites) (mg/g)
Solute (mg/l)
0
0.5
1
1.5
2
2.5
0
1
2
3
4
5
6
7
8

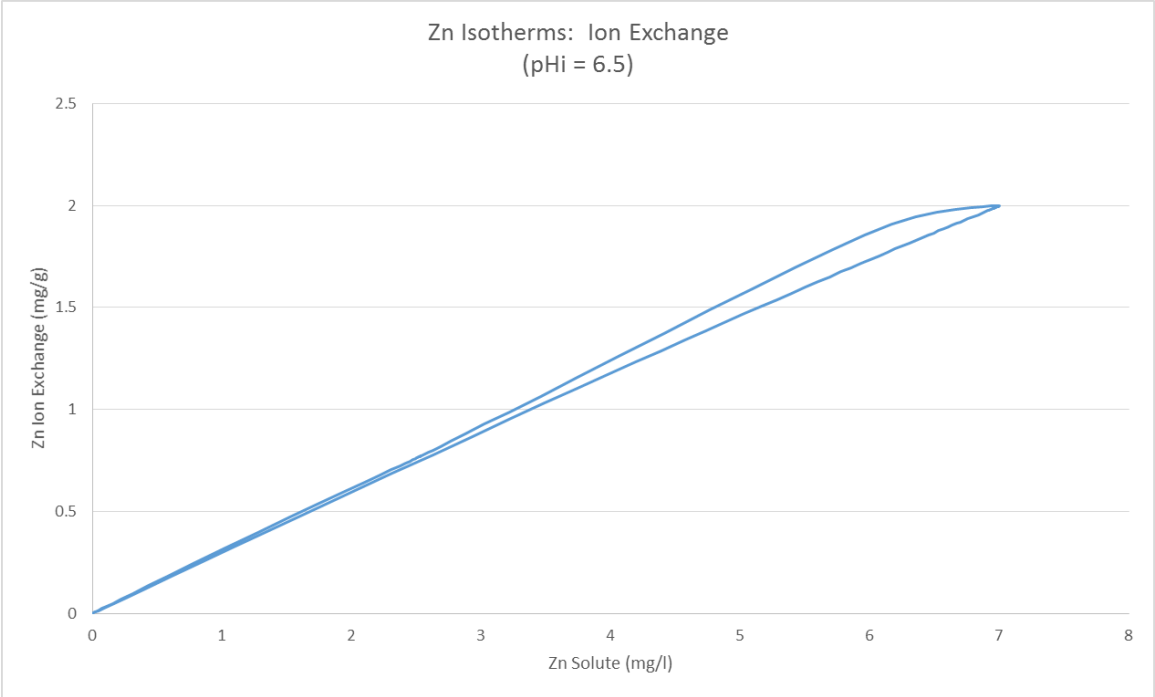
Zn Isotherms: Ion Exchange
(pHi = 6.5)
Zn Ion Exchange (mg/g)
2.5
2
1.5
1
0.5
0
0
1
2
3
4
5
6
7
8
Zn Solute (mg/l)

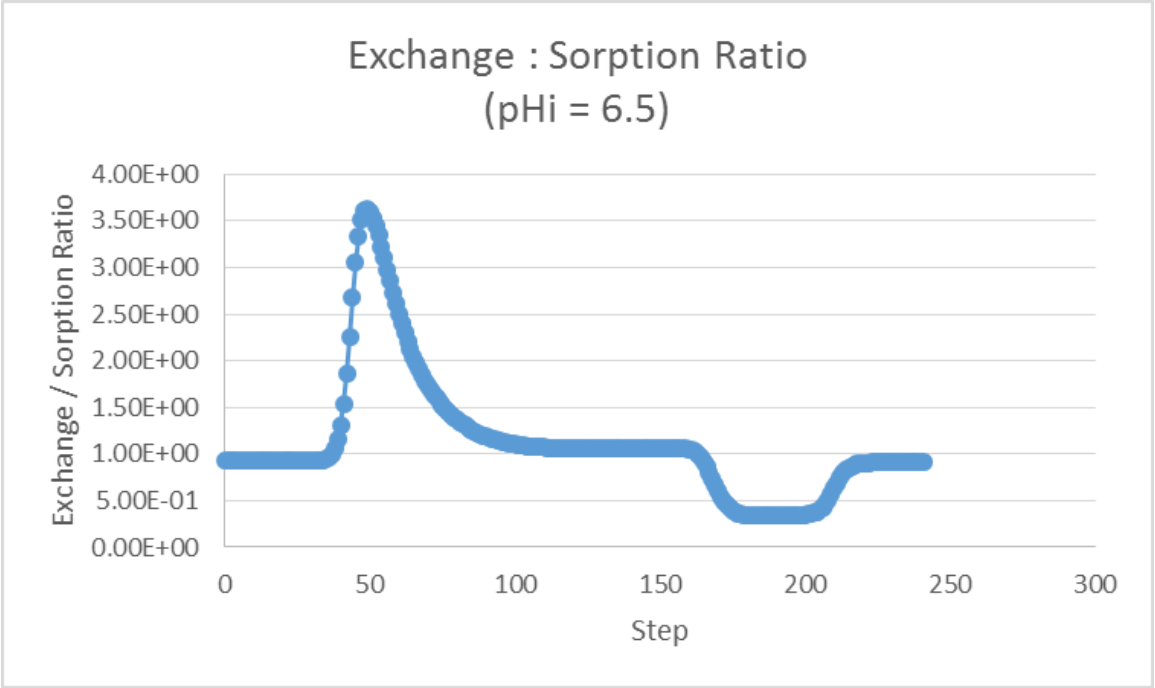
Exchange : Sorption Ratio
(pHi = 6.5)
Exchange / Sorption Ratio
4.00E+00
3.50E+00
3.00E+00
2.50E+00
2.00E+00
1.50E+00
1.00E+00
5.00E-01
0.00E+00
0
50
100
150
200
250
300
Step

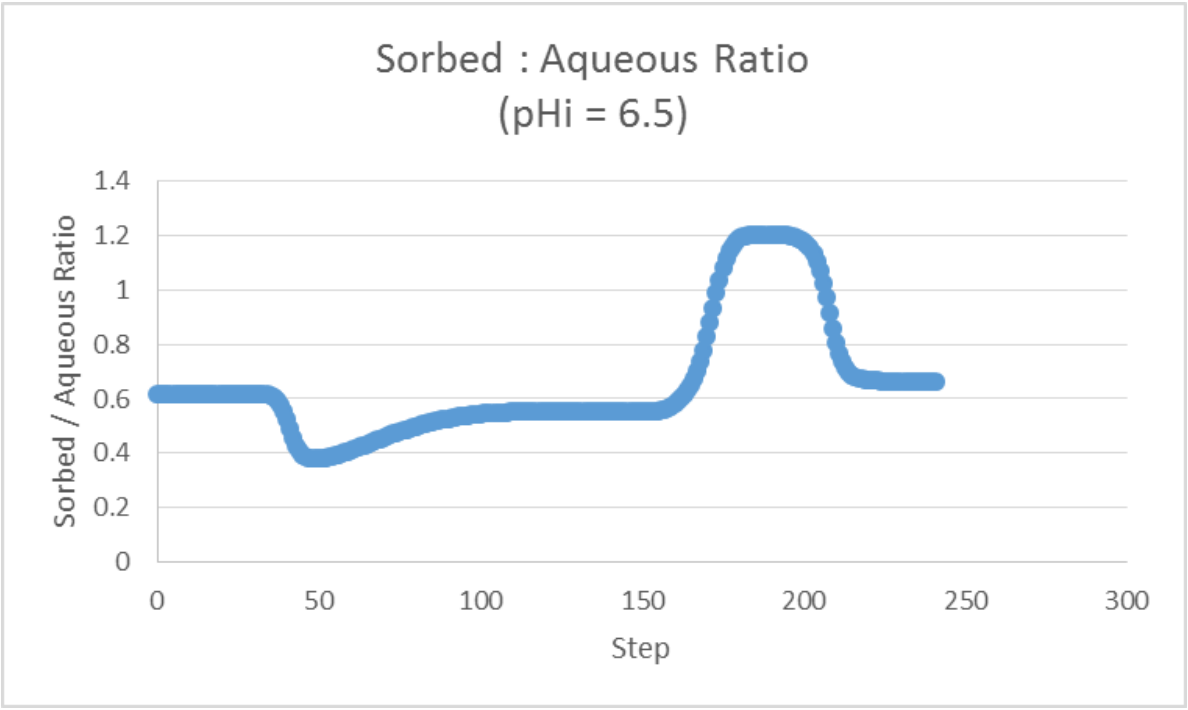
Sorbed : Aqueous Ratio
(pHi = 6.5)
Sorbed / Aqueous Ratio
1.4
1.2
1
0.8
0.6
0.4
0.2
0
0
50
100
150
200
250
300
Step

pH 7.0

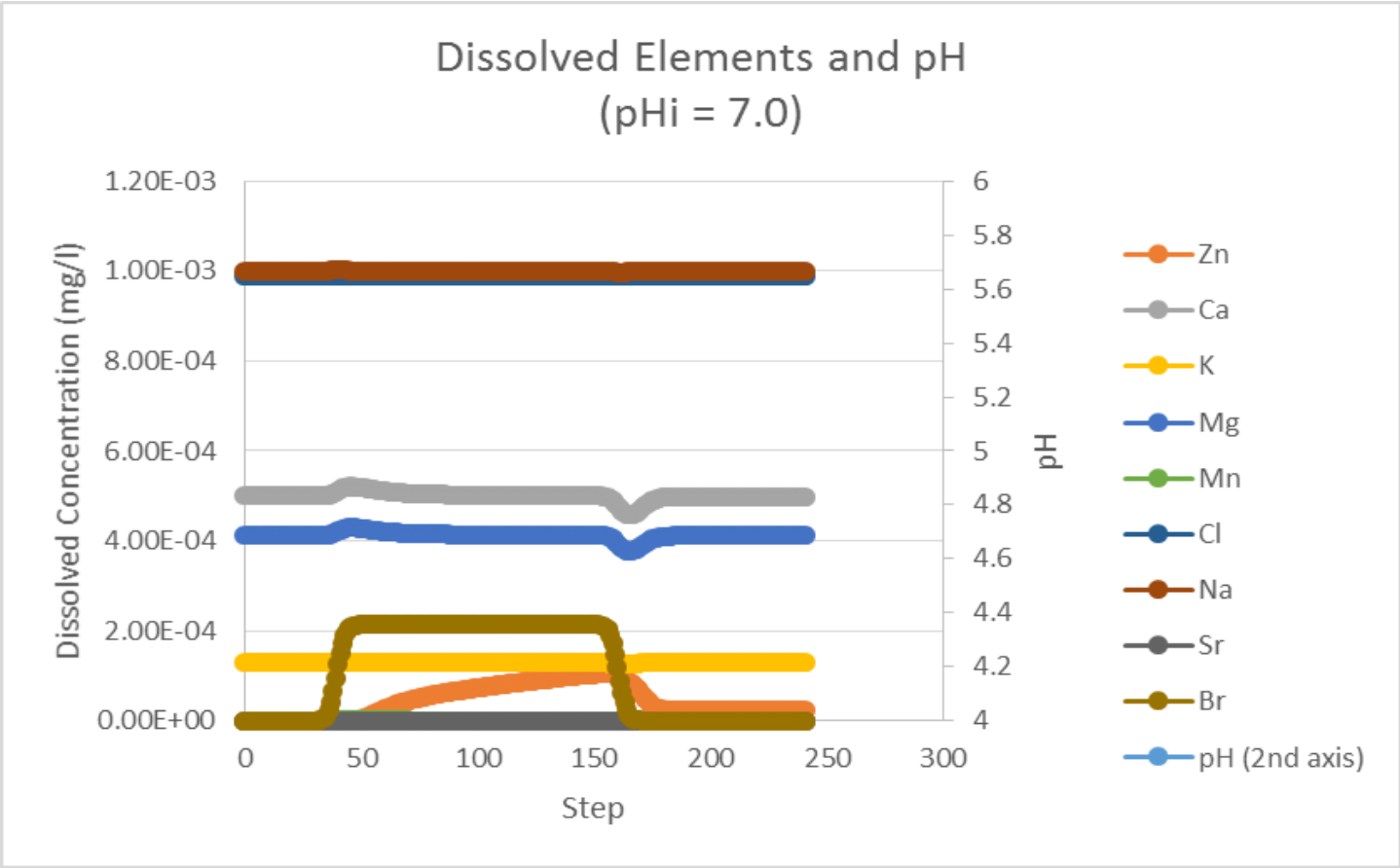
Dissolved Elements and pH
(pHi = 7.0)
Dissolved Concentration (mg/l)
1.20E-03
1.00E-03
8.00E-04
6.00E-04
4.00E-04
2.00E-04
0.00E+00
0
50
100
150
200
250
300
Step
6
5.8
5.6
5.4
5.2
5
4.8
4.6
4.4
4.2
4
pH
Zn
Ca
K
Mg
Mn
Cl
Na
Sr
Br
pH (2nd axis)

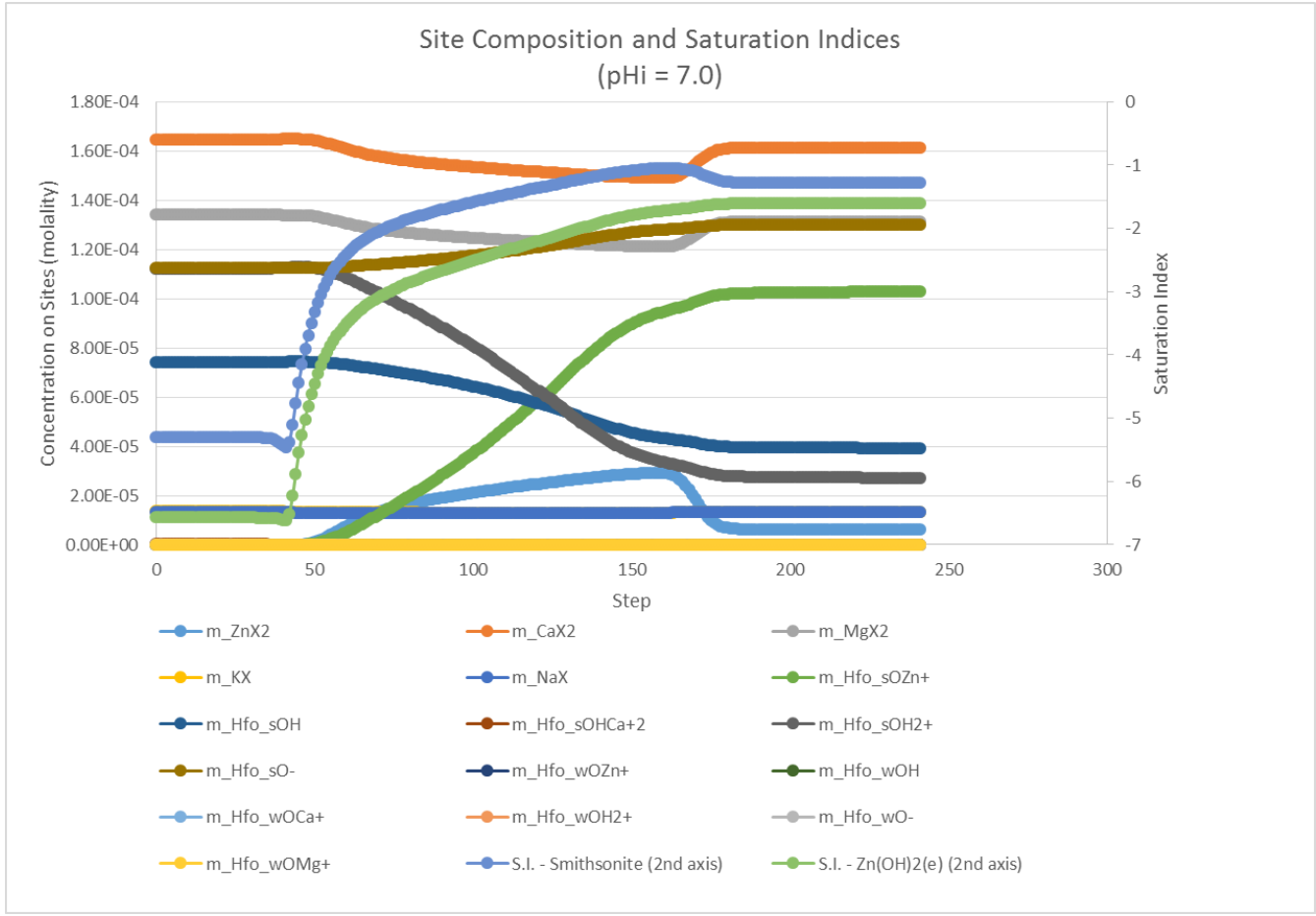
Site Composition and Saturation Indices
(pHi = 7.0)
Concentration on Sites (molality)
1.80E-04
1.60E-04
1.40E-04
1.20E-04
1.00E-04
8.00E-05
6.00E-05
4.00E-05
2.00E-05
0.00E+00
0
50
100
150
200
250
300
Step
Saturation Index
0
-1
-2
-3
-4
-5
-6
-7
m_ZnX2
m_CaX2
m_MgX2
m_KX
m_NaX
m_Hfo_sOZn+
m_Hfo_sOH
m_Hfo_sOHCa+2
m_Hfo_sOH2+
m_Hfo_sO-
m_Hfo_wOZn+
m_Hfo_wOH
m_Hfo_wOCa+
m_Hfo_wOH2+
m_Hfo_wO-
m_Hfo_wOMg+
S.I. - Smithsonite (2nd axis)
S.I. - Zn(OH)2(e) (2nd axis)

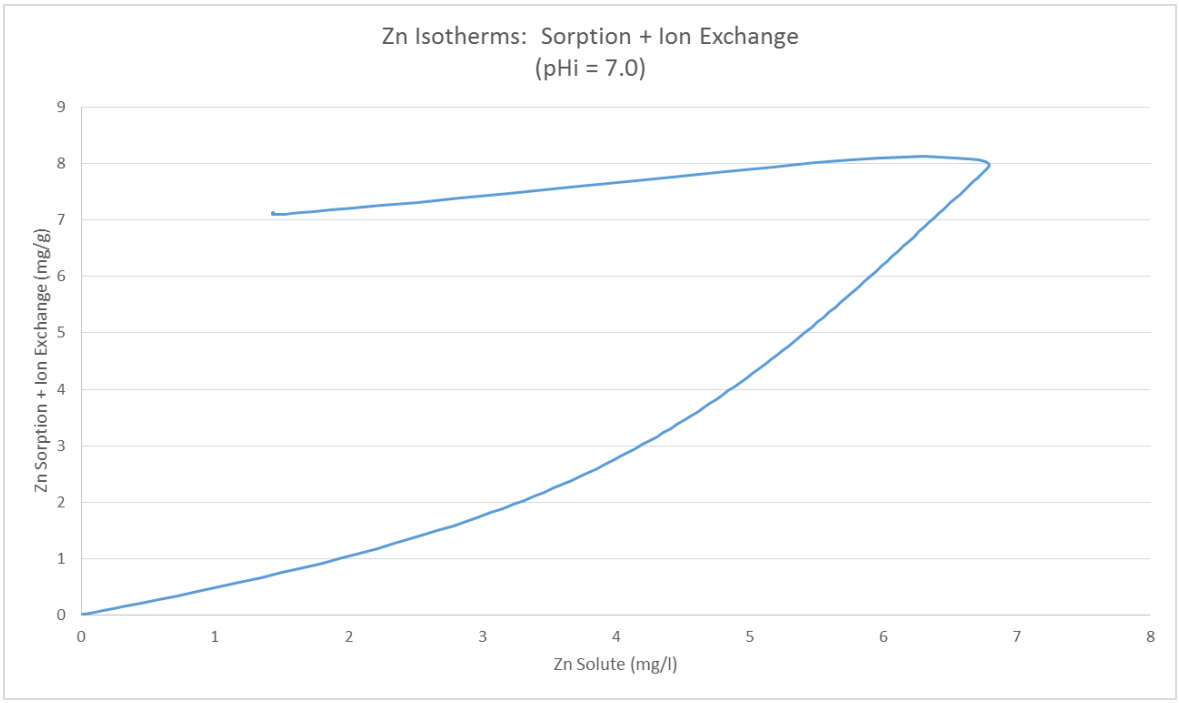
Zn Isotherms: Sorption + Ion Exchange
(pHi = 7.0)
Zn Sorption + Ion Exchange (mg/g)
Zn Solute (mg/l)
0
1
2
3
4
5
6
7
8
9

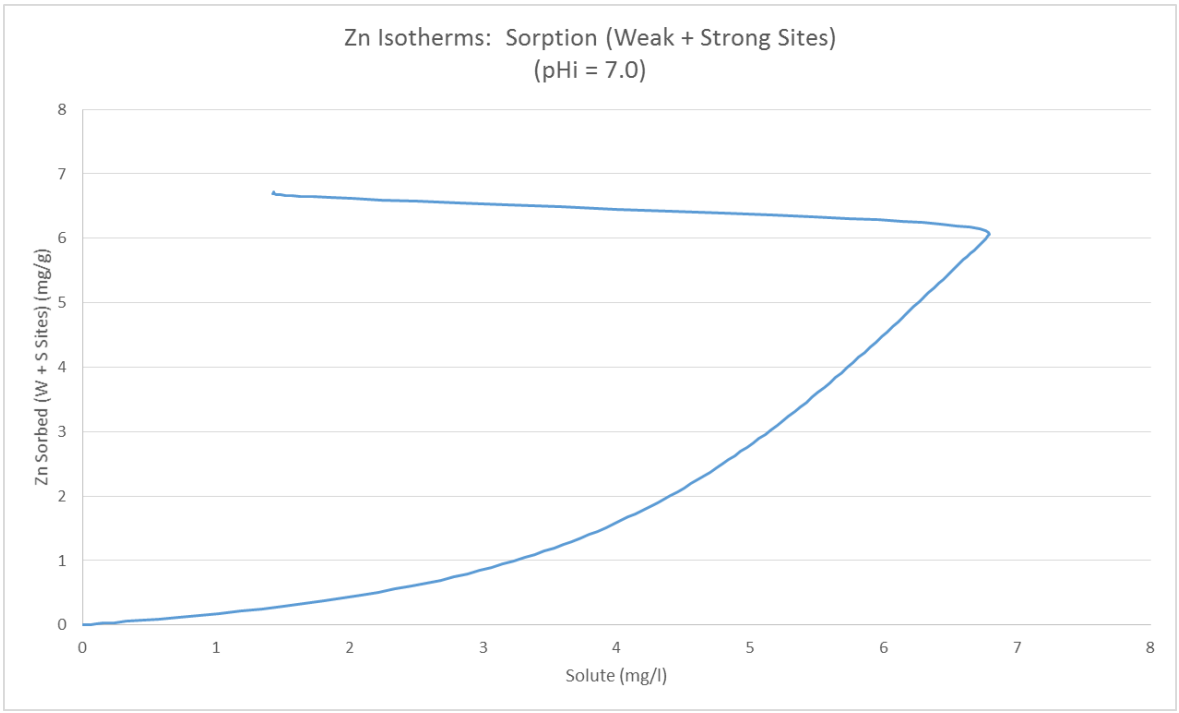
Zn Isotherms: Sorption (Weak + Strong Sites)
(pHi = 7.0)
Zn Sorbed (W + S Sites) (mg/g)
Solute (mg/l)
0
1
2
3
4
5
6
7
8

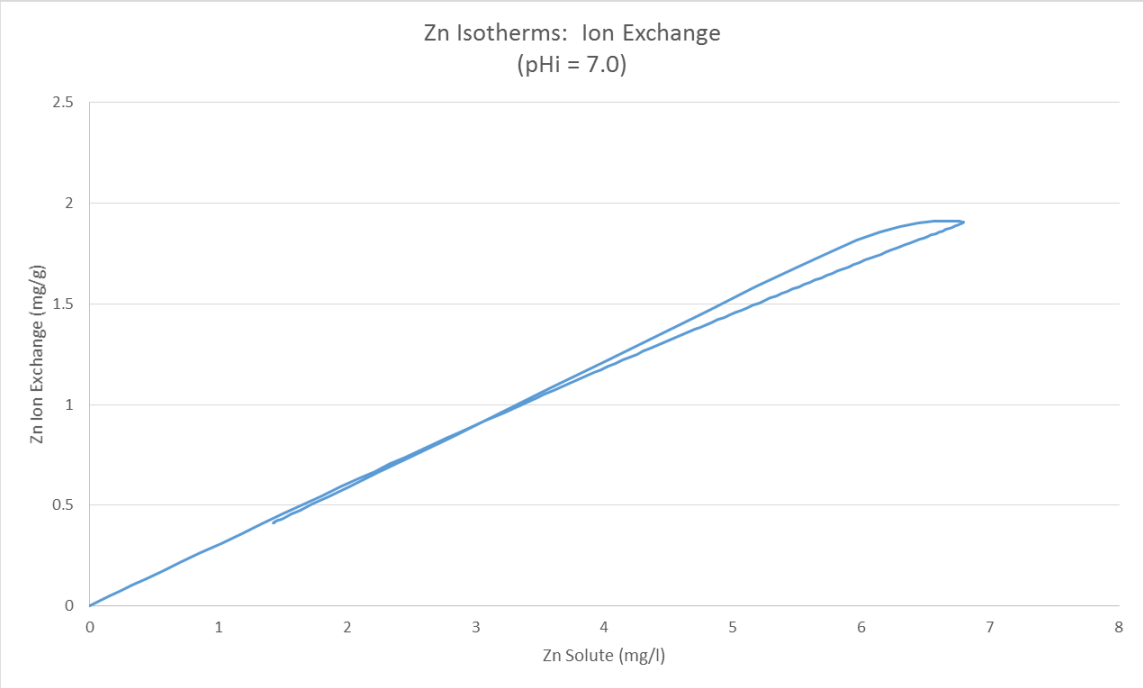
Zn Isotherms: Ion Exchange
(pHi = 7.0)
Zn Ion Exchange (mg/g)
2.5
2
1.5
1
0.5
0
0
1
2
3
4
5
6
7
8
Zn Solute (mg/l)

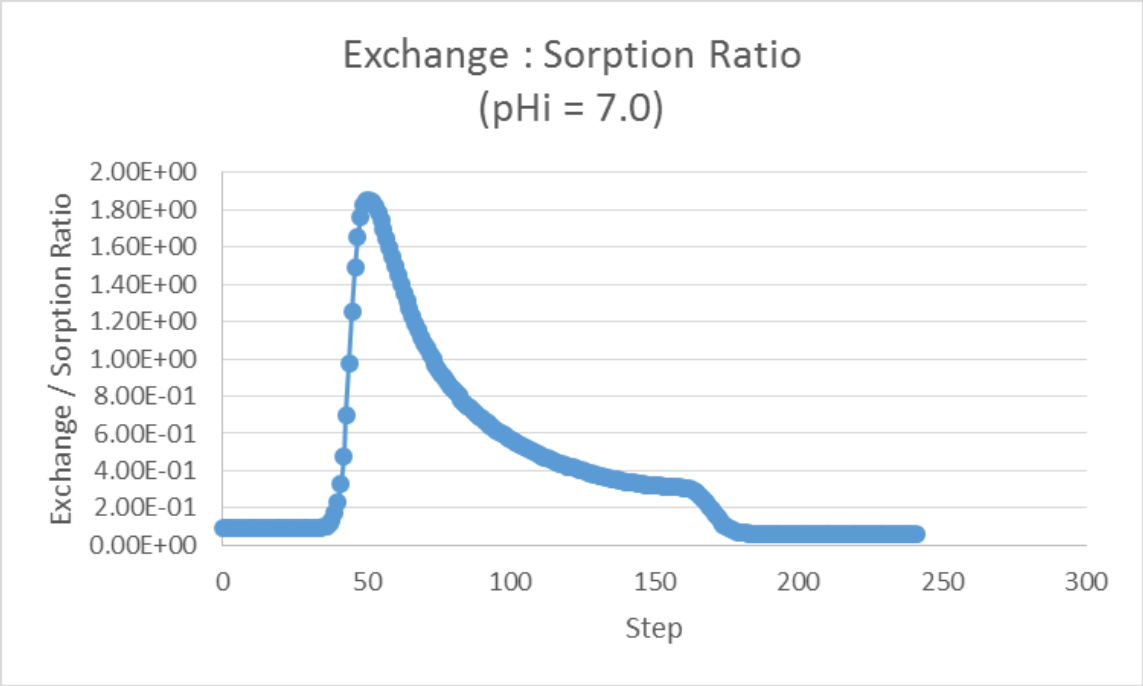
Exchange : Sorption Ratio
(pHi = 7.0)
Exchange / Sorption Ratio
2.00E+00
1.80E+00
1.60E+00
1.40E+00
1.20E+00
1.00E+00
8.00E-01
6.00E-01
4.00E-01
2.00E-01
0.00E+00
0
50
100
150
200
250
300
Step

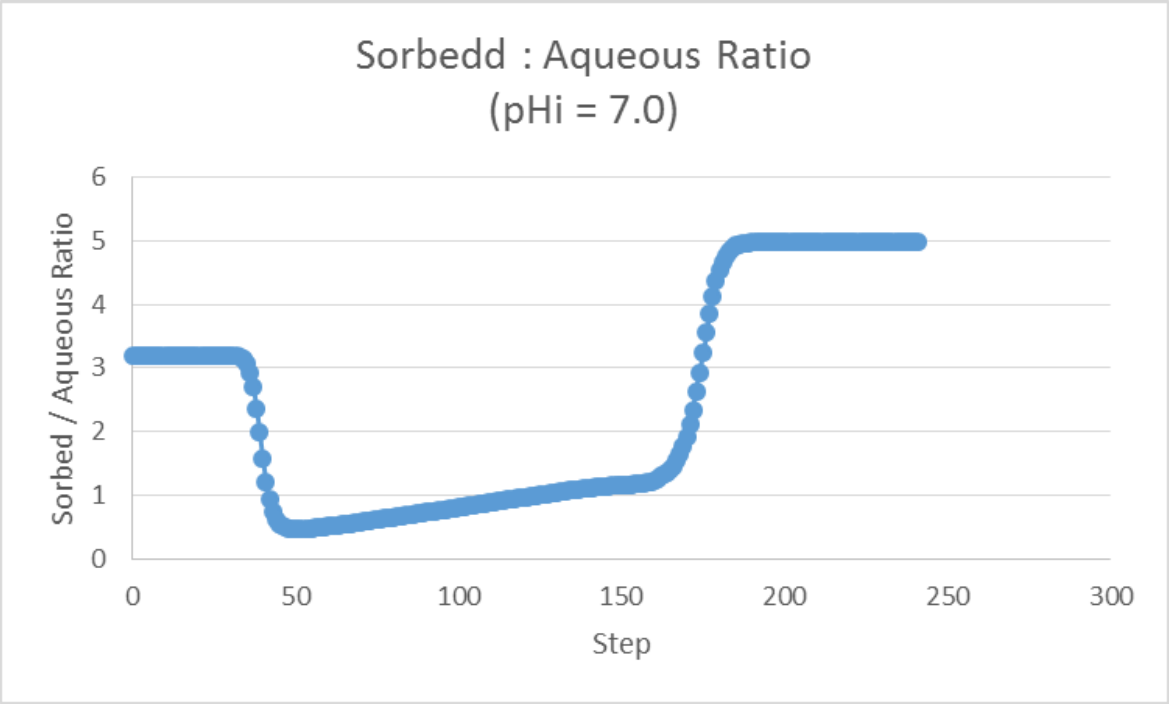
Sorbedd : Aqueous Ratio
(pHi = 7.0)
Sorbed / Aqueous Ratio
0
1
2
3
4
5
6
0
50
100
150
200
250
300
Step

pH 7.5

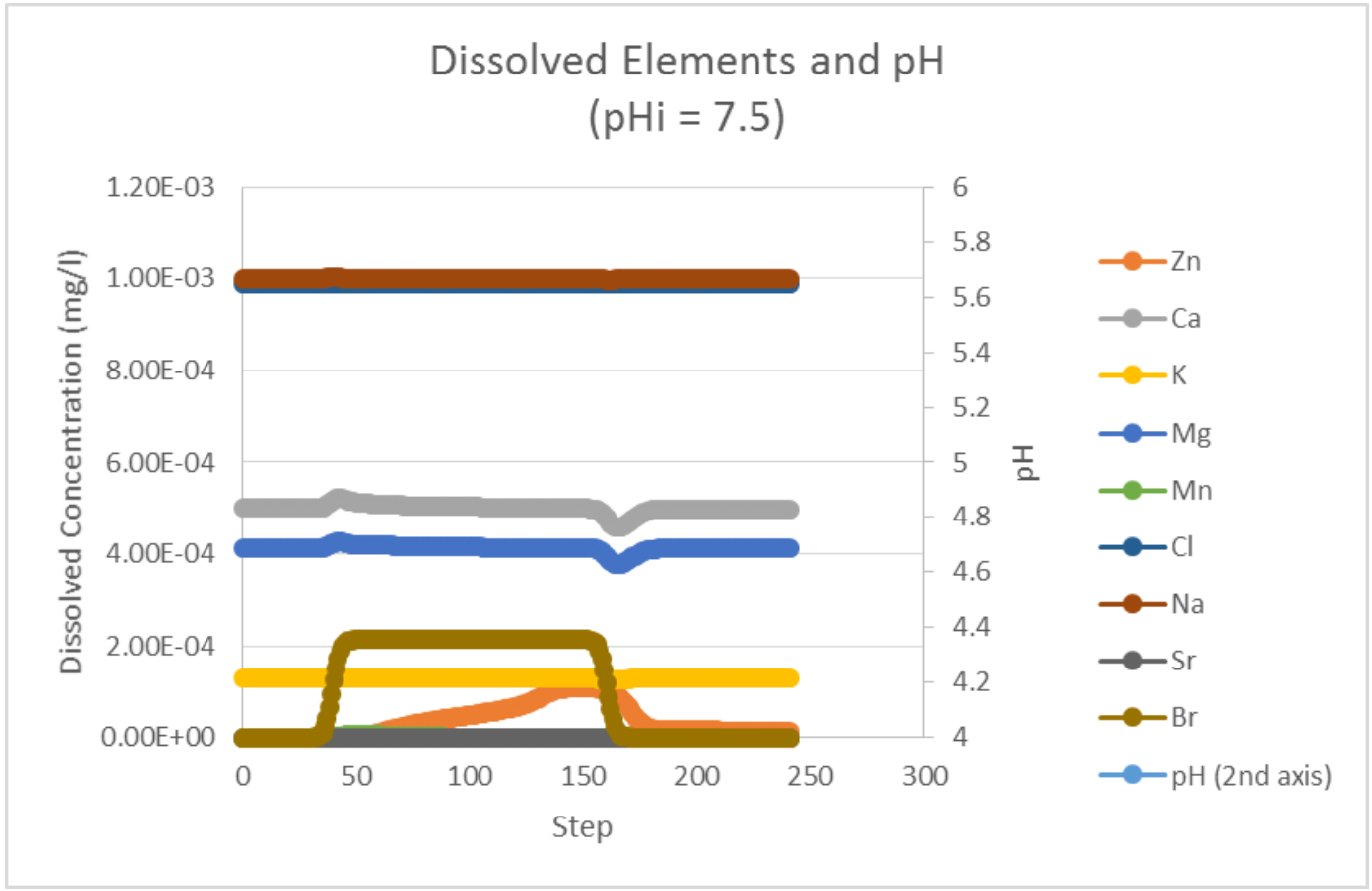
Dissolved Elements and pH
(pHi = 7.5)
Dissolved Concentration (mg/l)
1.20E-03
1.00E-03
8.00E-04
6.00E-04
4.00E-04
2.00E-04
0.00E+00
0
50
100
150
200
250
300
Step
6
5.8
5.6
5.4
5.2
5
4.8
4.6
4.4
4.2
4
pH
Zn
Ca
K
Mg
Mn
Cl
Na
Sr
Br
pH (2nd axis)

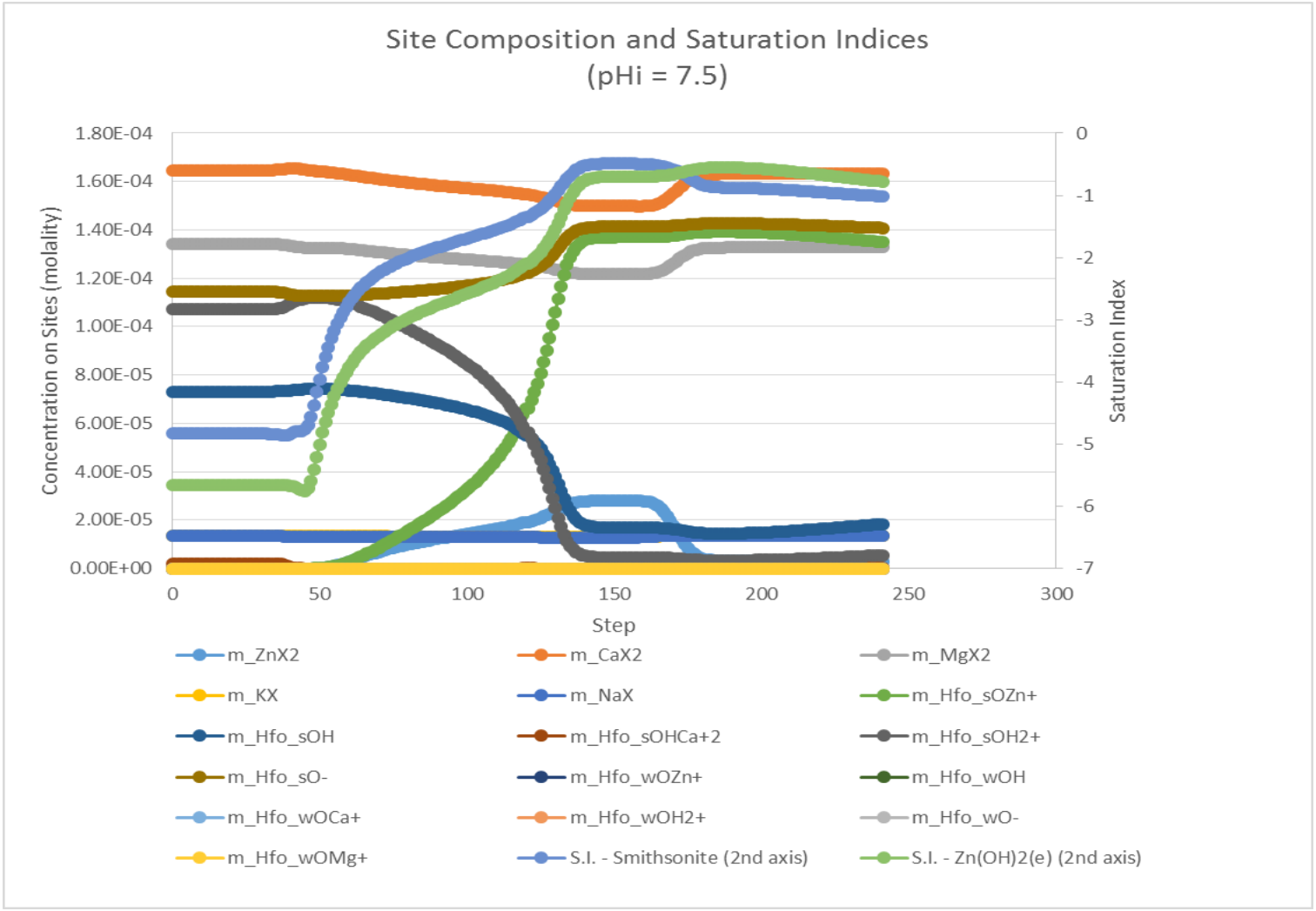
Site Composition and Saturation Indices
(pHi = 7.5)
Concentration on Sites (molality)
1.80E-04
1.60E-04
1.40E-04
1.20E-04
1.00E-04
8.00E-05
6.00E-05
4.00E-05
2.00E-05
0.00E+00
0
50
100
150
200
250
300
Step
Saturation Index
0
-1
-2
-3
-4
-5
-6
-7
m_ZnX2
m_CaX2
m_MgX2
m_KX
m_NaX
m_Hfo_sOZn+
m_Hfo_sOH
m_Hfo_sOHCa+2
m_Hfo_sOH2+
m_Hfo_sO-
m_Hfo_wOZn+
m_Hfo_wOH
m_Hfo_wOCa+
m_Hfo_wOH2+
m_Hfo_wO-
m_Hfo_wOMg+
S.I. - Smithsonite (2nd axis)
S.I. - Zn(OH)2(e) (2nd axis)

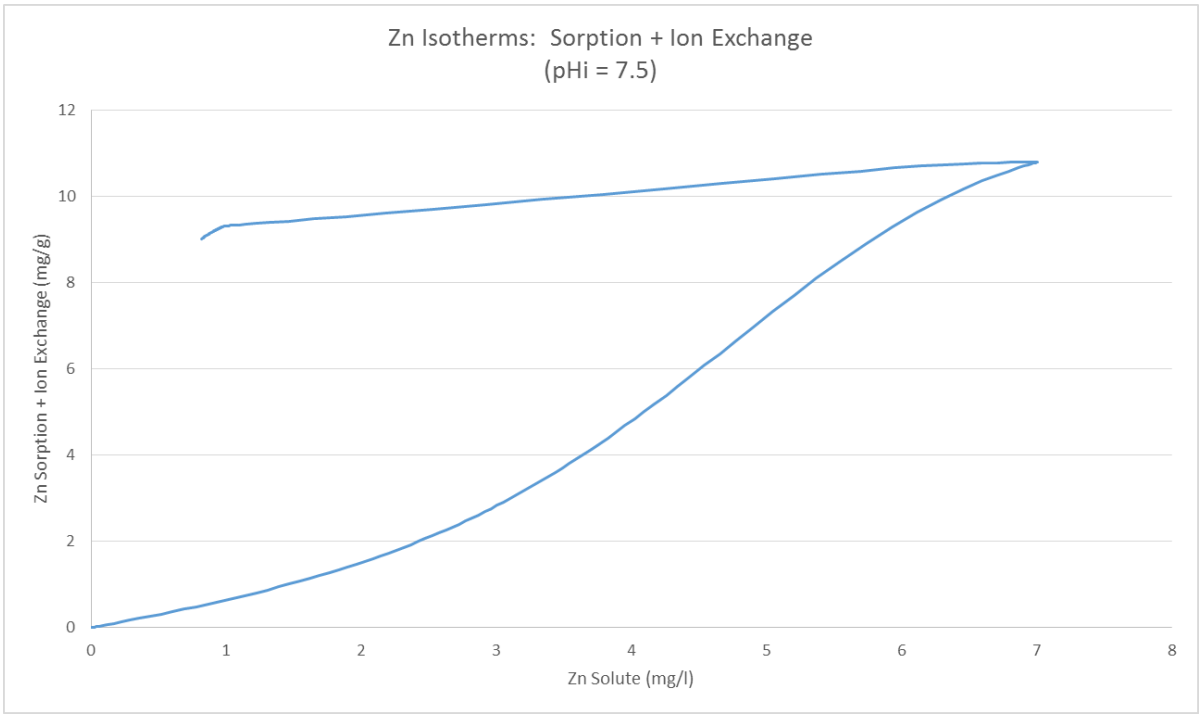
Zn Isotherms: Sorption + Ion Exchange
(pHi = 7.5)
Zn Sorption + Ion Exchange (mg/g)
Zn Solute (mg/l)
0
2
4
6
8
10
12
0
1
2
3
4
5
6
7
8

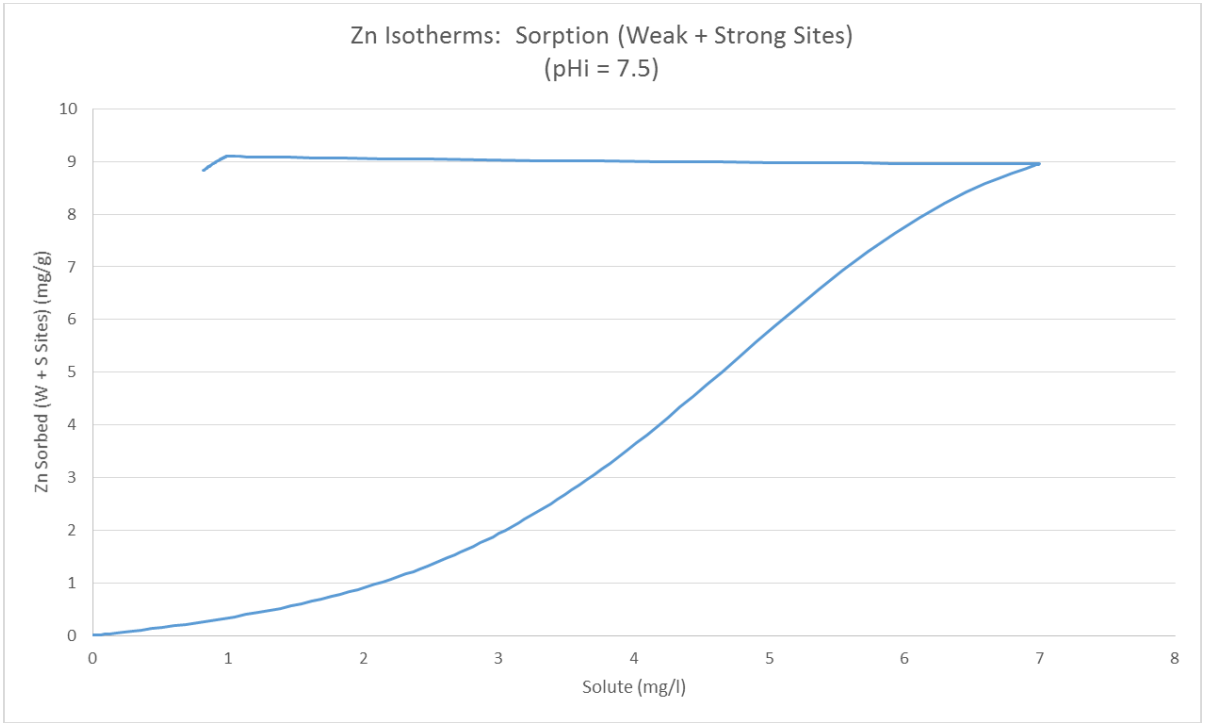
Zn Isotherms: Sorption (Weak + Strong Sites)
(pHi = 7.5)
Zn Sorbed (W + S Sites) (mg/g)
Solute (mg/l)
0
1
2
3
4
5
6
7
8
9
10
0
1
2
3
4
5
6
7
8

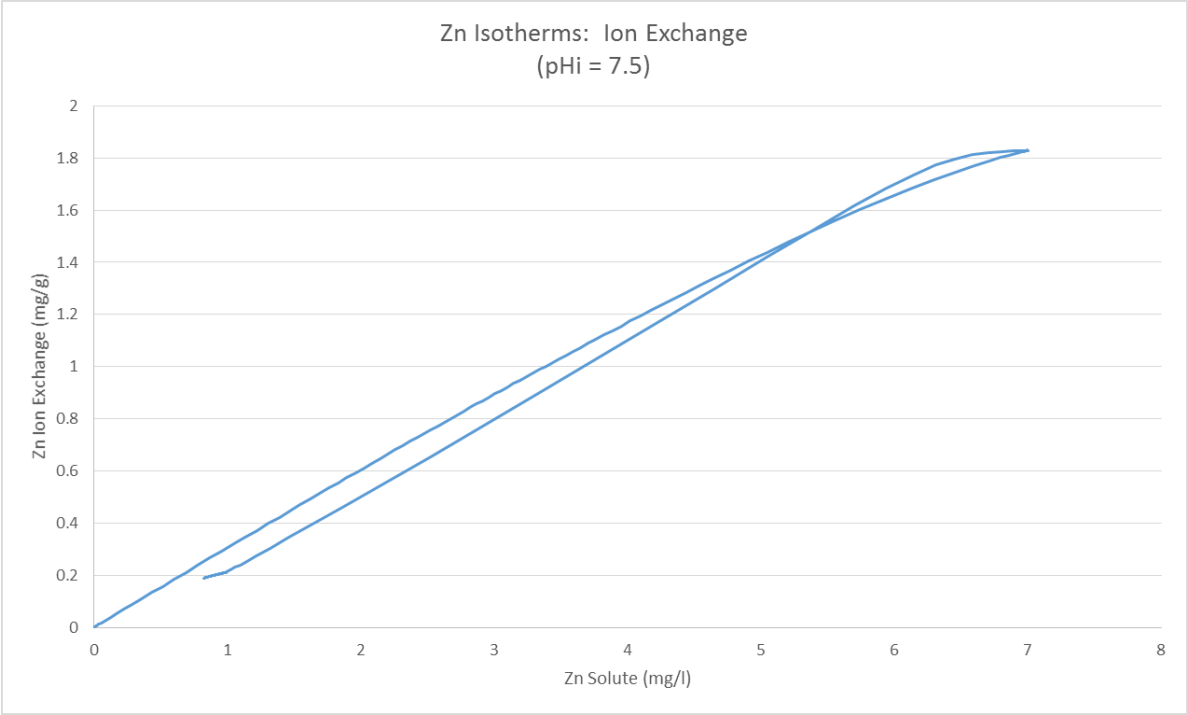
Zn Isotherms: Ion Exchange
(pHi = 7.5)
Zn Ion Exchange (mg/g)
2
1.8
1.6
1.4
1.2
1
0.8
0.6
0.4
0.2
0
0
1
2
3
4
5
6
7
8
Zn Solute (mg/l)

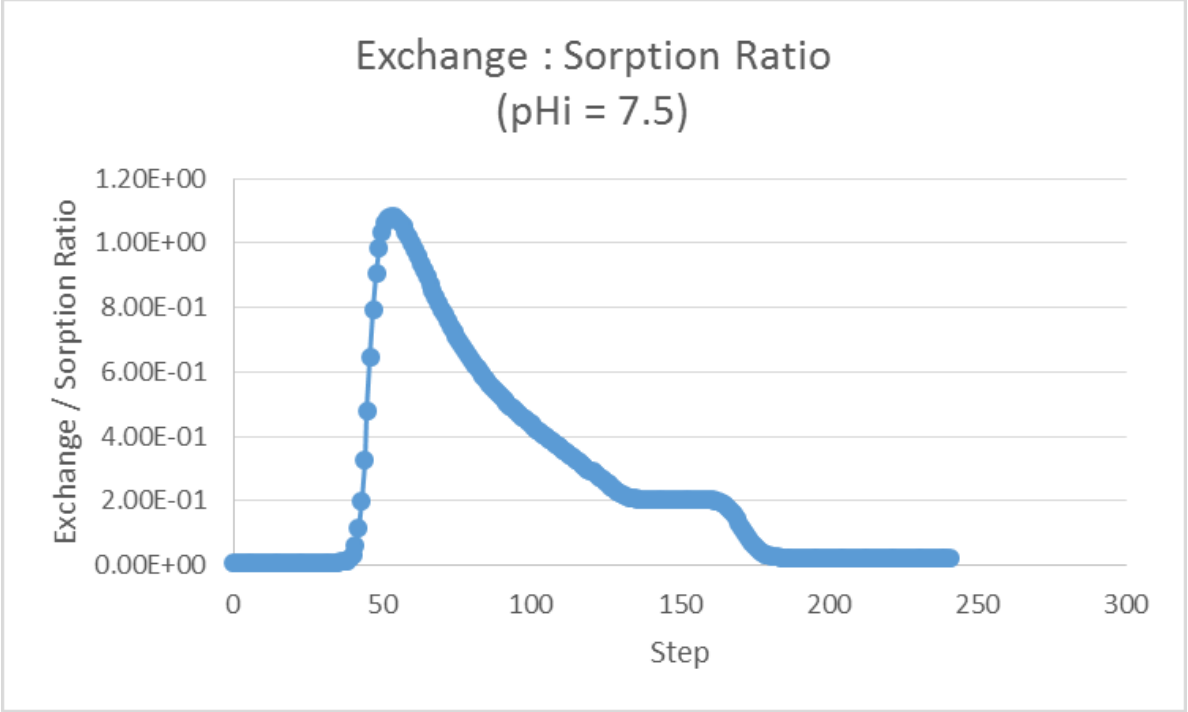
Exchange : Sorption Ratio
(pHi = 7.5)
Exchange / Sorption Ratio
1.20E+00
1.00E+00
8.00E-01
6.00E-01
4.00E-01
2.00E-01
0.00E+00
0
50
100
150
200
250
300
Step

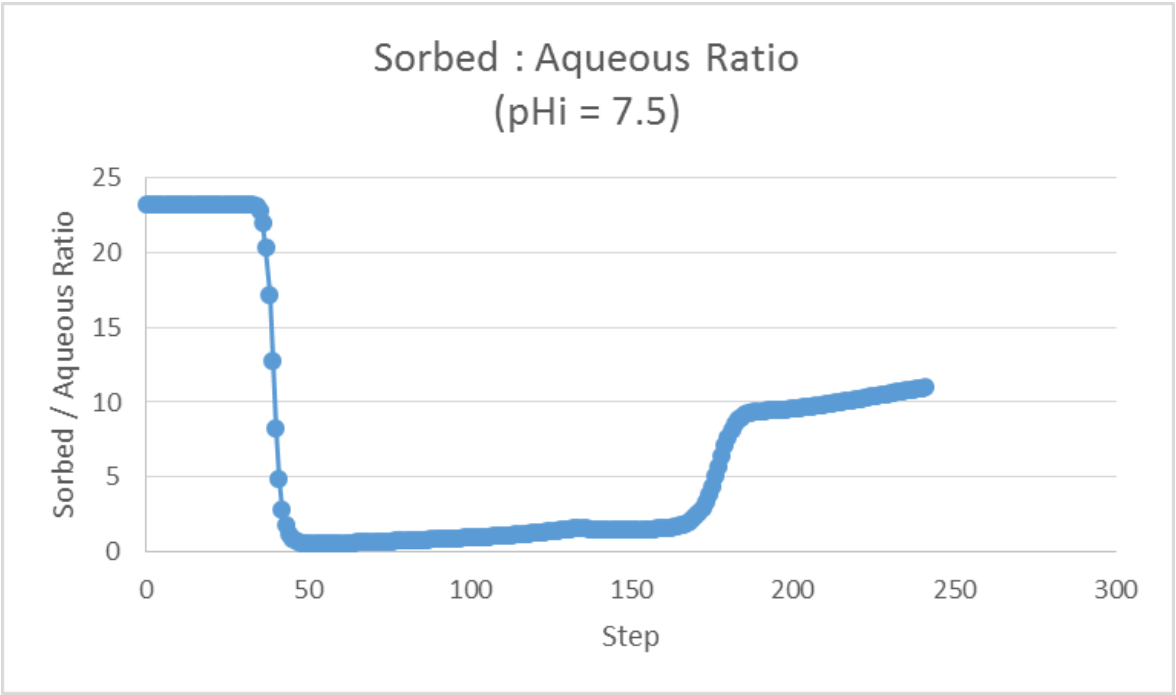
Sorbed : Aqueous Ratio
(pHi = 7.5)
Sorbed / Aqueous Ratio
25
20
15
10
5
0
0
50
100
150
200
250
300
Step

pH 8.0

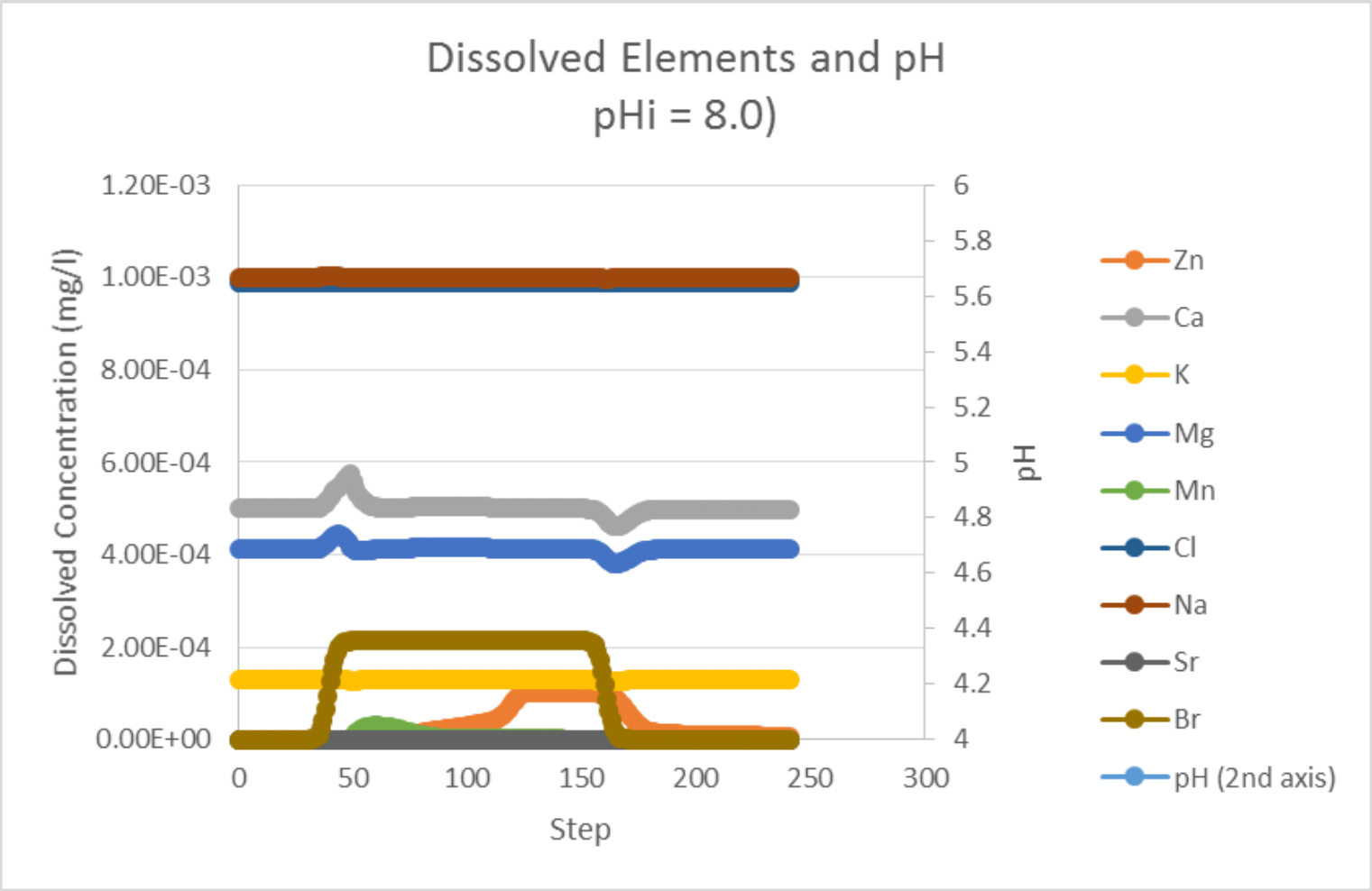
Dissolved Elements and pH
pHi = 8.0)
Dissolved Concentration (mg/l)
1.20E-03
1.00E-03
8.00E-04
6.00E-04
4.00E-04
2.00E-04
0.00E+00
0
50
100
150
200
250
300
Step
6
5.8
5.6
5.4
5.2
5
4.8
4.6
4.4
4.2
4
pH
Zn
Ca
K
Mg
Mn
Cl
Na
Sr
Br
pH (2nd axis)

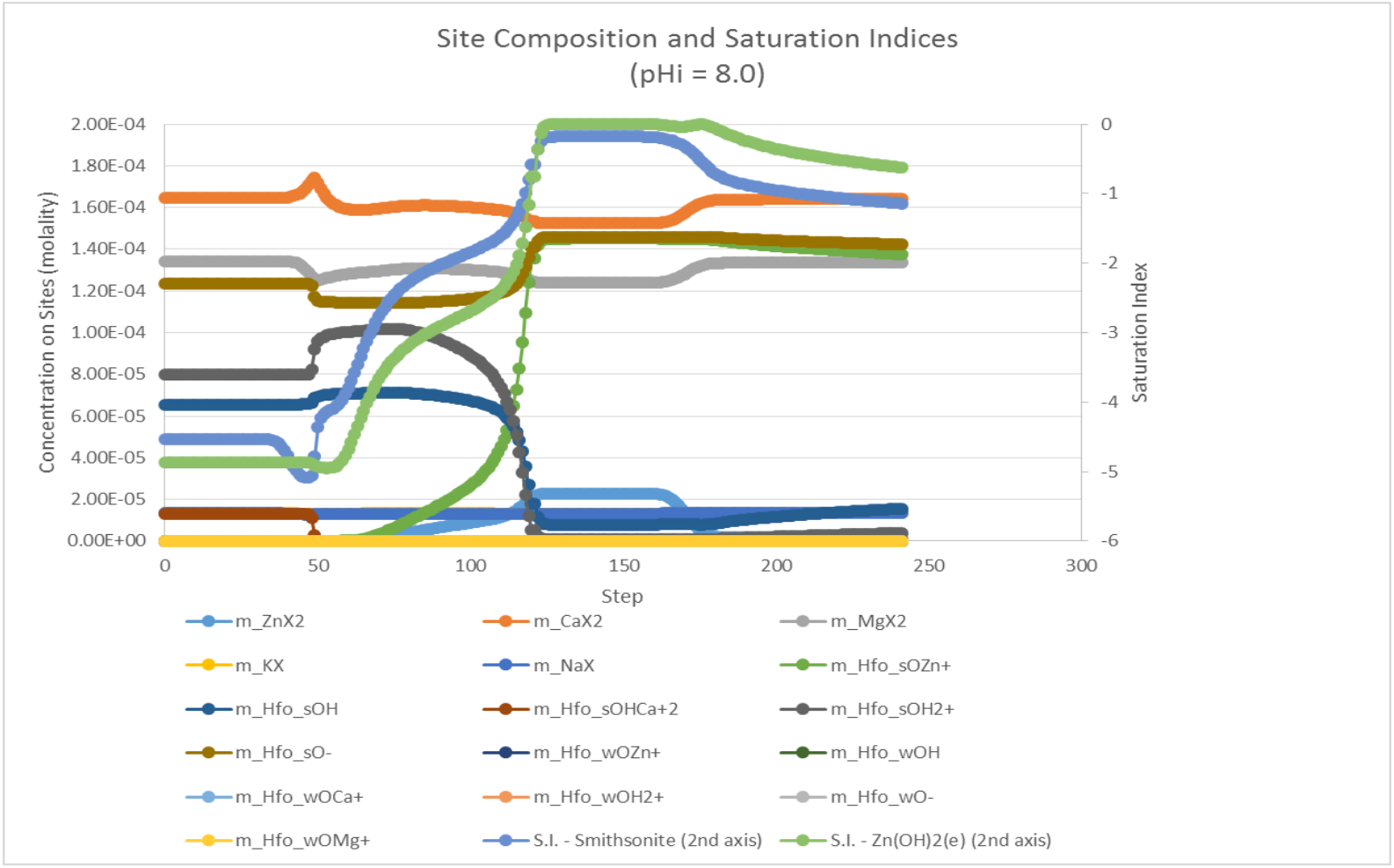
Site Composition and Saturation Indices
(pHi = 8.0)
Concentration on Sites (molality)
2.00E-04
1.80E-04
1.60E-04
1.40E-04
1.20E-04
1.00E-04
8.00E-05
6.00E-05
4.00E-05
2.00E-05
0.00E+00
0
50
100
150
200
250
300
Step
Saturation Index
0
-1
-2
-3
-4
-5
-6
m_ZnX2
m_CaX2
m_MgX2
m_KX
m_NaX
m_Hfo_sOZn+
m_Hfo_sOH
m_Hfo_sOHCa+2
m_Hfo_sOH2+
m_Hfo_sO-
m_Hfo_wOZn+
m_Hfo_wOH
m_Hfo_wOCa+
m_Hfo_wOH2+
m_Hfo_wO-
m_Hfo_wOMg+
S.I. - Smithsonite (2nd axis)
S.I. - Zn(OH)2(e) (2nd axis)

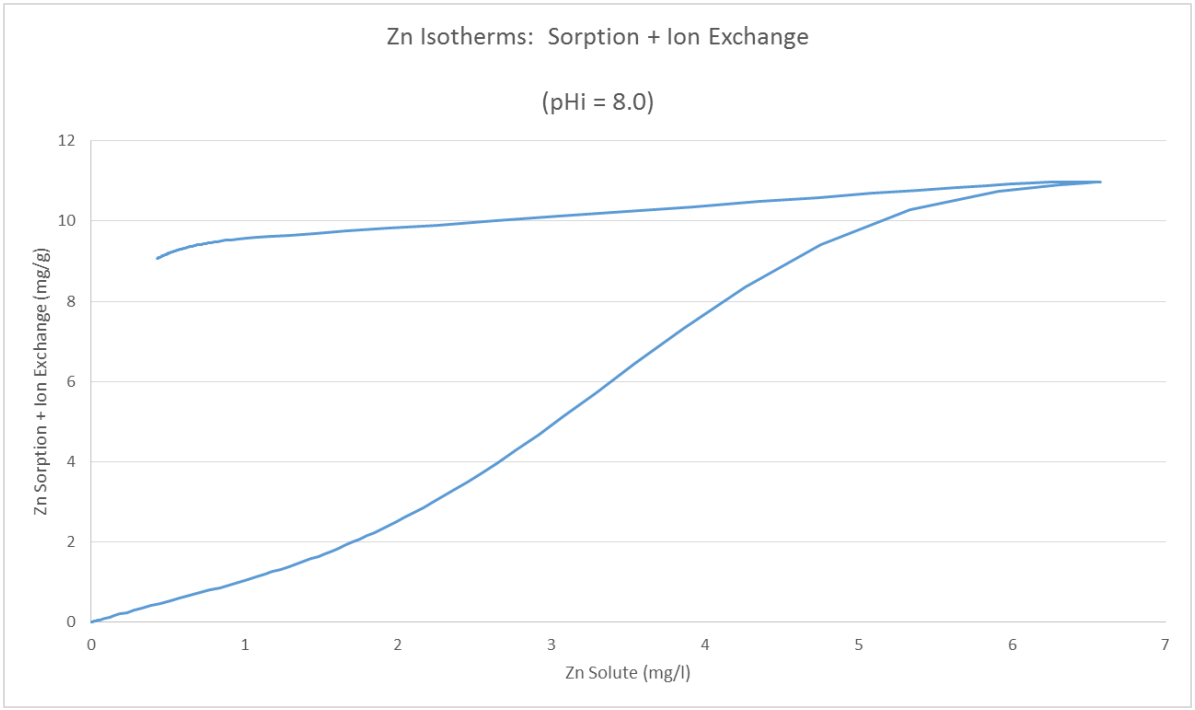
Zn Isotherms: Sorption + Ion Exchange
(pHi = 8.0)
Zn Sorption + Ion Exchange (mg/g)
Zn Solute (mg/l)
0
2
4
6
8
10
12
0
1
2
3
4
5
6
7

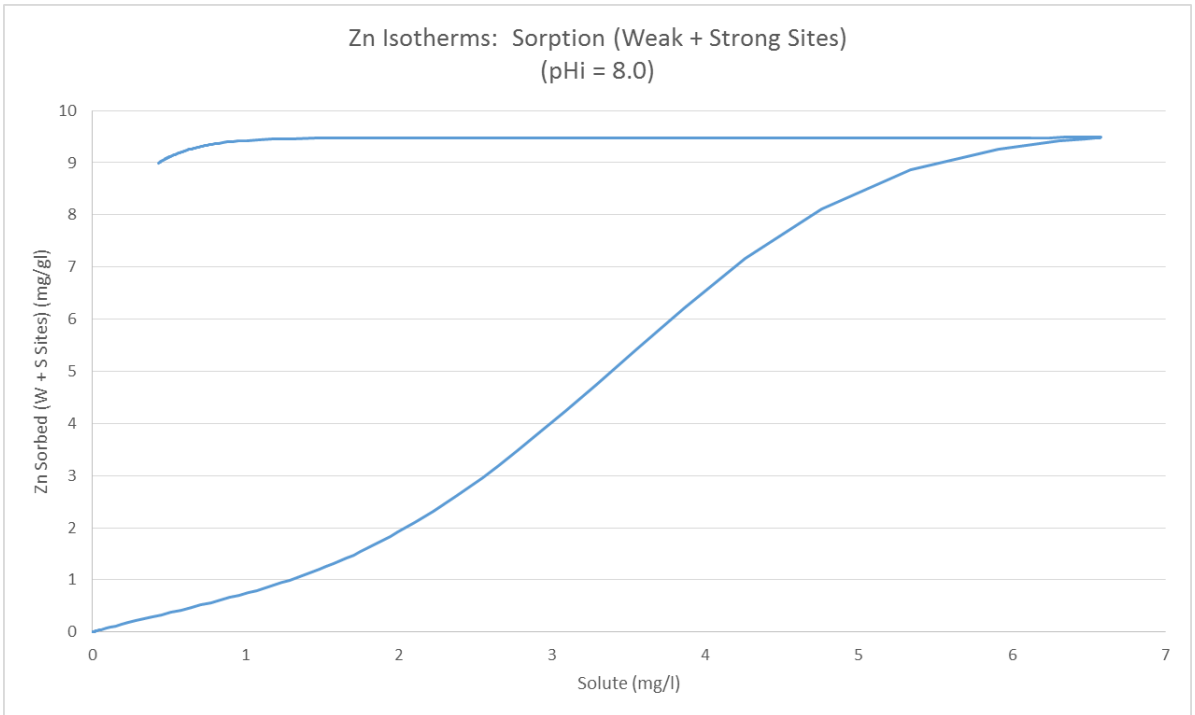
Zn Isotherms: Sorption (Weak + Strong Sites)
(pHi = 8.0)
Zn Sorbed (W + S Sites) (mg/gl)
Solute (mg/l)
0
1
2
3
4
5
6
7
8
9
10
0
1
2
3
4
5
6
7

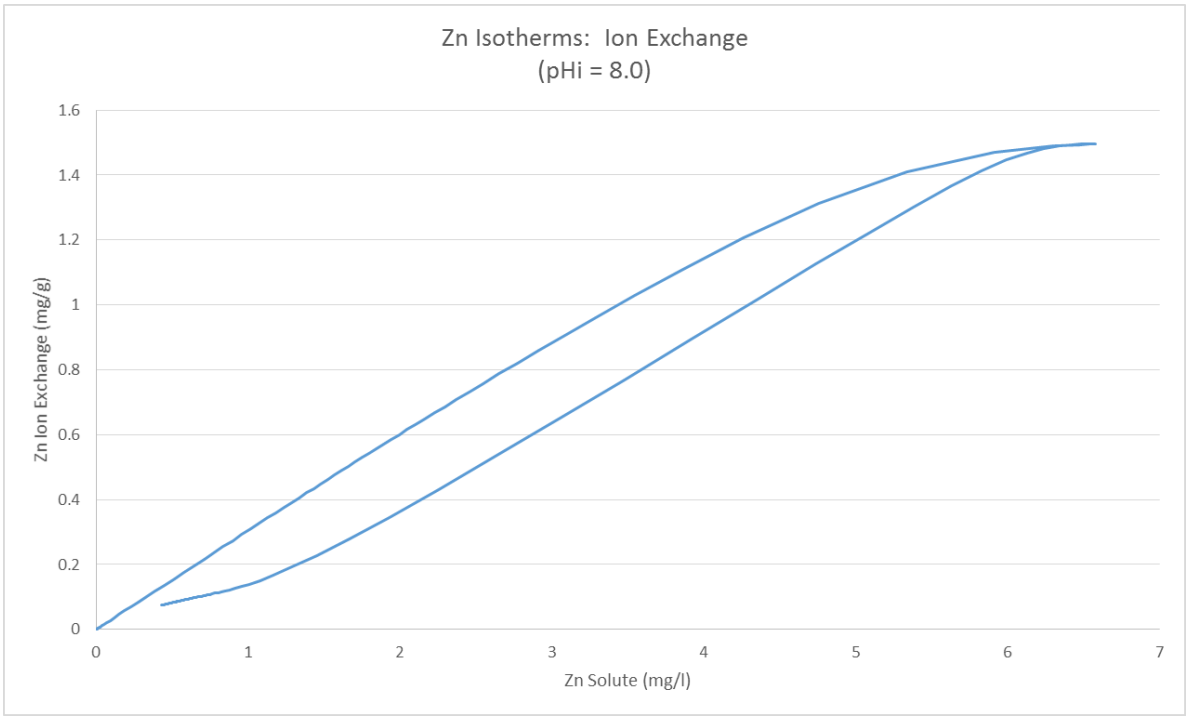
Zn Isotherms: Ion Exchange
(pHi = 8.0)
Zn Ion Exchange (mg/g)
1.6
1.4
1.2
1
0.8
0.6
0.4
0.2
0
0
1
2
3
4
5
6
7
Zn Solute (mg/l)

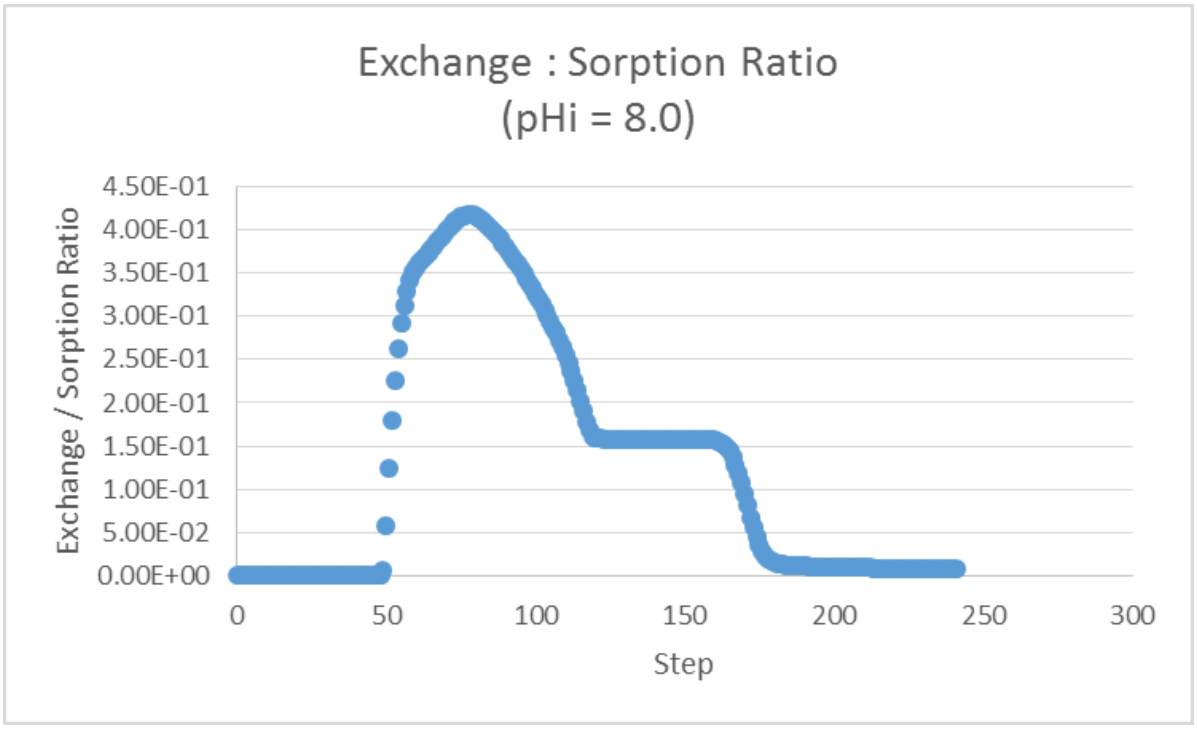
Exchange : Sorption Ratio
(pHi = 8.0)
Exchange / Sorption Ratio
4.50E-01
4.00E-01
3.50E-01
3.00E-01
2.50E-01
2.00E-01
1.50E-01
1.00E-01
5.00E-02
0.00E+00
0
50
100
150
200
250
300
Step

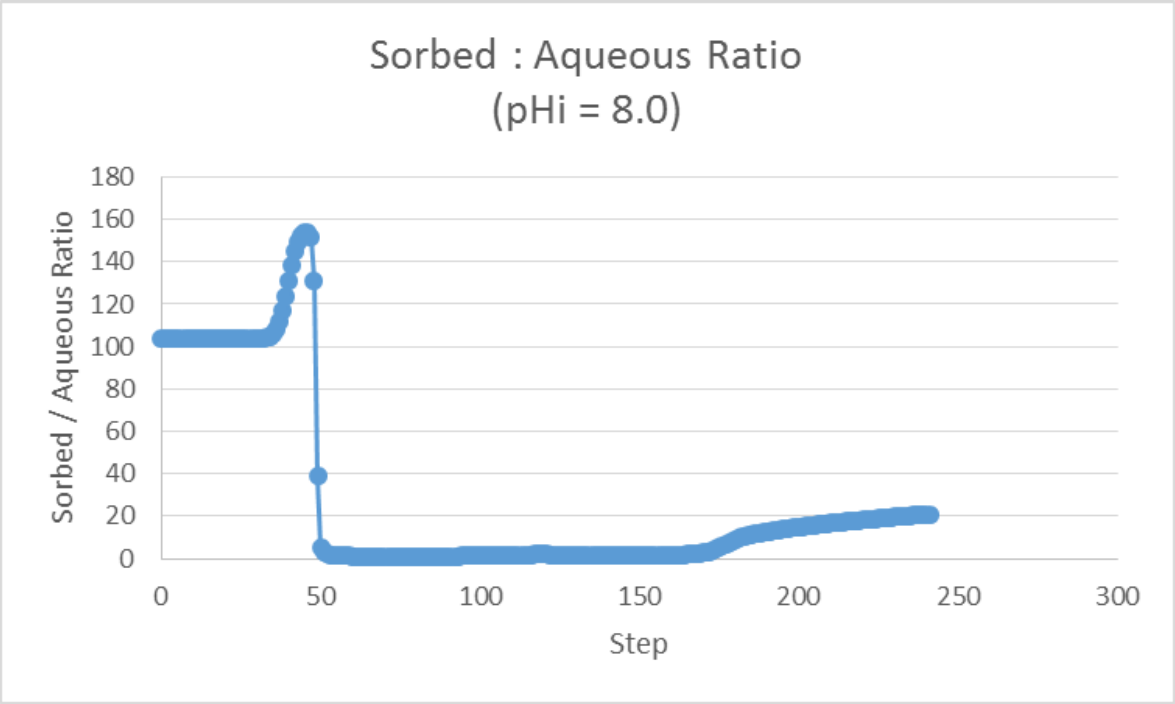
Sorbed : Aqueous Ratio
(pHi = 8.0)
Sorbed / Aqueous Ratio
180
160
140
120
100
80
60
40
20
0
0
50
100
150
200
250
300
Step

pH 8.5

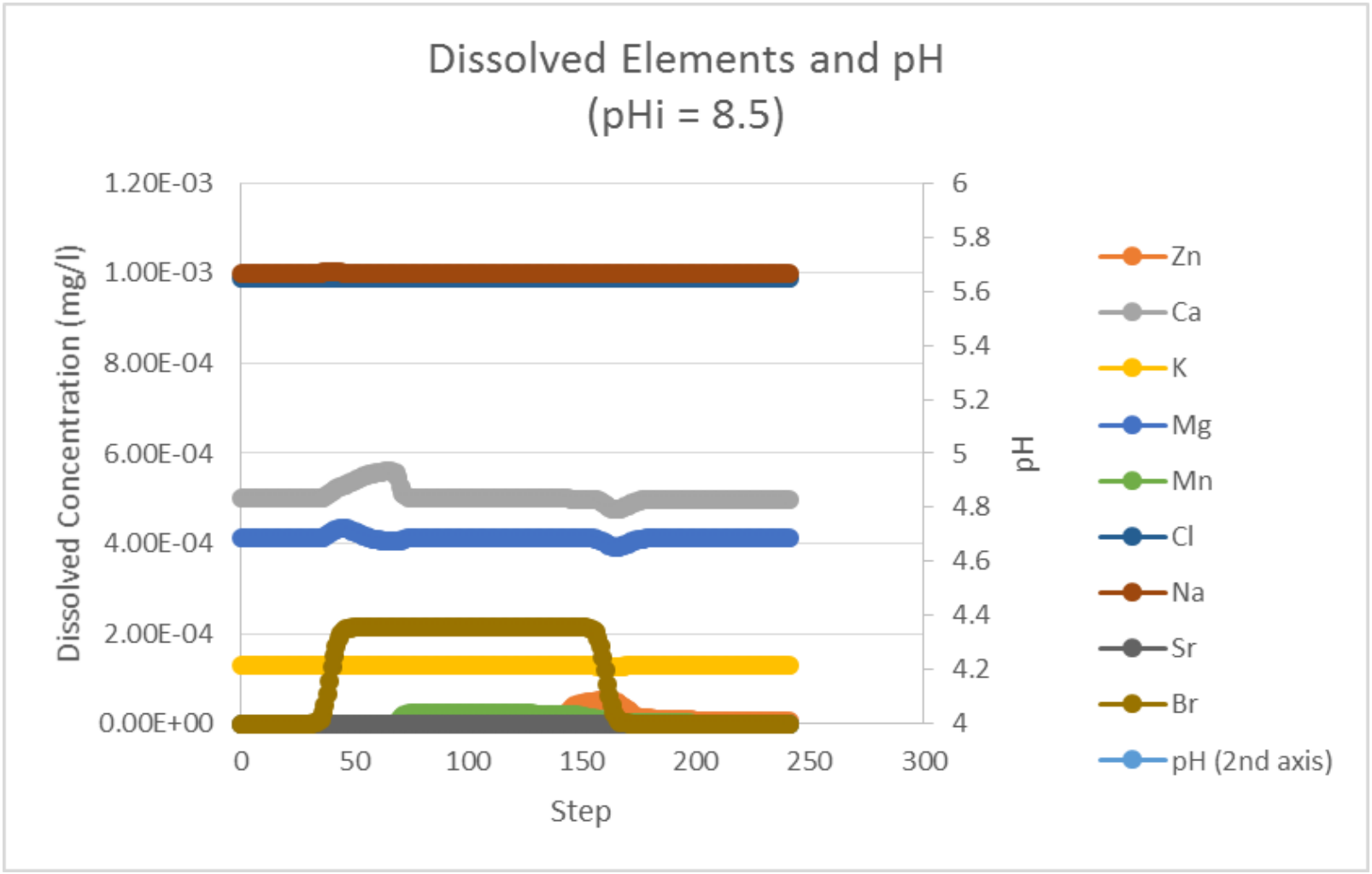
Dissolved Elements and pH
(pHi = 8.5)
Dissolved Concentration (mg/l)
1.20E-03
1.00E-03
8.00E-04
6.00E-04
4.00E-04
2.00E-04
0.00E+00
0
50
100
150
200
250
300
Step
6
5.8
5.6
5.4
5.2
5
4.8
4.6
4.4
4.2
4
pH
Zn
Ca
K
Mg
Mn
Cl
Na
Sr
Br
pH (2nd axis)

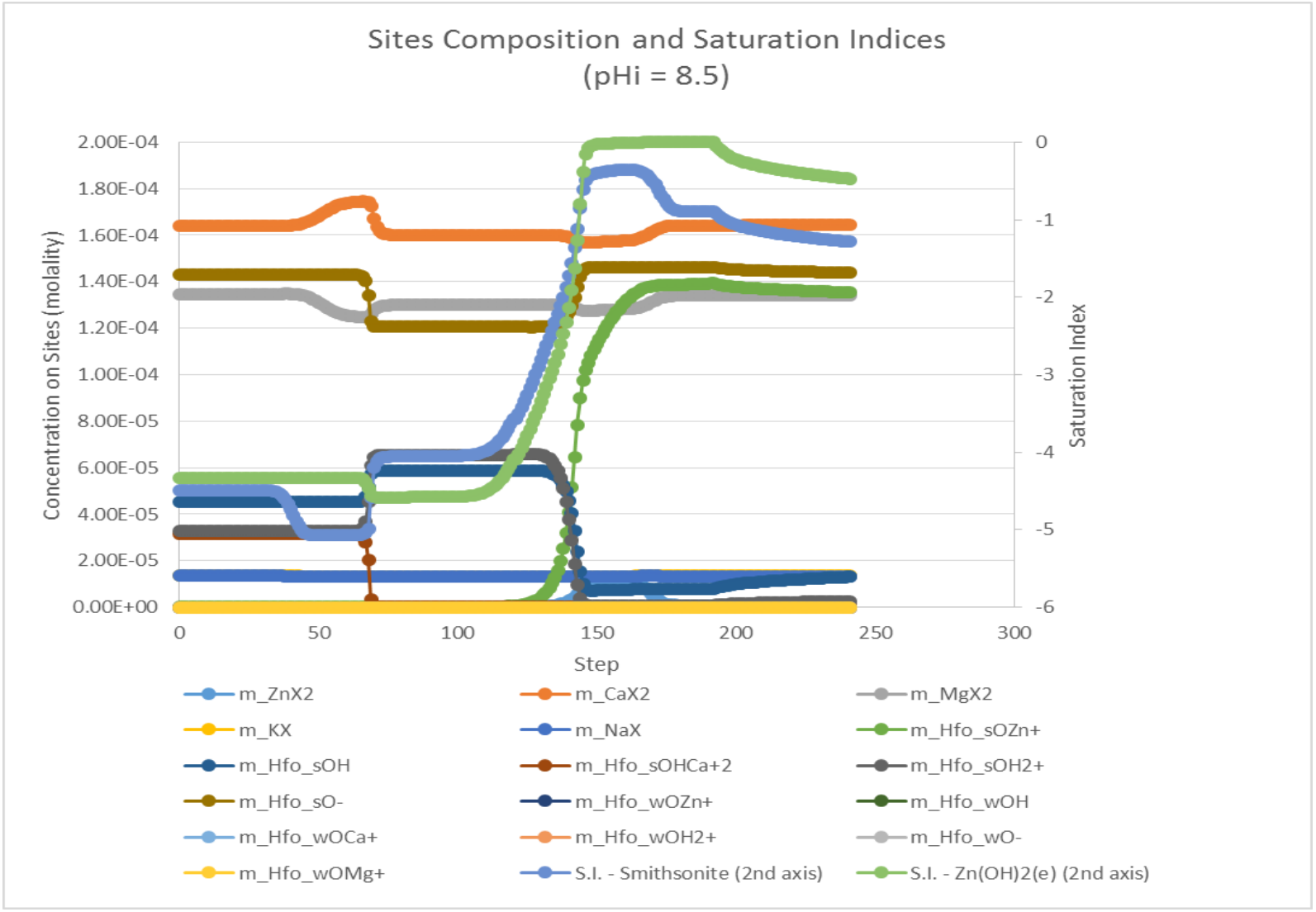
Sites Composition and Saturation Indices
(pHi = 8.5)
Concentration on Sites (molality)
2.00E-04
1.80E-04
1.60E-04
1.40E-04
1.20E-04
1.00E-04
8.00E-05
6.00E-05
4.00E-05
2.00E-05
0.00E+00
0
50
100
150
200
250
300
Step
Saturation Index
0
-1
-2
-3
-4
-5
-6
m_ZnX2
m_CaX2
m_MgX2
m_KX
m_NaX
m_Hfo_sOZn+
m_Hfo_sOH
m_Hfo_sOHCa+2
m_Hfo_sOH2+
m_Hfo_sO-
m_Hfo_wOZn+
m_Hfo_wOH
m_Hfo_wOCa+
m_Hfo_wOH2+
m_Hfo_wO-
m_Hfo_wOMg+
S.I. - Smithsonite (2nd axis)
S.I. - Zn(OH)2(e) (2nd axis)

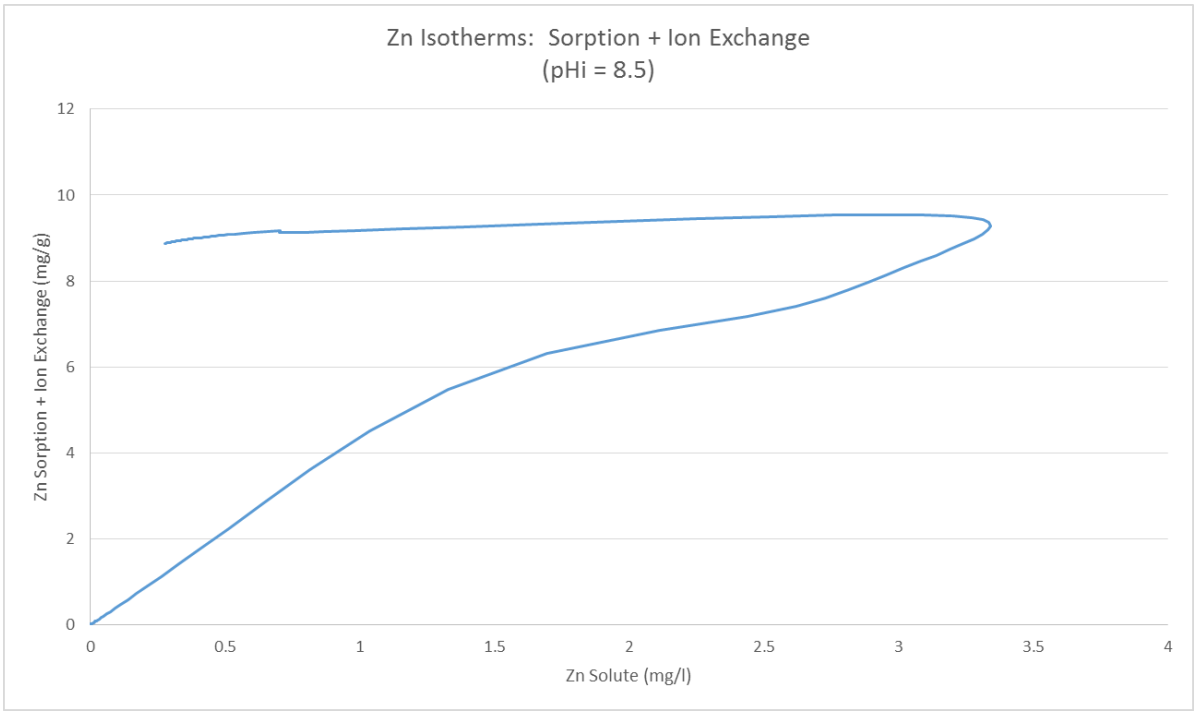
Zn Isotherms: Sorption + Ion Exchange
(pHi = 8.5)
Zn Sorption + Ion Exchange (mg/g)
Zn Solute (mg/l)
0
2
4
6
8
10
12
0
0.5
1
1.5
2
2.5
3
3.5
4

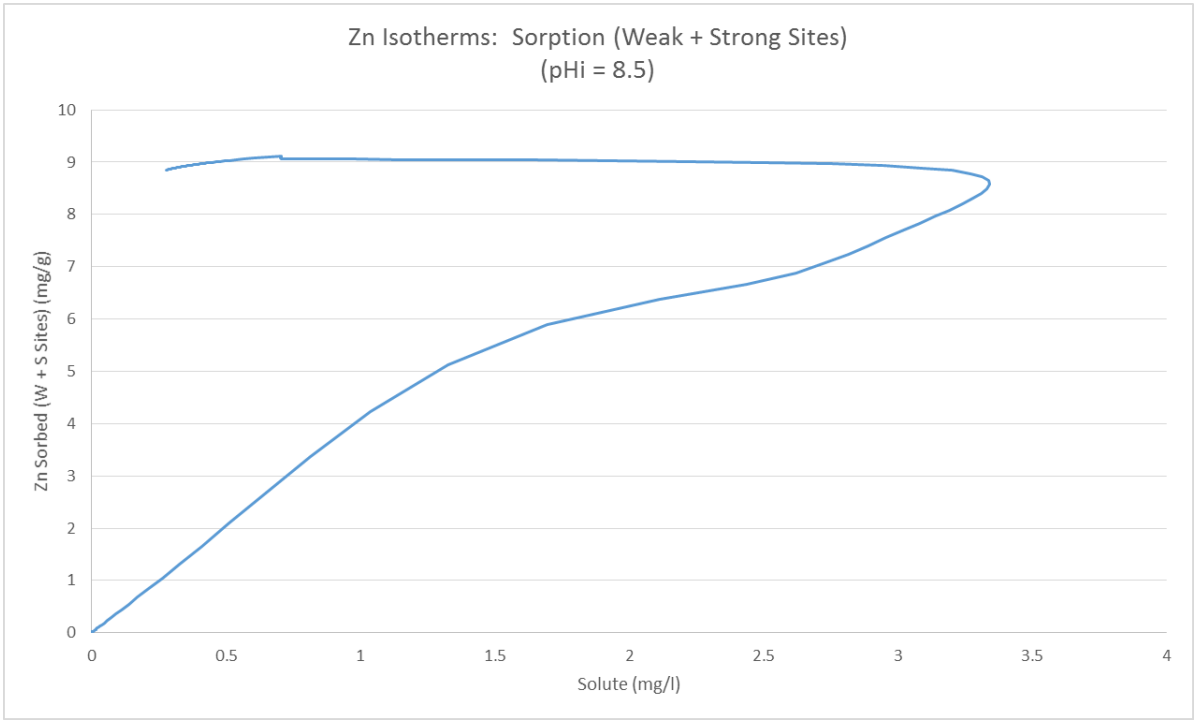
Zn Isotherms: Sorption (Weak + Strong Sites)
(pHi = 8.5)
Zn Sorbed (W + S Sites) (mg/g)
Solute (mg/l)
0
1
2
3
4
5
6
7
8
9
10
0
0.5
1
1.5
2
2.5
3
3.5
4

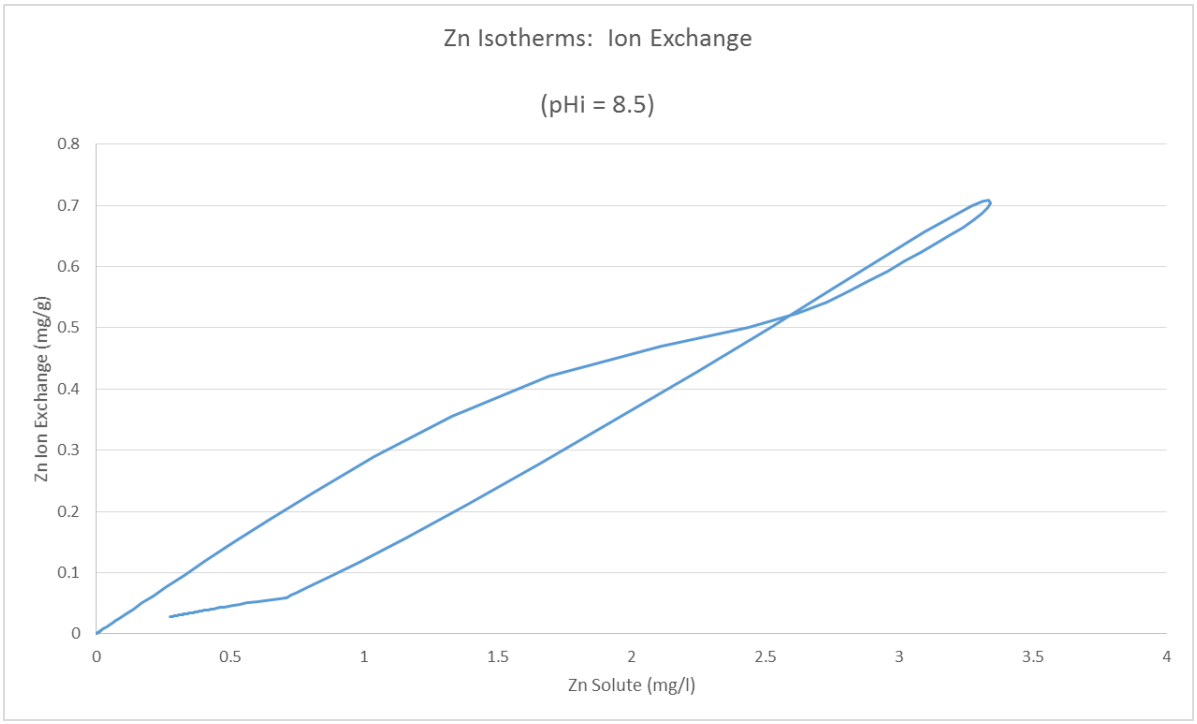
Zn Isotherms: Ion Exchange
(pHi = 8.5)
Zn Ion Exchange (mg/g)
0.8
0.7
0.6
0.5
0.4
0.3
0.2
0.1
0
0
0.5
1
1.5
2
2.5
3
3.5
4
Zn Solute (mg/l)

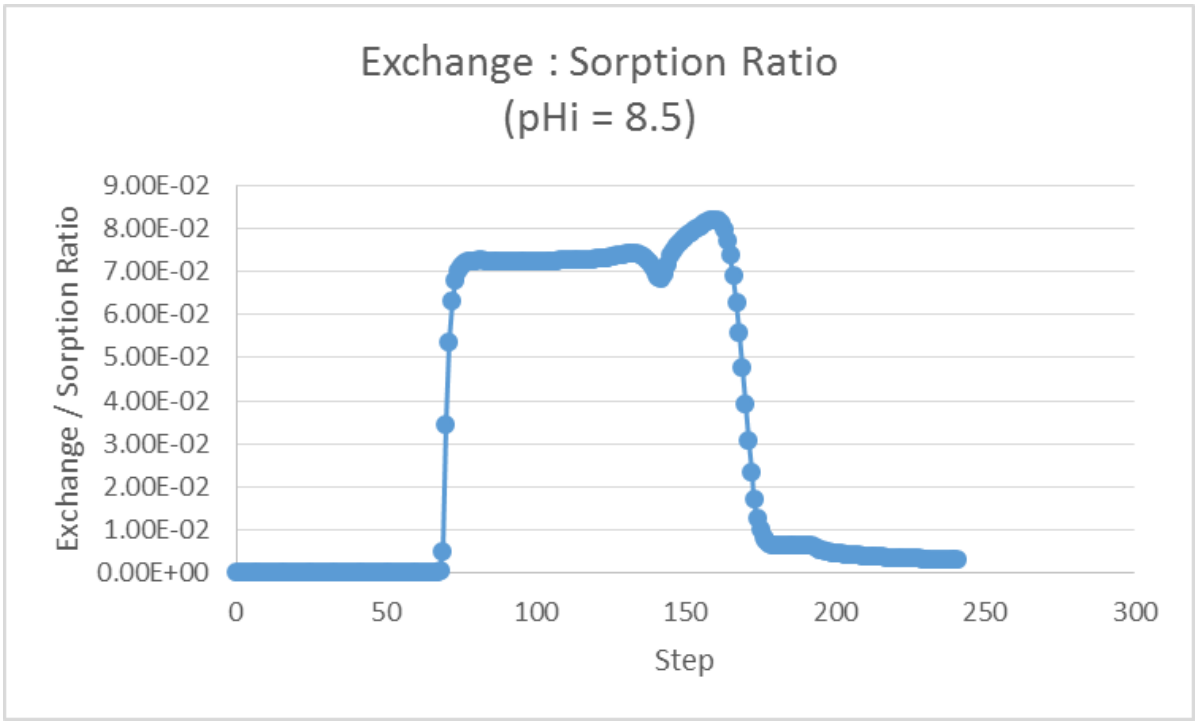
Exchange : Sorption Ratio
(pHi = 8.5)
Exchange / Sorption Ratio
9.00E-02
8.00E-02
7.00E-02
6.00E-02
5.00E-02
4.00E-02
3.00E-02
2.00E-02
1.00E-02
0.00E+00
0
50
100
150
200
250
300
Step

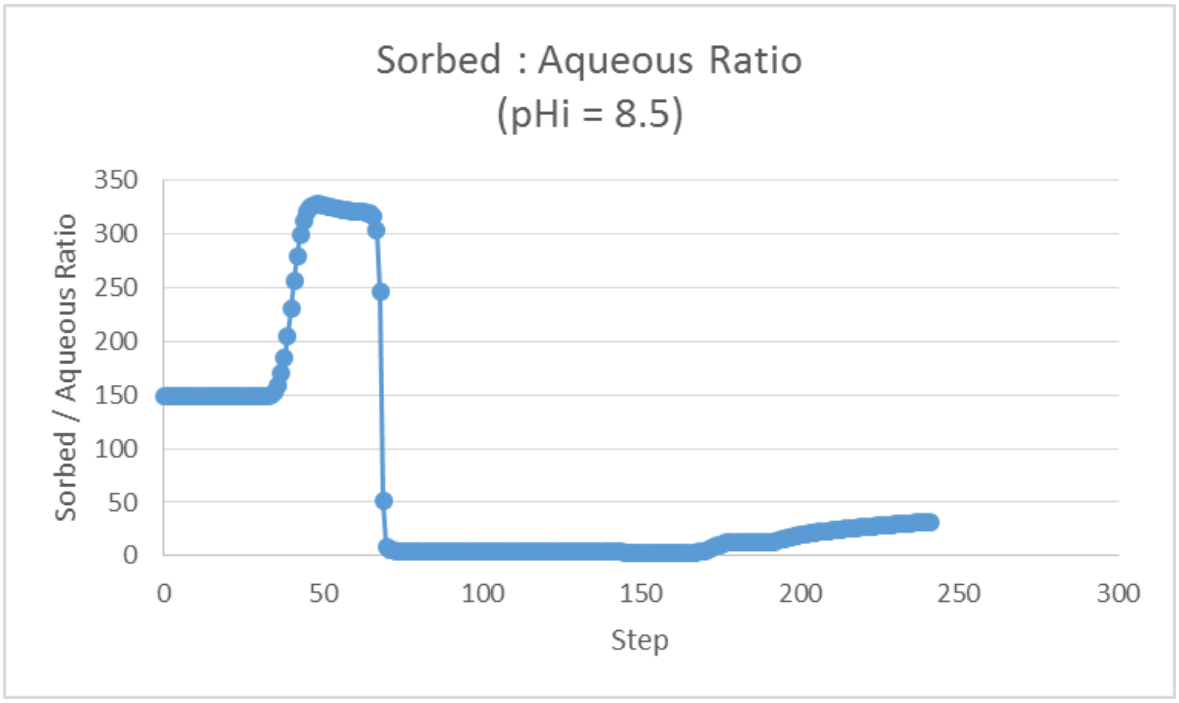
Sorbed : Aqueous Ratio
(pHi = 8.5)
Sorbed / Aqueous Ratio
350
300
250
200
150
100
50
0
0
50
100
150
200
250
300
Step

pH 9.0

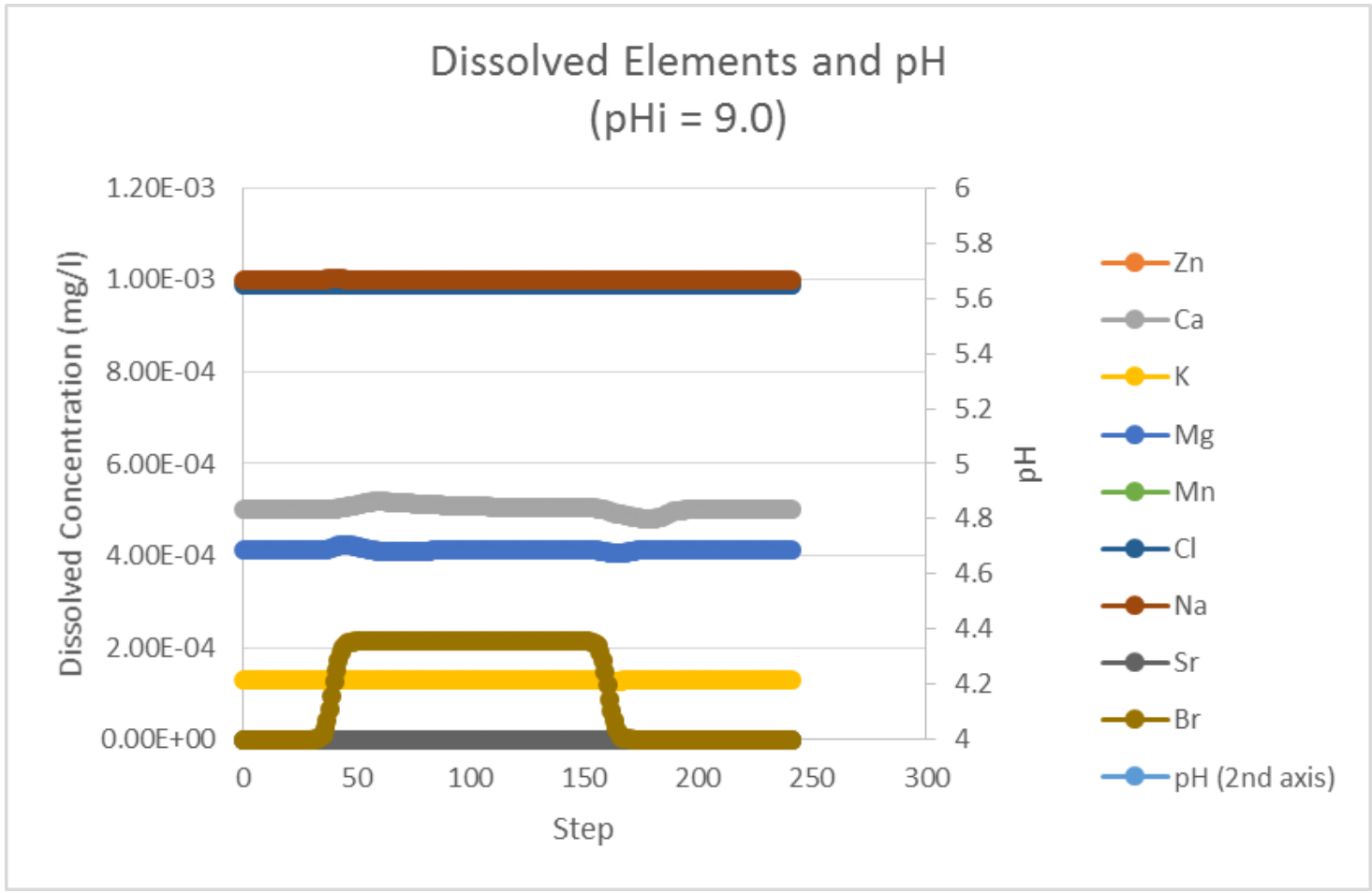
Dissolved Elements and pH
(pHi = 9.0)
Dissolved Concentration (mg/l)
1.20E-03
1.00E-03
8.00E-04
6.00E-04
4.00E-04
2.00E-04
0.00E+00
0
50
100
150
200
250
300
Step
6
5.8
5.6
5.4
5.2
5
4.8
4.6
4.4
4.2
4
pH
Zn
Ca
K
Mg
Mn
Cl
Na
Sr
Br
pH (2nd axis)

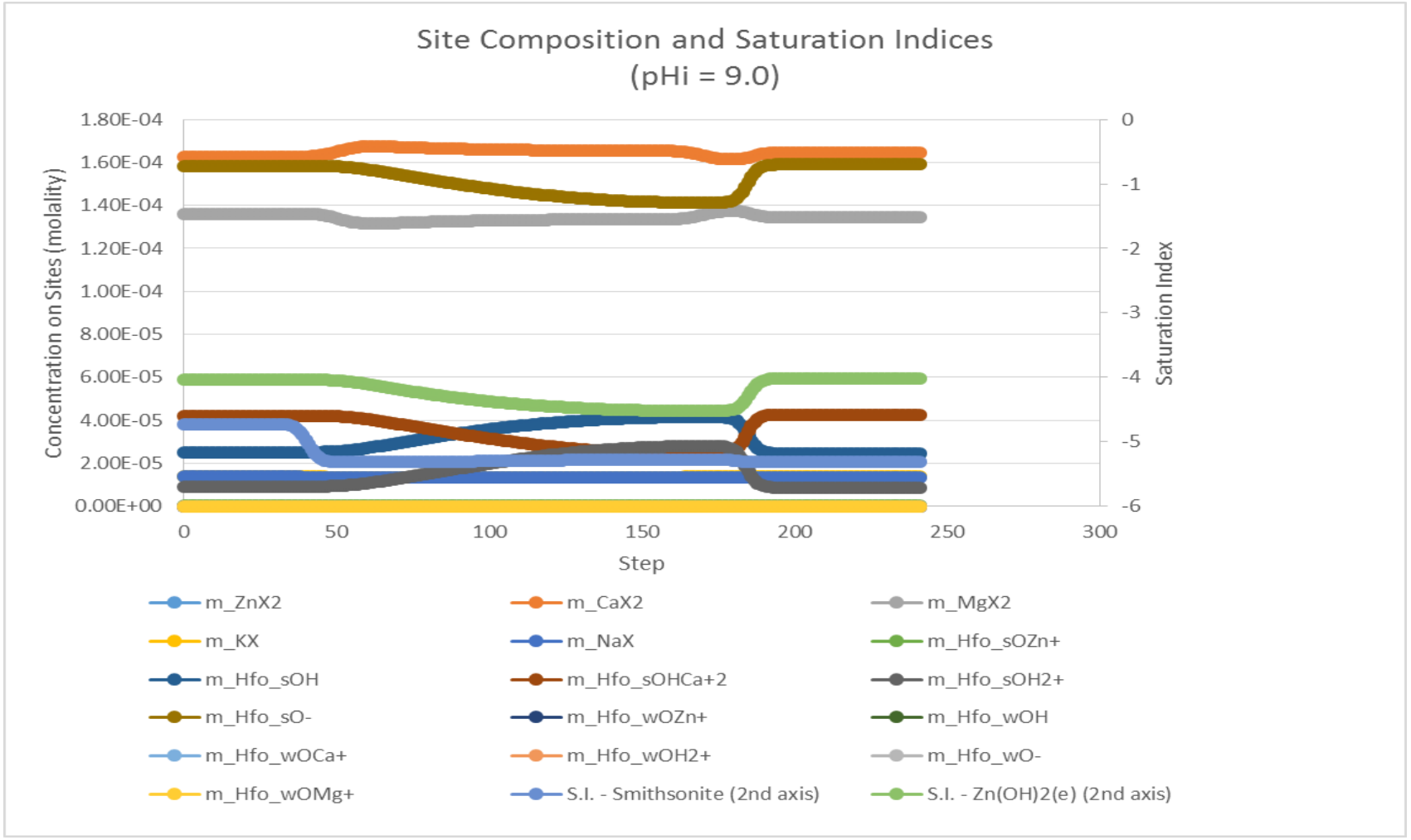
Site Composition and Saturation Indices
(pHi = 9.0)
Concentration on Sites (molality)
1.80E-04
1.60E-04
1.40E-04
1.20E-04
1.00E-04
8.00E-05
6.00E-05
4.00E-05
2.00E-05
0.00E+00
0
50
100
150
200
250
300
Step
0
-1
-2
-3
-4
-5
-6
Saturation Index
m_ZnX2
m_CaX2
m_MgX2
m_KX
m_NaX
m_Hfo_sOZn+
m_Hfo_sOH
m_Hfo_sOHCa+2
m_Hfo_sOH2+
m_Hfo_sO-
m_Hfo_wOZn+
m_Hfo_wOH
m_Hfo_wOCa+
m_Hfo_wOH2+
m_Hfo_wO-
m_Hfo_wOMg+
S.I. - Smithsonite (2nd axis)
S.I. - Zn(OH)2(e) (2nd axis)

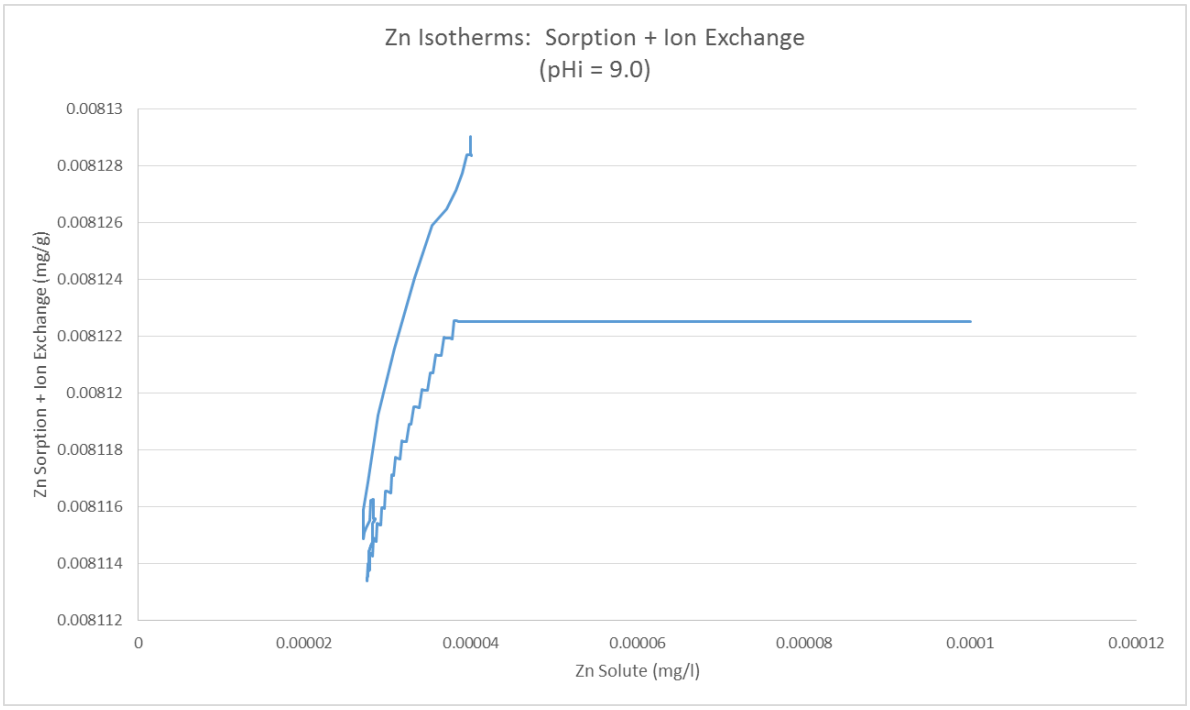
Zn Isotherms: Sorption + Ion Exchange
(pHi = 9.0)
Zn Sorption + Ion Exchange (mg/g)
0.00813
0.008128
0.008126
0.008124
0.008122
0.00812
0.008118
0.008116
0.008114
0.008112
0
0.00002
0.00004
0.00006
0.00008
0.0001
0.00012
Zn Solute (mg/l)

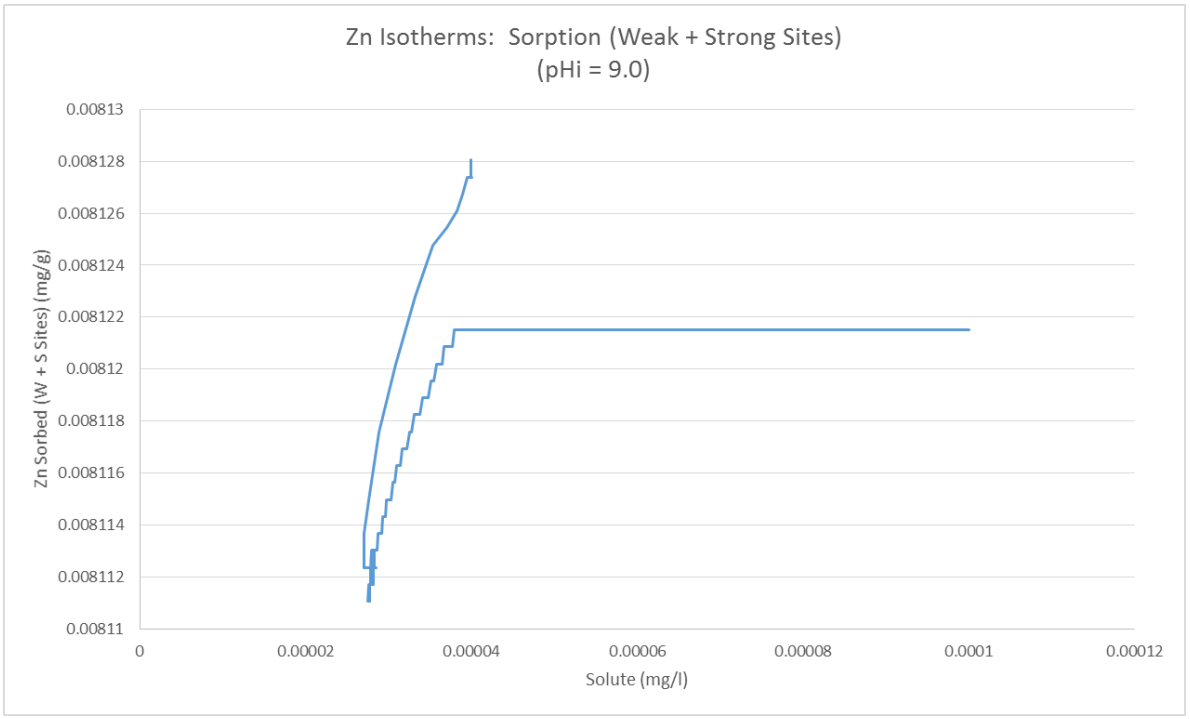
Zn Isotherms: Sorption (Weak + Strong Sites)
(pHi = 9.0)
Zn Sorbed (W + S Sites) (mg/g)
0.00813
0.008128
0.008126
0.008124
0.008122
0.00812
0.008118
0.008116
0.008114
0.008112
0.00811
0
0.00002
0.00004
0.00006
0.00008
0.0001
0.00012
Solute (mg/l)

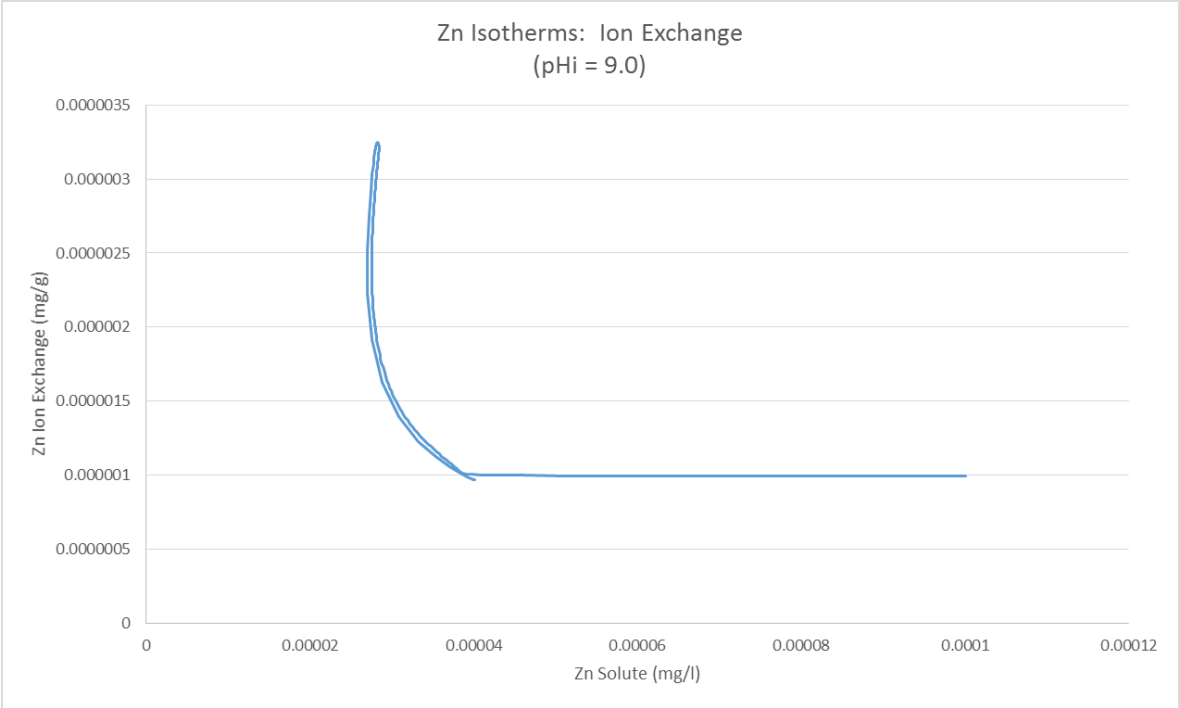
Zn Isotherms: Ion Exchange
(pHi = 9.0)
Zn Ion Exchange (mg/g)
0.0000035
0.000003
0.0000025
0.000002
0.0000015
0.000001
0.0000005
0
0
0.00002
0.00004
0.00006
0.00008
0.0001
0.00012
Zn Solute (mg/l)

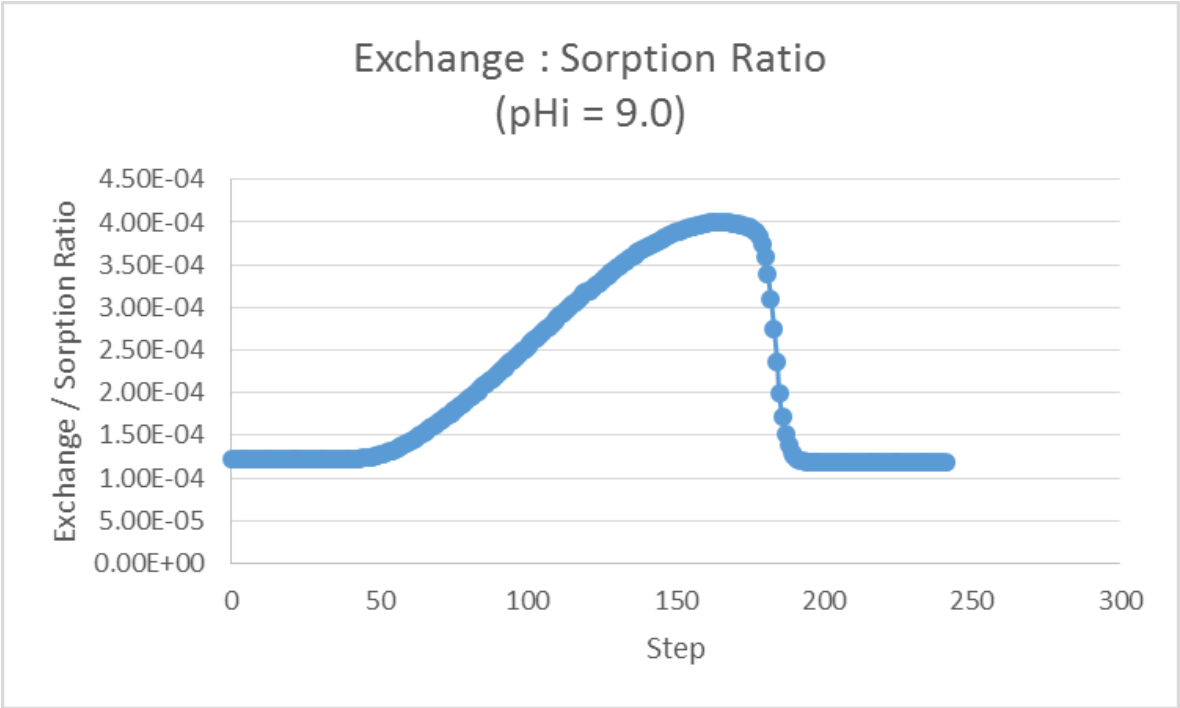
Exchange : Sorption Ratio
(pHi = 9.0)
Exchange / Sorption Ratio
4.50E-04
4.00E-04
3.50E-04
3.00E-04
2.50E-04
2.00E-04
1.50E-04
1.00E-04
5.00E-05
0.00E+00
0
50
100
150
200
250
300
Step

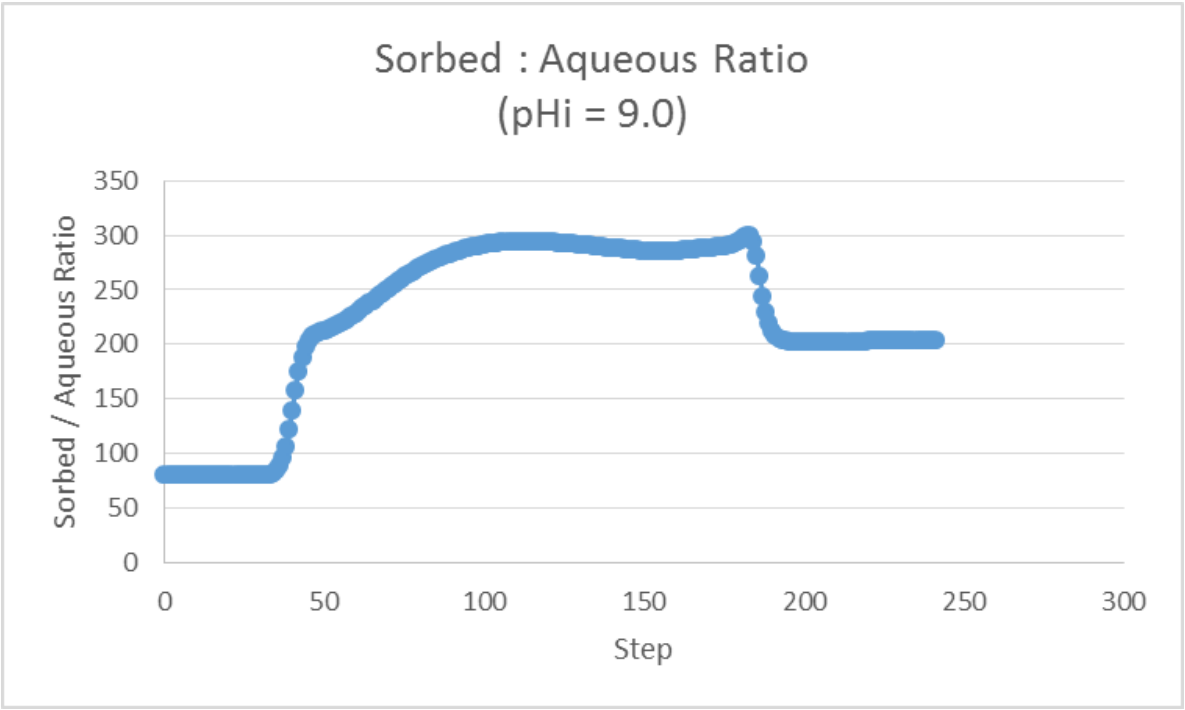
Sorbed : Aqueous Ratio
(pHi = 9.0)
Sorbed / Aqueous Ratio
350
300
250
200
150
100
50
0
0
50
100
150
200
250
300
Step